Development of novel therapeutics and *in vitro* models for spinal cord injury.

Michael Anthony McGrath
(B.Sc, M.Res)

A thesis submitted in fulfilment of the requirements of the University of Glasgow for the degree of Doctor of Philosophy

College of Medical, Veterinary and Life Sciences
Institute of Infection, Immunity and Inflammation
University of Glasgow

October 2016

Abstract

Spinal cord injury (SCI) is a devastating condition, which results from trauma to the cord, resulting in a primary injury response which leads to a secondary injury cascade, causing damage to both glial and neuronal cells. Following trauma, the central nervous system (CNS) fails to regenerate due to a plethora of both intrinsic and extrinsic factors. Unfortunately, these events lead to loss of both motor and sensory function and lifelong disability and care for sufferers of SCI. There have been tremendous advancements made in our understanding of the mechanisms behind axonal regeneration and remyelination of the damaged cord. These have provided many promising therapeutic targets. However, very few have made it to clinical application, which could potentially be due to inadequate understanding of compound mechanism of action and reliance on poor SCI models. This thesis describes the use of an established neural cell co-culture model of SCI as a medium throughput screen for compounds with potential therapeutic properties. A number of compounds were screened which resulted in a family of compounds, modified heparins, being taken forward for more intense investigation. Modified heparins (mHeps) are made up of the core heparin disaccharide unit with variable sulphation groups on the iduronic acid and glucosamine residues; 2-*O*-sulphate (C2), 6-*O*-sulphate (C6) and *N*-sulphate (*N*). 2-*O*-sulphated (mHep6) and *N*-sulphated (mHep7) heparin isomers were shown to promote both neurite outgrowth and myelination in the SCI model. It was found that both mHeps decreased oligodendrocyte precursor cell (OPC) proliferation and increased oligodendrocyte (OL) number adjacent to the lesion. However, there is a difference in the direct effects on the OL from each of the mHeps; mHep6 increased myelin internode length and mHep7 increased the overall cell size. It was further elucidated that these isoforms interact with and mediate both Wnt and FGF signalling. In OPC monoculture experiments FGF2 treated OPCs displayed increased proliferation but this effect was removed when co-treated with the mHeps. Therefore, suggesting that the mHeps interact with the ligand and inhibit FGF2 signalling. Additionally, it was shown that both mHeps could be partially mediating their effects through the Wnt pathway. mHep effects on both myelination and neurite outgrowth were removed when co-treated with a Wnt signalling inhibitor, suggesting cell signalling mediation by ligand immobilisation and signalling activation as a mechanistic action for the mHeps. However, the initial methods employed in this thesis were not sufficient to provide a more detailed study into the effects the mHeps have on neurite outgrowth. This led to the design and development of a novel microfluidic device (MFD), which provides a platform to study of axonal injury. This novel device is a three chamber device with two chambers converging onto a central open access chamber. This design allows axons from two points of origin to enter a chamber which

can be subjected to injury, thus providing a platform in which targeted axonal injury and the regenerative capacity of a compound study can be performed.

In conclusion, this thesis contributes to and advances the study of SCI in two ways; 1) identification and investigation of a novel set of compounds with potential therapeutic potential i.e. desulphated modified heparins. These compounds have multiple therapeutic properties and could revolutionise both the understanding of the basic pathological mechanisms underlying SCI but also be a powered therapeutic option. 2) Development of a novel microfluidic device to study in greater detail axonal biology, specifically, targeted axonal injury and treatment, providing a more representative model of SCI than standard *in vitro* models. Therefore, the MFD could lead to advancements and the identification of factors and compounds relating to axonal regeneration.

Table of Contents

List of Figures

List of Tables

List of Abbreviations

BACE-1	Beta-secretase-1
BBB	Blood brain barrier
BDNF	Brain derived neurotrophic factor
BrdU	Bromodeoxyuridine (5-bromo-2'-deoxyuridine)
BS	Bottenstein Sato
BSB	Blood spinal cord barrier
C2	Carbon position 2
C6	Carbon position 6
CM	Conditioned media
CNS	Central nervous system
CS	Chondroitin sulphate
CSF	Cerebrospinal fluid
CSPG	Chondroitin sulphate Proteoglycan
DAPI	4',6-diamidino-2-phenylindole
DMEM	Dulbecco's Modified Eagle Medium
DS	Dextran sulphate
DVT	Deep vein thrombosis
ECM	Extracellular matrix
EGF	Epidermal growth factor
FGF	Fibroblast growth factor
Fz	Frizzled
GAG	Glycosaminoglycan
GFAP	Glial fabrillary acidic protein
GLca	Glucuronic acid
GLcNS	N-substituted glucosamine
HA	Hyaluronic acid
HS	Heparan sulphate
IdoA	Iduronic acid
IL-1	Interleukin-1
IL1-ß	Interleukin-1ß
KS	Keratan sulphate
LMWH	Low molecular weight heparin
MAG	Myelin associated glycoprotein
MFD	Microfluidic device
MG	Microglia
mHeps	Modified heparins
MLC	Myosin light chain
MPSS	Methyl-prednisolone
N	N-Carbon position
NCAM	Neural cell adhesion molecule
NGF	Nerve growth factor
NO	Nitric oxide
NS	Neurosphere
NSC	Neural stem cell
NSCISC	National Spinal Cord Injury Statistical Center
NSM	Neurosphere medium
NT-3	Neurotrophic factor-3

OEC	Olfactory cell conditioned media
OL	Oligodendrocyte
OMgp	Oligodendrocyte myelin glycoprotein
OPC	Oligodendrocyte precursor cell
PBS	Phosphate buffered saline
PBS-T	Phosphate buffered saline - Tween
PDGF	Platelet derived growth factor
PDMS	Polydimethylsiloxane
PEG	Polyethylene glycol
PG	Proteoglycan
PGL	Polyglycolic acid
PLL	Poly-L-lysine
PLP	Proteolipid protein
RAG	Regenerative-associated gene
Re	Reynolds number
ROI	Region of interest
ROS	Radical oxygen species
RT	Room temperature
SC	Schwann cell
SCI	Spinal cord Injury
SD	Sprague Dawley
SO_3	Sulfuryl group
ST	Sulfotransferase
TGF-β	Tumor growth factor-β
TNF-α	Tumor necrosis factor-α

Acknowledgments

I would like to dedicate this thesis to my mum and dad for giving me every chance and opportunity. You are the reason why I am here, this PhD is a product of your love, care and support.

Special thanks to Kate, Chris and the munchkins Lily and Thomas your visits gave me such joy, you brought me a little piece of home up to Glasgow with every visit.

Also to my brothers; Andrew, Robert and Jack, you all kept me grounded and helped me more than you could imagine. Especially you Rob even coming up here to keep an eye on me, living with you was a highlight of my PhD.

To Síle, how lucky I was to find such a loving, caring person you make me happier than I thought possible. You helped me though the tough times and pulled me over the finish line, thank you so much.

I cannot express enough thanks to my supervisors Prof. Sue Barnett and Dr. Mathis Riehle for their continued support and encouragement from beginning to end. Their guidance helped me throughout my research and writing of this thesis.

The completion of this thesis could not have been accomplished without the support of fellow lab members past and present; special thanks to Susan and Paul for looking after me and helping me develop. Also to Steven, Katie and Cesc you three made me feel welcome when I first moved up here and we had some great nights out! Finally to Hulya, Mike, Sara, Tiia, Diana, Daniel and George what a cracking bunch of people, you lot made my time here such a laugh.

Author's Declaration

I declare that, except where explicit references is made to the contribution of others, that this dissertation is the result of my own work and has not been submitted for any other degree at the University of Glasgow or any other institution.

Signature _____

Printed name _____

Chapter 1

Introduction

1 The Spinal Cord

1.1 Physiology of the Spinal cord

The spinal cord is a thick bundle of nervous tissue situated in the vertebral column of vertebrates. It is one of the two major components of the central nervous system (CNS) along with the brain. The spinal cord is divided into four regions; cervical, thoracic, lumbar and sacral. Each region is segmented with a total of 31 nerve paired segments. These are divided unevenly between each region; cervical (7), thoracic (12), lumbar (5), sacral (5) and coccygeal (1) (Fig.1.1) (Kayalioglu 2009). The spinal cord averages between 40-45 cm long and is approximately 1.25 cm in diameter. It extends from the foramen magnum, becomes one with the medulla oblongata, and continues to the beginning of the lumbar region. Below this level the vertebral column is populated with spinal nerve roots. The spinal cord is supplied with blood from the meningeal net which is in turn supplied by segmental arteries (Johns 2014).

The spinal cord is composed of both white and grey matter. White matter is composed of bundles of myelinated axons, which give it its white colour while grey matter is made up primarily of nerve cell bodies. White matter is composed of three defined areas the posterior, anterior and lateral funiculi which are further subdivided into groups called fasciculi or tracts. Grey matter is composed of four parts: the posterior or dorsal horns, the anterior or ventral horns, the intermediate zones and the lateral horns (Fig.1.2) (Johns 2014). Dorsal and ventral nerve roots allow information to enter and leave the column, transmitting nerve impulses along the cord to appropriate targets, either the brain or peripheral regions (Crossman AR and Neary D 2010).

The spinal cord has two enlarged areas where large bundles of nerve fibres cross the CNS boundary. The first is the cervical enlargement where the spinal nerves exit the cord and form the brachial plexus, which supply nerves to the upper extremities. The second area, known as the lumbosacral enlargement, is where spinal nerves exit the cord and form the lumbar and sacral plexuses, which supply nerves to the lower extremities (Watson and Kayalioglu 2009). The anterior horns of the grey matter house the anterior nerve root cell bodies, whereas the posterior nerve roots cell bodies are housed as a mass of soma in the posterior root ganglia outside the cord.

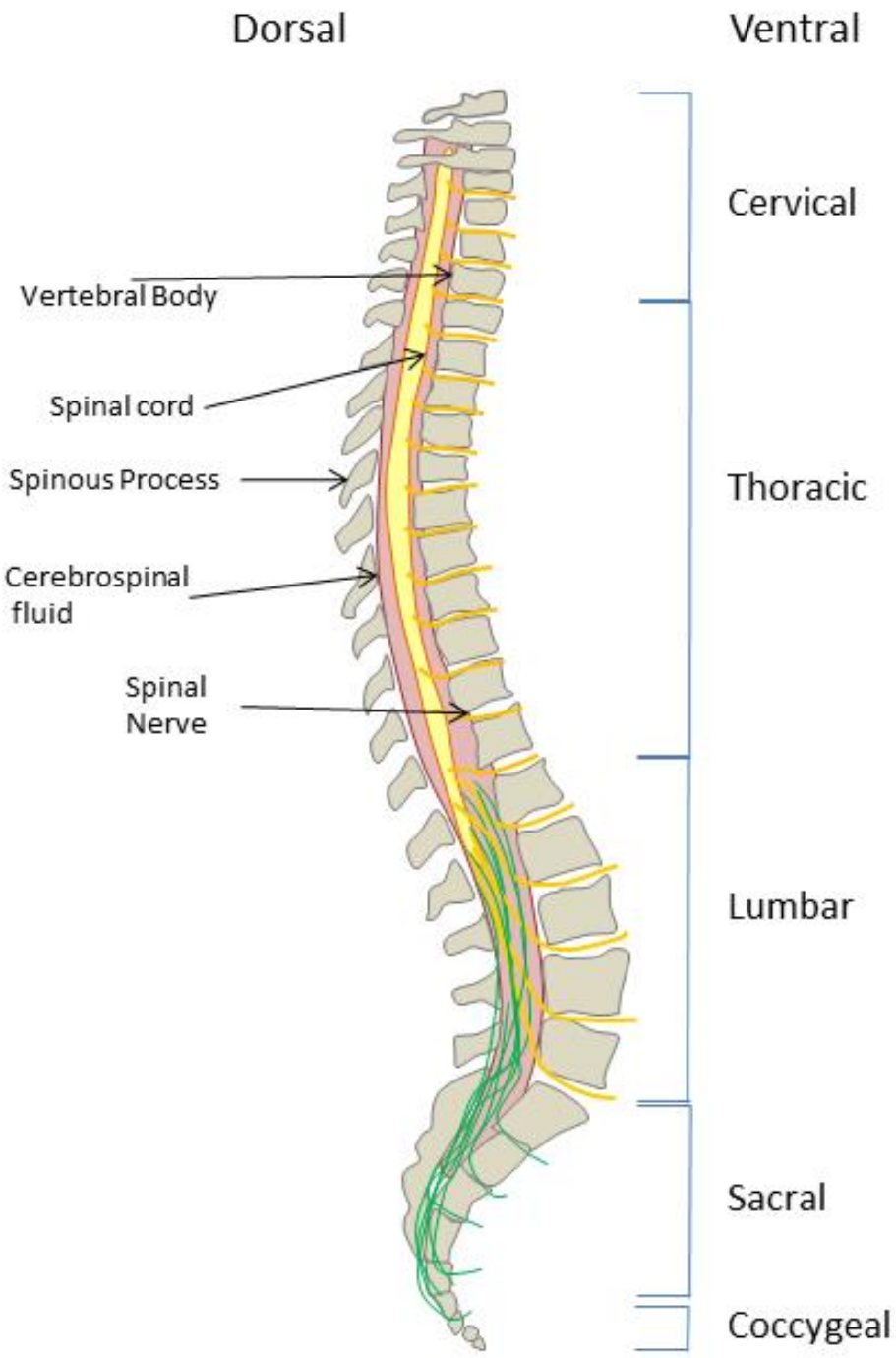

Figure 1.1 Spinal Cord

The spinal column can be split into 5 sections: cervical, thoracic, lumbar, sacral and coccygeal. The spinal cord extends from the brain to L4/5 region (yellow), past here the spinal nerve roots (green) extend down the rest of the column. Image adapted from (Drake et al. 2015)

The spinal cord is encased in meninges and cerebrospinal fluid (CSF). The meninges provide support and stability. The CSF surrounds both the brain and cord and it supports and cushions these whilst also removing waste products, which it returns to the blood stream (Scremin 2009).

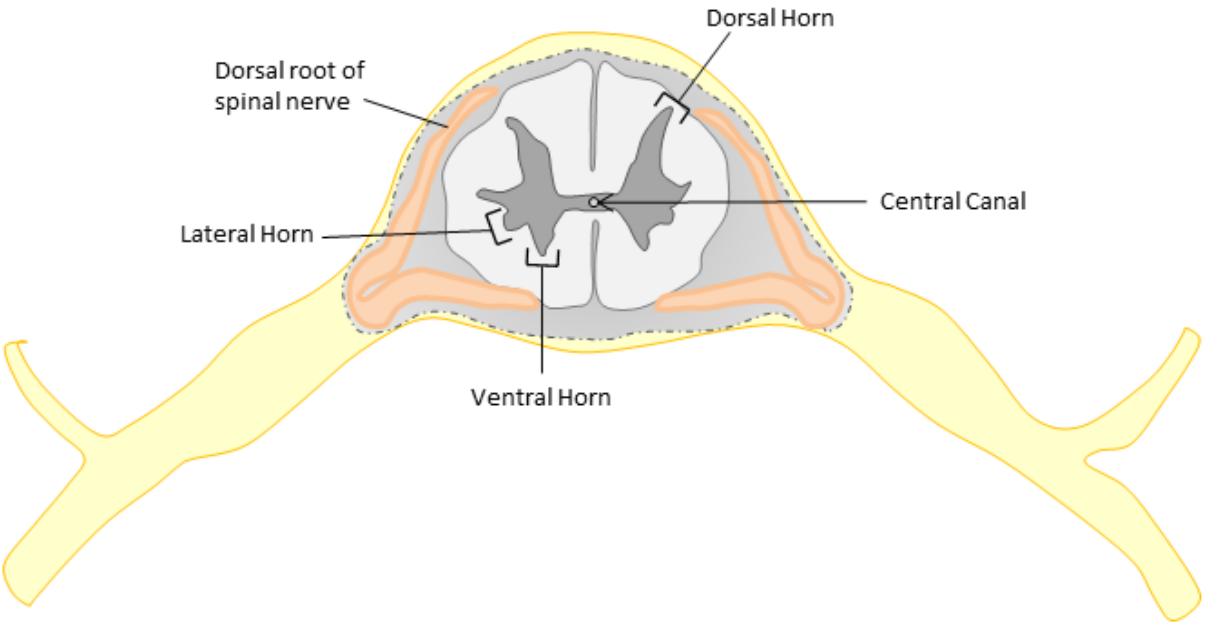

Figure 1.2 Cross section of the spinal Cord

The spinal cord can be seen here with the grey matter in the centre with the typical butterfly shape. This section is divided into dorsal, ventral and lateral horns containing sensory nerve tracts. The white matter houses the motor neuron tracts. Dorsal spinal nerves can be seen either side of the cord The nerves enter/leave the cord enabling communication with the CNS and the body. Adapted from (Drake et al. 2015)

The structure and organisation of the spinal cord is crucial to is function. The spinal cord is surrounded by aqueous CSF and is housed in the vertebral column, 31 bone sections designed to protect the cord within. The cord and vertebrae are sectioned into 5 distinct regions' cervical, thoracic, lumbar, sacral and coccygeal. The spinal nerves branch out of the cord through the vertebrae foramen and enter the peripheral nervous system.

Spinal cord development begins in the neural tube at around 21 days post fertilisation. Primitive nerve cells or neuroblasts arise from the neural epithelium within the neural tube. Neuroblasts found at the alter plate develop into the sensory neurons which reside in the dorsal horn, whereas those found at the basal plate differentiate into motor neurons within the ventral horns. Finally, neuroblasts differentiate into preganglionic sympathetic and parasympathetic neurons in the intermediate and lateral horns (Ashwell 2009). These mature neurons comprise of a cell body or soma with dendritic and axonal projections which deliver signals to and from the soma, respectively. Once these mature neurons have developed, cellular division ceases and these neurons remain in place for the rest of the organism's life (Eyre 2003).

The mature neurons lack the ability to dedifferentiate and divide. This absence of CNS cellular renewal presents a major clinical challenge as injury to the spinal cord often results in neuronal cell loss.

1.1.1 Clinical Pathology following spinal cord injury

Damage to the spinal cord causes a disruption in the communication between the brain and parts of the body that are innervated below the point of injury. Following SCI the extent of the injury is assessed medically, using an established international standard clinical tool known as the American Spinal Injury Association scale or ASIA scale. This characterises the injury and grades it on completeness, examining both sensory and motor outputs The classifications of the ASIA scale are:

- A=Complete: No sensory or motor function,
- B=Incomplete: sensory, but not motor function preserved below site of injury,
- C=Incomplete: motor function is preserved with key muscles at grade response 3 or less below site of injury,
- D=Incomplete: motor function is preserved with key muscles at grade response 3 or higher below site of injury, and finally,
- E=Normal: both sensory and motor function normally (Kirshblum et al. 2011).

Epidemiologically, the occurrence of traumatic SCI lies within four major areas; with motor vehicle accidents attributing 40-50%, sports related accidents at ~24%, falls 12-20%, and violence at 7-23% of cases. Non-traumatic injuries or illnesses include bone

cancers or osteoporosis, inflammation of the cord and multiple sclerosis and these can have similar pathological outcomes as traumatic injury (Figure. 1.3) (NSCISC 2013). The occurrence of any of these events can cause damage to the spinal cord by at least one of: direct trauma, compression by bone fragmentation, or ischemia (See Fig.1.4).

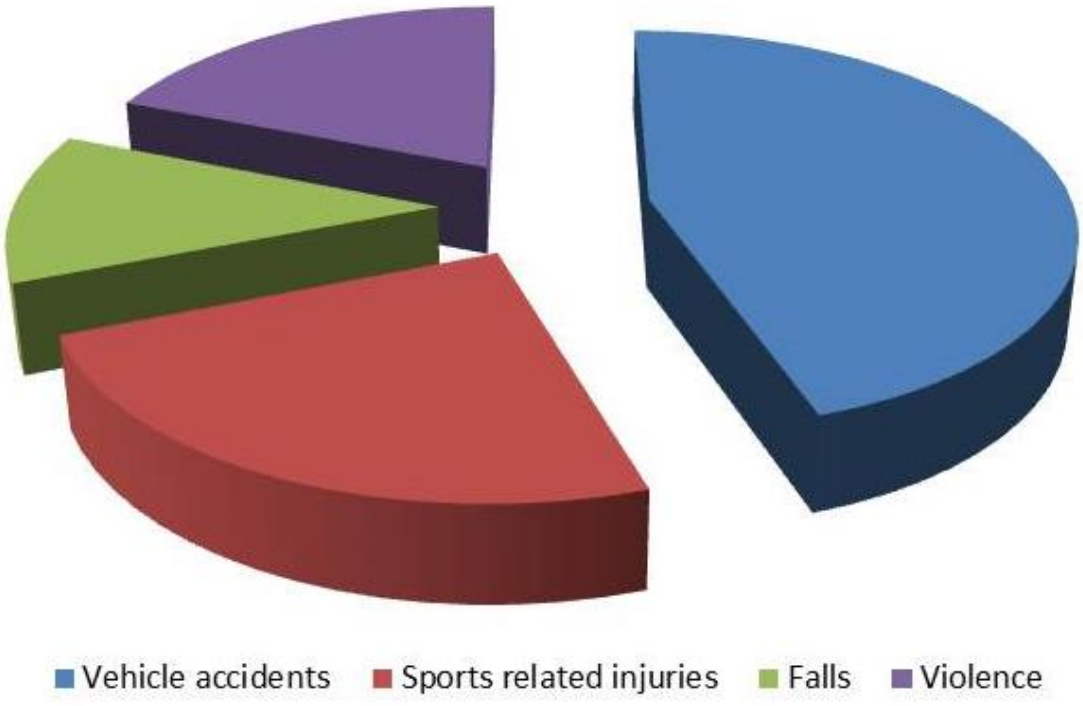

Figure 1.3 Percentage incidences of traumatic spinal cord injury

Motor vehicle accidents account for the highest incidence of SCI with 45% of cases with sports related injury at 24%, falls at 12% and violence accounting for 19%. Each injury causes damage to the cord leading many of the characteristics of SCI with paralysis being the most severe. (NSCISC 2013).

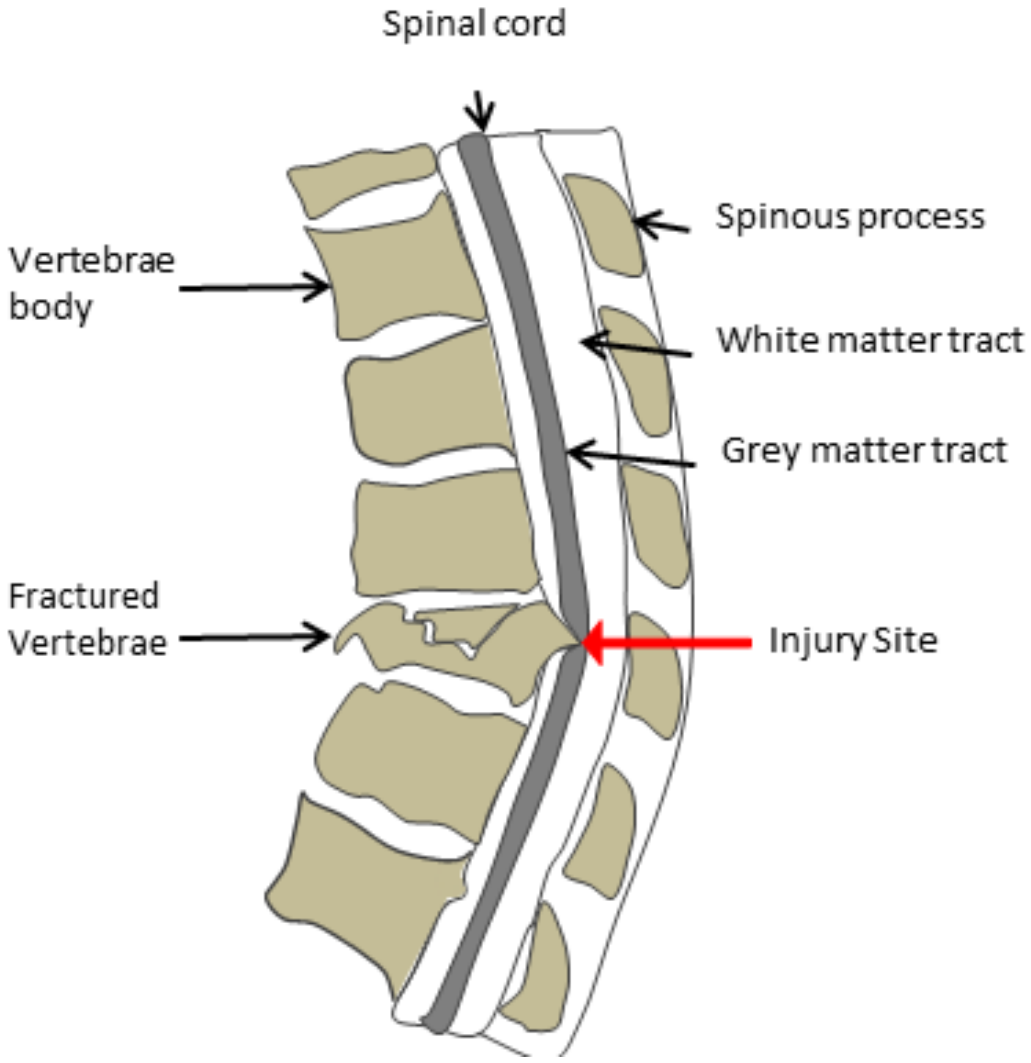

Figure 1.4 Traumatic SCI

Here is a depiction of a common injury to the spinal cord. A bone fragment is protruding into the spinal column and compressing the spinal cord and blocking arterial blood flow. Red arrow highlights the protrusion into the cord. This type of injury is commonly diagnosed using MRI and requires immediate surgery to stabilise the bone fragments, halting further movement and more damage. Image adapted from (Drake et al. 2015).

Life expectancy and mortality of SCI patients have improved drastically with the medical control of pneumonia (Berlly and Shem 2007) and urinary tract infection (Pannek 2011). However, the major causes of immediate mortality for SCI patients are pulmonary embolism and septicaemia (Thietje et al. 2011). Chronic psychological trauma also contributes to mortality with both alcohol-related death and suicide being prevalent amongst SCI patients (NSCISC 2013).

SCI sufferers are provided with constant pain management regimes and pain control is a key factor in quality of life. Rehabilitation programmes are available but the extent of recovery from rehabilitation relates to the extent of the injury. Unfortunately, many suffers experience little improvement, even with customised physiotherapy (Nagoshi et al. 2015).

1.2 Stages of SCI

1.2.1 Primary injury cascade

Immediately following spinal cord trauma the primary insult begins, this stage generally lasts under two hours. The initial site of injury manifests in the central grey matter with the white matter being largely spared at this time. The reason for this is not fully understood but it could potentially be related to the relatively softer consistency and vascularisation of the grey matter compared to white matter, making it more susceptible to mechanical stress (Wolman 1965).

In most cases of SCI there is evidence of disrupted blood flow and haemorrhage within the cord, through the loss of blood brain barrier (BBB) integrity. This disruption then leads to further damage from hypoxia and ischemia, which is detrimental to the surrounding tissue (Higashida et al. 2011). The insult then leads to neural loss, disruptions to axons and membrane integrity of the surrounding cells, which then triggers the cellular and molecular processes associated with the secondary cascade (Fitch et al. 1999). These are followed by the release of inflammatory mediators such as; IL-1β, TNFα and IL-6 triggering resident CNS immune cells (microglia) activation and migration (Pineau and Lacroix 2007) (Carlson et al. 1998) and oligodendrocyte loss/demyelination of spared axons (Li et al. 1999). The primary injury cascade is an important determinant of severity in SCI and a prime target for treatment and intervention.

1.2.2 Secondary injury cascade

Secondary injury is characterised by an immunological cascade with the influx of immunological factors resulting in wide spread cell death. The immunological cascade begins minutes after injury and can remain active for months following injury (Snyder and Teng 2012) (Leal-Filho 2011). The secondary phase can be characterised by vascular, biochemical and cellular consequences of injury (Mautes et al. 2000). These processes occur from progressive damage of the cord at the site of injury.

Vascular disruption involves breaching the blood brain barrier (BBB) or blood spinal cord barrier (BSB). This disruption results in oedema and invasion of systemic inflammatory cells, such as neutrophils and macrophages (Tator and Koyanagi 1997). In addition, the hypoxia caused by this vascular damage makes both glia and axons more susceptible to the detrimental effects of rising glutamate levels (Rothman and Olney 1986).

Biochemical events relate to the increase of extracellular excitatory amino-acid levels leading to glutamate receptor excitotoxic damage, which can induce local neuronal cell death (McAdoo et al. 2005). Additionally, Ca^{2+} ions are related to glutamate-cell death, with increased intracellular Ca^{2+} recorded in neurons at the injury site. Ca^{2+} is also related to the generation of free radicals through mitochondrial damage, which can induce further neural cell death (Park et al. 2004).

Cellular events are related to the influx of resident microglia and peripheral immune cells such as neutrophils and macrophages to the injury site. Microglia, which are the initial immune responders to injury in the CNS, migrate to the injury site (Dibaj et al. 2010). These activated microglia are not yet phagocytic macrophages as this phenotypic change only occurs following further activation through their exposure to certain cytokines and chemokines such as interleukin-1 (IL-1) and tumour necrosis factor-α (TNF- α) (Basu et al. 2002) (Probert et al. 2000). These then phagocytic microglia remove tissue debris and release neurotrophins such as nerve growth factor (NGF) and neurotrophin-3 (NT-3), to control the inflammatory response (Elkabes et al. 1996) (Nakajima et al. 2001). The peripheral immune cells can only enter the CNS following vascular damage (to the BBB) and chemotactic cues (Taoka and Okajima 2000). These cells are phagocytic and remove tissue debris from the site of injury. These cells also function to limit the BBB breach by accumulating at the site of vascular damage (Zhou et al. 2014).

1.3 Glial cells in CNS health and injury

Glial cells are known as the support cells of the CNS. '*Glia*' meaning 'glue' in Greek, this term coined by Rudolf Virchow in 1858 (Kettenmann and Verkhratsky 2008), are the major component of the CNS cellular environment (Purves D et al. 2001). Glial cells comprise a broad category of cells which include: astrocytes, oligodendrocytes microglia and ependymal cells with glial cells outnumbering neurons in the CNS (Jessen 2004).

Glial cells were deemed to be of little importance in SCI pathology with much research focusing on the neuron. However, studies are now suggesting that these cells play vital roles not only in neuropathology but in also neurogenesis (Jessen 2004), neuronal communication/ synapse formation and even in higher brain functions such as intelligence (Pfrieger and Barres 1997).

1.3.1 Astrocytes and myelinating glia in CNS

The focus of this thesis will be on astrocytes and myelinating glia known as oligodendrocyte progenitor cells (OPC) and oligodendrocytes (OL). The morphological and functional characteristic of these cell types are quite distinct.

1.3.1.1 Astrocytes

Astrocytes are intimately involved with many cells of the CNS. They are highly secretory cells and have many intricate processes, expanding outwards allowing interaction with thousands of surrounding neurons and glia (Araque et al. 1999). Astrocytes originate from the neuroectoderm as progenitor radial glial cells which become gliogenic and differentiate into astrocytes (Cepko et al. 1996; McConnell 1992). Within the grey matter the 'protoplasmic' astrocytes encase synapses whilst in the white matter 'fibrillary' astrocytes contact nodes of Ranvier and blood vessels (Bushong et al. 2002). Both of these astrocyte subtypes form gap junctions between distal processes of neighbouring astrocytes allowing astrocytic communication (Ogata and Kosaka 2002).

Astrocytes can have multiple different phenotypes depending on their position and the environment in which they reside, for example, triggering active and reactive astrocytic phenotypes in inflammatory environments (Khakh and Sofroniew 2015) (Sofroniew 2015).

Astrocytic functions in the CNS include energy metabolism, regulation of blood flow, immune system mediation and even adult neurogenesis. The main characteristic of the astrocyte to allow these functions is the mediation of signals between neural cells, glial cells and neuroendothelial cells within the CNS (Sofroniew and Vinters 2010).

Astrocytes are involved with the release of energy substrates and growth factors to the synapse. Astrocytes have been shown to endocytose certain neurotransmitters which can regulate and remove these molecules from the synaptic cleft which could otherwise result in overactive stimulation and nerve damage (Hamilton and Attwell 2010). They have vascular endfeet which are in direct contact with the blood vessel endothelial cells and express high levels of glucose transporters for passage of glucose (Kacem et al. 1998) to the dendrites, synapses and axons.

Astrocytes have been shown to have bidirectional interaction with blood vessels and synapses, forming a tripartite complex. Recent studies have shown astrocytes having the ability to control blood vessel dilation, thus altering blood flow to desired regions of the spinal cord (Abbott et al. 2006). Astrocytes have been observed encasing synapses forming a veil-like structure whilst extending other processes to contact capillaries, directly modifying the signals in an interaction termed neurovascular coupling (Haydon and Carmignoto 2006). Astrocytes have also been shown to be critical in synapse pruning and regulation in close association with microglia (Persidsky et al. 1999). Adult neurogenic niches are highly controlled areas within the CNS. Astrocytes have been shown to participate in CNS plasticity (Wilhelmsson et al. 2012). The activation and differentiation of adult neural stem cells (NSC) is crucial in memory formation. Astrocytes have been shown to mediate the differentiation of NSCs to neurons in the hippocampus through juxtacrine signalling and presentation of ephrin-B2 (Ashton et al. 2012). This is key, as new neurons are generated here, so the CNS has the capacity to form new neurons and connections, this may be the case following injury to the cord if the mechanisms behind this are fully understood.

1.3.1.2 Oligodendrocytes & progenitors

Oligodendrocyte precursor cells (OPC) are the progenitor cell that form oligodendrocytes (OL) and account for around 5%-8% of the CNS cell populations (Dawson et al. 2000). OLs are crucial in the CNS by allowing rapid saltatory signal transduction and neuroprotection as these specialised cells provide the lipid insulation or myelin sheaths around axons. OL morphological characteristics are very distinct from the astrocytes, even though still a process bearing cell, they can be seen to physically wrap axons with a myelin sheath (Simons and Nave 2015). A single OL can

form/contribute to up to 25 internodes of myelin, this number depends upon many factors such as the diameter of the axon and the region of the cord (Snaidero and Simons 2014).

OPCs are generated in the ventral neuroepithelium of the neural tube in early embryogenesis where they provide guidance for immature neuron migration. These cells are characterised by expressing the chondroitin sulphate proteoglycan-NG2 (NG2), and have now become known simply as NG2 cells. NG2 cells have both perinatal and adult forms (Noble 2000). OPCs can also arise from the dorsal spinal cord and hindbrain/telencephalon of the brain from early to post-natal development (Vallstedt et al. 2005). OPCs proliferate and migrate throughout the CNS during development and into adulthood, where they differentiate into mature oligodendrocytes forming myelin around axons (Simons and Lyons 2013). OPCs within the grey matter tend to have processes of a radial orientation whereas, in the white matter the processes are more longitudinal (Levine et al. 2001).

OPC proliferation, differentiation and migration are under the control of many endogenous factors. Astrocyte-derived growth factors include, insulin-like growth factor 1, (Komoly et al. 1992), platelet derived growth factor α and fibroblast growth factor-II. These factors promote the proliferation and inhibit the differentiation of OPCs (Noble et al. 1988) (McKinnon et al. 1990). Neuregulin is a neuron-derived factor which contributes largely to the survival of OLs and inhibits the proliferation of OPCs (Canoll et al. 1996). Myelinated axons actively inhibit the differentiation of OPCs through the release of ATP and certain neurotransmitters. Pre-myelinated axons, which initiate action potentials, release adenosine, which causes the resident OPCs to drop out of their proliferative state and begin differentiation towards a mature OL state, with the aim of myelinating the axon (Stevens et al. 2002). Perinatal OPCs have been shown to alter their differentiation to OL in the presence of CNS myelin (mature OL), with Notch 1 receptors being implicated as the receptor present on the OPC which inhibits differentiation in the presence of CNS myelin (Wang et al. 1998).

It is clear that astrocytes and OPCs/OLs are critical to spinal cord homeostasis. With astrocytes being central to glial and neuronal interactions, they are in a prime position for mediating the SCI response. With demyelination a key pathological outcome of trauma the reaction of OPCs/OLs to the injury site makes these cells high priority for targeting in the pursuit of CNS injury recovery, as these cells are crucial for cord homeostasis and protection of the axons. Therefore, understanding the processes that drive these cells during injury will allow for the identification of potential targets for clinical intervention.

1.3.2 Formation of the Glial scar

The pathological hallmark of SCI is the generation of the glial scar, which is seen as a major barrier for innate axonal regeneration (Yiu and He 2006). The glial scar contains a heterogeneous population of cells and factors which form both a chemical and physical barrier (See Figure. 1.5).

Ramon Y Cajal observed the limited regenerative capacity of the CNS in the early 1900s (Caja 1928). However, studies have shown that the CNS may have some intrinsic regenerative abilities. It has been observed that CNS neurons can regenerate if given a peripheral nerve environment (Richardson et al. 1980). This study demonstrated that the inhibition to growth within the CNS reflects a non-permissive environment as opposed to an innate inability of CNS axons to regenerate. This suggests that the components of glial scar which form the injury microenvironment around damaged axons can be responsible for the lack regeneration at the site of insult following SCI (Fehlings and Hawryluk 2010).

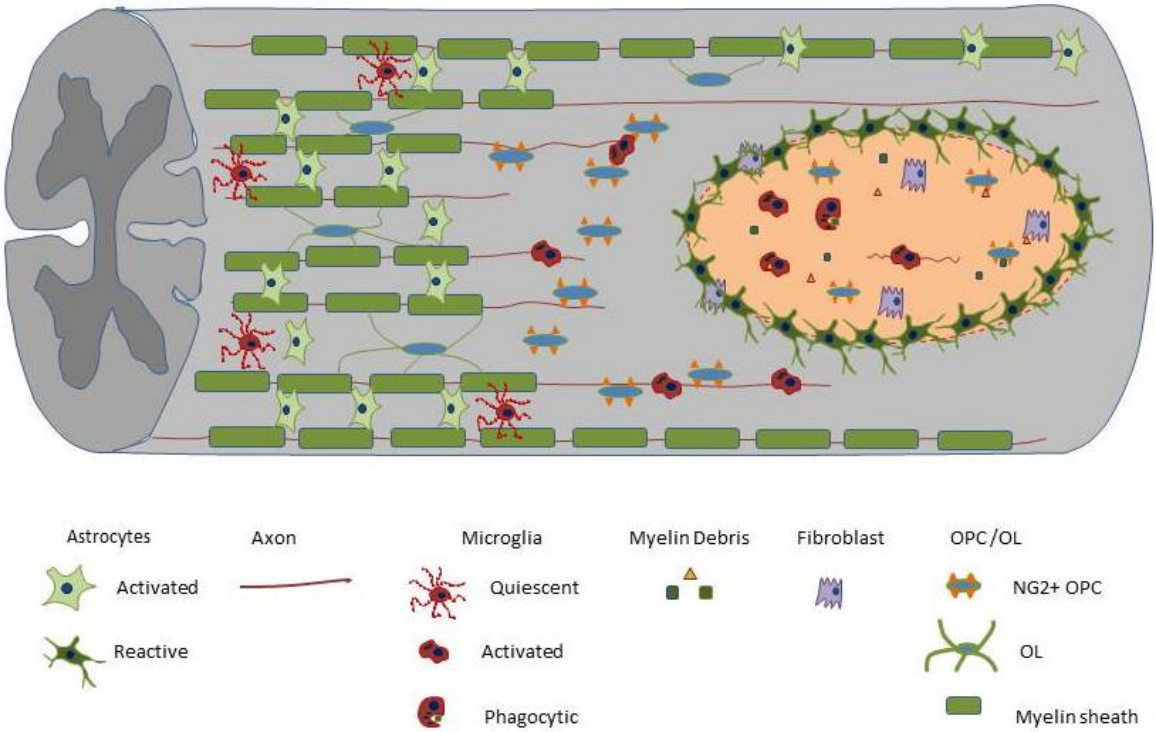

Figure 1.5 The glial scar

Trauma to the spinal cord elicits a major cellular and molecular response. The injury site is invaded by many different cells whose aim is to barricade the damaged area and remove any dead of damaged cells. The injury site is a non-regenerative environment with loss of axons and myelination a permanent feature of the injury leading to lifelong loss of function. The glial scar is the main target for therapies, it is known that a combinational approach is necessary due to the many components of injury. Image adapted from (Obermair et al. 2008).

The cellular composition of the glial scar includes, innate microglia, invading immune cells and fibroblasts from the peripheral vasculature, damaged axons, OL/OPC and astrocytes (Fig.1.5). Disruption of the BBB due to trauma contributes heavily to the glial cell component of the scar, as this enables an influx of immune cells, which adds to the cellular component of the glial scar (Fitch and Silver 1997). This disruption to the BBB is further exacerbated through the release of cytokines and chemokines, damaged cells, which leads to infiltration of systemic immune cells into the CNS or spinal cord space where the trauma has occurred (Leal-Filho 2011). The cellular components of the glial scar releases a plethora of molecules which have different effects on the cells constituting the glial scar and the surrounding tissue (Fitch and Silver 2008).

Astrocytes are major mediators of the glial scar. The astrocytes at the injury site and those which migrate to the site adopt a reactive phenotype altering their morphology, behaviour and function. Damaged cells release many factors, which contribute to

inducing the reactive phenotype of astrocytes including cytokines and growth factors (LIF, CNFT, TNFα and TGFß), small molecules such as ATP, oxidative stress molecules-radical oxygen species and nitrous oxide (ROS and NO) and cell damage leads to ischemia (hypoxia and glucose loss). Furthermore, it has been shown that in astrocyte depletion studies, neurite outgrowth can be achieved in the absence of the reactive astrocyte at the site of injury (Bush et al. 1999).

Other major constituents of the glial scar are both the OLs and their progenitor the OPCs. OL loss is a major event following injury to the CNS resulting in demyelination occurring during the secondary injury cascade (Levine et al. 2001). OPCs, similar to astrocytes alter their morphology and proliferation rate following injury, with accelerated OPC proliferation remaining high for up to a week following injury (Tripathi and McTigue 2007). Although OPCs' main function within the CNS is to differentiate into myelinating OLs, this function is inhibited following injury as OPCs are instead stimulated to proliferate by the glial scar factors. This results in focal demyelination in and around the site of injury (Fitch and Silver 2008).

A major molecular inhibitor within the glial scar is NG2, the chondroitin sulphate proteoglycan (CSPG), which is highly expressed on the cell surface of OPCs (Lytle et al. 2009). NG2+ OPCs have also been observed in the fibrotic core of the scar suggesting that these cells may be directly involved in the scar formation and may be promoting the inhibitory environment (Buss et al. 2009). $NG2^{+}$ OPCs have been shown *in vitro* to affect cells distal to the injury site, including OLs whose processes are altered, both in length and number, causing further spread of demyelination. NG2 has been shown to be a potent axonal repulsion guidance cue causing growth cone collapse and axonal retraction (Ughrin et al. 2003).

The final phase of glial scar formation sees the generation of a fluid-filled cavity or syrinx. The syrinx is a second form cavity comprised of a very dense astrocytic wall. This cavity is highly pressurised which can lead to further compression of the cord, however, the exact mechanisms of syrinx formation are unknown (Klapka et al. 2005) (Norenberg et al. 2004).

1.3.3 Preservation of function following astrocytosis and glial scar formation

Although it may seem that the reactive astrocytes are solely detrimental to regeneration, astrocytic response to injury has also been suggested as a protective

mechanism (Faulkner et al. 2004). This response of the astrocyte to insult leading to the formation of a reactive phenotype is conserved throughout vertebrate evolution (Larner et al. 1995). A study using GFAP-TK mice (thymidine kinase from herpes simplex virus targeted to reactive astrocytes), which removed dividing reactive astrocytes from the injury site showed that spinal insult to the mutant GFAP-TK mice was more detrimental than that same insult to wild type mice (Faulkner et al. 2004). Specifically in the GFAP-TK mice there was greater damage including failure of the BBB, leukocyte infiltration, severe cell loss in both neurons and glia (OL) with demyelination, compared to wild type (Bush et al. 1999). This study suggests that a primary function of reactive astrocytes and the glial scar is defensive and these cells should not necessarily be looked at as the enemy.

Similarly, the OPCs' role in the glial scar may have beneficial effects. A study which transplanted OPCs into an injury site. Lac-Z-transfected OPCs were transplanted into an irradiated cord, OPC survival was recorded and by 15 days there was a marked increase in remyelination (Franklin et al. 1996). Alterations to OPC phenotype have been suggested as having a potential regenerative role following injury. OPC 'activation' is required for remyelination to occur (Miron et al. 2011) and this activation leads to an altered phenotype both behaviourally and morphologically. Cellular hypertrophy and altered gene expression for certain genes, such as OLIG2 and NK2, are seen in activated OPCs (Fancy et al. 2004). OPCs require the inflammatory cascade to induce their activation or their priming for remyelination and their activation is proportional to the local inflammatory response (Chari et al. 2006). This understanding of the beneficial pro-remyelinating phenotype of the OPC suggests that treatments which dampen the immune response may be actually detrimental to the remyelination process.

1.4 Strategies for SCI repair and regeneration

SCI regeneration will be a combination of multiple therapeutic strategies. Regeneration encapsulates; cell survival, axonal growth, remyelination and synapse formation. Therefore, successful therapies will aim to promote a number of these regenerative factors.

1.4.1 Current Clinical therapies for SCI

Current therapeutic options for SCI are limited, with no adequate treatment available in the clinic to allow for complete functional repair. Numerous clinical trials have been carried out using both pharmacological and cellular strategies, with many yielding negative results, whether due to adverse effects of the drug or lack of statistical power

in the trial. Although in general these trials have been phase 1 and principally investigated for safety not efficacy, they still provide important insights into how we can improve and advance new therapies into the clinic.

Methylprednisolone Sodium Succinate (MPSS) is a corticosteroid used as a treatment in many inflammatory disorders such as arthritis and dermatosis (Hayball et al. 1992) (Goldberg and Barkoff 1960). It has also been posed as a potential treatment option for SCI, although controversially. Neurologically, MPSS has been shown to function through the enhancement of blood flow to the spinal cord and is also as a neuroprotective agent via the reduction of axonal die back post trauma (Hall 1992). There is also evidence that MPSS preserves OL death following injury (Lee et al. 2008). Furthermore, MPSS has been shown to be an anti-inflammatory agent reducing TNF-α and NFκß synthesis (Oudega et al. 1999). MPSS was originally thought to be most effective in the first few hours after injury (2002) and 5 clinical trials have been conducted looking at the therapeutic benefit of MPSS in SCI. However, following the trials, MPSS has been implicated in adverse side effects such as pulmonary compilations (Matsumoto et al. 2001). These adverse effects have left many clinicians divided, with some continuing to employ MPSS, feeling that the risks are justified in the context of the severe deficits that accompany SCI (Fehlings 2001).

Two other potential pharmacological therapies, gacyclidine (GK-11), an anti-glutamatergic agent (Feldblum et al. 2000), and Thyrotropin releasing hormone (TRH), a mediator of other excitotoxic agents (Dumont et al. 2001), also underwent clinical trials (Pitts et al. 1995). However, both trials suffer from poor experimental designs which lead to doubts over the outcomes.

GK-11 showed some potential therapeutic benefit 1 year post treatment for motor function following certain types of injury (cervical patterned injury) but the trial outcome was non-significant. However, the data obtained could be misleading due to non-significant statistical power, GK-11 is no longer being pursued (Bond and McKerracher 2014).

Similarly, TRH had shown promising results with statistical improvement following treatment with TRH versus untreated controls. However, only 20 patients were analysed so caution is needed as a statistical type I error could be confounding the true therapeutic effect of the drug (Pitts et al. 1995).

Following the pitfalls of past trials, newer more strictly controlled trials have been devised. Moreover, details for SCI trials conducted are published by scientists and

research organisations including, the International Campaign for Cures of Spinal Cord Injury Paralysis who have produced a publication to improve trial structure and design (Steeves et al. 2007). There are a number of promising neuroprotective treatments currently in clinical trials including Minocycline and Riluzole. Minocycline is a tetracycline derivative used in dermatological treatment but has been shown to be effective in animal models of stroke and multiple sclerosis (Festoff et al. 2006). Riluzole is an anti-convulsant used to treat amyotrophic lateral sclerosis patients (Bhatt and Gordon 2007). It has shown neuroprotective activity through the blocking of voltage-sensitive sodium channels release, which is dysregulated following insult to the spinal cord (Schwartz and Fehlings 2001).

1.4.2 Axonal outgrowth and removal of growth inhibition

The CNS has very limited innate axonal regeneration capacities (Fawcett 2006). It is believed that the inhibition of axonal outgrowth is due to both extrinsic and intrinsic factors. Extrinsic inhibitory factors are mainly released by cellular components of the glial scar into the injury environment and repel the axons from the site of injury (Fawcett and Asher 1999). Intrinsic inhibitory factors are synthesised within the damaged neurons/axons and inhibit the outgrowth into and across the site of injury (Filbin 2003).

A major proportion of extrinsic axonal outgrowth inhibitors is cellular debris from the myelin sheath such as myelin-associated glycoprotein, (MAG), oligodendrocyte myelin glycoprotein, (OMgp) and Nogo-A (Chen et al. 2002) (Wang et al. 2002) (Geoffroy and Zheng 2014) (Chong et al. 2012). MAG and OMgp are protein components of the myelin sheath and have been associated with causing OPC and OL death (Kotter et al. 2006). Moreover, these are the primary repulsion mediators leading to inhibition of axonal outgrowth into and across the injury site (Filbin 2003). The identification of these axonal outgrowth inhibitors has uncovered a potential treatment target. Experiments using antibodies blocking Nogo receptor-1, the receptor for MAG and OMgp, have been reported to facilitate long-distance regeneration and sprouting of corticospinal axons in rodent models (Zorner and Schwab 2010) (Fournier et al. 2001). However, targeting only the extrinsic inhibitor molecules has had limited regenerative success (Yiu and He 2006), suggesting that a two-pronged approach of both extrinsic and intrinsic targeting is necessary for adequate axonal outgrowth.

Due to the apparent intrinsic ability of peripheral neurons to regenerate following injury, this has led to intense studies into the differences between the PNS and CNS nervous tissue microenvironments which may hold the key to PNS regeneration (Huebner

and Strittmatter 2009). Gene profiling has been performed to identify genetic differences of the CNS and PNS neurons, and this has led to the identification of regenerative associated genes (RAG), active only in regenerating PNS neurons after injury (Schmitt et al. 2003) (van Kesteren et al. 2011). Therefore, a promising strategy for CNS axonal outgrowth is the targeted activation and up-regulation of these RAGs in the regenerating injured CNS neurons.

Studies have identified that successful regeneration requires the axons to synthesize proteins at the exact position along the axon which is injured (Jung et al. 2012). It has been shown that there is a difference in regenerative capacity in a given axon. This could depend on the number of ribosomes and other protein synthesis machinery present at the position of injury or at the growth cone (Court et al. 2008) (Sotelo-Silveira et al. 2006). Based on this observation, axons with low regenerative potential tended to have fewer ribosomes and protein synthesis machinery present at the injury site of the axon. The reason for variation in axonal ribosomal accumulation is not well understood (Verma et al. 2005). It is predicted that the CNS neurons have similar, if not the same, axonal protein synthesis machinery as the PNS neurons but the difference in axonal regeneration lies in their translational responses to nerve injury (Park et al. 2008). However, therapies which could activate or up regulate ribosomal presence at the site of axonal injury in the CNS could increase the regenerative capacity of the injured CNS neurons and promote axonal outgrowth (Gumy et al. 2010).

Similarly, the presence of mRNAs in the proximity of the site of injury of the axon can affect intrinsic axonal outgrowth (Kalinski et al. 2015). Studies have identified that the mRNA species present in axons and growth cones vary between axons within the CNS (Zivraj et al. 2010). These mRNAs are mostly related to the cytoskeleton and the control of cytoskeletal dynamics, but at varying levels (Willis et al. 2005). Therefore, the difference in regenerative capacities between axons at the injury site could be related to the mRNA species present within the axons at the site of damage. If we are able to understand these differences, a potential therapeutic approach could be to introduce or promote specific mRNA species to the axons at the site of injury.

1.4.3 Modulation of immune response

The role of the immune system in SCI regeneration is subject to debate, as to whether it is beneficial or not. Studies have provided evidence for both sides of the debate, with data suggesting a primary protective role of the native immune cells in injury and regeneration (Donnelly and Popovich 2008). Conversely, excess immune involvement can be detrimental to regeneration (Hausmann 2003) (Beck et al. 2010).

Following traumatic injury to the spinal cord, a number of events lead to immune involvement in the injury site and the surrounding area. Inflammatory cytokines and chemokines are released from damaged or dying cells (Bartholdi and Schwab 1997) (Lee et al. 2010). These signal to neighbouring cells which then respond to the damage by releasing more cytokines and chemokines, further recruiting cells to the injury site (Pineau and Lacroix 2007). The initial responder immune cells are the native microglia which migrate to the injury site and proliferate and begin phagocytosing the damaged and dead cells. Depending on the injury, the BBB may be breached, which then allows peripheral immune cells to respond to the injury. Both native microglia and peripheral immune cells help to establish the secondary cascade and initiate the immunological phase of SCI (Zhou et al. 2014).

Treatment options which focus on the mediation of the immune response look to control the chronic inflammatory phase which persists long after the initial immune activity has ceased. Treatment options here have two focuses; targeting the cells directly or their damaging excretory products. One approach is to target the pro-inflammatory factors on the cell surface of immune cells. TNF, a family of pro-inflammatory cytokines, is a prominent target in immune-mediated therapy with the identification and development of TNF inhibitor molecules (He et al. 2005). TNF-α has been implicated in cFOS activated glutamate-mediated cell death (Hermann et al. 2001) and activation of NF-kß, a key regulator of inflammation and cell death (Orange and May 2008) (Brambilla et al. 2005). Transforming growth factor-ß2 (TGF-ß2) is another therapeutic target. TGF-ß2 is expressed on astrocytes and is involved in the early inflammatory response (McTigue et al. 2000). A study which inhibited TGF-ß2 resulted in significantly decreasing the spread of scarring and tissue loss (Logan et al. 1999).

Another approach to modulate the immune response to SCI is the addition of autologous primed immune cells, specifically peripheral macrophages, into the injured cord (Rapalino et al. 1998b). These cells have been shown to play a role in active PNS regeneration (Perry et al. 1987). Activated autologous macrophages were the very first cells to be transplanted into the injured cord and reach clinical trials (Knoller et al. 2005). Furthermore, it was shown that macrophages primed with peripheral myelin products could promote regeneration and functional recovery in the CNS (Rapalino et al. 1998a). Activated macrophages also were shown to benefit CNS regeneration through the synthesis and release of beneficial trophic factors; interleukin-1B (IL-1B) and brain derived neurotrophic factor (BDNF) at the injury site (Rapalino et al. 1998b). However, it has been shown that depletion of peripheral macrophages leads to tissue sparing and increased neural sprouting following injury (Perry et al. 1987), suggesting that the role of macrophages is complex having seemingly contradictory effects on SCI.

1.4.4 Bioscaffolds

Bioscaffolds have been widely employed as both physical scaffolds and as drug delivery vehicles for SCI (Nomura et al. 2006). They have been constructed with many components of the extracellular matrix (ECM) including collagen (Marchand et al. 1993), fibronectin (Sterne et al. 1997) and hyaluronic acid (HA) (Rochkind et al. 2002). Bioscaffolds have also been fabricated out of naturally occurring polymers such as alginate/agarose and chitosan (Freier et al. 2005), as well as synthetic polymers such polyglycolic acid (PGA) (Chen et al. 2010) and polyethylene glycol (PEG) (Luo and Shi 2004). These materials have been selected as they are non-immunogenic and so do not elicit an immune response (Shoichet MS et al. 2008). Bioscaffolds have two major functions as a treatment for SCI; to provide physical guidance channels for regenerating neurons/axons and as a delivery medium for repair and regenerative treatments, both pharmacological and cellular (Nisbet et al. 2008), or occurring as a combination of the two.

Bioscaffolds aim to reconstruct the damaged or lost ECM of the spinal cord (Straley and Heilshorn 2009; Straley et al. 2010). They are often tubular structures, with porous fibre-like membranes which provide physical guidance for regenerating axons to grow along (Dalton et al. 2002), whilst also allowing therapeutic molecules to be bound for increased therapeutic effect (Wells et al. 1997). Bioscaffolds can also occur as gels which are semisolid liquids and have the quality of being able to fill cavities and gaps created by the injury. This type of structure could potentially lead to the prevention of astrocytosis and the spread of extrinsic inhibitory molecules at the injury site (Nomura et al. 2006).

Many treatments for SCI are introduced systemically and there is the possibility that the BBB may inhibit some molecules from entering the CNS, as well as the potential of undesirable systemic effects (Rossi et al. 2013) (Kabu et al. 2015). However, the introduction of a bioscaffold at the site of injury addresses this problem as certain molecules can be bound to the scaffold and be delivered specifically to the site of injury. A study using a nanowire scaffold to locally deliver therapeutic molecules to the injured cord resulted in enhanced neuroprotective effects of these treatments compared to standard non-scaffold delivery (Tian et al. 2012).

Hyaluronic acid hydrogels are emerging as one of the most important sources of artificial scaffolds in the tissue engineering field (Collins and Birkinshaw 2013). A recent study adopted a HA hydrogel, modified with multi-tubular structures, bound with anti-Nogo receptor antibody, and a cocktail of BDGF and VEGF for transplantation into a

rat spinal cord lesion (Wen et al. 2015). They observed retardation of gliosis and inflammation as well as large nerve fibre outgrowth and even new blood vessels in and around the implant. This approach encapsulates in its entirety the possibilities of bioscaffolds, with gel structure for cavity filling, combined with physical structure for outgrowth and binding of therapeutics for drug delivery.

Biomaterials have also shown promise as part of a combined treatment strategy with transplanted cells. One study used bioscaffolds to provide physiological cues for axonal outgrowth and cellular support for damaged or lost cells at the injury site (Zhong and Bellamkonda 2008).

Bioscaffold are a promising candidate for a 'combined therapeutic approach' to SCI treatment as this strategy enables; pharmacological, cellular, physical guidance and localised delivery approaches in one single treatment.

1.4.5 Cellular transplantation

Cell transplantation is a promising therapeutic strategy for SCI injury and has been studied extensively (Tewarie et al. 2009) (Mothe and Tator 2012). Stem cells have been intensively study as a potential SCI treatment. However, somatic cells such as unipotent and terminally differentiated cells from the glial cell lineages such as, OPC, Schwann cells (SC) and olfactory ensheathing cells (OEC) have arisen as potential candidates for transplant-mediated repair.

The consensus by the SCI research community is that a combinational treatment approach to SCI is needed and cellular transplantation appears to be the first name on the treatment option team sheet.

1.4.5.1 Glial cell therapy

Promising candidates for transplant-mediated repair for SCI are glial cells. There are three well documented options, which include two resident CNS glia; OPC/OL and OEC with the candidate from the PNS being the SC (Crang and Blakemore 1991) (Ramon-Cueto 2000) (Kuhlengel 1988).

Due to the role of OPCs as precursors of myelinating OL, cell therapies have investigated introducing these cells into the damaged cord with the aim of promoting re-myelination after trauma. OPCs can and have been isolated from neural stem cells which in turn can be used in transplant-mediated repair (Zhang et al. 1998).

SCs are the peripheral myelinating glial cell, providing myelin sheaths for PNS axons allowing rapid saltatory signal transduction (Villegas 1972). SCs were identified as potential candidates for SCI as far back as the 1970s (Blakemore 1977). Although these cells are the myelinating glial cells of the PNS, if presented with the correct diameter of axons in the CNS they can in fact myelinate CNS axons. These cells are extracted from peripheral nerve grafts and can be expanded in culture to increase the number of cells available for transplant (Kuhlengel et al. 1990). Interestingly, SCs have been shown to invade the CNS following trauma to the cord and can myelinate the resident CNS axons at the site of injury (Beattie et al. 1997). The SCs in the periphery have many other functions unlike their CNS counterpart, OLs, such as phagocytosing damaged cells and moderating the immune response (Reichert et al. 1994) (Hirata and Kawabuchi 2002). These combined therapeutic effects led to SC transplantation into patients with acute thoracic spinal cord injury performed at The Miami Project, University of Miami Miller School of Medicine 2013. This phase 1 clinical trial used autologous SCs from the sensory nerve in the leg, cultured up to 5 weeks then surgically transplanted into the injury site (NCT01739023). Although these cells have gone into clinical trial, there has been evidence calling into question the benefit of SC in the repair process. Studies have shown that the SC may interact negatively with the astrocyte and exacerbate the glial scar (Higginson et al. 2012). This study used an *in vitro* confrontational assay where astrocytes were plated as a strip in front of a strip of SCs and allowed to migrate towards each other. It was found that SCs approached the astrocytes but did not cross into their domain but formed a boundary. This had been likened to the undesirable response seen *in vivo* as exacerbating the glial scar.

OECs have also been put forth as a candidate for transplant-mediated repair (Graziadei and Graziadei 1979) (Graziadei 1973). These cells are specialised glial cells that have been shown to play a role in olfactory nerve regeneration in the olfactory bulb, the only known site within the CNS which has regenerative capabilities in the mature CNS (Graziadei and Graziadei 1979). OECs support the outgrowth of olfactory nerves during normal cell turnover (Farbman 1990). These glial cells do not reside in the spinal cord, they originate in the outer layer of the olfactory bulb, which is a transitional zone between the PNS and CNS (Barnett et al. 1993). Using the confrontation assays described above and in (Lakatos et al. 2000), it was shown that unlike SCs, OECs can mingle with astrocyte and do not form a boundary. Thus, it is believed that due to their inherent property to coexist with astrocytes, they could be a better candidate for SCI therapy than SCs (Higginson et al. 2012). However, using incomplete injury models it has been shown OECs promote neuroprotection and re-myelinate demyelinated axons (Toft et al. 2012). The precise mechanisms of the regenerative abilities of OECs are still poorly understood but research so far has shown promise.

1.5 Sulphation and signalling mechanisms in SCI

Data from the Barnett lab and others suggest modifying the level of sulphation of resident cell surface sugars around a lesion may be a beneficial strategy in SCI repair (Higginson et al. 2012; Properzi et al. 2008) (Hering et al. 2015) (Rauvala and Peng 1997). Sulphation is the biochemical process of enzymatic conjugation of a sulphate group from a donor molecule to another molecule (Chapman et al. 2004). Sulphation is implicated in a wide variety of biological processes including detoxification, hormone regulation and importantly cell signalling (Rosen and Lemjabbar-Alaoui 2010).

Cell signalling encapsulates all cellular communication. The signalling process involves a ligand and a receptor and in some cases a co-factor which mediates the ligand-receptor binding. In many cases the co-factor is a sulphated sugar moiety present at the site of signal initiation (Rosen and Lemjabbar-Alaoui 2010).

There are many types of cell signals which are usually chemical in nature. Their function in biological activities is dictated by cell signalling molecules such as growth factors, immune factors, neurotransmitters and even components of the ECM (Alberts B et al. 2002). Many of these signals can be sent to the immediate surroundings, as seen in paracrine signalling, as opposed to endocrine signalling, which can travel vast distances via the vascular system. There is also juxtacrine signalling that occurs between two cells in very close contact, where their surface receptors interact directly.

There is great variation in the receptor profiles found on the extracellular cell surface of glial/neuronal cells and this receptor line up is dictated by the role of that cell in the tissue. The signalling cascade cannot be initiated without the binding of a ligand to its appropriate receptor. In the case of certain specific pathways, such as the fibroblast growth factor (FGF) family, the signalling cascade cannot be initiated without a sulphated extracellular co-factor (Turner and Grose 2010). Biochemical studies have demonstrated that certain members of the heparan sulphate (HS) class of glycosaminoglycans (GAG) are necessary for FGF to bind and dimerise its receptor (Turnbull et al. 2001). The sulphation of these HSs play a role in strengthening the ligand-receptor binding. In some cases, signalling ligands which require sulphated co-factors also require a concentration gradient of the ligand to initiate the signalling cascade (Jullien and Gurdon 2005). The diffuse positioning and binding strengths of these HS molecules on the cell surface or in the ECM form this concentration gradient and are highly controlled to fine tune cell signalling pathways (Yan and Lin 2009).

1.5.1 Injury and changes in sulphation

The ECM is a supportive network of molecules which can mediate cellular interactions (Bowers et al. 2010). The ECM is a fundamental component of any cellular network as it is crucial in maintaining homeostasis. The ECM in the CNS also plays a role in the mediation of neuronal firing. A major class of molecules dominant in the ECM are the proteoglycans (PG) and their bound sulphated GAG. These are major regulators of the cellular interactions which occur in the ECM and are major factors in the injury environment.

Once the ECM and the sulphated cell surface GAG become disrupted following trauma, they induce sustained dysregulation of the surrounding cellular populations, exacerbating the injury. This makes the ECM and associated GAGs an attractive target for therapeutic intervention, as ameliorating their detrimental effects on injury might limit the pathology of SCI.

1.5.1.1 GAGs and PGs

Sulphated GAGs have a negative charge, which then can interact with a diverse set of proteins, and are involved in many biochemical processes. PGs are a family of proteins, all of which contain a core protein where one or more covalently attached GAG chains are bound (Sarrazin et al. 2011). GAGs bound to the PG consist of a linear polysaccharide backbone, which are made from repeating units of amino sugars specifically, N-acetylglucosamine (N), N-substituted glucosamine (GlcNS) or N-acetyl-galactosamine (GalNAc) and uronic acid specifically, glucuronic acid (GlcA) or iduronic acid (IdoA). The major functions of the GAG-PG are largely determined by the GAG side chain, as these dominate the chemical nature of the structure dictating their interactions at the biochemical level. GAGs are extremely important in the CNS and are characterised based on their disaccharide backbone. The major groups are; chondroitin sulphate (CS), heparan sulphate (HS), dermatan sulphate (DS), keratan sulphate (KS) and hyaluronic acid (HA) (Cui et al. 2013). The sulphation state of these molecules provides a specific charged structure and is key to their binding properties, with each CS, HS, DS and KS all having various sulphation state, with HA being the only sulphate null GAG (Small et al. 1996).

HS and CS are the two major abundant GAGs present as PGs throughout the CNS (Swarup et al. 2013) commonly referred to as HSPG and CSPG. HS is composed of mainly GlcA with some IdoA and has on average one sulphate group per disaccharide unit (Castillo et al. 1998), which is far less sulphated moieties compared to its isomer Heparin which

contains 2.7 sulphate groups per disaccharide unit (Lindahl et al. 1998). CS is composed of GalNAc which is attached to GlcA and IdoA via a glyosidic bond. The sulphation state of CS can vary with multiple positions in which the disaccharide can be sulphated, such as at 4- and 6- position of the GalNAc and 2- position on GlcA with combinations of these creating sub types of the CS (Silbert and Sugumaran 2002).

Changes in the sulphation state of the GAGs are both cell type and growth condition specific. Alterations to the cell environment such as trauma, cause a change in the orientation, pattern and level of sulphate moieties present on the GAGs (Swarup et al. 2013). This change in microenvironment also leads to a change in the presence/level of the proteoglycans which in turn alters the availability of the GAGs which are to be sulphated (McKeon et al. 1995).

1.5.1.2 GAG Sulphation

Sulphation of the GAGs occurs in the Golgi apparatus, with a sequential enzymatic process, which adds sulphate moieties to the sugar backbone in a non-template process (Silbert and Sugumaran 2002). There are two forms of sulfotransferase (ST) both catalysing the transfer of a sulfuryl group (SO_3) from the doner molecule to the GAG chain (Bishop et al. 2007). Cytosolic ST sulfonate intracellular molecules such as hormones and tends to be more promiscuous in their targeting, whilst membrane-associated ST sulfonate large extracellular molecules such as carbohydrates and tends to be more specific in its targeting (Chapman et al. 2004).

Studies have identified large numbers of ligands which interact with HS but relatively few are known for CS, KS and DS, suggesting alternative roles for sulphation of the GAG than just ligand interaction (Tumova et al. 2000).

A factor which may also determine the greater ligand binding capabilities of HS and Heparin over their fellow GAG members could be related to the conformational and sequence composition of the sugar residues in their backbone (Coombe and Kett 2005; Fuerer et al. 2010; Turnbull et al. 2001; Xu and Dai 2010). HS and Heparin have high sequence heterogeneity and contain highly modifiable domains in their oligosaccharide structure (Turnbull et al. 2001; Xu and Dai 2010). Following the initial binding of a ligand, there is a conformational change in the sugar residue position to enhance binding, which does not occur in CS, KS and DS. This suggests that there may be more to the GAG binding than the sulphation level of the saccharide unit, that the flexibility and conformation in the sugar residues play a huge role in ligand interaction. Therefore,

studying sulphation in isolation may not provide a complete picture of the whole process.

1.5.1.3 CSPGs and HSPGs in CNS homeostasis and injury

As mentioned earlier, CSPG and HSPG are the two most abundant proteoglycans present in the ECM of the CNS (Swarup et al. 2013). CSPGs have crucial roles in the developing CNS. They are highly expressed in the embryonic nervous system and brain. They function by providing guidance cues for neurite outgrowth (Masuda et al. 2004). CSPGs also negotiate cellular migration and certain classes of CSPG have been shown to aid proliferation of neural crest cells in the developing brain (Kubota et al. 1999). Moreover, in the mature CNS, CSPGs have been shown to be present at high concentrations in the perineuronal nets that occur around the soma and proximal dendrites aiding in synapses stabilisation (Miao et al. 2014). The HSPGs are known to provide co-factor binding and signal stabilisation for a number of signalling complexes, importantly, the growth factors required for proliferation, differentiation and migration in the CNS (Bernfield et al. 1999). HSPGs are thought to lead to active growth responses in axons (Johnson et al. 2004).

The field of SCI repair is littered with research focusing on the CSPG involvement in injury mechanism, rather than the HSPG aspect. CSPGs have been considered as the primary inhibitors of CNS axonal outgrowth and regeneration. CSPGs are highly expressed within the glial scar (Buss et al. 2009). Chondroitinase ABC is a potent CSPG degrading enzyme showing promise in initiating axonal outgrowth and functional recovery following SCI (Bradbury et al. 2002). It is thought that the CSPG are the yin to the HSPG yang in axonal growth and guidance (Laabs et al. 2005). There is little evidence, however, which clearly shows the HSPGs role during the injury response and their role in the chronic phase following the insult (Jones et al. 2003). The role of HSPGs in development suggests that HS-mediated signalling could possibility be a factor in CNS repair and regeneration.

1.5.2 Signalling disruption and SCI pathology

Cell signalling and communication come in many different molecular forms and there are a wide variety of signal transmitters ranging from simple gases to complex proteins. The signalling range varies with certain signals transmitting over long distances such as between organs systems, while others act locally, such as on neighbouring cells. Certain signalling cascades are initiated through the release of ligands from neighbouring cells but also from the ECM.

The ECM houses many ligand depots (binding sites), which can modulate many signalling cascades. Therefore, ECM remodelling enzymes can have profound effects on signalling cascade activation. Heparanase is the only endo-glucuronidase found in mammals (Vlodavsky et al. 2007). The enzyme breaks down HS specifically, but also other Heparin-like structures bound to the cell surface or present in the ECM (Zhang et al. 2015). Therefore, heparanase is a major ECM remodelling factor, liberating any tethered growth factors, immune related factors and enzymes bound to the ECM, freeing these to exert their effects on surrounding cells. In addition to releasing bound factors, the small HS fragments are able to further interact with additional ligands and mediate their activity (Escobar Galvis et al. 2007). Heparanase has been implicated in multiple pathologies, including an increased expression by migrating astrocytes in cerebral ischemia and even following SCI (Li et al. 2012a) (Zhang et al. 2006).

The vastly complex molecular signalling mechanisms involved following trauma and progression of the pathological state in the CNS remain largely unknown. Many signalling pathways have been investigated and are dysregulated after SCI (Fancy et al. 2009) (Chen et al. 2005). Following a traumatic event, certain signalling cascades can alter the phenotype of a cell. Cellular priming is defined as a state in which an agonist alters the phenotype of the affected cell (Friese et al. 1994). Cellular priming can be beneficial, in that the altered phenotype attempts to alleviate further spread of the injury, as seen with reactive astrocytes following SCI. However, cellular priming can also be detrimental, leading to a chronic negative state after injury, as seen with activated immune cells present at the site of injury which sustain a pro-inflammatory state, leading to further damage to the surrounding spinal cord cells (Fitch and Silver 2008).

Many signalling cascades are activated and deactivated during SCI (Abe and Cavalli 2008). Injury can lead to altered secretion of certain ligands and alterations to the expression of certain cell surface receptors.

1.6 *In Vitro* models of CNS injury and regeneration

The complex nature of SCI creates many challenges in the pursuit of identifying potential therapies. Many models have been developed with the aim of providing a platform to study SCI and the regeneration processes. The history of SCI modelling dates back to 1911, with the first documented *in vivo* experiments using weight-drop techniques on dog spinal cord (Allen 1911). *In vivo* models have been employed to study the primary and secondary events of injury and therapeutic potential of novel compounds. However, due to the complexity of the *in vivo* system and the restricted

follow up studies due to ethical consideration, this results in investigations of the basic underlying mechanisms of any biological process being extremely difficult. To this end, *in vitro* models have been developed to simplify the investigation of complex CNS mechanisms. Using both *in vivo* and *in vitro* models in parallel create a more complete approach to understanding SCI and regeneration.

In vitro models offer a more controlled study of the cellular and molecular aspect of the injury and regenerative process compared to *in vivo* models. The most common animal species employed in SCI research are rodents specifically; rats, mice, gerbils and hamsters (Kundi et al. 2013). Rat models are most frequently used as they are inexpensive, relatively easy to care for and can be maintained in large numbers. The spinal injury response of a rat has been likened to that of humans, specifically the occurrence of a fluid filled cyst at the site of injury (Lee and Lee 2013). Mice have been employed ever increasingly for SCI modelling due to large transgenic libraries available. However, their relative small size limits their use for *in vivo* studies. Also, the injury site begins to shrink over time and there is no fluid filled cyst at the injury site (Inman et al. 2002). However, mouse models offer more in terms of genetic studies and genetic manipulation. The use of transgenic mice species has provided valuable understanding of cellular and molecular aspect of SCI (Lee and Lee 2013). For example a study generated transgenic mice expressing multiple fluorescent proteins within neuronal populations, allowing detailed imaging of these multiple neuronal populations (Feng et al. 2000). *In vitro* mouse models allow the use of transgenic tissue samples and can be harvested so that specific interactions can be investigated in great detail.

1.6.1 Cell culture techniques

The major advantage with the use of *in vitro* models is the ability to monitor the progression of neuronal change following the introduction of compounds to injury, with the ability to assess these responses in real time. Cell culture techniques can be considered complex or simple. A complex cell culture contains multiple different cell populations interacting in one dish/well, in contrast to simple cell culture which is the study of a single cell type or population, or even a single cell in isolation.

The study of SCI through cell culture has generated many *in vitro* models, using a range of different tissue sources. Cell culture can also utilise a range of different source material from invertebrate system to rodent models. However, cell culture can utilise immortalised cell lines (specifically human cell lines) for the study of specific parts of SCI pathology including axonal regeneration. Human cell lines allow for a more

translatable model for study of effectiveness of drugs and high-through put screening for CNS repair and regeneration.

Simple *in vitro* models utilise cell lines such as PC12, an pheochromocytoma cell (Greene and Tischler 1976). Models have been used with particular focus on neurite outgrowth, with studies highlighting the effects of nerve growth factor (NGF) and its mechanisms on outgrowth. These studies demonstrated multiple potential mechanisms for NGF activity (Kumar et al. 2012) (Wang et al. 2011). Cell lines are often employed as a high-through put screening tool, and are used in complex *in vitro* models for more detailed studies (Allen et al. 2005).

Using the complex culture models usually involves the incorporation of multiple cell types. Complex primary cell cultures can be used to study specific differentiated cellular functions, such as the more complex biological process myelination (Thomson et al. 2008).

Previously in the Barnett lab, a complex culture system has been set up that is termed myelinating cultures. These cultures were devised by C Thomson & A Sørensen (Thomson et al. 2008) (Sorensen et al. 2008b). This culture method is a complex system which uses a monolayer of neurosphere-derived astrocytes on top of which a mixed embryonic spinal cord cell population is seeded. These cultures were modified to represent SCI by making a cut across layers of cells using a flat edge scalpel and shown to recount many of the features of SCI *in vivo* (Boomkamp et al. 2012).

This culture has been used to study the formation of myelin, and the mechanisms involved from the perspectives of different cell types. For example, this culture method has highlighted the role of astrocytes in the myelination process, displaying a dual function of these cells, showing that the phenotypic state, whether quiescent or activated determines levels of myelination and this relates to factors the astrocytes release (Nash et al. 2011a; Nash et al. 2011b). Moreover, using these cultures, FGF-9 has been implicated as an astrocytic factor which inhibits myelination through the induction of a pro-inflammatory environment as well as inhibiting OPC maturation, resulting in a failure of re-myelination (Lindner et al. 2015). In addition, this culture method demonstrated that OECs and not SCs promote axonal myelination *in vitro* (Lamond and Barnett 2013).

The development of this culture system into one where injury mechanisms can be studied, was established in the Barnett lab (Boomkamp et al. 2012). Here, the mechanically induced injury (using flat edge scapel blade) in the myelinating culture

has many characteristics of a SCI lesion with focal demyelination, loss of neurite density and lack of spontaneous neurite outgrowth. Furthermore, this study demonstrated that astrocytes appear reactive with altered morphologies. This new injury culture model has been used to demonstrate the therapeutic effect of combinatorial treatment with well-known SCI therapeutic compounds. It has been shown that Rho-ROCK inhibitors, C3 and the ROCK inhibitor Y23627 have a synergistic therapeutic effect, as opposed to either compound alone leading to both increased myelination and promotion of neurite outgrowth (Boomkamp et al. 2012). Rolipram was also studied in this culture system and evidence of its mechanisms of action was uncovered. Furthermore, Rolipram was shown to be an inhibitor of the high-affinity binding site of the cAMP degradation enzyme PDE4, and this effect was mediated through the activation of the EPAC pathway, not the commonly thought PKA pathway (Boomkamp et al. 2014). This study further demonstrated the merit of this culture system through the dissection of individual mechanistic pathways following drug treatment.

1.6.2 Limitations in current *in vitro* methodologies

Although *in vitro* cell culture models have provided great insight into SCI pathology and regeneration as detailed above, they are not without their limitations.

Primary cells are difficult to manipulate and often require specialist training and are very time-consuming. Furthermore, depending on the requirement, primary cells can be very sensitive to passage, which can lead to both altered phenotypes and senescence (Astashkina et al. 2012). Also, primary cells proliferate slowly and have temperamental metabolic capacities (Astashkina et al. 2012). However, primary cells are of more benefit in functional studies than cell lines. This is due to the fact that they can have differentiation properties which are rarely seen in immortalised cell lines, making primary cells more suited for toxicity studies (Ekwall 1980).

Another limitation from *in vitro* techniques is due to the abnormal cellular organisation as the cell is removed from its normal physiological architecture, which could alter many cellular processes. The intricate spatial cellular position within tissue is fundamental to its purpose as an organ (Greek and Menache 2013). Cells in culture are removed from their original structure and organisation, then artificially grow on a substrates unlike its original microenvironment (Bhatia and Ingber 2014).

Conventional cell culture methods have allowed for a deeper understanding of the mechanisms of injury and have identified key regulators in these processes. However, they lack the ability to precisely control the cellular microenvironment (Whitesides

2006). The feeding methodology for cultures are basically the standard 'bath' feeding where the cultures (whether that is cells on cover slips or tissue sections) are flooded with growth media. This growth media creates a molecular equilibrium where each individual cellular secretion becomes dispersed throughout the culture media. This does not reflect how factors are presented to cells in a normal physiological environment with concentration gradients being a feature of many tissue environments. So, to estimate the response of a cell in a mixed population creates problems as the *in vitro* environment is 'contaminated' with irregular cell communication and cross talk.

1.6.3 Advancements in *in vitro* techniques

New *In vitro* models of SCI have subsequently been developed with the goal of overcoming the limitations of current *in vitro* models, outlined above. Of particular interest are 3D cell culture and lab-on-chip device models.

1.6.3.1 3D cell culture model of SCI

A major caveat with *in vitro* models of SCI is the standard 2D platform in which cell culture takes places, whether that is a culture flask or a glass coverslip (Fawcett et al. 1989). This topography is unnatural and will affect the cultured cells in unknown ways causing the cells to act in a way unlike what is seen physiologically. There has been an increasing use of 3D culture platforms in CNS *in vitro* modelling. The aim of 3D cultures is to allow the cells to be in an environment which allows a more natural 3D conformation of the cell, and not to be deformed by a rigid 2D surface such as glass. As previously described, these 2D platforms are not an accurate representation of a normal cellular microenvironment (Fawcett et al. 1989).

A common approach to 3D-like cultures is through the use of basement membrane matrices enabling the study of proliferative abilities of differentiated neurons (Ajioka et al. 2011), a line of study not possible using standard 2D techniques. 3D micropillars have been employed to study the ensheathment by OLs, allowing a high-throughput compound screen to be carried out, with focus on concentric wrapping of the OL being the parameter measured (Mei et al. 2014).

1.6.3.2 Lab-on-chip devices

Lab-on-chip is the broad term for small scale investigations using miniaturised compartmentalised cell culture devices. The dimension and precise design of these devices allow for the manipulation of the fluidic microenvironment to provide a more

accurate representation of the fluidic physiological environment (Andersson and van den Berg 2003).

Lab-on-chip technologies have been used successfully in other areas of research, specifically the study of HIV. Engineers at the University of New Jersey have identified a method of HIV testing through the development of a lab-on-chip device which uses miniscule quantities of expensive chemical assay compounds for identification of the virus, potentially reducing the cost of this expensive test (Ghodbane et al. 2015). Similarly, this technology could benefit many laboratories in that expensive reagents or potential treatments can be used in extremely small quantities.

The study of axonal injury and regeneration has been advanced in recent years due to the advent of the lab-on-chip devices. These devices provide a unique resolution to the study of axon specific mechanisms (Taylor et al. 2005). Lab-on-chip devices allow the researcher to design highly specific compartmentalisation devices in which to study multiple cellular populations interacting or in isolation (Tharin et al. 2012) (Wang and Lu 2008). Additionally, they have the ability to manipulate cellular microenvironments, through the control of hydrostatic pressure therefore, creating a far more powerful technique than standard *in vitro* methods. Many early lab-on-chip devices overcame some limitations created by standard *in vitro* techniques such as the lack of fluidic control and the inability to study cells entrapped in 3D constructs. However, in the pursuit of a more representative *in vitro* model of the *in vivo* cellular environment an even more advanced version of the lab-on-chip has been developed known as organ-on-chip (Bhatia and Ingber 2014).

Organ-on-chip is a microfluid device which is aimed at artificially interconnecting the different tissue levels found in specific organs. Multiple organs have been studied in this fashion including heart, liver and bone (Grosberg et al. 2011; Lee et al. 2007; Zhang et al. 2011). Even the different cellular populations found in the spinal cord and BBB can be cultured in a multi-chambered device with interconnected microchannels where the fluid microenvironment can be manipulated to try to recapitulate the interactions *in vivo* (Booth and Kim 2012) (Achyuta et al. 2013). Theoretically, a multi-chambered device could be devised to have several interconnected cell seeding platforms containing peripheral dorsal root cells connected to endothelial cells found in the BBB to spinal cord cells, mimicking the PNS/CNS divide or dorsal root entry zone. This would allow for the investigation of therapeutics at an almost systemic level. The possibilities are many with the only limiting factor being the innovation of the researcher. Organ-on-chip devices are a potentially extremely powerful tool in the study of cellular interactions at organ level.

1.7 Conclusion

It is clear that the pathology of SCI is complex. It seems we have only scratched the surface of understanding spinal cord trauma and are very much in the dark concerning repair and regeneration. The primary and secondary injury cascades have been somewhat characterised and research has demonstrated how these lead to the formation of the glial scar. The glial scar has been at the centre of therapeutic intervention strategies with multiple therapies attempting to overcome the inhibitory environment of the glial scar. However, looking at the glial scar as being solely detrimental to repair is inaccurate, with studies highlighting the advantages of the glial scar in limiting the spread of damage. Other strategies for SCI regeneration have focused on many aspects of the injury such as the promotion of axonal outgrowth, modulation of the immune response, creation of bioscaffolds and cellular transplantation. However, few studies have focused on the sulphation state and the role of HS-mediated cell signalling during injury, which could identify HS as a target for therapeutic intervention for SCI. SCI research relies heavily on *in vitro* cell culture models of the pathology but current systems fail to completely mimic the injury process. However, novel *in vitro* technologies such as microfluid devices are being devised which may better encapsulate SCI processes and provide a greater knowledge in the pursuit of fully understanding SCI pathology and regeneration.

1.8 Aims

The overall aim of my thesis was to identify novel compounds for the treatment of SCI using a well-established neural cell co-culture model of SCI (SCI model). This was carried out by the following:

1) Using the existing SCI model to carry out a medium-through put screen of novel therapeutic compounds identified for other applications. Following this, I aimed to identify the potential mechanisms of action for potential effective compounds.

2) Developing a novel *in vitro* model of SCI where the cells are compartmentalised, ultimately allowing therapeutic molecules to be applied to specific groups of cells in isolation. This was carried out by the modification of the well-established SCI model in combination with a microfluidic device, where the cell bodies are separated from other cellular compartments e.g. the axonal compartment, so that drugs or cells could be directly applied to either the neuronal cell bodies or to the axonal compartment.

Chapter 2
Materials and Methods

2 Materials and Methods

2.2 Neurosphere and astrocyte culture

Neurospheres (NS) were generated by harvesting of the striata from 1-day-old Sprague Dawley rat forebrains, modified from the method developed by (Reynolds and Weiss 1996). The tissue was triturated using a glass pasture pipette in L-15 media (Invitrogen, Paisley, Scotland). The newly homogenised tissue was centrifuged at 1200 revolutions per minute (rpm) for 3 mins. The supernatant was removed and the pellet resuspended in 20 ml neurosphere media (NSM) containing Dulbecco's Modified Eagle Medium/F12 (DMEM/F12, 1:1, DMEM containing 4,500 mg/L glucose), enriched with 0.105% $NaHCO_3$, L-glutamine, 5,000 IU/mL penicillin, 5 µg/mL streptomycin, 5.0 mM HEPES (all from Invitrogen, Paisley, Scotland), 100 µg/mL apotransferrin, 25 µg/mL insulin, 60 µM putrescine, 20 µM progesterone, and 30 µM sodium selenite, supplemented with 20 ng/ml of Epidermal growth factor (EGF) (Peprotech,UK). The cell suspension was transferred to an uncoated $T75^3$ vented flask (Greiner, Stonehouse, UK) and incubated at 37ºC in an atmosphere of 7% CO_2/93% air. The culture was fed every 2-3 days with an addition of 5 ml NSM and 4 µl EGF(20 ng/ml). Following 5-7 days in culture (when cellular spheres are visible), the suspension was triturated using a glass pasture pipette to produce a smaller cell sphere suspension. The cells were centrifuged at 1200 rpm for 3 mins. Removing the supernatant and adding 10% foetal bovine serum with 2 nM l-glutamine the cells were triturated for a final time. The suspension was transferred to 13 mm poly-$_L$-lysine (PLL) coated coverslips in a 24-well plate, where they were incubated for a further 5-7 days at 37ºC in an atmosphere of 7% CO_2/93% air, until a confluent monolayer of cells was present.

2.3 Myelinating spinal cord culture

The protocol for generating the myelinating co-culture was based on, with some alterations, the model previously developed (Sorensen et al. 2008a). The pregnant female was culled using CO_2 overdose followed by removal of uterus containing embryos via cervical dislocation. The embryos were removed from the amniotic sac and transferred to a dish containing L-15 media (Invitrogen, Paisley, Scotland) and the cranial section (5-6 mm) of the spinal cord was dissected. The cords were then transferred to a fresh dish containing L-15 media, the meninges were stripped and the exposed cord placed on ice in a vial containing 1 ml L-15 media. Four-six cords were placed per 1 ml vial per cell preparation. The cords were mechanically disassociated by trituration using glass pasture pipette, then enzymatically by incubation with trypsin

(100 µl of 2.5%, Invitrogen) and collagenase (100 µl of 1.33%, ICN Pharmaceuticals, Basingstoke, UK), for 15 min. The enzyme activity was stopped by adding 1 ml of a solution containing 0.52 mg/ml soybean trypsin inhibitor, 3.0 µg/ml bovine serum albumin and 0.04 mg/ml DNase (SD, Sigma). The cell suspension was triturated to ensure complete enzymatic activity was stopped, and then centrifuged for 5 mins at 800 rpm. The pellet was re-suspended in 2 ml plating media (PM) containing 50% DMEM, 25% horse serum, 25% Hanks balanced salt solution (HBSS) with Ca^2+ and Mg^2+, and 2 mM L-glutamine (Invitrogen). The astrocyte monolayer coverslips were removed from the 24-well plates and transferred to a sterile 35 mm Petri dish prior to spinal cord mix being added. The disassociated spinal cord cells used for standard myelinating culture were plated onto coverslips supporting the astrocyte monolayer at 300,000 cells per 50 µl. The cells were left to adhere for 2 hours at 37ºC then supplemented with 300 µl PM and 500 µl differentiation medium which contained; DMEM (4,500 mg/mL glucose), 10 ng/mL biotin, 0.5% hormone mixture (1 mg/mL apotransferrin, 20 mM putrescine, 4 mM progesterone, 6 mM selenium (formulation based on N2 mix of (Bottenstein and Sato, 1979) 50 nM hydrocortisone), and with or without the addition of 0.5 mg/mL insulin known as DM+ (insulin positive) or DM- (insulin negative) (all reagents from Sigma). Each culture dish containing the myelinating culture was fed 3 times a week by removing 400 µl and adding 500 µl fresh DM+ for the first 12 days, then DM- for the proceeding 12+ days. Cultures were sustained for 24+ days in an atmosphere of 7% CO_2, 93% air, at 37ºC.

2.4 Injury induction

For injury experiments, 24 day old myelinating cultures were subjected to a lesion created by an 11 mm single edge razor blade (WPI, Aston, UK). The culture which was to be injured was first removed from the culture dish and placed on a sterile blue roll. Then, in a guillotine-like fashion, the blade was lowered to the surface of the coverslip and with little pressure, the lesion occurs before finally returning the coverslip back to the dish. Injured cultres were treated where appropriate, 1 day post injury (25 DIV). Treatment stratagies were either; 1 single treatment with two further recovery feeds (modified heparins) or 3 treatments administered over the course of a week (ROCK inhibitors).

2.5 Oligodendrocyte progenitor cell and microglia culture

Generation of Oligodendrocyte progenitor cell (OPC) and Microglia (MG) culture was performed by isolating the floating cell fraction of 7 day old cortical astrocyte cultures. The cortical-derived astrocytes were generated by dissecting the outer layers of the

cortex from postnatal day 1 (P1) Sprague Dawley rat pups, as previously described (Noble and Murray, 1984) with slight modifications. The tissue was placed in a vial containing L-15 media then triturated and incubated with collagenase (500 µl 1.33%) for 20 min at 37ºC. The reaction was stopped as described previously with SD, and centrifuged at 1200 rpm for 3 mins. The cellular pellet was re-suspended in 10% FBS DMEM and cultured for 5-7 days in a PLL-coated T75 vented flask before the floating fraction was collected. The culture was fed 3 times a week with removal of 4 ml and adding 5 ml 10% FBS. The OPCs and MG were detached following controlled agitation of flasks, followed swiftly by plated onto a 90 mm culture dishes for 15-20 min allowing separation of OPCs from MG (and other glia cells) due to differential adhesion. The OPCs remained in the supernatant, which was removed, centrifuged at 1200 rpm 5 mins, resuspended in Sato media (adapted from Bottenstein and Sato, 1979) containing 0.5 mg/ml insulin in 10 mM HCL (Sigma, UK), glutamine (100 mM; Sigma, UK, human transferrin (Sigma, UK) and gentamycin (100 mg/ml; Sigma, UK), supplemented with the growth factors; fibroblast growth factor (FGF-2) at 10 ng/ml and platelet derived growth factor (PDGF) at 2 ng/ml (both Peprotech, UK). The OPCs were cultured in the presence of the growth factors for 5 days, before incubation in Satos media alone +/- the required treatment for the duration of the experiment. Similarly, with the MG, the difference being cultured in 10% FBS containing DMEM high glucose 4.5 g/l for the entirety of the experiment, even at the stage of required treatment. The pure OPC and MG culture was then counted using a haemocytometer and seeded into a 24-well plates containing PLL-coated coverslips at a density of 5,000 cells in a volume of 50 µl at 37ºC for 15 mins to allow cells to attach. Then an additional 400 µl of Sato media or 10% FBS high glucose (MG) was added to each well. Both cultures were fed 3 times a week with the removal of 250 µl and the addition of 300 µl.

2.6 Microfluidic device preparation

The microfluidic device was fabricated in polydimethylsiloxane (PDMS) using soft lithography. A positive replica mould was produced using thin sheet silicon and two patterned layers of SU8 photoresist (3000 series, MicroChem, US). The first layer contained the positive relief patterns of the microchannels connecting the three chambers resulting in a thickness of 7 µm. The second layer contained the positive relief patterns for the cell reservoirs resulting in a final thickness of 9 µm. The positive silicon relief master (master) was then exposed to ultra vilot (UV) light and developed in a photomask (JD PhotoTools, UK) and MicroPosit EC solvent (Rohm and Haas, US). In addition the master was silanised by vapour deposition of 1*H*,1*H*,2*H*,2*H*-perfluoroctyl-trichlorosilane (Sigma Aldrich, UK) for 1 hour. The PDMS (Dow Corning) was cast onto the master with the PDMS at a base to curing agent ratio of 10:1 at 80ºC for 3 hours.

After curing the PDMS was peeled off the master cut to size (approx. 24 mm by 60 mm) and punched out the cell reservoir chambers with 6 mm diameter biopsy punch (Stiefel, UK). The newly formed device and coverslip (where the device is to be mounted) was sterilised in 70% ethanol for 90 seconds in a sonication bath. The device assembly was initiated by firstly exposing the two surfaces, the coverslips and PDMS device (micro-patterned size up) to plasma by placing them in an O_2 plasma machine, settings at 50% power and exposed for 6 seconds. The two surfaces are now coated in plasma and ready for bonding. Bonding was done by very carefully lifting the PDMS and inverting it so the patterned surface will meet the coverslip, then lowered the PDMS down and with slight pressure bonding occurred instantly. PLL coating of the devices was done by adding 100-200 µL per well. Coating needed to occur within 30 mins of O_2 plasma exposure whilst the PDMS was temporarily hydrophilic (so the PLL will coat the chambers and microchannels), left for 1.5 hours at 37ºC. PLL solution was washed from all wells with dH_2O, making sure not to allow the device to dry out. The devices were finally sterilised under UV for 45 mins.

2.7 Microfluidic device cell seeding

Prior to cell seeding, the cell reservoirs are washed with appropriate medium (astrocyte-10% FBS, neurons-DM$^-$ or OPC-enriched Satos medium). The devices were placed in individual Petri-dishes (9 cm diameter, two devices per dish). The surrounding area of the dish was flooded with 5-10 ml of medium (5x gentamycin concentration). Following the previously described astrocyte and spinal cord cell preparation (sections 2.1 and 2.2) with only slight modification. Neurospheres were cultured, and then differentiated into astrocytes using 10% FBS in a T75 culture flask prior to seeding into the device. Astrocytes were trypsinised centrifuged at 1200 rpm for 3 mins, then re-suspended in 1 ml of 10% FBS, and counted using a haemocytometer. Astrocytes were seeded at a concentration of $4*10^3$/µl per reservoir chamber. Before seeding the astrocytes the resident media in the devices was removed leaving some residue, so not to dry out the device and the cell suspension was pipetted into the inlet reservoir. The cell suspension flooded into the chamber and cells attached to the PLL surface, and were left for 1 hour to allow full adhesion before being filled with fresh culture medium, 200 µL per well. Cultures were incubate and fed as instructed previously (section 2.1) in an atmosphere of 7% CO_2 93% air at 37ºC. Seeding of disassociated spinal cords cells into the devices followed the same cell preparation method as descried previously (section 2.2), creating a final cell concentration of $1.5x10^5$ in each cell chamber

2.8 Nanofiber preparation

Polycaprolactone (PCL) electrospun nanofibers (Nanofiber Solutions, Ohio USA) were PLL treated the same as standard glass cover slips. Both aligned and random 700 nm diameter fibre 24-well culture inserts and 96-well culture plates were used for OPC/OL myelination experiments.

2.9 Western Blotting

The western blotting method, involving injured cultures required three lesions per coverslip. Cultures were lysed using lysis buffer (Millipore, Watford, UK) and the protein concentration calculated using the NanoDrop spectrophotometer (Thermo Scientific, USA). To harvest the cell lysates, 40 µl of CellLytic M Cell Lysis Reagent was added to each coverslip and incubate at room temperature (RT) for 10 mins, followed by scrapping of the cells with a 21G needle, and transfer of lysate to an eppendorf tube where the cells were triturated with the same 21G needle. Protein concentrations were calculated using Nanodrop (Protein A280, 1 Abs=1 mg/ml). Protein samples (10 µg protein per lane) were prepared per well in 6 µl of 43 Laemmli sample buffer and 2.4 µl NUPAGE reducing agent 103 (Invitrogen) at 80ºC for 10 mins. The samples were run on a NUPAGE NOVEX Tris-acetate gel (4–12%; Invitrogen) at 200 volts for 45 mins. The gel was then transferred to a PVDF membrane using the iBlot Western Detection system (Invitrogen, Paisley, UK). The membrane was incubated in blocking buffer containing 5% skimmed milk powder and 0.2% Triton-X100 in PBS (PBS-T) overnight at 4ºC. The membranes were then incubated with primary antibody (Table 2.1) diluted in blocking buffer for 1 hour at RT on an orbital shaker. Following three wash steps for 5 mins each in PBS-T, the blots were incubated with the appropriate horse radish peroxidise-conjugated secondary antibodies for 1 hour at RT on a shaker. After three washes in 0.2% Triton-X100 and a final wash in PBS, the membranes were treated with ECL-plus (1:1, Amersham, GE Healthcare, UK), and exposed to film (Amersham). The intensities of the protein bands were determined using densitometer Gels tool on Image J software.

2.10 Immunohistochemistry

For cell surface antigen labelling, the cultures were incubated with primary antibodies (diluted in relevant media) for 20 mins at RT (Table 2.1). Cells were washed in PBS and incubated with the appropriate secondary Alexa fluorophore-conjugated antibody (diluted in relevant media) (Table 2.2) for 20 mins at RT. The cells were fixed in ice-cold methanol for 15 mins in the freezer. For co-labelling with intracellular antibodies,

cells were washed in PBS and incubated with primary antibodies, diluted in blocking buffer (containing PBS with 0.1% Triton X-100 and 0.2% porcine gelatine) for 45 mins at RT. The coverslips were washed with PBS and the appropriate secondary Alexa fluorophore-conjugated antibodies added for 45 mins at RT. The cells were washed in PBS followed by dH_2O and mounted in Vectashield (Vector Laboratories, Peterborough, UK) and sealed with nail varnish or HardMount. For intracellular labelling alone, the cultures were fixed in 4% paraformaldehyde for 20 mins at RT followed by washes in PBS and permeabilization in 0.2% Triton- X100 for 15 mins at RT. The cultures were washed 3 times in PBS. The primary antibodies were added, diluted in blocking buffer, and the cells incubated for 45 mins at RT. After 3 washes in PBS, the cultures were incubated with the appropriate secondary antibodies at RT for 45 mins. The cells were washed in PBS followed by dH_2O, mounted in Vectashield (Vector Laboratories, Peterborough, UK) and sealed with nail varnish or Hardmount.

Table 2-1 Primary Antibody List

Antigen	Raised in	Isotype	Dilution	Fixation method	Internal/ External	Source
AA3 (PLP)	Rat	IgG1	1:100	4% PFA	Internal	Hybridoma
SMI31	Mouse	IgG1	1:1500	4% PFA	Internal	Abcam
MBP	Rat	IgG2a	1:100	4% PFA	Internal	Abcam
A2B5	Mouse	IgM	1:1	Ice cold methanol	External	Hybridoma
04	Mouse	IgM	1:1	Ice cold methanol	External	Hybridoma
NG2	Rabbit	IgG	1:200	Ice cold methanol	External	Chemicon
GFAP	Rabbit	IgG1	1:1000	4% PFA	Internal	DAKO
Nestin	Mouse	IgG1	1:200	4% PFA	Internal	Abcam
BrdU	Mouse	IgG1	1:20	Ice cold methanol	Internal	DAKO

Table 2-2 Secondary Antibody List

Antibody	Conjugate	Dilution	Source
Goat anti-mouse IgG1	Alexa Flour: 555 and 488	1:600	Molecular Probes
Goat anti-mouse IgM	Alexa Flour: 555 and 488	1:600	Molecular Probes
Goat anti-rat IgG	Alexa Flour: 488	1:600	Molecular Probes
Goat anti-mouse IgG_{2a}	FITC	1:100	Southern Biotech
Goat anti-rabbit IgG	Alexa Flour: 488	1:600	Molecular Probes

2.11 BrdU immunohistochemistry

For the detection of proliferating cells Bromodeoxyuridine (5-bromo-2'-deoxyuridine), BrdU, was employed (BD Bioscience). BrdU is incorporated into newly synthesised DNA or replicating cells. During S-phase replication BrdU can also be delivered to daughter cells therefore, tagging any cell which are in a proliferative state. Using this technique in our culture system, BrdU (5 µg/ml) was added to the medium and left for 18-24 hours. The BrdU-treated cultures were washed in PBS, prior to fixing the cells in ice cold methanol for 10 mins at -20ºC. This was followed by mild permeableization in PBS-T and brief fixation in 0.02% PFA for 1 min at RT. The coverslips were washed and incubated in fresh 0.07 M NaOH diluted in PBS-T at RT for 10 mins. In addition to detection of proliferating cells via antibody detection of the incorporated BrdU co-staining can be performed, staining for any desired marker to confirm cell specific proliferation. Anti-BrdU (BrdU, mouse, 1:20) was added for 45 mins at RT. After another washing step, Goat anti-mouse (Alexa 488, 1:500) was added for 30 mins at RT. The coverslips were the mounted in Vectashield with DAPI (Vector Laboratories, Peterborough, UK).

2.12 Microscopy and Image analysis

Cells were imaged using Olympus BX51 or LAS AF Leica DM4000 B fluorescence microscopes, a Zeiss LSM 510 confocal microscope or an Etaluma Lumascope 500 inverted fluorescent microscope. For quantitative analysis of injury; neurite density, myelination and neurite outgrowth, the entire lesion site was imaged adjacent (0–670 µm from the lesion edge) to the actual injury site with each condition being blinded to

the experimenter. Similarly, for the non-injury quantification of neurite density and myelination, each condition was blinded to the experimenter and standardised random sampling was performed. For cell counting analysis (OPC/OL, MG and astrocyte) 20x magnification was used with 10 images per coverslip and the cells of interest counted per field of view and divided by the total number of DAPI-positive cells. For neurite density, myelination and neurite outgrowth studies images were taken at 10x magnification with 20 images per coverslip (with each experimental sample contained technical triplicates).

2.13 Myelination quantification

Firstly neurite density was quantified using CellProfiler Image Analysis software (Broad Institute). The pixel value for SMI-31 immunoreactivity was measured by dividing that pixel threshold level by the total number of pixels. We refer to all SMI-31-positive processes as neurites and processes ensheathed by myelin as axons. To calculate the percentage of myelinated axons, immunoreactivity associated with PLP (AA3) positive myelin sheaths was also measured using CellProfiler Image Analysis software. A pipeline program which tracks the myelin sheaths over axons, and the percentage of myelin calculated using the area obtained for the highlighted myelin divided by the area. All experiments were carried out at least three times using technical duplicates. For intensity studies specific marker staining was calculated using ImageJ software by measuring the integrated density of the individual colour per image and normalizing the value to the number of DAPI-positive nuclei. Cell size was determined using ImageJ software and a sample of cells were taken per image and drawn around using a define region of interest size, then the area calculated by threshold intensity.

2.14 Neurite outgrowth and lesion size quantification

A neurite outgrowth was defined as a SMI-31 positive projection with enters and crosses the lesion site. Each image was subject to scoring of each neurite which crosses the lesion site, any areas which appear to be uninjured they are excluded from the analysis. The number of neurites per images was then averaged across the lesion and given as a number of neurite per field of view. Using the same images the length of the lesion was calculated using ImageJ software. Multiple points per images were measured and averaged across the entire lesion per condition.

2.15 Statistical analysis

Graphpad Prism software was used for data presentation and statistical testing. For simple comparison paired-students t-test was employed to determine statistical significance. For multiple condition comparisons One-way repeated measures ANOVA test was employed to data sets followed by Dunnett's multi-comparison test to calculate potential significant difference. Asterisks are used to represent significance less than *$p<0.05$, **$p<0.01$, **$p<0.001$ and inserted onto graphed data. All errors are depicted as standard errors of the mean (SEM).

Chapter 3
Neural co-culture model of SCI as a medium throughput screening tool for therapies in SCI repair

3 Introduction

The processes underpinning SCI and regeneration are complex and it is possible that there are many potential therapeutic targets. To test these compounds *in vivo* requires large numbers of animal cohorts which have ethical and practical problems. This has led to the development of *in vitro* throughput screening tools (Krishna et al. 2014), using primary animal tissue for the rapid assessment of therapeutic compounds for SCI regeneration.

A challenge in developing an *in vitro* screen to identify potential regenerative therapeutics is the complex neurobiology underlying CNS injury, as this is not completely understood and cannot be completely modelled by an *in vitro* system (Fawcett and Asher 1999). However, SCI involves several global processes that can be encapsulated *in vitro* including, but not limited to, focal demyelination from OL cell loss, OPC proliferation/differentiation, focal neurite density loss, neurite retraction and lack of outgrowth (Boomkamp et al. 2012).

Classically, compound screens involved the investigation of multiple compounds to one specific target or pathway. However, in this study we modified this approach by employing several compounds targeting different processes involved in SCI and repair in order to ascertain which processes were the most responsive to therapeutic intervention. The SCI model first described in (Boomkamp et al. 2012) can be employed for this purpose by providing a collection of experimental parameters; myelination, neurite density and neurite outgrowth. These parameters were examined following exposure of the culture to a set of 5, potentially therapeutic, compounds. These compounds were selected for this screen as they have shown therapeutic benefit even though not exclusively related to CNS injury. Table 3.1 provides a short description of the compounds that were used in the screen.

Table 3-1 Compounds screen candidates

Compound Name	Previous effects	Provided by	Published findings	Predicted cellular target
A specific ROCK inhibitor: SC336 SC76 SC96	Stem cell survival	Dr. J. Mountford	Under patent	Multiple cellular targets
Olfactory ensheathing cell conditioned media	Promotion of myelination	Current lab members	(Lamond and Barnett 2013)	OPCs and neurons
Modified Polysaccharides (chemically modified Heparin)	Reduction of Astrocytosis	Dr. J. Turnbull	(Higginson et al. 2012)	ECM/cell surface

3.1 Aims

The primary aim of this study was to identify novel compounds in CNS repair and regeneration. This was be carried out by screening a diverse set of compounds at a range of concentrations, using the SCI model.

3.2 Results

3.2.1 Novel ROCK inhibitors' role in CNS repair and regeneration

Rho-kinase (ROCK) is a serine/threonine kinase and a major downstream effector of the small GTPase Rho. Rho-GTPases are molecular switches which regulate signal transduction and 20 Rho-GTPases have been described. The ROCK pathway is involved in many cellular functions specifically controlling the actin cytoskeleton, microtubule dynamics and membrane transport, leading to regulation of cellular behaviour, proliferation, migration and morphology (Nobes and Hall 1999). The ROCK pathway is involved in the stabilisation of the actin cytoskeleton, through the inactivation of myosin light chain phosphatase, which leads to an accumulation of phosphomyosin, which in turn induces cytoskeletal reorganisation (Coleman et al. 2001). Most importantly, the inhibition of ROCK has been associated with functional recovery in SCI (Chan et al. 2005).

The diverse roles of Rho-ROCK within the cell and the plethora of dysregulations observed at the injury site suggest that this pathway may be implicated in the injury response with changes observed in both neurons and glia. In particular, it has been associated with increased proliferation states seen in astrocytes and OPCs (McTigue et al. 2001) (Bush et al. 1999), changes in cellular behaviour and migration as seen with microglia invasion and activation to phagocytic macrophages to the injury site (Carlson et al. 1998) (Rolls et al. 2008) and microtubule depolymerisation leading to neurite retraction and lack of neurite outgrowth.

It is well documented that there are three injury-related myelin-associated inhibitors of axonal outgrowth signalling through the Rho-ROCK molecular switch; Nogo, myelin-associated glycoprotein (MAG) and oligodendrocyte-myelin glycoprotein (OMgp) (Mimura et al. 2006). Each have different initial activation mechanisms (Filbin 2003) but converge on the activation of the ROCK response to actin/microtubule rearrangement and subsequent lack of neurite outgrowth. Previous studies have looked to the use of ROCK inhibitors for therapeutic use in SCI (Fournier et al. 2003) (Chan et al. 2005). However, our collaborators have provided three novel ROCK inhibitors (SC76, SC96 and SC336), each of which show a highly specific inhibition of the ROCK pathway (unpublished data) compared to that of Y27632. Thus, it has been hypothesised that these inhibitors would be more useful in SCI treatment as they are more specific inhibitors of the ROCK pathway. The ROCK inhibitors used in this screen were shown to have high specificity targeting only the ROCKII pathway identified using a kinase array. The results of this kinase array are currently in preparation for publication and the

compounds are currently undergoing the patenting process. Therefore, the specifics and actual results of the kinase array and the chemical composition cannot be divulged.

3.2.1.1 Result: ROCK inhibitor

The SCI-myelinating culture was established as described previously (Boomkamp et al. 2012). Briefly, the myelinating cultures were incubated until day 24 before then being injured using a flat edged scalpel blade. The injury created a focal decrease in neurite density and myelination levels adjacent to the lesion. The cultures were treated with the ROCK inhibitors at a range of concentrations as advised by Dr. J. Mountford – SC76: 30 nM and 45 nM, SC96: 15 nM, 30 nM and 45 nM and SC336: 25 nM, 50 nM and 75 nM, from day 25 to day 31. The cultures were then fixed at day 33 and stained for the myelin marker, PLP, and the neurofilament marker, SMI31. The cultures were imaged using an Axio fluorescent microscope at a 10x magnification, adjacent to the cut site as described in (Boomkamp et al. 2012) for the entire lesion length. Neurite density was calculated based on the SMI31 pixel intensity compared to the total pixels per image. Myelination was quantified by calculating the percentage PLP pixel staining overlying the SMI31 staining but only at a uniformed longitudinal structure with predetermined dimensions. Neurite outgrowth was analysed by scoring the neurites that were seen entering and crossing the lesion site. Images were taken by focusing on the lesion site with each neurite which entered and crossed the lesion classified as 'outgrowth'.

Untreated control cultures had neurite density and myelination scores of 35.3% and 5.8% respectively (Fig.3.1.G and H). Treatment of the injured cultures with inhibitor SC76, led to increased neurite density and myelination compared to untreated controls (Fig.3.1. G and H). Neurite outgrowth showed a promotion at 45 nM (Fig.3.2. D) with an average increase of 16 neurites per field of view.

Inhibitor SC96 promoted neurite density at 15 nM but a decrease was observed at 30 nM and 45 nM with density levels dropping below those of the control to 29.6% and 31.2% respectively (Fig.3.3.). An increase in myelination was observed at all concentrations of SC96 (Fig.3.3. I and J). No promotion of neurite outgrowth was observed with SC96, with neurite outgrowth not exceeding control levels (Fig.3.4.E).

The ROCK inhibitor SC336 did not have any observable positive effects on neurite outgrowth at any concentrations tested (Fig.3.6.E). Treatment with 50 nM appeared to cause an increase in neurite density (Fig.3.5.B and I), however, at the same concentration there is a marked decrease in myelin levels (Fig.3.5 G and J). Treatment with the 25 nM concentration had no apparent effect on either neurite density or

myelination with levels similar to that of control (see Fig.3.5.B,F and I-J). SC336 at 75 nM appears to promote myelination, however, no increase in neurite density was observed (Fig.3.5.I and J).

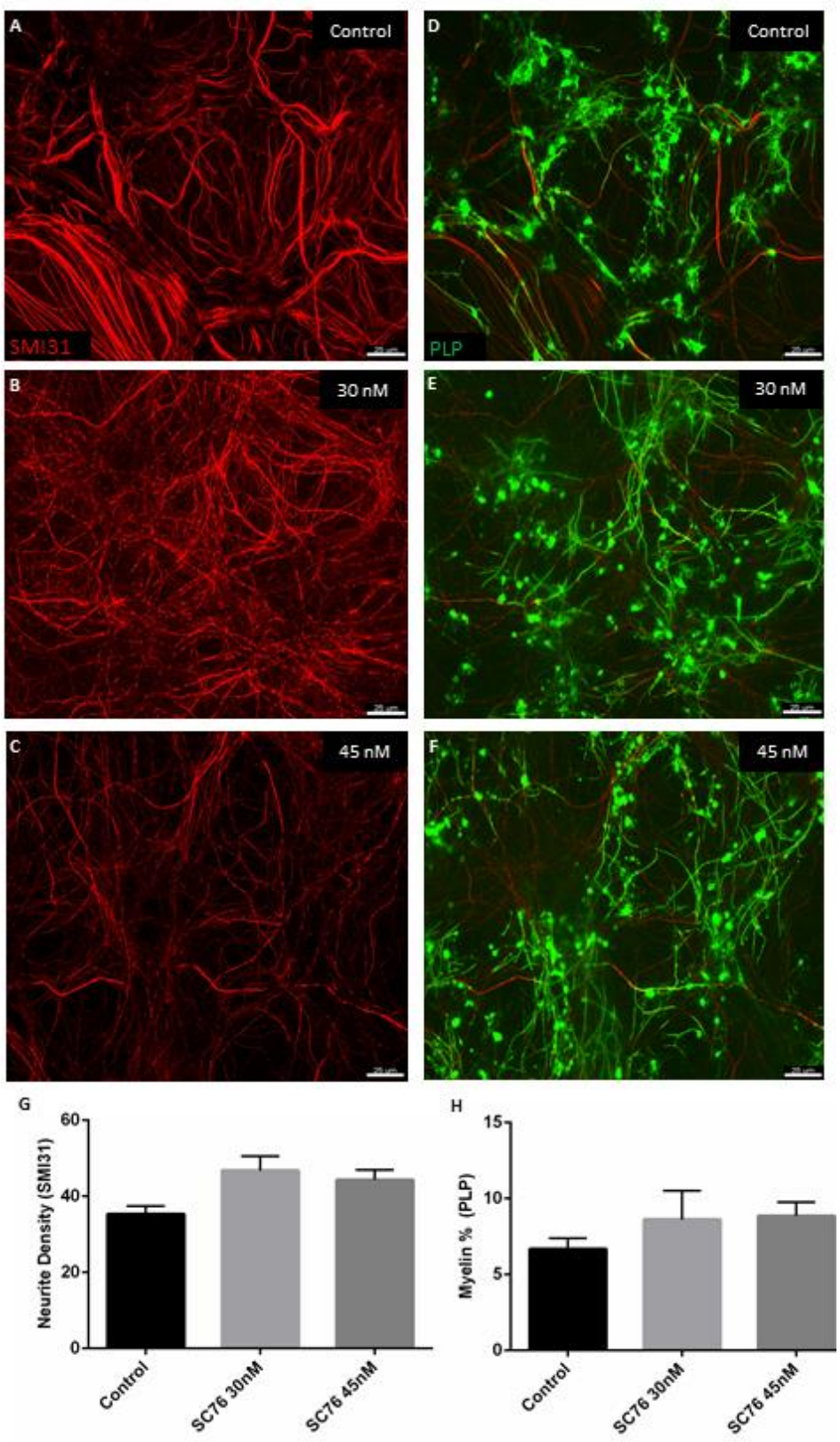

Figure 3.1 ROCK inhibitor SC76 promotes both neurite density and myelination following injury.

The myelinating cultures were injured after 24 DIV and treated with ROCK inhibitor for a further 5 days. The ROCK inhibitor was used at two concentrations 30 nM and 45 nM with both showing a trend towards promotion of neurite density (SMI31, Red) and myelination (PLP, green) relative to the untreated control (A and D). SC76 at a concentration of 30 nM (B and E) was more potent than 45 nM as the former had greater increase of neurite density and myelination adjacent to the lesion (G and H) (C and F). N=2 and error bars-SEM, scale bar-25 µm.

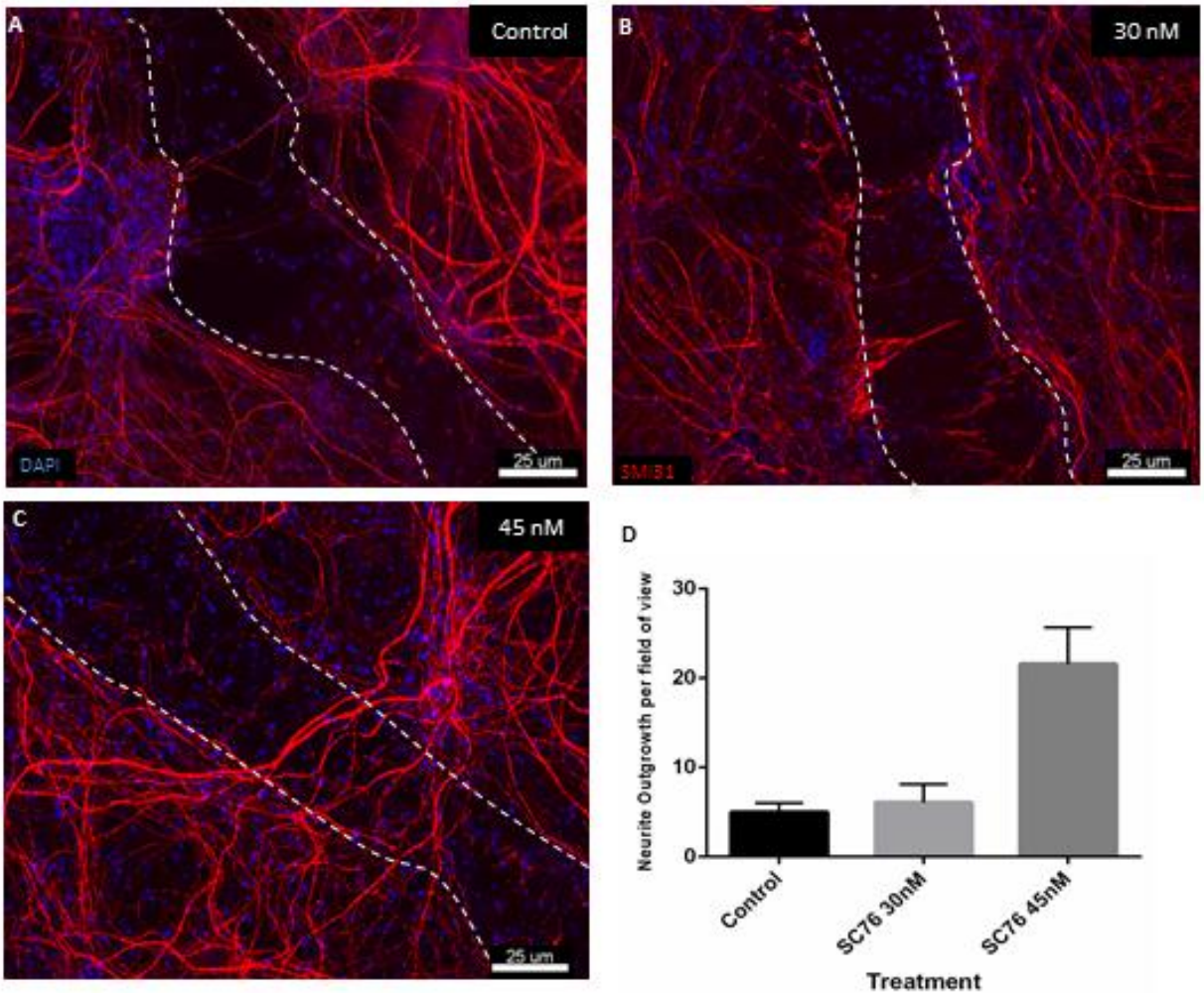

Figure 3.2 ROCK inhibitor SC76 promotes neurite outgrowth at 45 nM concentration.

Neurite extension was assessed by scoring the number of neurites which cross the lesion site, marked by dashed line and identified by a decrease in the nuclei density (DAPI, blue) seen down the entire cut area (A- control). SC76 at 45 nM (C and D) appears to promote neurite extension following a 5 day treatment course with neurite numbers above that of cut control. There was no recorded difference to the number of neurite (SMI31, red) which cross the lesion following the same treatment at 30 nM (B and D) when compared to control (A). N=2, error bars-SEM, scale bars-25 µm.

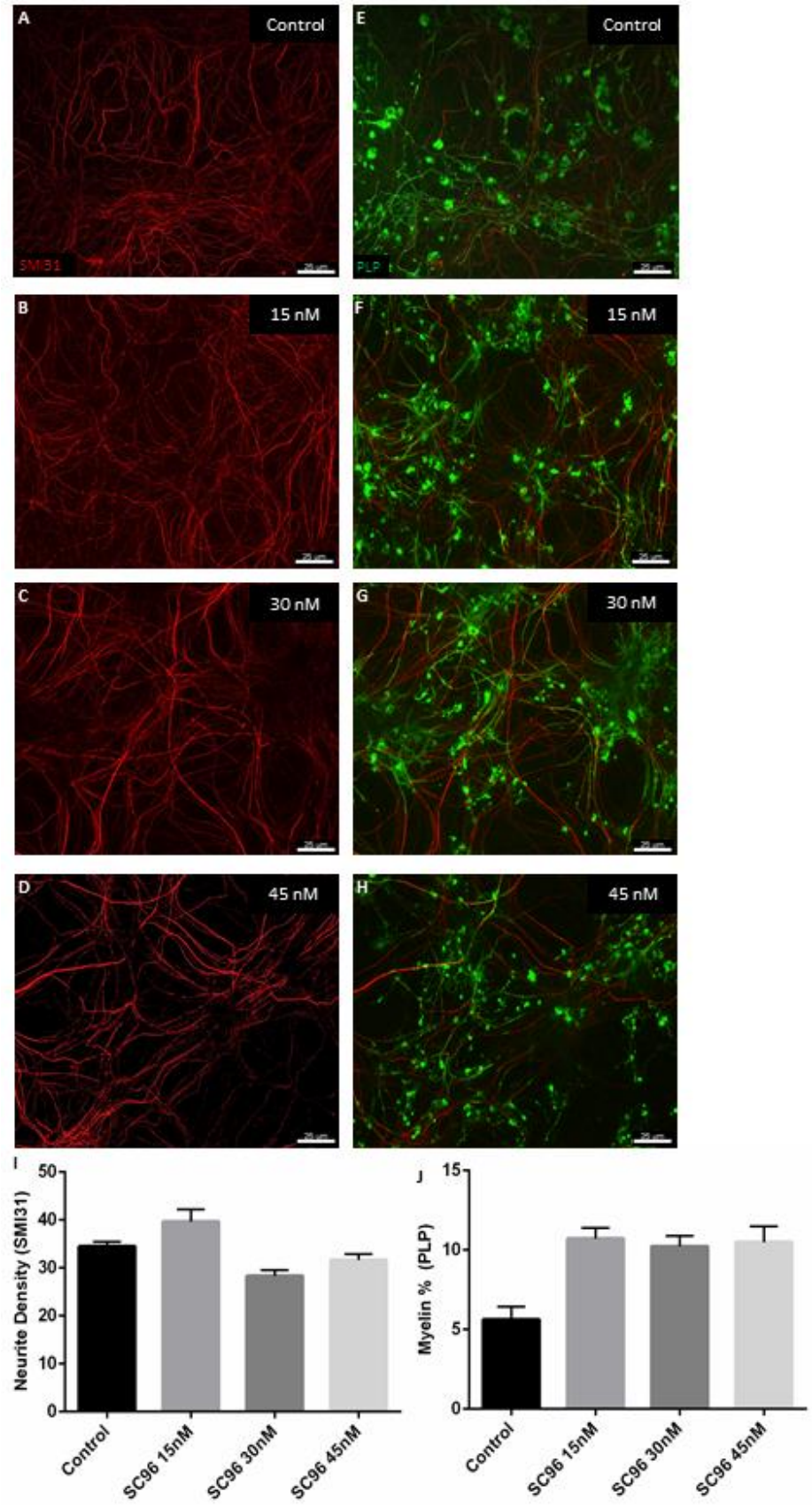

Figure 3.3 ROCK inhibitor SC96 elevates and myelination following injury.

Following a 5 day treatment with SC96 at a range of concentrations from 15 nM-45 nM, neurite density (SMI31, red) was promoted at 15 nM only (B-D and I). However myelination (PLP, green) was promoted at all concentrations (F-H and J). N=2, and error bars -SEM, scale bar-25 µm.

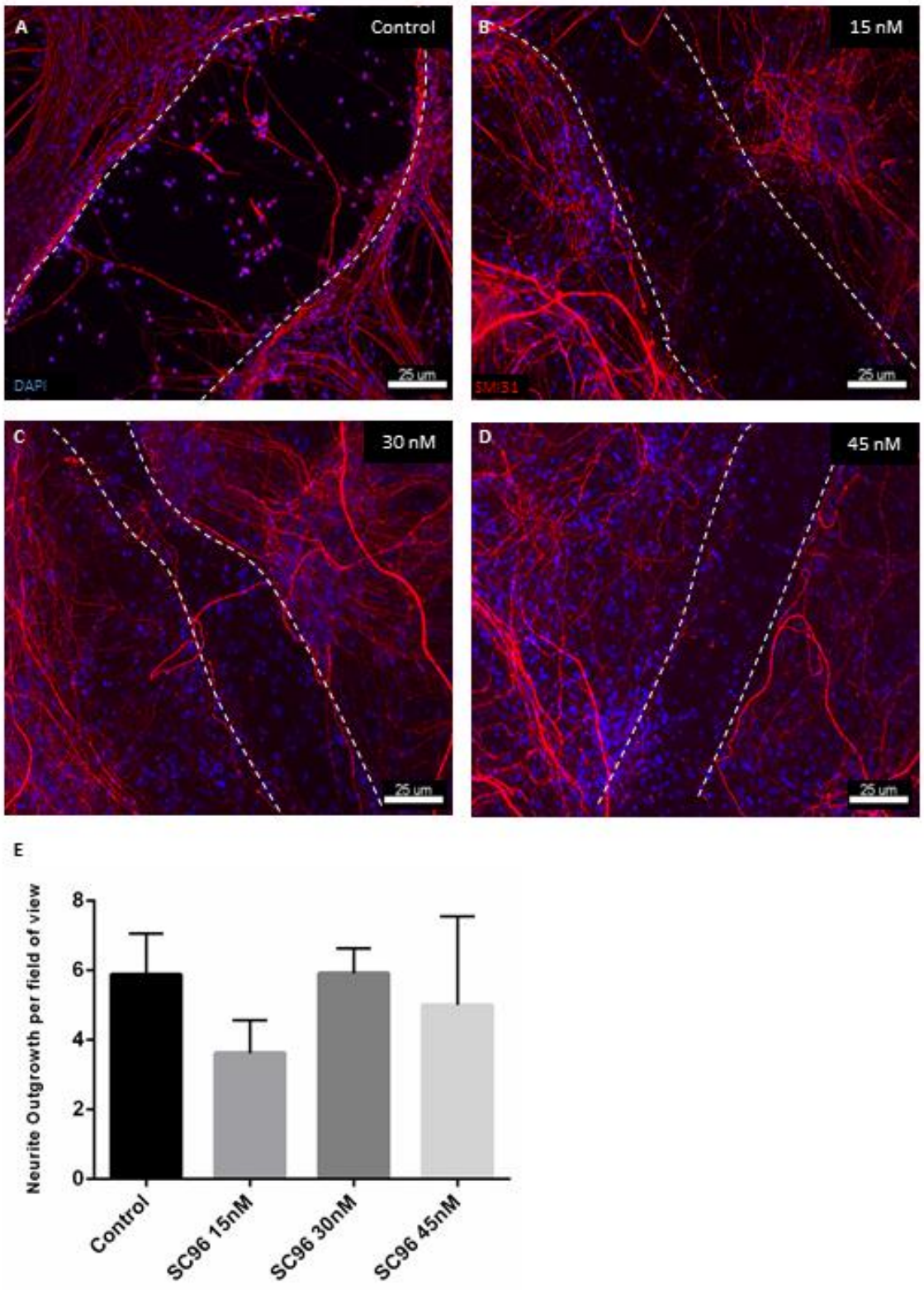

Figure 3.4 ROCK inhibitor SC96 does not promote neurite extension at any concentration

Treatment with SC96 at concentrations of 15 nM-45 nM did not have any effect on neurite outgrowth (B-D). The number of neurite scored crossing the lesion site did not surpass that of control (A and E). Lesion marked by dashed line and identified by a decrease in the nuclei density (DAPI, blue) seen down the entire cut area (A). N=2, and error bars -SEM, scale bar-25 µm.

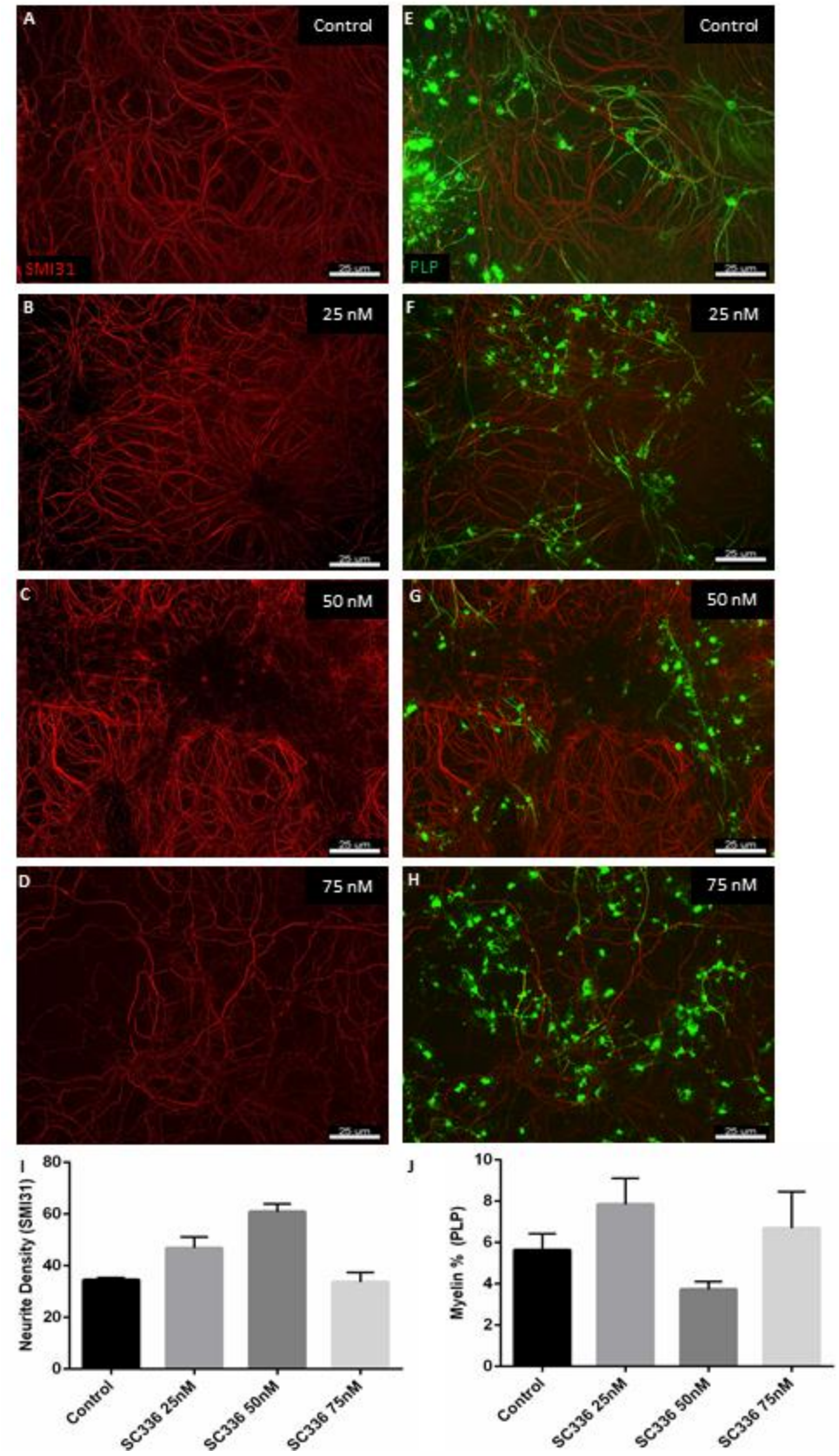

Figure 3.5 Inhibitor SC336 elevates both neurite density but myelination is unaffected.

The myelinating cultures were lesioned at 24DIV and treated with inhibitor SC336 for a further 5 days. The inhibitor was used at three concentrations 25, 50 and 75 nM, with only 50 nM having any effect. A potential promotion of neurite density (SMI31, Red) at 50 nM occurs (C, I) but myelination (PLP, green) was seen to decrease to levels below control (E, J). 25 nM and 75 nM (B and D, F and H) did not have an effect on either neurite density or myelination (I and J). N=2 and error bars-SEM, scale bar-25 µm.

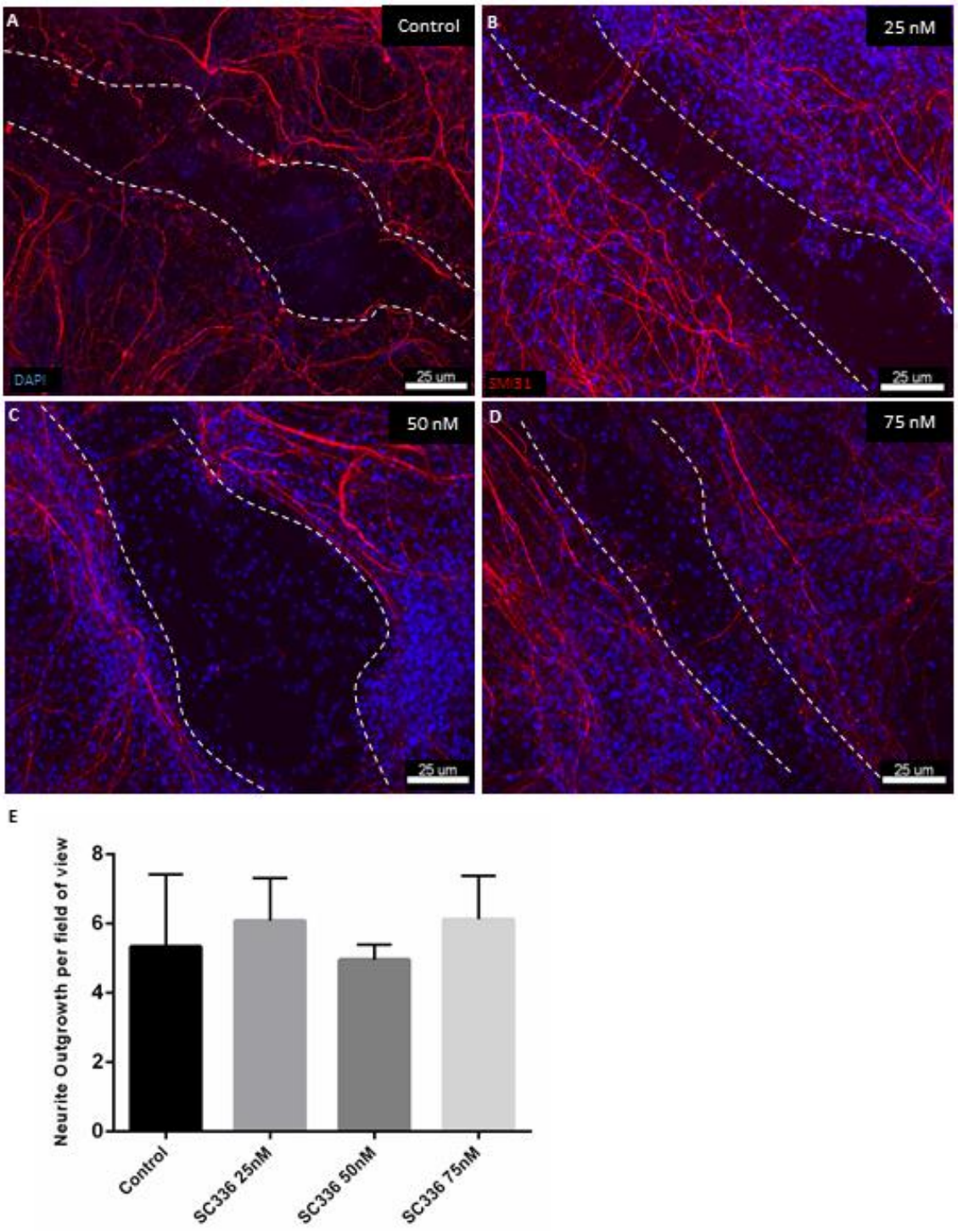

Figure 3.6 Inhibitor SC336 does not promote neurite extension after injury.

Following a 5 day treatment at no concentration used displayed any promotion in neurite extension (B-D, E), with number of neurites per field of view not surpassing control levels (A-D, E). Lesion site marked by dashed line (A) and a decrease in the nuclei density (DAPI, blue) observed down the entire area. N=2 and error bars, SEM, scale bar-25 µm.

3.2.2 Repair and regenerative properties of olfactory ensheathing cell conditioned media

Glial cell transplantation is a promising approach to SCI repair. Both *in vitro* and *in vivo* studies have outlined various modes of function for OECs in the repair process (Kocsis et al. 2009). OECs are a unique glial cell type which can myelinate axons of a small diameter and support the growth and regeneration of olfactory neurons (Fairless and Barnett 2005). Although OECs have been shown to have similar characteristics astrocytes and Schwann cells, they appear to have advantages over these cells for CNS repair (Barnett and Riddell 2004). OECs have been shown to provide trophic support to surrounding neurons through the secretion of; NGF, BDNF, GDNF, and FGF (Lipson et al. 2003). Interestingly, OECs have been shown to actively migrate to the injury site. A study demonstrating TNF-α was secreted by reactive astrocytes which could attract OECs to the site of injury (Su et al. 2009). Many studies discuss the beneficial interaction, in terms of CNS repair, of the OECs on the surrounding neuron and glial populations. For example, they can intermingle with astrocytes, downregulate GFAP (Lakatos et al. 2003) and do not induce astrocyte hypertrophy (Lakatos et al. 2000).

In this screen we treated injured myelinating cultures with OEC conditioned medium (OEC-CM) to investigate if the beneficial associated processes for repair reported in the formentioned study occur from an OEC secreted factor as opposed to direct cellular interaction. OEC-CM has been shown to be beneficial in the development of myelin in an *in vitro* model (Lamond and Barnett 2013). If a promotion in myelination, neurite density and outgrowth is observed following the treatment with OEC-CM, this would merit further investigation into the exact composition of the medium to identify components which may be driving the repair processes recorded.

3.2.2.1 Result: OEC-CM promotes both neurite outgrowth and myelination following injury

The SCI model was followed as described previously (Boomkamp et al. 2012). Briefly, the myelinating cultures were incubated until day 24 before then being injured using a flat edge scalpel blade. The injury created a focal decrease in neurite density and myelination levels adjacent to the lesion. The cultures were treated with OEC conditioned medium at 1:2 and 1:4 dilutions with standard DM- culture media (see Materials and Methods section 2.5), at day 25 until day 31, treating every other day. The cultures were then fixed at day 33 and stained for the myelin marker, PLP and neurofilament marker, SMI31. The cultures were imaged using an Axio fluorescent microscope at a 10x magnification, adjacent to the cut site as described in (Boomkamp et al. 2012) for the entire lesion length. Neurite density was calculated based on the

SMI31-red pixel intensity compared to the total pixels per image. Myelination was quantified by calculating the percentage PLP-green pixel staining overlying the SMI31-red staining only at a uniformed longitudinal structure with predetermined dimensions. Neurite outgrowth was analysed by scoring the neurites that were seen entering and crossing the lesion site. Images were taken by focusing on the lesion site with each neurite which entered and crossed the lesion classified as 'outgrowth'.

OEC-CM treated cultures following injury promoted both myelination and neurite density at both 1:4 and 1:2 relative to untreated controls. The ratio of 1:4 promoted myelination to a greater percentage over 1:2, with myelin levels reaching 11.3% and 6.45% respectively (see Fig.3.7 B, C and E, F). However, following treatment with OEC-CM at 1:2, the cultures had a slightly higher neurite density percentage adjacent to the lesion compared to 1:4, with density levels increasing to 44.9% and 41.4% respectively.

Following treatment with both dilutions of OEC-CM, there was a promotion of neurite outgrowth compared to controls (Fig.3.8. C,D) with 1:2 and 1:4 ratios increasing the number of neurite per field of view to averages 12 and 18 neurites per field of view respectively compared to average untreated control levels of 5 (Fig.3.8. D).

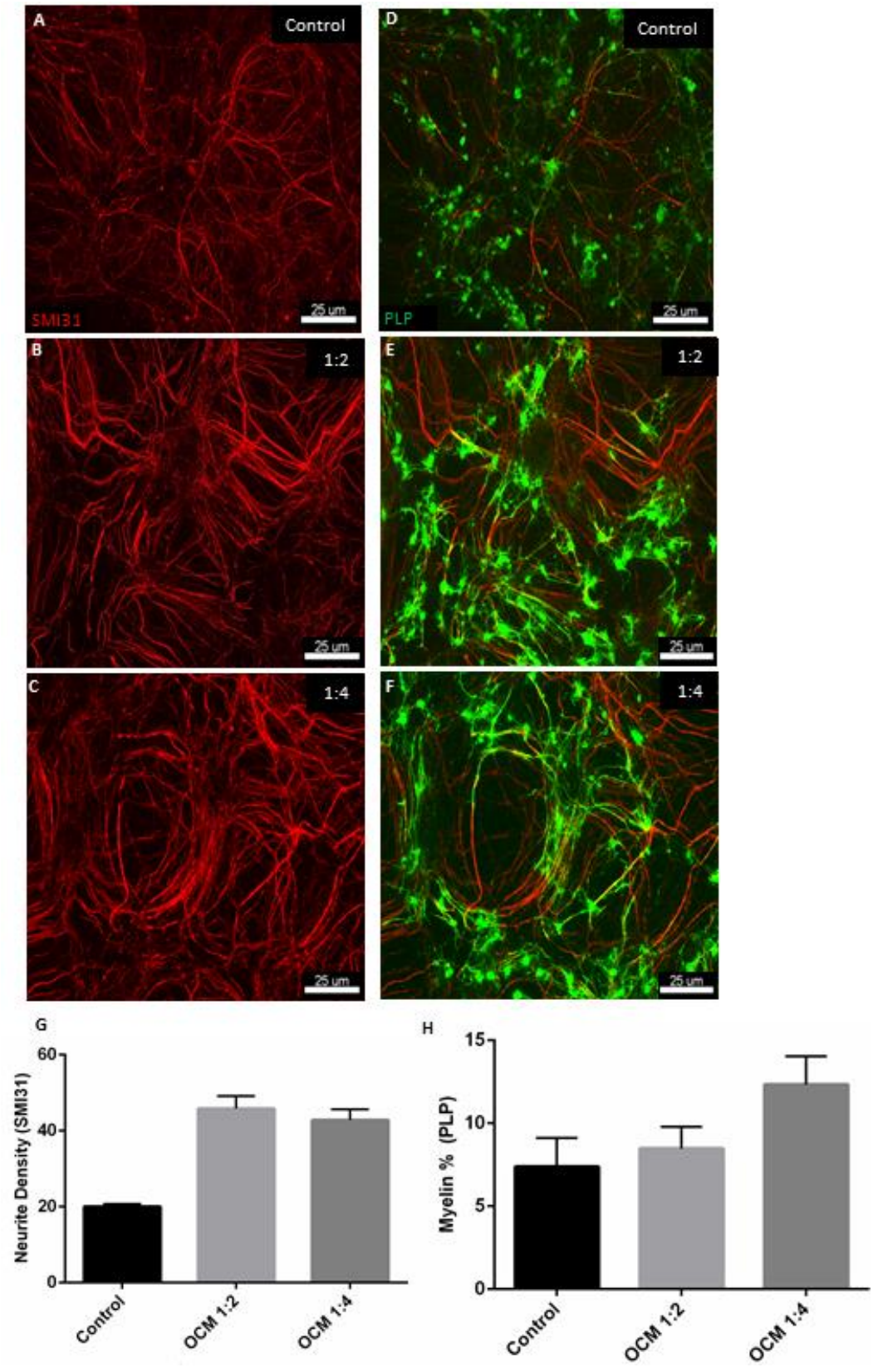

Figure 3.7 OEC-CM promotes both myelination and neurite density following injury.

The myelinating cultures were set up and injured after 24 DIV and treated for a further 5 DIV with OEC-CM at 1:2 and 1:4 ratios. Treatment with OEC-CM at both ratios showed a promotion of neurite density (SMI31, Red) (B and C, G) and myelination (PLP, green) (E and F, H). N=2 and error bars-SEM, scale bar-25 µm.

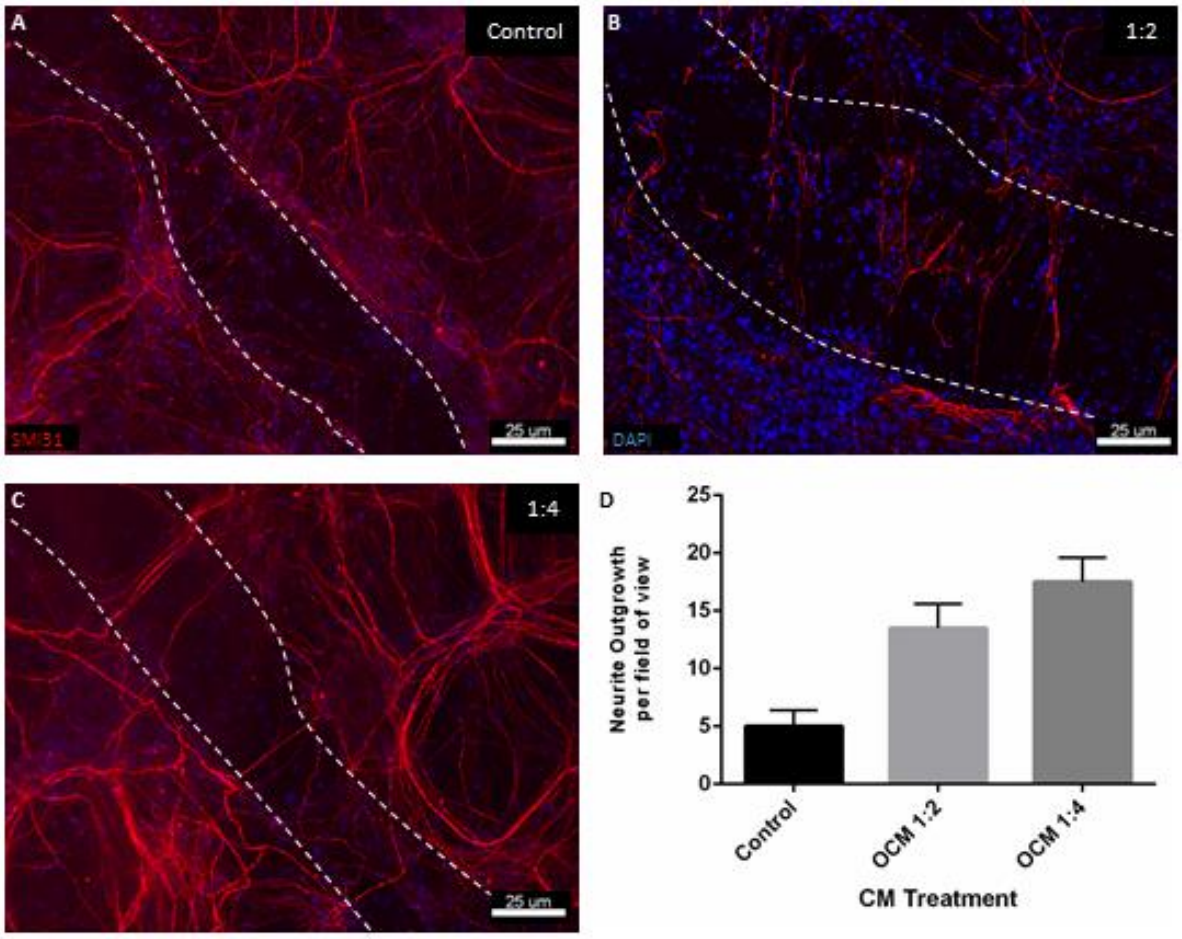

Figure 3.8 OEC-CM promotes neurite outgrowth following injury.

Myelinating cultures were set up and cut with a scalpel blade after 24 DIV. Following a 5 day treatment with OEC-CM. A promotion in neurite outgrowth was recorded at 1:2 and 1:4, with number of neurites per field of view surpassing control levels (A-D). Lesion site marked by dashed line (A) observed down the entire area. N=2 and error bars-SEM, scale bar-25 µm.

3.2.3 Modified heparin as a novel approach to SCI therapy

Following the promising repair-associated processes of the OEC-CM treated injury cultures, I sought to identify the factor(s) present within the OEC-CM which were pro-repair. Following (Higginson et al. 2012), which examined the OEC-CM composition, I hypothesised that the degree of sulphation of HSPG may be a factor associated with the repair processes promoted in the OEC-CM treated cultures. In this study, the sulphation state of HSPG was seen to be the factor which allowed for another repair-associated process, astrocyte mingling, to occur which merited the investigation of HSPG sulphation in our injury myelinating culture system.

Heparin has been proposed as a potential CNS therapy. A study found that proteoglycan accumulation and the inflammatory response in brain regions affected by senile dementia could be resolved by treatment with heparin. They found that this was due to the competitive inhibition of proteoglycan accumulation by heparin and its anti-inflammatory activities (Ma et al. 2007). SCI also involves changes in proteoglycan accumulation and an inflammatory response suggesting a role for heparin as a treatment for repair.

Heparin is an analogue of the HS side chain of HSPG and both are chemically and structurally similar (Sarrazin et al. 2011) (Xu and Dai 2010). HSPGs mediate a plethora of signalling pathways, and signalling dysregulation is prevalent in many CNS pathologies (Cui et al. 2013). It is thought that exogenous Heparin, or modified heparin, could mimic HSPG and mediate certain ligand-receptor binding leading to either suppressing detrimental or activating beneficial HSPG-associated pathways to promote SCI repair (Smith et al. 2015).

Modified heparins (mHep) are compounds which have been artificially altered, changing their degree of sulphation, with an emphasis on the number of sulphate and n-acetyl groups bound to the sugar residue. The mHeps used for the screen were previously used by Higginson and colleagues (Higginson et al. 2012). In this study multiple mHeps were generated with mHep6 (a 2-*O*-monosulphated heparin) having the greatest impact on mingling, meriting it being chosen for this study. It has been modified via desulphating the C2 position on the carbon chain and been shown to be more potent in reducing astrocyte reactivity (Higginson et al. 2012).

The injury mechanisms following trauma are becoming more apparent with signalling disruptions, changes in proteoglycan accumulation and sulphated side changes potentially underling SCI pathology. Using these mHeps to manipulate or ‘reset’ the

signalling disruptions by endogenously adding these signalling co-factor mediators could be a suitable option in SCI therapy.

3.2.3.1 Result: Modified Heparin polysaccharides

The SCI cultures was incubated until day 24 then injured using a flat edge scalpel blade. The lesion created an initial cell free space at a length of ~300 µm. This creating a focal decrease in neurite density and myelination levels adjacent to the lesion. The cultures were treated with mHep6 at a range of 1 ng/ml to 50 ng/ml, at day 25 then allowed to recover for a further 8 days. The cultures were then fixed at day 33 and stained for appropriate myelin marker: PLP and neurofilament marker SMI31. The cultures were imaged using an Axio fluorescent microscope at a 10x magnification, adjacent to the cut site as described in (Boomkamp et al. 2012) for the entire lesion length. Neurite density was calculated based on the SMI31-red pixel intensity compared to the total pixels per image. Myelination was quantified by calculating the percentage PLP-green pixel staining overlying the SMI31-red staining only at a uniformed longitudinal structure with predetermined dimensions. Neurite outgrowth was analysed by scoring the neurites that were seen entering and crossing the lesion site. Images were taken by focusing on the lesion site with each neurite which entered and crossed the lesion classified as 'outgrowth'.

Following a single treatment of mHep6 it can be seen that the 1 ng/ml concentration significantly promotes myelination, p-0.0353 (Fig.3.9.G and L) and neurite density, p-0.0035 (Fig.3.9 B and K). There was no promotion in either neurite density or myelination with increasing concentrations of mHep 6 (10-50 ng/ml) when compared to the untreated control (Fig.3.9.L and K). Precise myelin and neurite density p-values can be seen in table 3.2 below with significant results highlighted in bold.

Table 3-2 mHep Myelination percentages, Neurite density and P-values

Concentration ng/ml	Myelination (%)	p-value/ Significance	Neurite density (%)	p-value/ Significance
1	**9.03**	**0.0353/Y**	**64.89**	**0.0035/Y**
10	6.707	0.6039/N	52.67	0.1899/N
25	6.250	0.8768/N	43.67	0.9985/N
50	4.500	0.7360/N	40.33	0.9665/N

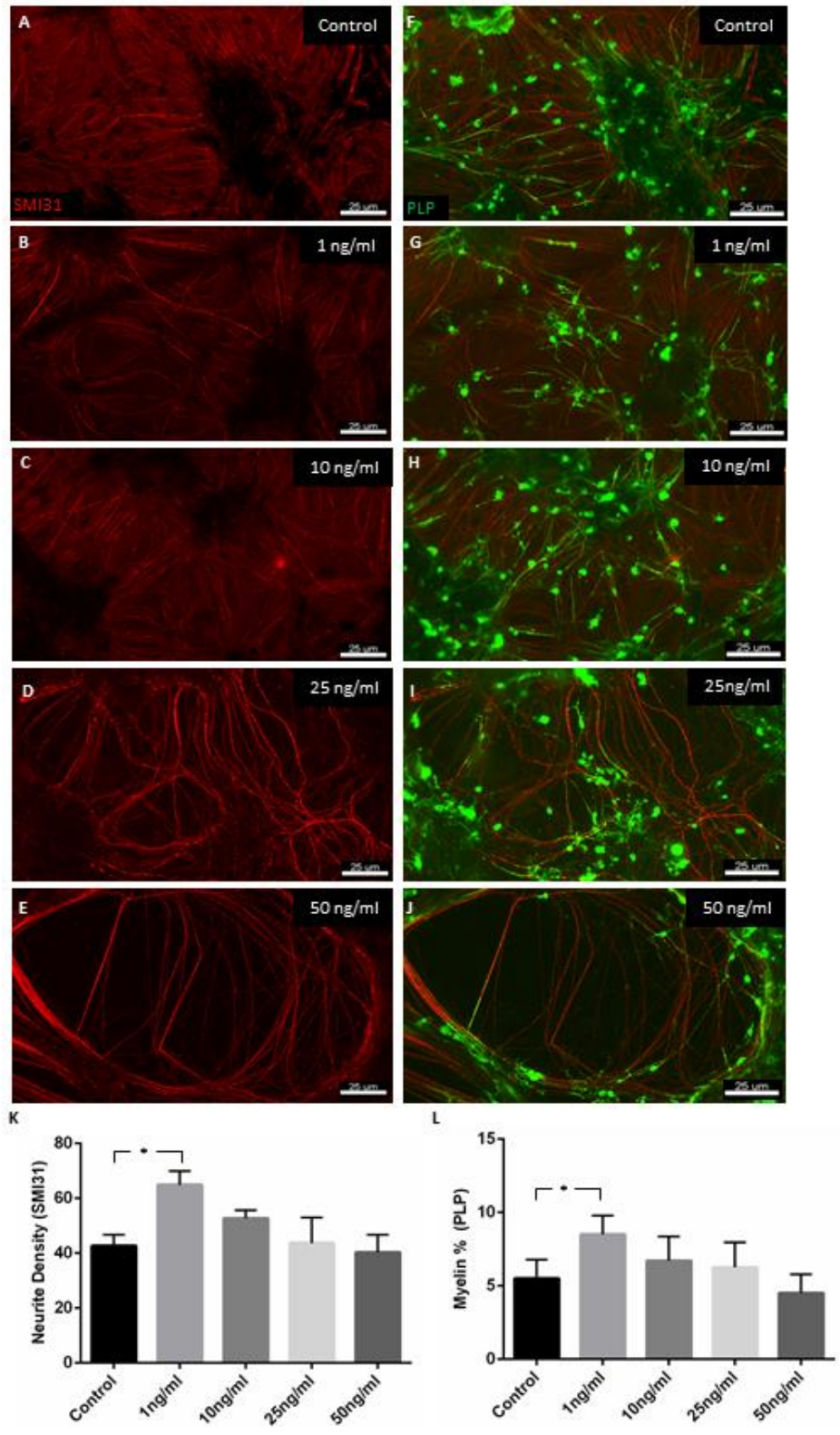

Figure 3.9 mHep 6 promotes myelination and neurite density at 1 ng/ml.

The myelinating cultures were set up and injured after 24 DIV and treated for a further 5 DIV with varying concentrations of mHep 6. mHeps 6 was used at four concentrations from 1-50 ng/ml with only 1 ng/ml showing a significant promotion of neurite density (SMI31, Red) (B and K) and myelination (PLP, green) (G and L). The higher concentrations of mHep6, 10-50 ng/ml (C, D and H, I) appeared to have a negative correlation of concentration verses effect on both neurite density and myelination (K and L). Statistical test used was one-way ANOVA with post-hoc multi-comparison correction, $p<0.05$ represented * in graph (K and L). N=3 and error bars-SEM, scale bar-25 µm.

Following mHep6 treatment there is a promotion neurite outgrowth across the lesion significantly at 1 and 10 ng/ml (Fig.3.10.B-C and F). mHep6 at 25-50 ng/ml concentrations (Fig.3.10. D-F) had no effect on the number of neurites crossing the lesion compared to control (Fig.3.10. A and F). Precise values can be seen in the table 3.3 and significant concentrations in bold.

Table 3-3 mHep6 neurite outgrowth and P-values

Concentration ng/ml	Number of Neurite outgrowth	p-value/ Significance
1	**10.00**	**0.0098/Y**
10	**11.50**	**0.0018/Y**
25	2.000	0.7193/N
50	1.500	0.5323/N

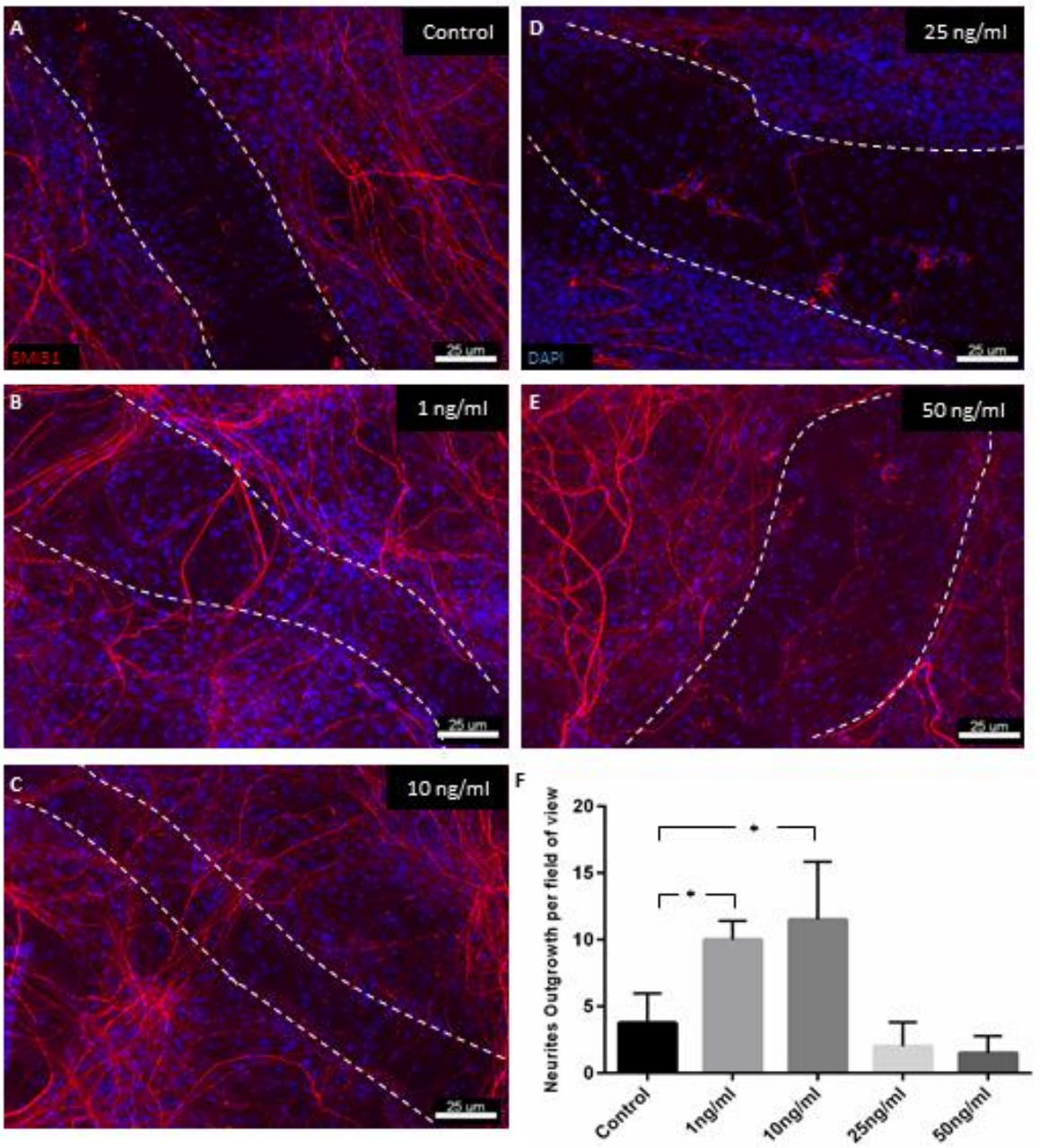

Figure 3.10 The mHep 6 treatment promotes neurite outgrowth

Myelinating cultures were set up and cut with a scalpel blade after 24 DIV. Following a 5 day treatment at 1-50 ng/ml of mHep 6. Significant neurite outgrowth was recorded at 1 ng/ml and 10 ng/ml with number of neurites per field of view surpassing control levels (A-C and F). There was no significant neurite outgrowth following treatment of mHep6 at 25 ng/ml and 50 ng/ml (D-F). Lesion site marked by dashed lines (A). Statistical test used was one-way ANOVA with post-hoc multi-comparison correction, $p<0.05$ represented * in graph (F) N=3 and error bars, SEM, scale bar-25 µm.

3.3 Discussion

In an effort to identify potential therapeutic compounds for CNS repair, we screened a range of potential therapeutics on a SCI model which has key SCI experimental parameters to identify therapeutics for further study.

3.3.1 Neural co-culture model of SCI compound screen

The SCI model was used to screen 5 different compounds (See Table 3.1) at a range of concentrations. The culture was sensitive enough to determine effects from compounds at low concentrations (1 ng/ml range for mHep). In addition, certain compounds were seen to have effects on either myelination, neurite outgrowth or in certain case, both, as seen after treatment with the SC76, OEC-CM and mHeps.

Moreover, the demand to assess large numbers of compounds for SCI therapeutic benefit in a cost- and time-efficient manner highlights the need for throughput assays, such as the compound screen used here. However, this system could be further developed to incorporate, high-content approaches such adapting the culture to a 96-well plate, as well as automated microscopy, particularly to evaluate myelination and neurite outgrowth. Incorporating these adaptions could advance this culture system to an even more high-throughput screening tool for SCI therapeutics.

3.3.2 Highly specific ROCK inhibitor SC76 has multiple beneficial therapeutic effects in our *in vitro* model of SCI

The ROCK pathway is involved in many aspects of cell motility, specifically cellular migration and processes extension and neurite outgrowth (Riento and Ridley 2003). This pathway becomes activated following SCI and contributes to many of the injury-related processes (Fujita and Yamashita 2014). Therefore, inhibiting the ROCK pathway is a justified target in SCI treatment (Dergham et al. 2002).

SC76 appeared to promote myelination and neurite density and outgrowth (Fig.3.1). Myelination and neurite density were promoted at both concentrations tested whereas neurite outgrowth was only promoted at 45 nM (Fig.3.2). SC96 showed promotion of myelination at all concentrations tested (Fig.3.3), however, no promotion of neurite outgrowth was observed (Fig.3.4). Even though SC336 showed promise in aspects of stem cell biology (protected data, under patent, J. Mountford, University of Glasgow) it seems to lack any repair effect on myelination, neurite density and outgrowth (Fig.3.5-3.6). These results were generated from two biological repeats so the data can only

suggest trends towards an effect. Further repeats are required for statistical analysis to conclusively assess the true therapeutic potential of these novel ROCK inhibitors.

The ROCK inhibitors used in this study were more highly selective inhibitors of the ROCK pathway than the previously used ROCK inhibitor, Y27632, based on a kinase assay undertaken by J. Mountford (unpublished data).

The SC76 inhibitor data from this screen suggests that the activation of the ROCK pathway following injury may have a role in the OPC/OL demyelination, which backs up previous data from other studies in the literature (Boomkamp et al. 2012) (Pedraza et al. 2014). This could be due to actin reorganisation in the OL following SCI which destabilises the myelin sheath (Kippert et al. 2007).

The ROCK pathway mediates myosin light chain MLC via the accumulation of phosphomyosin, leading to microtubule depolymerisation and neurite retraction following injury. Data from this screen suggests that inhibiting the ROCK pathway solely following injury leads to neurite outgrowth across the injury site. This could be due to the inhibition of phosphomyosin accumulation and depolymerisation of microtubules. This potential mechanism has been implicated previously, in a study using the less specific Y-27632 ROCK inhibitor (Lingor et al. 2007).

This screen does not identify the target cell(s) which receive the most therapeutic benefit from ROCK inhibition. However, due to the multiple beneficial effects including the promotion of myelination and neurite outgrowth, this suggests several cellular targets.

SC96 and SC336 did not show the same effects on myelination and neurite outgrowth as SC76. The kinase array performed by Dr. Mountford demonstrated the same ROCK inhibitory effects of all three inhibitors. However, this is beyond the scope of this screen. Even though the ROCK inhibitor data from this screen seems promising, due to the similarities these novel ROCK inhibitors have compared to the well-known ROCK inhibitor Y27632 in term of myelination and neurite outgrowth further research using these compounds is potentially redundant. Therefore, no further experimentation will be carried out using these ROCK inhibitors.

3.3.3 OEC secrete a positive factor which promotes myelination and neurite outgrowth in our model of SCI

A potential treatment option for SCI is cellular transplantation, with autologous OEC shown to be promising (Raisman 2001) (Tabakow et al. 2013). To determine if the OEC pro-repair element was a secreted factor, the SCI culture was treated with OEC-CM. CM promoted myelination and neurite outgrowth following injury, suggesting a secreted factor from the OEC is responsible for these repair associated processes at the injury site (Franssen et al. 2007). The CM contains multiple signalling mediators and trophic factors which could be promoting these repair-associated processes. Following the Higginson study, we were particularly interested in assessing the role of HSPGs in mediating these repair processes. HSPGs have been associated with signalling pathways involved in myelination and neurite outgrowth (Hantaz-Ambroise et al. 1987) (Properzi et al. 2008). Thus, it was hypothesised that the degree of sulphation on the expressed HSPGs could be playing a role in promoting myelination and neurite outgrowth in our SCI model.

Therefore, the OEC-CM line of inquiry was continued using the mHeps to determine the role of sulphation in SCI-associated processes. Thus, using the most promising mHep highlighted in the Higginson experiments, mHep6, at varying concentrations we screened for its potential therapeutic benefit for treatment of SCI.

3.3.4 mHeps could be a novel repair therapeutic in SCI

Much research has been carried out relating to sulphated GAGs at the injury site, specifically chondroitin sulphate proteoglycans (CSPG) (Jones et al. 2003). However, there has been little investigation into the role of HSPG at the injury site (Properzi et al. 2008). mHep6 is a heparin desulphated at carbon-2 position of the uronic acid residue of the heparin disaccharide repeating unit. It was produced chemicoenzymatically altering the level of sulphation of heparin (Yates et al. 2004). mHep6 that was shown to promote astrocyte mingling (Higginson et al. 2012). Therefore, this mHep was selected as a proof-of-principle that the sulphation state of the injury site contributes to the repair outcome.

In this culture system, a single treatment with mHep6 at a concentration of 1 ng/ml promoted myelination and neurite density, but not at higher concentrations. At concentrations of 1 and 10 ng/ml, mHep6 promoted neurite outgrowth.

Interestingly, the higher concentrations of mHep6 did not promote myelination, neurite density or neurite outgrowth. This could be explained by the chemical structure of mHep6 (Fig.4.1.C). At a certain point the low sulphation status of mHep6 becomes redundant with the injury site becoming saturated by sulphate groups, thus negating the therapeutic effects of the compound.

3.3.5 Conclusion

Use of the screen demonstrated that the SCI cultures can be used to evaluate effects of many therapeutics on CNS injury repair using the parameters; myelination, neurite density and neurite outgrowth. Following the identification of mHeps as a potential treatment for SCI, this compound was taken forward for further study. However, using the SCI model alone is insufficient to gain a better understanding of the potential of the therapeutic and the mechanism underlying this activity.

Thus, the model has certain limitations which need to be addressed:

1. The response of each of the individual cells present in the culture to the therapeutic needs to be addressed such as the proliferation and differentiation of OPC and the phenotypic shift of astrocytes. This is due to the complex nature of neuronal-glial and glial-glial cross-talk which carry out processes such as myelination and neurite outgrowth. This limitation needs to be addressed through the use of monocultures, looking at each of the key cell types in the SCI model to determine the effects the therapeutics have on the isolated cell population.

2. In addition, with all its merits the culture does not accurately represent some features of the *in vivo* environment. It lacks defined cellular orientation, specifically, the neuronal cell body and neurite compartmentalisation. This somewhat limits our ability to study the specific mechanisms relating to neurite outgrowth.

This SCI culture has identified two new avenues of study. Firstly, the prospect of a novel therapeutic strategy for CNS repairs and secondly, the requirement for further development of this model to better investigate repair-related processes such as neurite outgrowth

Of the 5 compounds examined here, three have shown benefit in both promotion of myelination and neurite outgrowth; SC76, OEC-CM and mHep6 (both at 1 and 10 ng/ml).

However, due to the dual benefit of mHep6 combined with the limited reports in literature using heparin mimetics in SCI and repair we took this compound forward for further study.

This led to the formation of the hypothesis: '*The sulphation level of the heparin mimetic effects the level of myelination and neurite outgrowth following injury*'

Chapter 4

Modified Heparin mimetics as a novel treatment option for SCI repair and regeneration

4 Result: Modified Heparin mimetics as a novel treatment for SCI repair and regeneration

4.1 Introduction

GAGs, HSPGs and heparin could potentially provide a novel opportunity for the development of carbohydrate-based therapeutics for many pathologies, including SCI. Advancements in our understanding of GAG interactions has enabled the generation of GAG mimetics with desirable chemical properties, ones which allow for highly controlled interventions of certain pathological mechanisms.

4.1.1 Heparin treatment

Heparin is a well-known potent anticoagulation and antithrombotic drug (Damus et al. 1973). It was first described in 1916, commercial manufacture started in the 1920s, and improved purification methods led to animal studies and the first clinical trials in the 1930s (Barrowcliffe 2012). Through intense structural and interaction studies it was found that the thrombin affinity occurred through binding to only one third of the heparin chains (Hirsh 2001). Further studies into the structural functions of Heparin identified two prominent forms of Heparin; Low- dose Heparin, used for prevention of deep vein thrombosis (DVT) (McCarthy et al. 1977), and low-molecular-weight heparin used in anticoagulation treatments (Weitz 1997) demonstrating that Heparin has been modified to best suit certain biological activities.

Heparin, like heparan sulphates (HS), exerts its effects on a variety of biological processes through interactions with growth factors, cytokines, adhesion molecules and extracellular matrix enzymes (Capila and Linhardt 2002) (Powell et al. 2004). Heparin treatment has also been associated with having tissue repair properties, for example, heparin has been investigated as an anti-inflammatory agent with its use as a treatment for burns (Ferreira Chacon et al. 2010) and for smoke inhalation damage (Miller et al. 2009). Heparin mediates its effects through competitive binding to release growth factors tethered to the ECM, allowing the growth factors to participate in tissue repair processes (Pike et al. 2006). These studies demonstrate that heparin has many potential therapeutic benefits. However, the potent anticoagulation and antithrombotic effects of heparin could potentially result in an undesirable side effect when developing towards other therapeutic possibilities.

4.1.2 Heparin mimetics

'Heparin mimetics' is a term for a class of chemically modified HS GAGs and heparin. Numerous diverse heparin mimetics have been designed which are structurally distinct from naturally occurring sulphated GAGs. There is high structural and chemical similarity between Heparin, GAG chains of HSPGs and heparin mimetics. Therefore, heparin mimetics have been used as a tool to help understand the role of GAGs/HSPGs in multitudes of biological processes in both physiology and pathology (Freeman et al. 2005).

Heparin mimetics are classified based on their starting compound and the type of modifications they have undergone. A high proportion of heparin mimetics are carbohydrates, whether that is oligosaccharide (between 2-10 monosaccharide residues) or polysaccharide (>10 to several hundred monosaccharide residues). There is also a growing number of non-carbohydrate based mimetics which are adding to this ever expanding class of therapeutics (Coombe and Kett 2012).

There are many structural features which add to the diversity of the mimetics. The size and molecular weight of the starting molecule is a common chemical modification target with investigators normally reducing the size of the polysaccharide in the pursuit of increased specificity and effectiveness. However, this can potentially impact the compound's effect, as alterations to size also alters the overall sulphation state and final molecular conformation (Lindahl 2007). The degree and orientation of sulphation is also a critical target for modification (Wessel et al. 2005). Due to the limitation and inconsistency of the sulphation and desulphation techniques, typically a heterogeneous population of products is formed, potentially leading to highly variable results.

Each modification, however complex, is limited by the ability to produce the mimetic on an industrial scale. Each of these potential drugs has to be commercially viable and translate to clinical relevance in the form of mass production (Lord and Whitelock 2014). There are few heparin mimetics in clinic (Table 4-1), however, this appears to be changing with many mimetics now entering clinical trials

4.1.3 Heparin mimetics as a therapeutic strategy

Heparin mimetics have been developed to broaden the therapeutic potential. Heparin modifications aim to increase the potency of interactions between the mimetic and the target protein.

Table 4-1: To date seven heparin mimetics have been approved for clinical use, compounds adapted from (Barrowcliffe 2012). These include:

Trademark Name	Chemical Name	Structure and composition	Treatment
Sucralfate®	sucrose octasulphate	sulphate sucrose derivative and aluminium hydroxide	Gastric and duodenal ulcers
SP54®, Elmiron®	pentosan polysulphate	a derivative of Pentosan Polysulfate	Interstitial cystitis
Dextran sulphate	dextran sulphate	sodium or potassium dextran sulphate derivative	Inhibition of peptic ulcers
Hirudoid®	oversulphated heparin	mucopolysaccharide polysulfuric acid	Thrombophlebitis Soft tissue injuries
Macugen®	pegaptanib sodium	twenty-eight oligonucleotide modified with nucleotidesmonomethoxy polyethylene glycol (PEG)	Neovascular age-related macular degeneration
Suramin®	Sodium sulfonate	6-sodium sulfonate	Onchocerciasis and sleeping sickness
Cacipliq20®	Heparan sulfate analogues	Heparan sulfate analogues-poly glucose backbone	Diabetic ulcers and chronic wounds

It is clear that the design and modification of heparin-like compounds and their use extend beyond just the anti-coagulation field. Therefore, the modifications need to overcome the apparent innate anti-coagulation of heparin activity whilst maintaining and strengthening their other, less well defined, biochemical activities (Wall et al. 2001) (Lapierre et al. 1996).

A number of studies suggest the use of chemically modified heparins as a potential drug treatment strategy. A large amount of research in the field of oncology evaluates the use of chemically modified heparin as an anti-metastatic and anti-angiogenic therapy (Casu et al. 2010) (Casu et al. 2004). Heparin mimetics have been shown to be an effective inhibitor of heparanase (Naggi et al. 2005). Heparanase has been shown to play a role in tumour cell proliferation, metastasis and neovascularisation, making the targeting of heparanase a promising treatment strategy (Nadir and Brenner 2014). The heparin mimetic sulphation positions, specifically: 2-*O*-sulphate and 3-*O*-sulphate have been shown to be key in inhibiting heparanase and also decreases the anti-coagulant side effect of the mimetic (Lapierre et al. 1996). This study suggests that at least one negatively charged sulphate group is required to inhibit the heparanase enzyme. This

study has also highlighted that the placement and orientation of the sulphate groups on the heparin moiety is crucial in understanding the interaction of the mimetic with a target protein.

4.1.4 Heparin and heparin mimetics in neuroscience

It is known that heparin and its related GAGs are involved in the pathomechanism of the neurodegenerative disorders, Alzheimer's disease and also in CNS trauma (Snow et al. 1989) (Snow et al. 1987). Additionally, GAGs have been recently shown to be neuroprotective in animal studies suggesting an entirely new avenue in the treatment of neurodegenerative diseases and neurological trauma (Dudas and Semeniken 2012).

Heparin could potentially be exerting its effects through the heparin-binding region of neural cell adhesion molecule (NCAM) (Cole et al. 1986) suggesting heparin mimetics can mediate specific neurological processes.

A study using a panel of selectively desulphated heparin compound to demonstrate the role of FGF signalling in astrocyte and SC/OEC boundary formation, a measure of astrocyte reactivity, which could have implications for glial cell transplantation in CNS injury (Higginson et al. 2012). The same selective desulphated heparin panel has been used in a study of selective inhibition of Alzheimer's ß-secretase 1 (BACE-1), an enzyme which cleaves the amyloid precursor protein and a key protein in Alzheimer pathology. Here one of the heparin mimetics, which contained N-acetyl, 2-*O*- and 6-*O*-sulfates, was effective in the BACE-1 inhibition (Patey et al. 2006). Additionally, heparin has recently been suggested as a treatment for limiting neurological injury that follows subarachnoid haemorrhage (Simard et al. 2010). Promising studies have also demonstrated a role for heparin and GAGs in the suppression of apoptotic processes through regulation of the death receptor ligands and their receptors (Belmiro et al. 2009). This has implications in SCI and suggests a potential treatment approach in repair and regeneration.

It has been suggested that heparin mimetics could exert their therapeutic benefit by regulating ligand-receptor binding and signalling activation. With signalling dysregulation a feature of many neurological disorders and trauma, mimetics could be introduced to intercede and provide therapeutic benefit. Studies have demonstrated the role of HSPGs as co-factors for several key pathways, including the neurite outgrowth and myelination associated Wnt and FGF pathway (Wade et al. 2014).

Is has become apparent that activation of Wnt signalling in the injured CNS could be important in the regenerative process which may be in part due to Wnt being able to

activate other signalling pathways (Gonzalez et al. 2012). The initiation of the canonical pathway begins with the binding of the ligand with its receptor Frizzled (Fz). Wnt proteins are lipid-modified glycoproteins which are reliant on the HSs on the cell surface and in the ECM to stabilize the ligand (Fuerer et al. 2010), maintain the solubility of the ligand, distribute the ligands along the morphogenic gradients and initiate the signalling cascade (Ai et al. 2003). Wnt signalling could potentially have protective roles in neurogenesis and blood brain barrier restructuring (Briona et al. 2015) (Stenman et al. 2008) (Liebner et al. 2008). Moreover, there is evidence to suggest that following SCI there is a down regulation of the mRNAs for many Wnt ligands, suggesting Wnt signalling is largely repressed after injury (Gonzalez-Fernandez et al. 2014). This suggests that a potential treatment which could mediate or even activate Wnt signalling could aid regeneration.

The stabilisation and/or activation of the Wnt pathway as a treatment would re-establish the signalling cascade which has been demonstrated to be down regulated following injury. Studies have alluded to the activation of the canonical Wnt pathways as a potential treatment in CNS regeneration specifically for neurite outgrowth, with focus on the stabilisation of the ß-catenin messenger molecule or inhibition of ß-catenin degrading molecule GSK3-ß (Cuzzocrea et al. 2006). Wnt signalling has been shown to be a mediator of axonal guidance with several Wnt proteins being shown to stimulate the extension of axons through controlled gradients which attract the axons towards the brain once they cross the midline from the dorsal spinal cord (Lyuksyutova et al. 2003).

However, Wnt signalling activation may have differential effects depending upon the cell type involved. A study has been reported showing that if the Wnt pathway is repressed in OPCs through exon targeted knockdown, it leads to decreased OPC proliferation following trauma, with an increase in neurite outgrowth observed (Rodriguez et al. 2014). This study highlights that this specific pathway may not have a global benefit in the injury response. It is clear that Wnt play important roles in injury and repair-associated processes, but many of the precise mechanisms are unknown. Therefore, employing modified heparins (mHeps) in the treatment of SCI could allow for the elucidation of the exact mechanism of Wnt in SCI and repair.

FGF signalling has been implicated in SCI but has been recorded to have both beneficial and pathological roles (Koshinaga et al. 1993). FGF signalling has been shown to decrease astrocytosis and promote neurogenesis by inducing glial progenitor-like phenotypes which are supportive of axonal regeneration (Goldshmit et al. 2014). The majority of research has focus specifically on FGF2 and it's role in SCI pathology and

regeneration (Adeeb and Mortazavi 2014). Similarly, other studies have suggested a neurotrophic effect of FGF2 and subsequent upregulation promoting regeneration. However, there is a recorded increase in FGF2 after spinal cord injury contusion, which suggests that FGF signalling could have a neuroprotective role (Mocchetti et al. 1996). However, this suggests that even though upregulation of FGF2 is recorded after SCI, FGF2 appears to have little regenerative potential, beyond the limited innate regenerative capacity of the spinal cord. In addition, FGF signalling has been shown to promote OPC proliferation and could potentially attribute to the lack of OL differentiation and subsequent myelination adjacent to the lesion. FGF signalling and OPC proliferation and OL differentiation is a complex interaction, with the developmental stage of the OPC/OL dictating the effect the FGF signalling has, this is due to the change in receptor prolife as the cell matures (Bansal et al. 1996).

FGF signalling has a long history which goes hand in hand with HSPG. HSPG are well characterised co-factors which initiate FGF signalling, through the specific sulphation moieties found on the GAG chain. Therefore, using selectively desulphated mimetics the injury response could be beneficially altered and provide more understanding of the role of FGF2 signalling in repair and regeneration.

It is clear that heparin and it's analogues interact with a wide variety of biological mechanisms and highlighting a place for heparin mimetics in CNS injury and treatment. Using the modified heparin (mHep) panel utilised in the Higginson and Patey experiments we can evaluate the use of mHeps as a treatment for SCI (Higginson et al. 2012; Patey et al. 2006).

4.2 Aims

- To utilise the selectively desulphated mHep panel and ascertain effects on:
  - myelination and neurite outgrowth following injury
  - the maintenance of myelination
- To understand the mHep mechanism of action.

4.3 Results: Effects of odified Heparin panel on promotion of myelination and neurite outgrowth

To date, heparin mimetics have not been studied in SCI and repair. The SCI myelinating cultures were employed as a tool to study the effects of variably desulphated mHeps on myelination and neurite outgrowth following injury to establish the therapeutic potential of these mHeps, and to study the role of heparan sulphation at the injury site.

The mHeps used here were provided by Dr. E.A. Yates, and in collaboration with Dr. J. Turnbull University of Liverpool, UK. The compounds were produced by a semisynthetic, selective desulphation of the commercial available heparin. Each modified version of heparin was structurally distinct and therefore, had different biochemical capabilities. Each mHep and the chemical modification it underwent are described in Table 4.2 and Fig 4.1.

Table 4-2: Selectively desulphated mHeps panel with chemical modification. (Adapted from Patey et al., 2006)

Modified Heparin	Chemical modification	No:SO_{3-}
mHep1	No modifications. Complete iduronate 2-*O*, glucosamine 6-*O*-sulphation and *N*-sulphation	3
mHep5	Selective removal of iduronate 2-*O*-sulfate. (concomitant modification in the small number of *N*- and 3-*O*-sulfated glucosamine units)	1
mHep6	Selective removal of glucosamine 6-*O*-sulfate and *N*-sulphate	1
mHep7	Complete removal of O-sulphates (achieved using solvolytic de-sulfation)	1
mHep8	Complete desulphation of iduronate/glucosamine *O*-sulphates and *N*-sulphates with *N*-acetylation	0

A

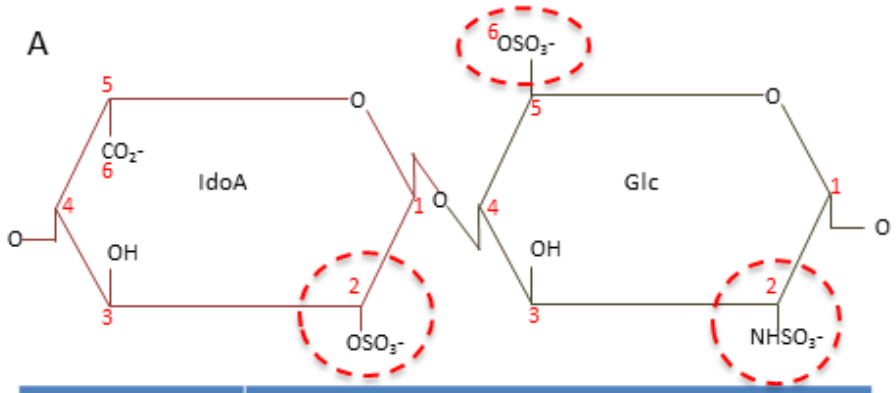

Heparin	Modification
1	Sulphate modification positions: IdoA–2-*O* Glc – 6-*O* and *N*-sulphate

B

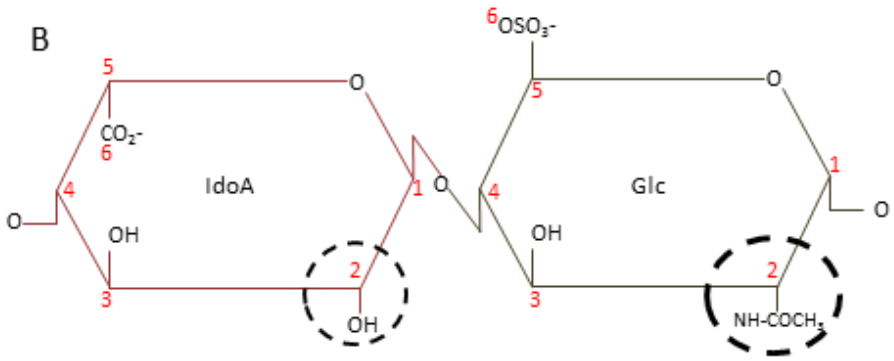

mHep	Modification
5	*O*-sulphated at C6 of GlcNAc *N*-acetylated at C2 GlcNAc and desulphated at C2 IdoA

C

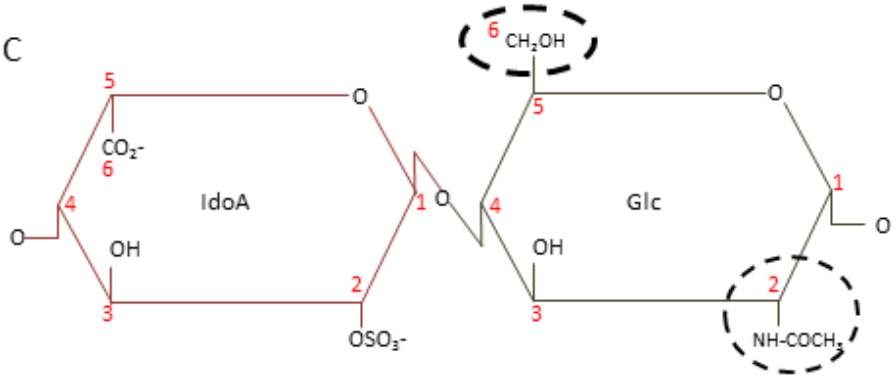

mHep	Modification
6	*O*-sulphated at C2 of IdoA *N*-acetylated at C2 GlcNAc and desulphated at C6 GlcNAc

D

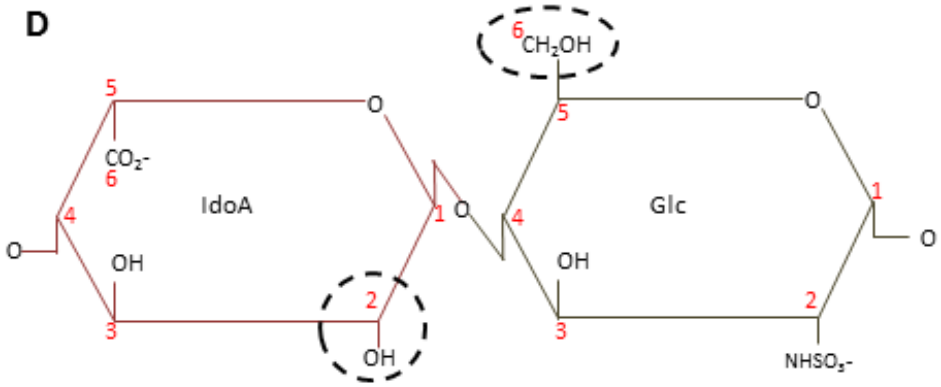

mHep	Modification
7	*N*-sulfated at C2 GlcNAc ($GLcNSO_3$-) desulphated at C2 of IdoA and desulphated at C6 GlcNAc

E

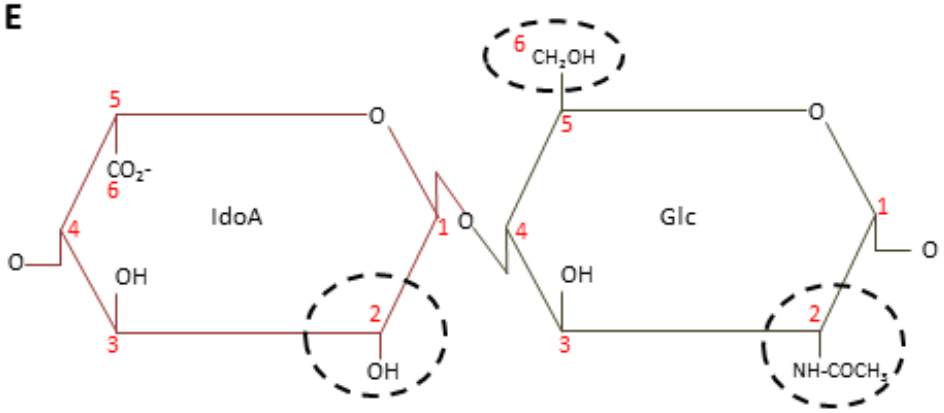

mHep	Modification
8	*N*-acetylated at C2 and desulphated at C6 of GlcNAc desulphated at C2 of IdoA

Figure 4.1 Heparin Disaccharide unit and modifications

Commercial heparin was selectively desulphated at three possible positions: 2-*O*-iduronic acid (IdoA), 6-*O* and *N*-glucoasmine (Glc/NAc), marked dashed red circle (A). mHep5 sulphation profile, 6-*O*-sulphated (B), mHep6 sulphation profile, 2-*O*-sulphated (C), mHep7 sulphation profile N-sulphated (D) and mHep8 total desulphated (E) each desulphated positions marked black dashed circle and list of modifications tabled below each disaccharide unit.

4.3.1 mHep effect on neurite density and myelination following injury

To investigate the effects of the mHeps on neurite density and myelination following injury, myelinating cultures were carried out a previously described (Section 2.2). Cultures were incubated until day 24 at which time a cut was made across the cultures using a flat edge scalpel blade. The lesion created a focal (650 μm) decrease in neurite density and myelination levels adjacent to the lesion (Boomkamp et al. 2012). The cultures were treated with each mHep compound (for chemical structure, Fig 4.1) at a concentration of 1 ng/ml for a single treatment at day 25 before being allowed to recover for a further 5 days with no treatment applied.

The cultures were then fixed and stained for SMI31 for axons and an anti-PLP antibody was used to visualise mature myelin. The cultures were imaged at 10x magnification adjacent to the cut site for the entire length of the lesion (region of focal effect). Neurite density was calculated based on the red pixel intensity (red, SMI31/neurite) compared to the total pixels per image. Myelination was quantified as described previously (2.2) by calculating the percentage of green pixels (AA3/myelin) over laying red pixels (SMI31/axon) only at a uniformed longitudinal structure with define dimensions.

Neurite density was significantly promoted after treatment with 2-*O*-sulphate mHep6 compared to the untreated control (Fig.4.2. D and H). The other desulphated forms of mHep5,7 and 8 had no significant effect on promoting neurite density with values not exceeding 48%, 54% and 52% respectively (Fig.4.2. G). Normal heparin (mHep1) had no effect on neurite density (56%), with no statistically significant difference compared to the untreated control (44%) (Fig.4.2.G).

mHeps 6-8 significantly promoted myelination compared to control (Fig. 4.2.D-F and H). Partially desulphated mHep5 did not affect myelination levels, with levels not exceeding 5% (Fig. 4.2.C and H). mHep1 significantly decreased the level of myelination compared to the control with 2.6% myelination compared to 5% (Fig.4.2. H).

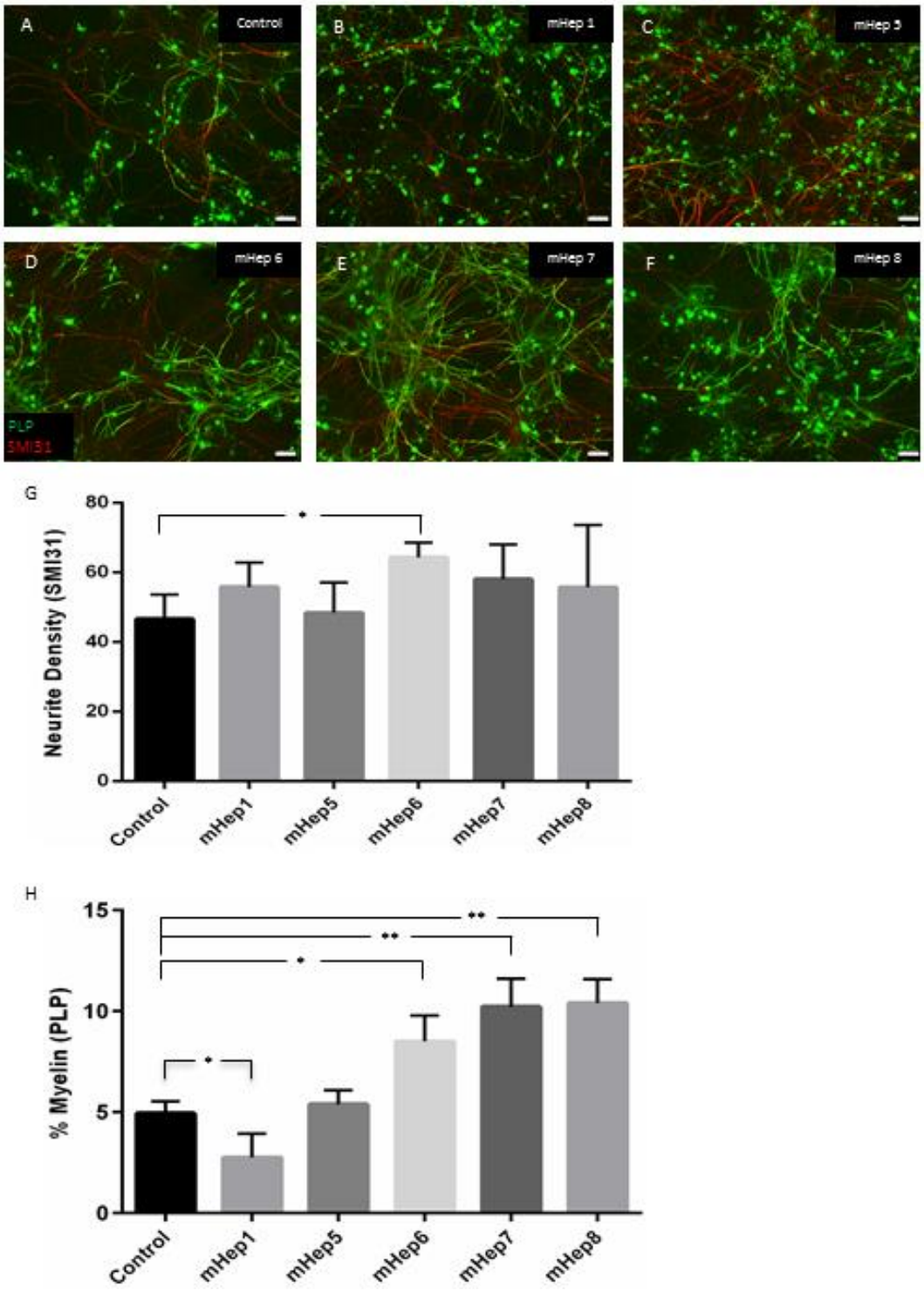

Figure 4.2 The Desulphated forms of mHep have positive effects on myelination and neurite density following a single treatment.

mHep6 promoted neurite density (SMI31, red) following treatment at 1ng/ml (D and G). With no other mimetic having any statistical effect on neurite density. mHep 6-8 significantly promoted myelination adjacent to the lesion following a single treatment, with percentages raising above 9%-mHep6, 10%-mHep7 and 10%-mHep8 compared to the control 5% (.H). mHep5 did not statistically promote myelination with levels reaching slightly greater than 5% (H). mHep1 significantly decreased the levels of myelination with percentages of 2.5% (H). Statistical test used was one-way ANOVA with post-hoc Dunnett's multi-comparison correction, *p<0.05, **p<0.01 represented in graph (G and H). N=6 and error bars SEM, scale bar, 25 µm.

4.3.2 Desulphated mHeps promote neurite outgrowth following a single treatment

Injury was achieved using a flat edge scalpel blade which created an initial cell free space with very low numbers of neurites, average of three, crossing the lesion. Following the same treatment plan and time course as previously described, cultures were fixed and stained for the axonal marker SMI31 and DAPI for nuclei. Neurites which entered and extended across the entire cut site were counted and determined to be neurite outgrowth.

Desulphated forms of the mHep 5-8, all significantly promoted neurite outgrowth across the lesion compared to the untreated control (Fig.4.3. C-F and graph G). mHep5 and mHep7 were the most effective promoters of neurite outgrowth with the number of neurites per field of view increasing to, on average, 14 per field of view, compared to 3 neurites in control cultures. mHep6 and mHep8 both promoted neurite outgrowth but to lower levels, averaging 10 neurites per field of view each (Fig.4.3. G). mHep1 did not promote neurite outgrowth following the same treatment course with neurite numbers not rising about 2-3 neurites per field of view (Fig.4.3. B and G).

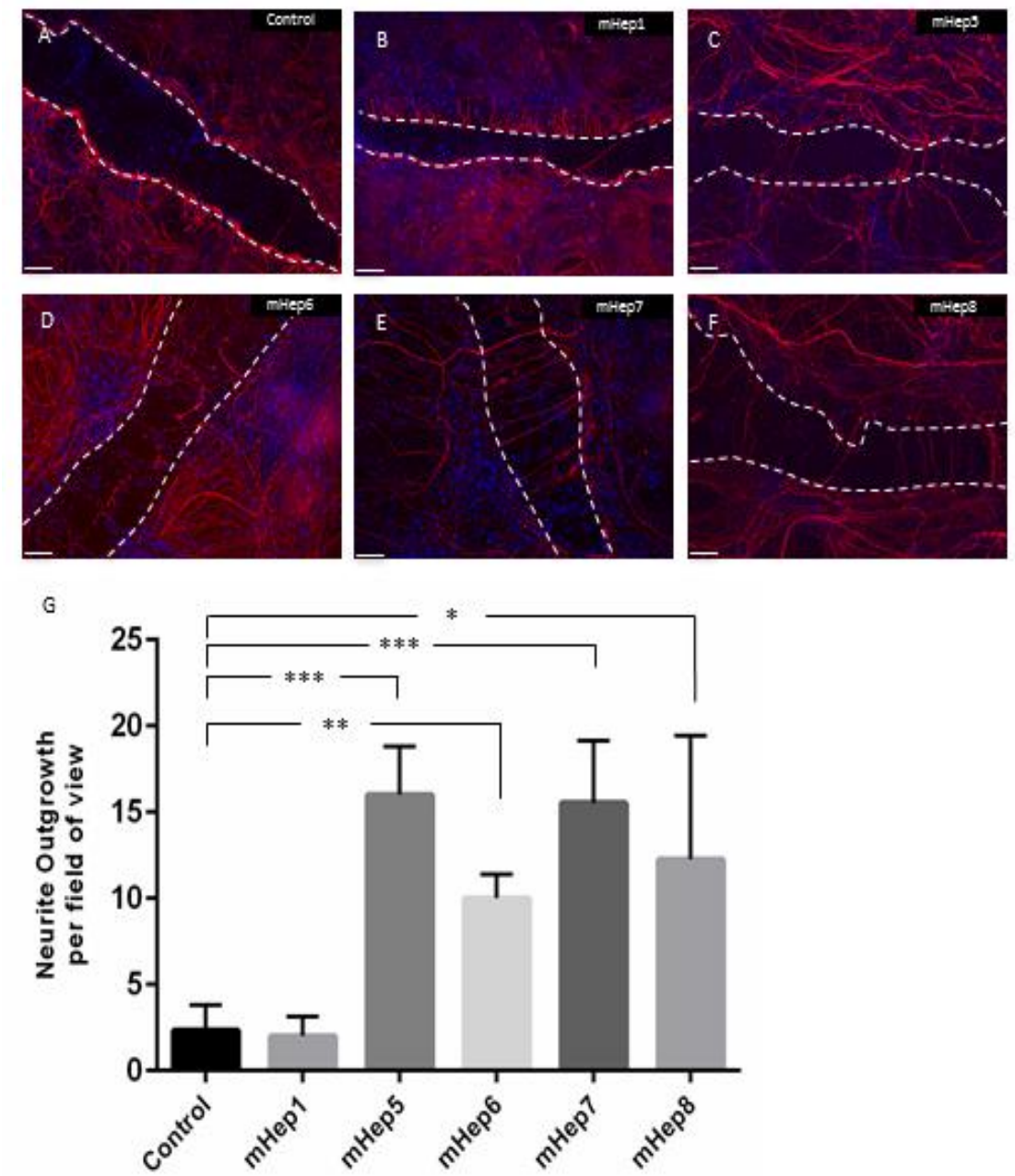

Figure 4.3 The mHep5, 6, 7 and 8 all significantly promote neurite outgrowth following a single treatment.

Lesion site marked by dashed line and a decrease in the nuclei density (DAPI, blue) observed down the entire area. Significant neurite outgrowth across the lesion was seen with mHep5-8 with numbers of neurites per field of view surpassing control levels (C-F and G). There was no effect on neurite outgrowth with mHep1 following a single treatment course (L). Statistical test used was one-way ANOVA with post-hoc Dunnetts multi-comparison correction, *p<0.05, **p<0.01, ***p<0.001 represented in graph (L) N=3 and error bars-SEM, scale bar-25 µm.

4.3.3 Highly sulphated mHep increases the size of the lesion site

Following injury, the lesion site was initially a cell free space about 400 μm across. The lesion size was defined as the area lacking nuclei and neurites. 10 images were taken for each condition. The size of the lesion was calculated using ImageJ LineTool, by drawing a line from one edge of the lesion to another which was then converted to the actual size in μm.

Highly sulphated mHep1 significantly increased the lesion size to 564 ± 27.47 μm compared to the untreated control of 400 ± 20.04 μm (Fig.4.4.G). The desulphated mHeps, mHep5-8, did not have any statistically significant effect on the lesion size (Fig.4.4.D), with average lesion sizes being 380 ± 18 μm (mHep5), 315.16 ± 46.8 μm (mHep6), 405 ± 48.65 μm (mHep7) and 316.6 ± 56.22 μm (mHep8).

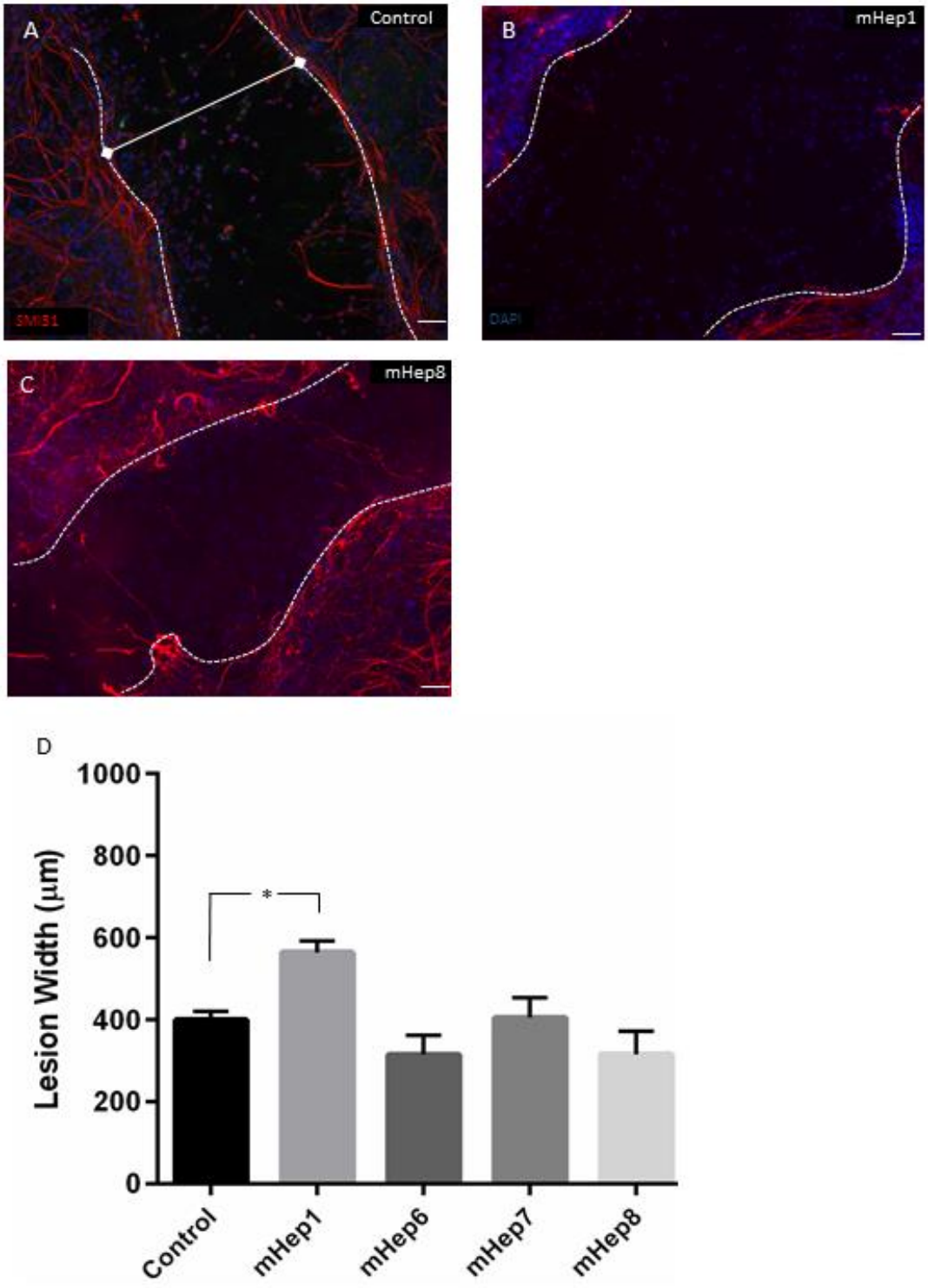

Figure 4.4 High levels of sulphate significantly exasurbates the lesion size following a single treatment.

The lesion edge was marked and 10 measurements were taken per image at even spaced intervals. Significant increase in lesion size was observed with Heparin (mHep1) (B and D) with the average lesion size reaching 564.5 µm, when compared to control lesion 400 µm. Desulphated mHep 6-8 did not have any effect on the lesion size with no statistical difference (D). Statistical test used was one-way ANOVA with post-hoc Dunnett's multi-comparison correction, $p<0.05$, * represented in graph (D) N=3 and error bars-SEM, scale bar-25 µm.

4.3.4 Desulphated forms of mHep cause an increase in the active astrocytic marker nestin

Following injury the lesion site is invaded by astrocytes which have an altered morphology and reactive phenotype. For astrocytosis experiments, western blotting was carried out on protein lysates extracted. Protein level comparisons were performed using semi-quantitative densitometry analysis using imaging software, ImageJ.

mHep1 significantly increased GFAP protein levels following injury (Fig.4.5.A and D) whereas the desulphated forms, mHep6 and mHep7, did not significantly alter the GFAP levels (Fig.4.5.A,C and D). There was no statistically significant change in nestin levels following treatment with mHep1 (Fig.4.5.B and E). However, both desulphated mHep6 and mHep7 induced a statistically significant increase in Nestin protein levels compared to the untreated control (Fig.4.5.B and E).

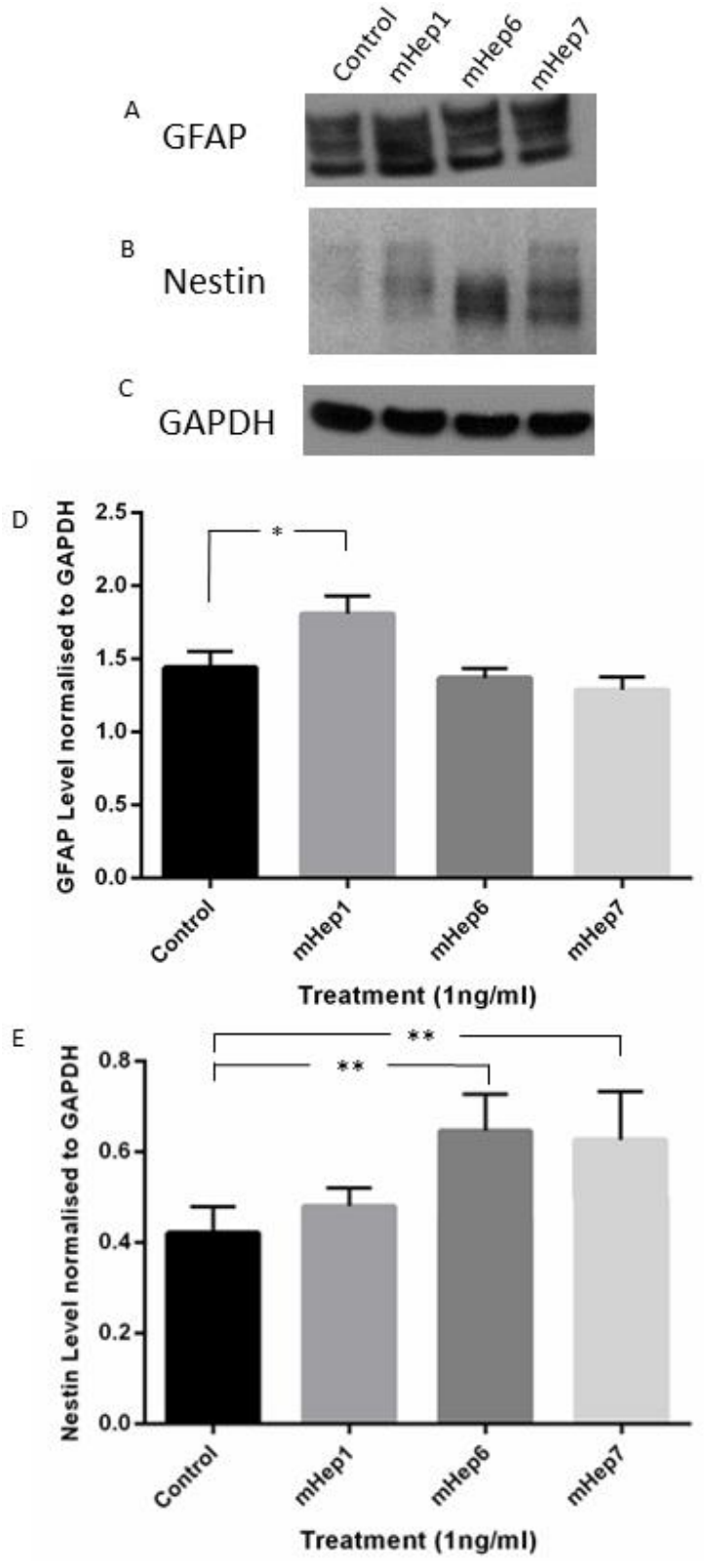

Figure 4.5 Desulphated forms of mHeps cause an increase in the active astrocytic marker nestin following a single treatment

GFAP was significantly increased following mHep1 treatment (A) and Nestin was significantly increased following mHep6 treatment (B) Loading control being GAPDH which is expressed ubiquitously (C). There was no significant change in GFAP levels following treatment with mHep6 or 7 (A and D). However, mHep1 significantly increase GFAP (A and D, *). There was a significant increase in Nestin levels following treatment with mHep6 and mHep7 compared to control (B and E, **). There was no change in the nestin levels following treatment with

mHep1 (B and E). Statistical test used was one-way ANOVA with post-hoc Dunnett's multi-comparison correction, p<0.001 represented ** in graph (E) N=3 and error bars, SEM.

4.3.5 Desulphated mHeps cause a decrease in OPC proliferation

In order to assess the effects of the mHeps on OPCs, OPCs were seeded at a concentration of 500 cells/µl in Bottenstein Sato (BS) media containing PDGFα and FGF2 and maintained for 5 days. The BS enriched media was then switched to BS media with or without mHeps at a concentration of 1 ng/ml. Cultures were used for proliferation, morphology and differentiation assays.

For proliferation studies the cultures were co-incubated with BrdU at the same time as the mHeps for 12 hours before being subjected to fixation and staining. Controls for this experiment were cultures incubated with BS alone to show basal proliferation and cultures incubated with BS plus PDGFα and FGF2 as a positive control for proliferation. Following fixation the cultures were co-stained for BrdU and the appropriate differentiation marker; either immature OL marker (04) or myelin marker (PLP) and DAPI (nuclei). The cultures were blinded to the experimenter and each culture was imaged at 10x magnification in a random sampling fashion. Quantification was performed using a CellProfiler pipeline which simultaneously counts the total number of nuclei and the BrdU positive cells producing a ratio of proliferating cells (BrdU+) verse total number of cells. BS control was used to compare each treatment and is the baseline level of proliferation.

The BS only control had an average of 32% proliferating cells (Fig.4.6.B and E). mHep1 promoted proliferation of OPC with the average percentage of 53% (Fig.4.6.A and E). Desulphated mHep6, 7 and mHep8 decreased the number of proliferating OPCs with the average percentage number of BrdU+ cells falling to 29% (Fig.4.6.B-E).

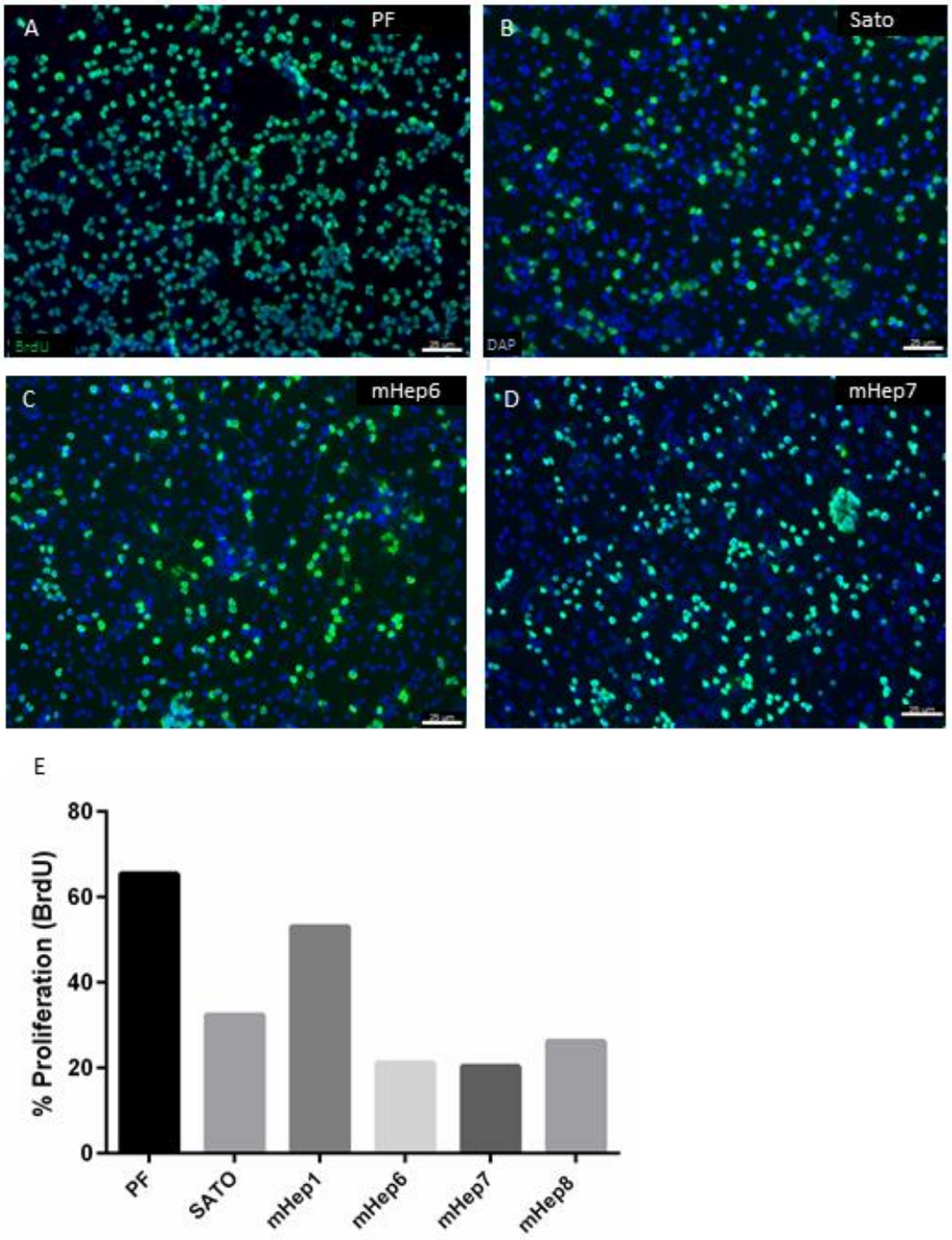

Figure 4.6 Desulphated mHeps causes a decrease in OPC proliferation

The cultures were co-stained for BrdU (green) and nuclei-DAPI (blue). PDGF and FGF positive control (A). Each treatment was compared to SATO control (B), desulphated mHep6-8 (C and D mHep6 and 7 respectively, E) reducing proliferation of OPCs with mHep1 promoting OPC proliferation (E). N=1, scale bar-25 µm.

4.3.6 OL numbers are rescued adjacent to the lesion following treatment with desulphated mHeps

Following treatment of the injured myelinating cultures with mHeps, the cultures were fixed and stained with SMI31 for axons and AA3 for mature OLs. The cultures were blinded and imaged at 10x magnification adjacent to the cut site for the entire length of the lesion (region of focal effect), 10 images per coverslip. OL number were quantified directly adjacent to the lesion site, using a CellProfiler plugin, which counts the number of green (PLP+) circles over laying blue (DAPI+) circles per image. Mature OLs were defined as PLP+ cell bodies.

mHep1 displayed a significant decrease in OL number adjacent to the lesion compared to the untreated control (Fig.4.7.C). mHep5 and mHep6 did not significantly promote OL number adjacent to the lesion with PLP+ cells not exceeding control numbers (Fig.4.8). However, desulphated mHep6, 7 and 8 did significantly promote/rescue the number of OLs adjacent to the lesion site with mHep8 having the greatest impact on OL number (Fig.4.8.C).

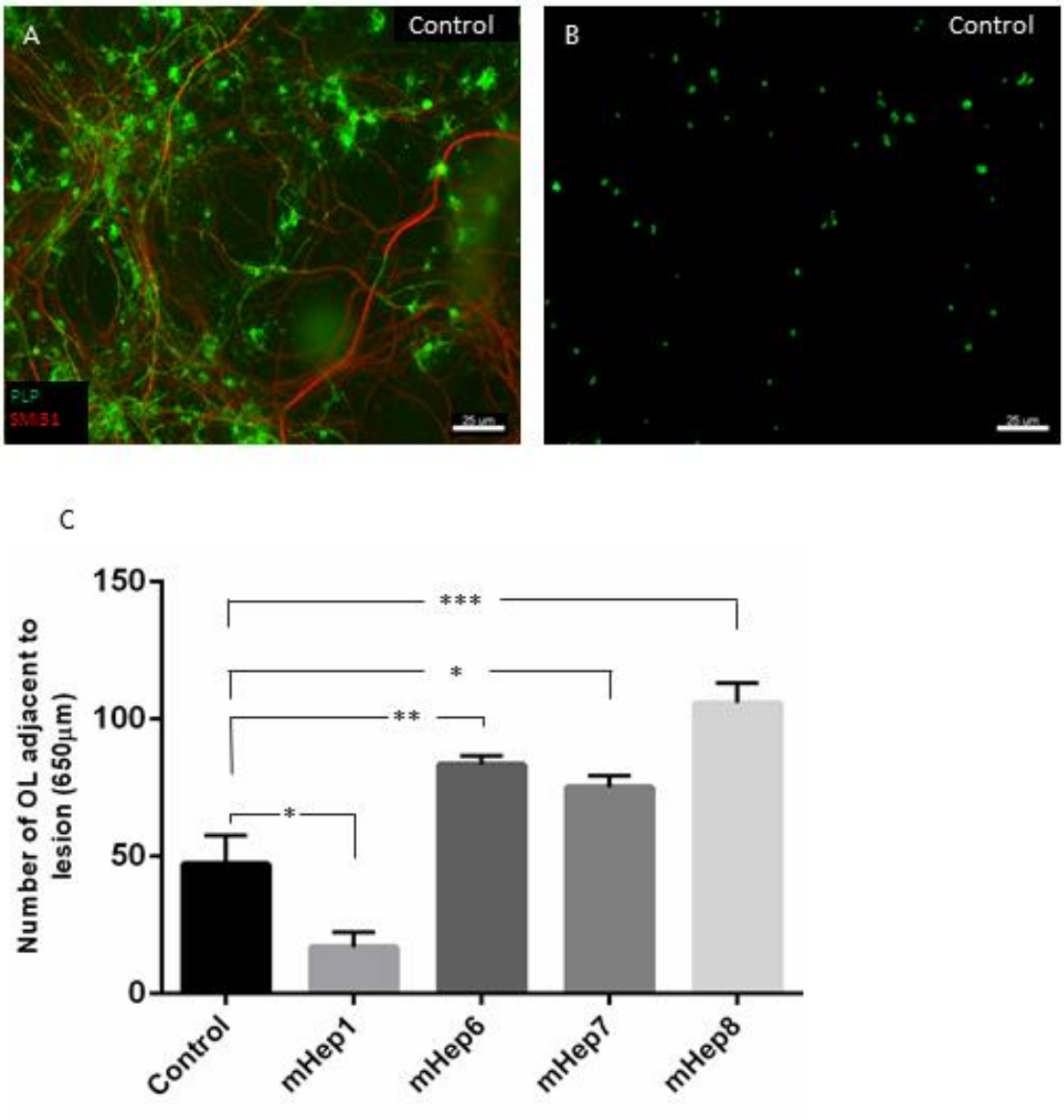

Figure 4.7 The Desulphated forms of mHep promote the number of OL adjacent to the lesion

OL quantification was performed using CellProfiler pipeline which calculate green spherical objects (B) at a set dimension each mHep treatment was compared to control OL number (A). As the sulphation level decreases mHep1-8 we see an increase in the number of OL adjacent to the lesion. Highly sulphated mHep1 significantly decrease the number of OL compared to control levels (C). Desulphated mHep6, 7 and 8 both significantly promote the number of OL adjacent to the lesion with number reaching 85, 78 and 109 respectively (C). Statistical test used was one-way ANOVA with post-hoc Dunnett's multi-comparison correction, $p<0.05$, $p<0.001$ and $p<0.0001$ represented *, **, * in graph (C). N=3 and error bars-SEM, scale bar- 25 µm.**

4.3.7 mHep6 and 8 promote myelin sheath length and mHep 7 increases OL size

OPCs were seeded onto PLL coated nanofiber culture inserts (Nanofiber Solutions ^{TM}) at a concentration of 500 cells/µl in a volume of 50 µl, then made to a final volume of 250µl in BS media containing PDGFα and FGF2 for 5 days. The OPC media was then switched to BS media with mHep treatment at 1 ng/ml for 7 days. Controls (BS only, growth factor BS) were also maintained for 7 days. The cultures were co-stained with the appropriate OPC/OL markers; either immature OL marker (04) or mature myelin marker (PLP) and nuclei (DAPI). The cultures were blinded to the experimenter and each culture was imaged at 10x and 40x magnification 10 per coverslip, in a random sampling fashion. Sheath length was quantified by measuring a single internode (PLP+ process) per cell, from cell body to outmost internode using the imaging software ImageJ LineTool and Measure function. Cell area was quantified using the imaging software ImageJ. The cell size was defined by the green (PLP+) pixel threshold compared to the total pixel intensity and individual cells were marked with region of interest (ROI) tool to allow single cell analysis.

The OL sheath length of the untreated control (BS only) averaged 166.6 ± 20.37 µm with the growth factor control sheath size only reaching 87.3 ± 31.24 µm (Fig. 4.8.A). mHep1 had no significant effect on the sheath length with the average length reaching 150.6 ± 57.94 µm. Similarly, the desulphated mHep 7, had no significant effect on the sheath length with average lengths measuring 196.9 ± 60.18 µm (Fig.4.8.E and G). Desulphated mHep6 and 8 significantly promoted the OL sheath length compared to control with an average length 298.64 ± 84.31 µm and 317.4 ± 66.7 µm respectively (Fig.4.8.D, F and G).

The cell size of OLs was significantly increased following treatment with mHep7, 289.17 ± 49.75 μm^2 compared to control, 139 ± 16.9 μm^2 (Fig.4.8.B,E and H). mHep, 6 and 8 did not show any statistically significant difference on cell size (157.87 ± 41.9 and 141.9 ± 36.86 μm^2, respectively) (Fig.4.8.D, F and H). However, mHep1 significantly decreased the overall cell size, 79.65 ± 8.31 μm^2 (Fig.4.8.C and H).

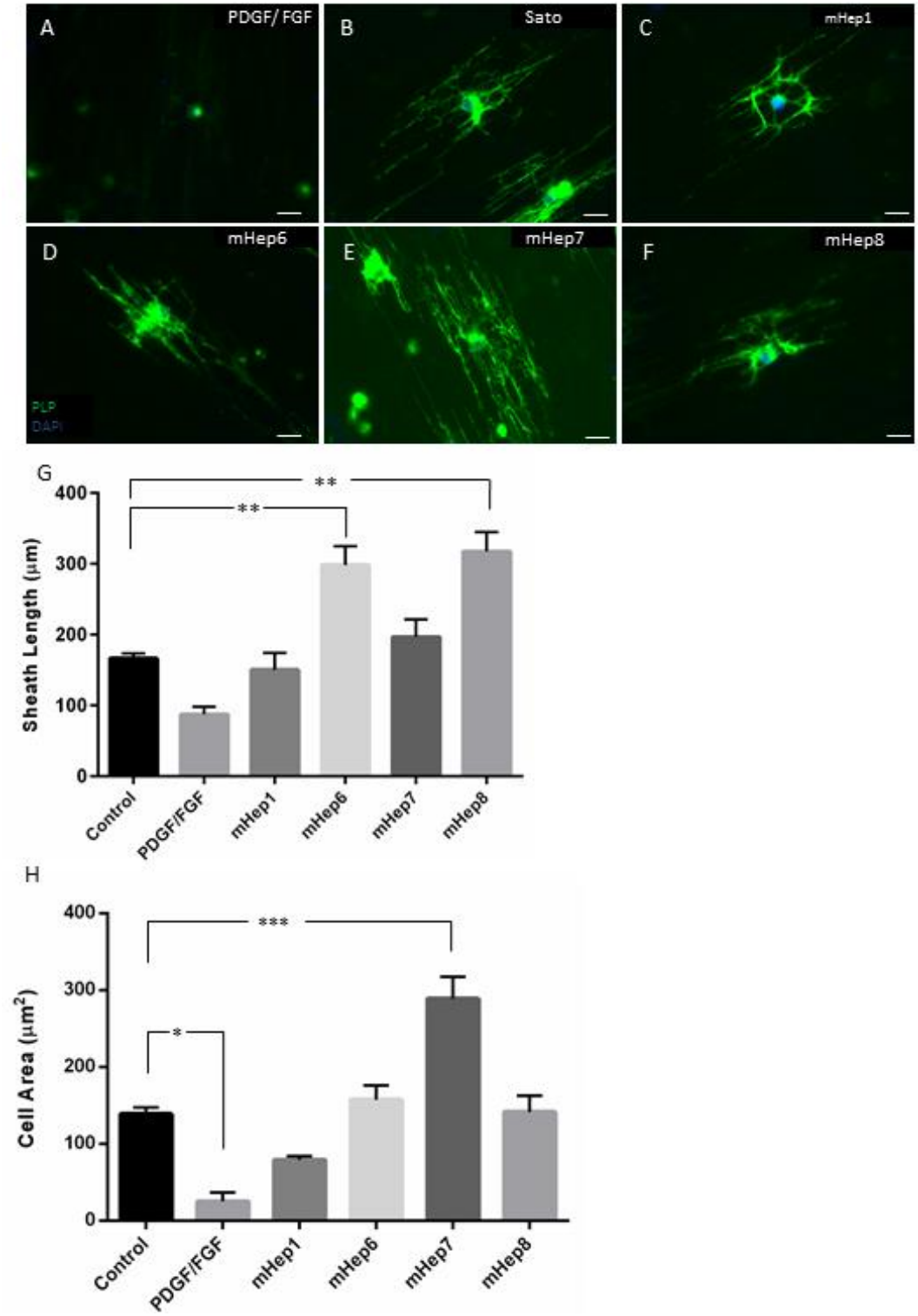

Figure 4.8 Promotion of myelination by Desulphated mHep maybe due to process stabilisation and increased cell size

Desulphated mHep7 caused a statistical increase in the OL cell size following treatment, with an increase of 170 µm compared to control (E and H). mHep6 and 8 statistically promoted sheath length compared to control (D, F and G). Statistical test used was one-way ANOVA with post-hoc Dunnett's multi-comparison correction, $p<0.05$ * $p<0.001$ **and $p<0.0001$ * represented in graph (A-B) N=4 and scale bars-25 µm error bar-SEM.**

4.3.8 2-*O*-sulphated mimetic inhibits OPC proliferation by binding FGF2 ligand but not the FGFR

To determine whether mHeps inhibit FGF2 signalling by binding to the FGF2 ligand but not presenting the ligand to the receptor, monocultures of OPCs were treated with FGF2 (a known activator of proliferation) and with mHeps to assess whether the mimetics blocks FGF2 activity.

OPCs were seeded on to PLL-coated coverslips at a concentration of 500 cells/μm^2 in 500µl of BS media containing; PDGFα and FGF2 and maintained for 5 days. The OPC media was then switched to BS media containing a combination of mHeps (1 ng/ml) plus FGF2 (50 ng/ml).

Treatment with FGF2 alone induced OPC proliferation compared to BS control, with an average of 61% proliferation versus 41% (Fig.4.9.E). FGF2-mHep6 co-treatment reduced the mitogenic activity of FGF2 alone, with levels decreasing to 21% (Fig.4.9.C-E). Treatment with FGF2 plus mHep1 enhanced OPC proliferation compared to FGF2 alone, with an average percentage of BrdU incorporation increases to 70% (Fig.4.9.E).

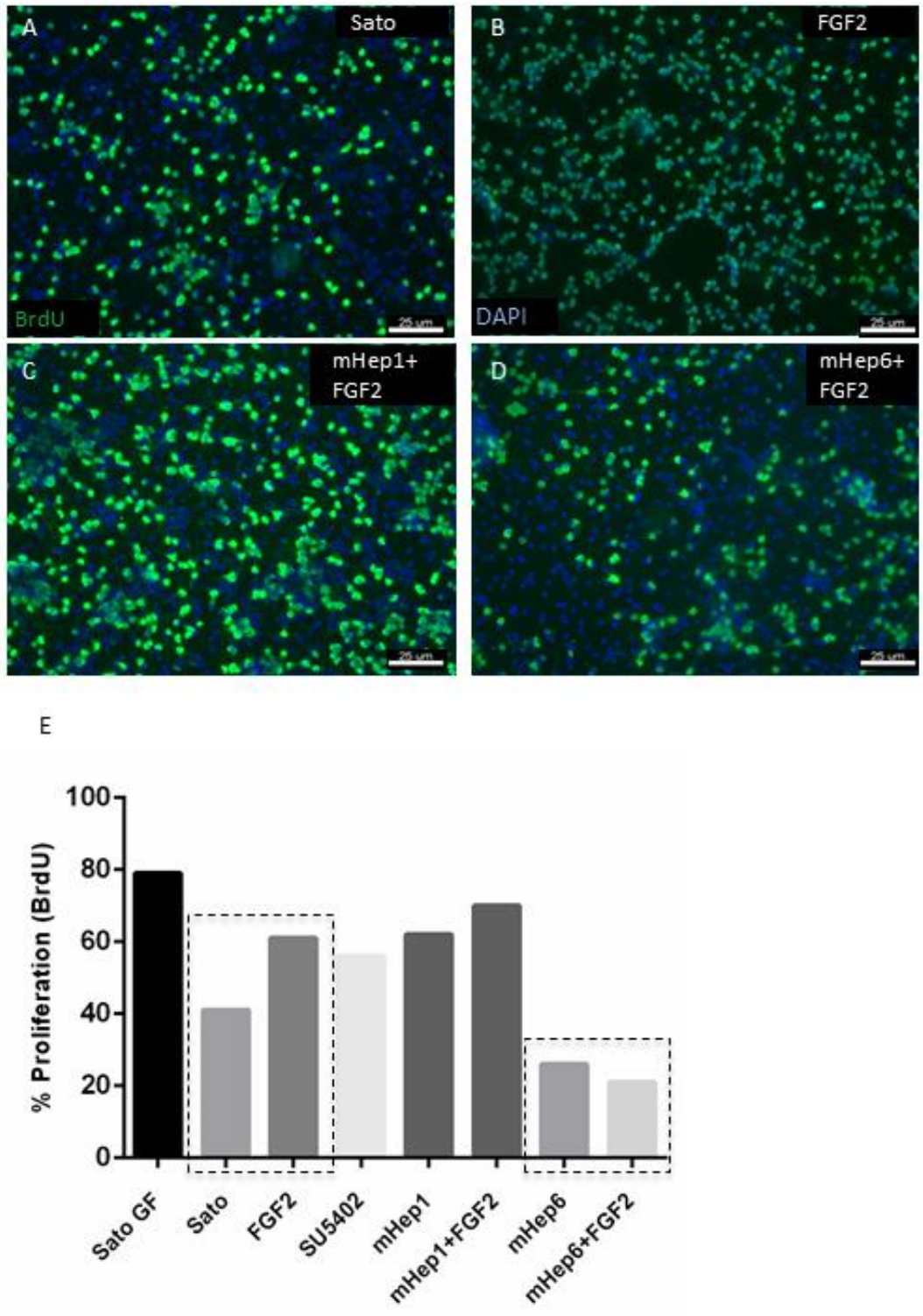

Figure 4.9 2-*O*-sulphation (mHep6) can immobilise FGF2 ligand and inhibit signalling activation leading to a decrease in OPC proliferation

OL ensheathment experiments the cultures were treated with each mHep compounds at 1 ng/ml for 7 days. The cultures were co-stained with appropriate OPC/OL markers either immature OL marker (04, red) or myelin marker (PLP, green) and DAPI (nuclei, blue). FGF2 treatment alone promotes 60% OPC proliferation an increase on Sato alone 41% (A-B and E, marked black dashed box). mHep6/FGF2 co-treatment removes the proliferative effect of FGF2 to 23% which is similar to mHep6 alone 26% proliferation (C-E, marked black dashed box). mHep1/FGF2 co-treatment slightly enhances the FGF2 proliferative effect compared to mHep1 but increase dramatically compared to Sato control (E). N=1 and scale bars-25 µm.

4.3.9 *N*-sulphation position (mHep7) has demyelinating effects in established myelinating cultures

For myelin maintenance experiments, the uninjured myelination cultures were treated with each mHep compound at 1 ng/ml for a single treatment at day 25 for 5 days at which point cultures were fixed, stained and analysed.

No significant effect was recorded on neurite density following with any mHep treatment (Fig.4.10. A-E). Highly sulphated mHep 1 significantly decreased the levels of myelination with myelin percentages falling to 5.3 ± 2.3% compared to control 12.5 ± 2.25% (Fig.4.10 B and F). Desulphated mHep7 had similar effects on the level of myelin, with 7.2 ± 0.9% average myelination, mHep6 and mHep8 had no statistically significant effect on myelin values; 10.7 ± 2.5% and 10.3 ± 2.9% (Fig.4.10.F).

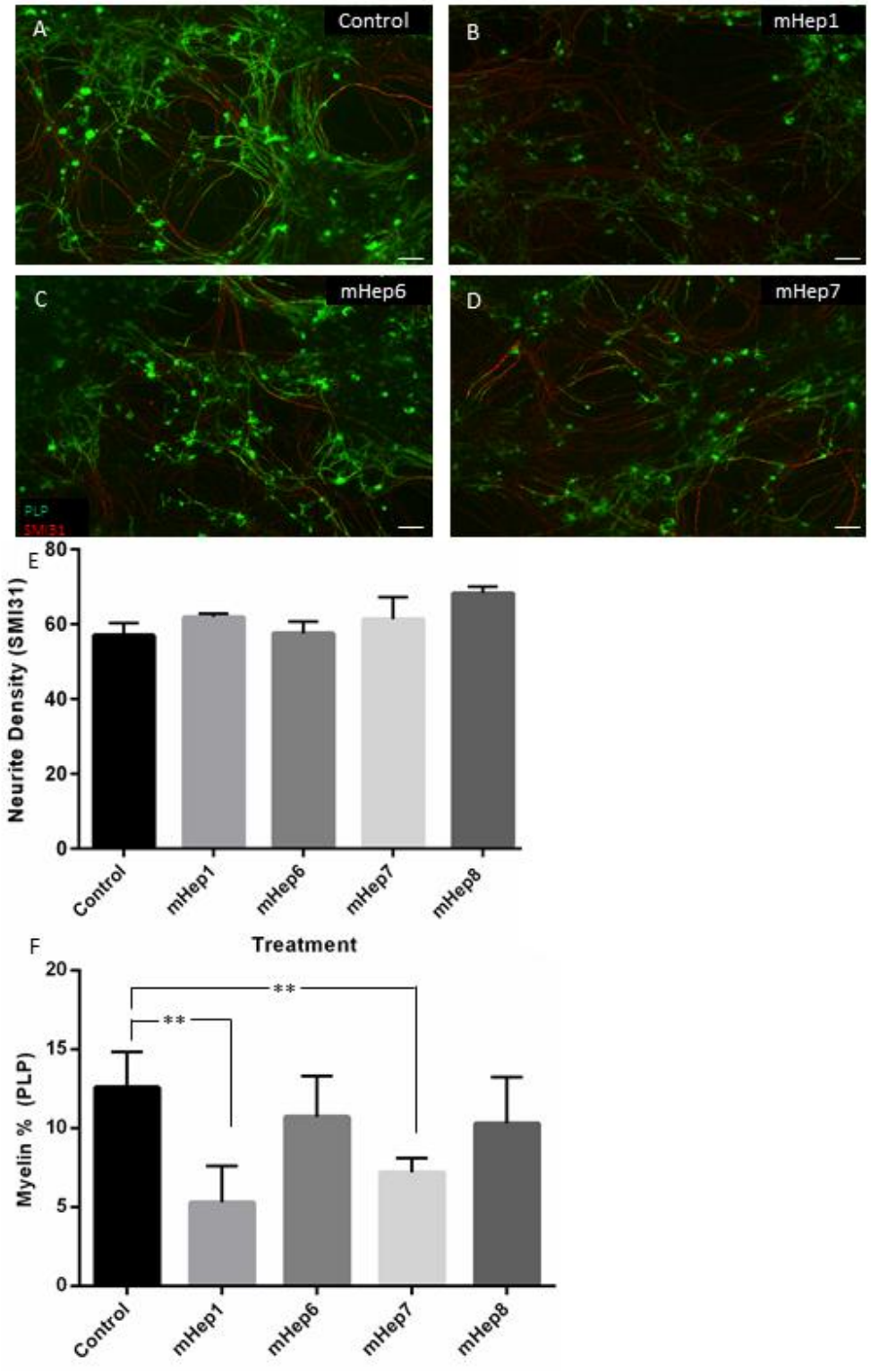

Figure 4.10 Desulphated mHep7 and sulphated mHep1 have demyelinating effects on healthy cultures following a single treatment.

No effect was seen on neurite density (SMI31, red) following treatment with any mimetic (E). mHep 1 (B) and mHep7 (D) significantly decreasing myelination following a single treatment, compared to control (A and F). mHep6/8 did not statistically promote myelination with levels reaching slightly greater than 10% (C [representative of 10% myelination] and F). Statistical test used was one-way ANOVA with post-hoc Dunnett's multi-comparison correction, $p<0.001$ represented ** in graph (F). N=6 and error bars-SEM, scale bar-25 µm.

4.3.10 *N*-sulphation and 2-*O*-sulphation could be promoting myelination through the activation of the canonical Wnt pathway.

The myelinating cultures were incubated until day 24 then a cut was made across the cultures using a flat edge scalpel blade. The lesion created a focal (650 µm) decrease in neurite density and myelination levels adjacent to the lesion. Cultures were subject to a single treatment on day 25 with mHep6 and 7 at a concentration of 1 ng/ml. Mechanisms by which the mHeps might work was investigated by treating the cultures with mimetics plus a specific signalling pathway inhibitor. XAV inhibitor (blocks the canonical Wnt pathway by inhibiting ß-catenin) was used at a concentration of 200 nM. Following treatment, cultures were incubated for 5 days before being fixed, stained and analysed for neurite density and myelination.

There was no significant effect on neurite density after co-treatment with mimetics and XAV inhibitor compared to mHeps alone and control (Fig.4.11.G).

As seen in Results: 4.3.1, mHep6 and 7 can promote myelination following injury to the myelinating culture. The promotion in myelination observed with mHep6 was removed following co-treatment with XAV (Fig.4.11.C-D and H) and significantly decreased when compared to mHep6 alone (4.11.F). mHep7 co-treatment with XAV significantly decreased myelination compared to mHep7 alone and was similar to that of the control level (Fig.4.11.D and F). XAV treatment alone decreased myelination but not significantly when compared to controls (Fig.4.11.B and F).

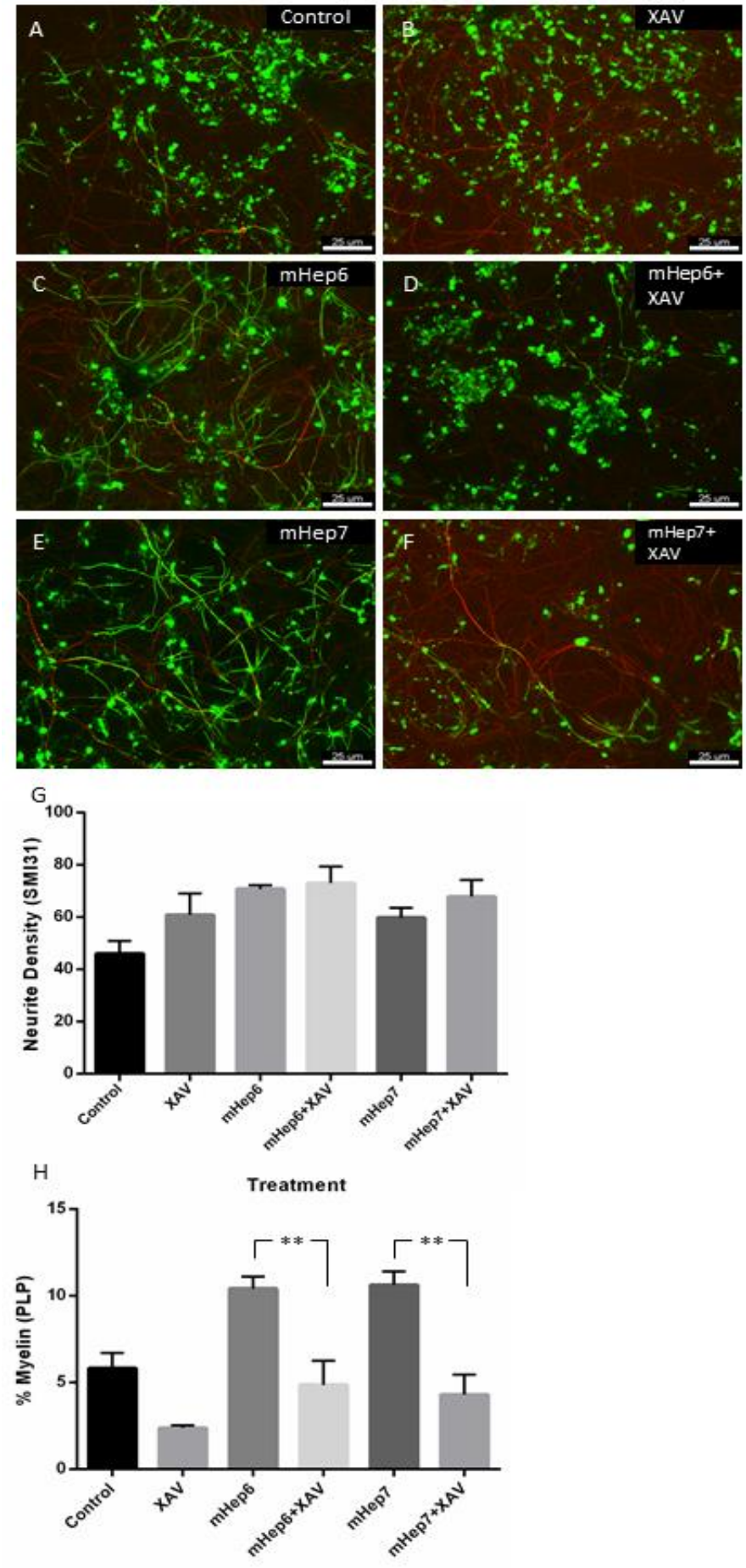

Figure 4.11 Canonical Wnt signalling pathway activation could be in part involved in mHep6 and mHep7 promotion of myelination.

XAV inhibitor alone (B) was not significant compared to control (A) There is a significant reduction in the mHep6 (C) and 7 (E) effect on myelination following the inhibition of β-catenin mHep6+XAV (D) and mHep7+XAV (F), graphed in H. There is no statistical change in the neurite density effects following the same treatment course on neurite density (G). Statistical test used was one-way ANOVA with post-hoc Dunnett's multi-comparison correction, p<0.01 represented ** in graph (H). N=6 and error bars SEM, scale bar- 25 µm.

4.3.11 mHep7 promotion of neurite outgrowth is mediated through the Wnt pathway.

Injury to the cultures results in an initial cell free space with very low numbers with averages of 3 neurite acrossing the lesion. The cultures were co-treated with mHep6 and or 7 at 1 ng/ml and XAV inhibitor at 200 nM on day 25, then allowed to recover for a further 5 days at which point cultures were fixed, stained and assessed for neurite outgrowth across the lesion.

Desulphated mimetics mHep6 and 7 significantly promoted neurite outgrowth across a lesion compared to the untreated control (Fig.4.12.C,E and G). XAV inhibitor alone promoted the number of neurites per field of view to 17 compared to the untreated control with 4 (Fig.4.12.A-B and G).

XAV inhibitor-mHep6 co-treatment did not remove the promotion of neurite outgrowth created by mHep6 alone with number of neurites per field of view averaging at 15 compared to 13 in mHep6 alone (Fig.4.12.C-D and G)

Following mHep7- XAV co-treatment there was a significant decrease in neurite outgrowth compared to treatment with Hep7 alone (Fig.4.12.E-G). However, neurite outgrowth of the co-treatment was still significantly increased compared to the untreated control (Fig.4.12.F-G).

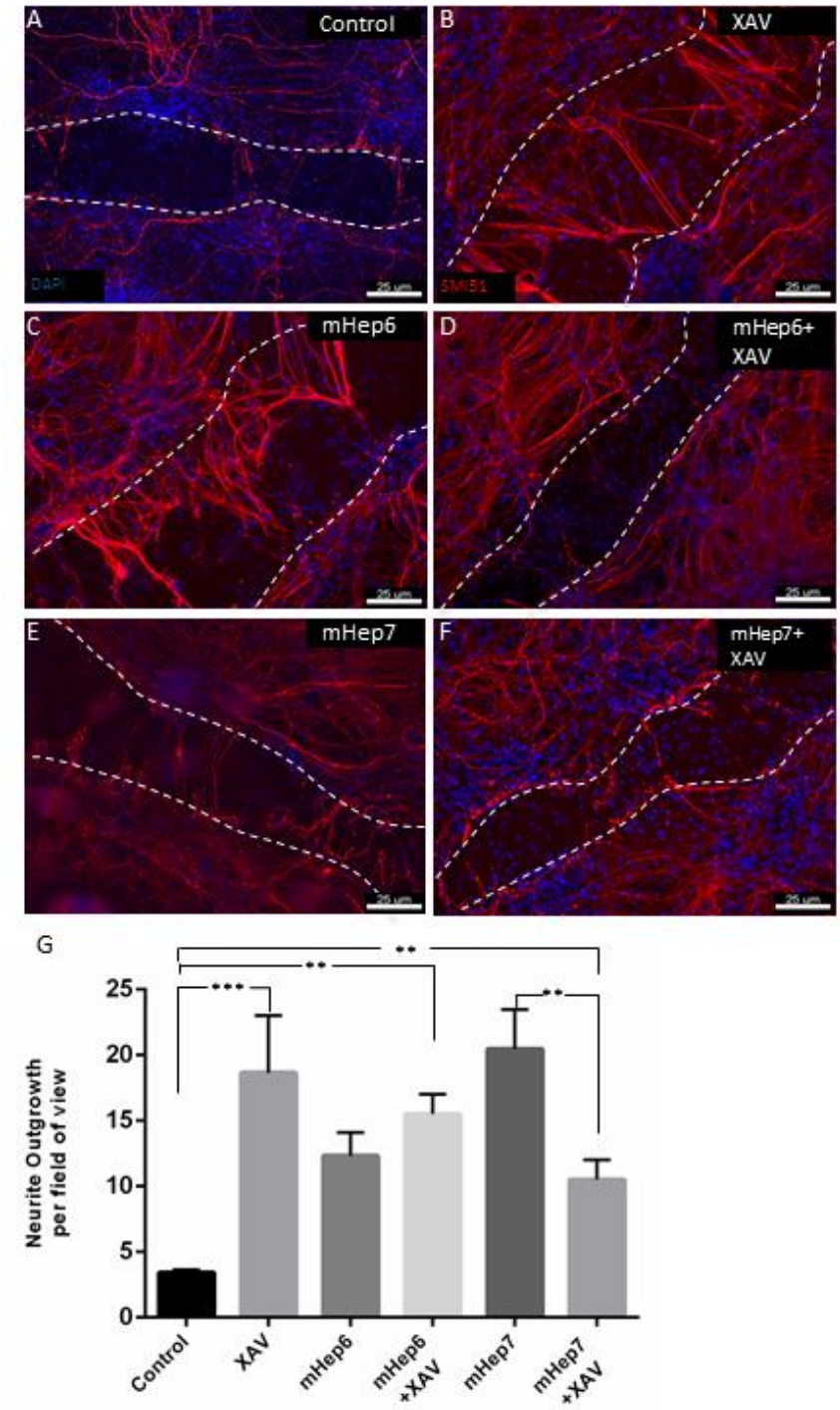

Figure 4.12 Canonical Wnt signalling pathway activation could be in part involved in mHep6 and mHep7 promotion of neurite outgrowth.

XAV inhibitor alone cause a significant increase in neurite outgrowth compared to control (A-B and G). mHep6/XAV co-treatment did not result in a removal of neurite outgrowth activity (C-D and G). Whereas, mHep7/XAV co-treatment saw a significant reduction in neurite outgrowth compared to mHep7 alone (E-G). However, mHep7/XAV co-treatment increased neurite outgrowth number is significant compared to control (A, F-E). Statistical test used was one-way ANOVA with post-hoc Dunnett's multi-comparison correction, p<0.01 and p<0.001*** represented in graph (H). N=6 and error bars-SEM, scale bar-25 µm.**

4.4 Discussion

It has been shown that Heparin and its mimetic derivatives have many binding targets (Coombe and Kett 2012). It has been suggested that modulation of certain factors (mimetic-binding-proteins) within an injury site could have therapeutic benefit. For these reasons, several heparin mimetics were created in the pursuit of tissue repair properties heparin may possess.

This has led to the investigation and hypothesis that the introduction of desulphated heparin mimetics can have multiple therapeutic benefits and used for the treatment and understanding of SCI.

Four heparin mimetics, mHep6 (2-*O*-sulphated), mHep7 (*N*-sulphated), mHep8 (total desulphated/*N*-acetylated) and mHep1 (commercial heparin), were examined for their capacity to promote myelination and neurite outgrowth following injury in a complex *in vitro* CNS injury model. This type of assay, where multiple cells types are interacting to create a complex CNS myelinating culture which can be injured which then mimics many key features of SCI, is a powerful screening tool for potential therapeutics (Boomkamp et al. 2014; Boomkamp et al. 2012).

mHep6 and mHep7 have been shown in this study to have potential therapeutic benefit, both showing promotion in both myelination and neurite outgrowth. However, with continued investigation the mimetic with *N*-sulphation (mHep7) demonstrated demyelinating effects on healthy established cultures suggesting a duality in effect; beneficial in injury and detrimental in steady state. This potentially has far-reaching effects in that off-target effects of mHep7 could undermine benefits and be potentially catastrophic to SCI patients.

Following the recorded promotion in myelination and neurite outgrowth, the successful mimetics were carried forward for more detailed investigation. This entailed looking further with the SCI model and monocultures of individual cell types contained in the culture.

Turning to monoculture experiments, it was shown by two different methods that mHep6 and mHep7 even though thet had myelin promoting properties, their effects on OPCs and OLs were quite different. However, the experimental options available for detailed neurite outgrowth investigation are limited.

In this study we suggested a novel therapeutic approach in the form of mHeps for SCI repair. The principle finding of this study was; partially and fully desulphated heparin mimetics promote neurite density, myelination and neurite outgrowth following a single treatment after injury. From this finding, a secondary hypothesis was formed that the mHeps act by altering the availability and thus change activity of certain signalling pathways. This was investigated using commercially available receptor blockers to identify specific pathways involved during mimetic treatment.

By understanding the individual mHep mechanisms and cellular responses, we can in turn further suggest how to best modify the mHep compounds to increase treatment potency and potentially further promote the beneficial effects associated with a given mHep.

4.4.1 mHeps' effects on myelination

This study recorded an increase in myelination adjacent to the lesion following a single treatment of mHeps 6, 7 and 8, at 1 ng/ml concentration 1 day post injury (4.3.1). The complex nature of the culture makes identifying the specific cells and mechanisms involved very difficult. Therefore, OPC/OL monocultures were used to assess the effects of the mHeps on these cells which directly involved in myelination, investigating, proliferation, differentiation and OL; ensheathment and internode length (4.3.5 and 4.3.7).

4.4.2 mHeps and myelinating glia

The recorded promotion of myelination by mHeps 6, 7, 8 and the reduction in myelination by mHep1 (Fig.4.2) resulted in the investigation of the mimetics on OPCs and OLs as these are the specialised cells responsible for myelin sheath formation and axonal ensheathment.

It was found that treatment with desulphated mimetics, mHep 6 and 7, in an OPC monoculture decreased OPC proliferation, suggesting the inverse response of differentiation. These observations implicate 2-*O*-sulphate and *N*-sulphate positions (mHep6 and 7 respectively) as key mediators of certain signalling pathways resulting in OPC proliferation and differentiation (Fig.4.6). However, mHep8 which lacks both of these sulphate moieties (Fig.4.1.D) also yields increases in myelination. This result, coupled with the results from the mHep6 and 7 experiments, suggests that introduction of desulphated mimetics is more beneficial than their more sulphated counterpart; mHep1.

The shift to OPC differentiation was supported by counting the number of OLs adjacent to the lesion in the complex culture, with an increase in OLs compared to untreated control following treatment with desulphated mHeps 6, 7 and 8 (Fig.4.7). This suggests that the increase in myelination following treatment with desulphated mimetics on injured cultures could be in part due to the inhibition of proliferation and the induction of OPC differentiation and maturation. Thus, increase OL number corresponds to the mimetic inducing OPC differentiation and inhibition of OPC proliferation.

Similar observations have been made relating to neural cell proliferation in the developing brain and in an *in vitro* study of spinal cord neural precursor proliferation. These studies concluded that, sulphation is crucial in the proliferative state of a cell, demonstrated by treatment with sodium chlorate which inhibits sulphation of the HSPG, thus, leading to a disruption in proliferation of a cell line (Ford-Perriss et al. 2003) (Karus et al. 2012). Therefore, by introducing desulphated mHeps into the injured culture we are disrupting the proliferative state of the OPCs and could be inducing differentiation to myelinating oligodendrocytes which would allow for promotion of myelination of spared axons.

Inversely, treatment with a highly sulphated mimetic (mHep1) lead to an enhancement of OPC proliferation. A similar observation was made by Becker-Catania and colleagues, but here they suggest that heparin potentiates OPC proliferation through the mitogenic factor such as FGFa (Becker-Catania et al. 2011). OL number adjacent to the lesion was also reduced following mHep1 treatment suggesting that OPC proliferation (potentially even increased) is maintained at the injury site. These responses to mHep1 treatment could potentially lead to a reduction in myelination following injury. Heparin has also been shown to have proliferative effects on non-neuronal cells, specifically smooth muscle cells. This study concluded that the proliferation relates to the level and position of the sulphate groups on the heparin polysaccharide. It was shown that substitutions of *O*- and *N*-sulfo groups relates to the heparin anti- proliferative activity (Garg et al. 2008). The data using the SCI in vitro model also recorded an anti-proliferative activity on OPCs by the desulphated mHeps (4.3.5).

The variations in the chemical composition of each of the mimetics could lead to different ligand/receptor interactions within the injury environment. For instance, mHep6 (desulphated at C6, sulphated at C2, Fig.4.1.C) may be mimicking the sulphation state of the endogenous OPC HS-GAG sulphation pattern which has a similar chemical structure to mHep6. Properzi and colleagues observed an increase in HS sulphated at C2 following injury to the CNS. They concluded that OPCs have increased 2-*O*-sulphated HS GAG chains compared to OL suggesting an immaturity and an inability to bind certain

growth factors which would otherwise elicit proliferation (Properzi et al. 2008). Therefore, treatment with exogenous soluble heparin mimetics which are 2-*O*-sulphated could be indirectly competing for the ligands/receptors which would otherwise bind to the OPC cell surface HS and elicit a proliferative injury response.

Both *in vivo* and *in vitro* studies have demonstrated that there is a loss of myelination adjacent to and at the site of injury even though OPCs are present. However, these OPC do not differentiate into mature myelin forming OL. Mimetic treatment induces OPC differentiation and OL myelination of the spared axons. The data generated in this study suggests that the OPCs at the site of injury have the capacity to mature and form myelin-producing OL but the injury microenvironment is not permissive to elicit this process. Therefore, the mimetics counteract the injury microenvironment and promote the recovery of myelination.

The desulphated mimetics create an environment permissive for myelination to occur. Evidence has been provided suggesting that the mimetics directly impact the OPC/OL state at the site of injury. The exact mechanism in which the mimetics are acting still remains elusive, however, looking to the potential role of mimetic acting as a co-factor for cell signalling may provide an answer.

4.4.2.1 Mimetic promotion in myelination potentially through ligand immobilisation and signalling deactivation

It has been known for some time that heparan sulphates act as a co-factor for FGF signalling. Using biochemical techniques it has been shown that the sulphate moieties on the GAG chain specifically the 2-*O* and 6-*O* carbon position on the iduronic acid and glucosamine residues are crucial for ligand binding (2-*O*-sulphate) and receptor activation (6-*O*-sulphate). With this knowledge we hypothesised that the mimetic treatment may be interfering with FGF signalling, and FGF signalling has also been well known to dictate OPC proliferation. Therefore, it was theorised that mHep6 could be acting as a 'sponge' or blocker for the ligand and inhibiting FGF signalling, as it lacks the appropriate sulphate moiety required to bind to and activate the receptor (Fig.4.1.C). Therefore, endogenous mHep6 (sulphated at only C2) blocked FGF signalling and caused OL differentiation leading to increased myelination. This appeared to be the case, following OPC co-treatment with mHep6 and FGF2 ligand (Fig.4.9). FGF2 has been shown to induce OPC proliferation (it is actually a part of the BS DMEM enriched media required for OPC culture). Here, it is evident that FGF2 ceased to induce OPC proliferation when it was co-treated with mHep6, suggesting that mHep6 is mopping up the FGF2 ligand, and due to mHep6 lacking 6-*O*-sulphated moiety it cannot form the

FGF-HS-FGFR complex leading to silencing of FGF signalling and in turn OPC proliferation. As a proof of principle FGFR blocker SU5402 was introduced to the OPC culture which led to similar observation on OPC proliferation generated by mHep6 (Fig.4.9.E).

Under the same hypothesis, treatment with mHep1 or heparin which has both 2-*O* and 6-*O*-sulphates, would therefore, promote OPC proliferation. Increased OPC proliferation was observed in monoculture and enhanced proliferation in the presence of mHep1/FGF2 co-treatment, when compared to BS-Sato control and to mHep6 (Fig.4.9.E). Therefore, this suggests that mHep1 did not promote myelination following injury due to its role in enhancing OPC proliferation, preventing OL differentiation and subsequent myelination of spared axons.

FGF signalling is one of many cell signalling pathways which mediate their signalling through the sulphated HSPGs. Therefore, other pathways were considered, which have been shown to play a role in myelination which signal via HSPG involvement. This has led to the use of specific signalling inhibitors.

These FGF2 co-treatment experiments were a proof of principle experiment testing the hypothesis of ligand immobilisation (or ligand 'sponge'). The mimetic mode of action has by no means been uncovered, what has been demonstrated here is that mimetics which lack certain sulphated moieties can bind to but not act as co-factors for certain signalling complex activation. There are many more signalling ligands and receptors in which our mimetics are interacting with but it has been demonstrated that interceding in injury mediated signalling disruption can be an effective approach to SCI therapy.

4.4.2.2 Promotion in myelination by mHeps and activation of Wnt signalling

In parallel with identifying the cellular target of the mHeps, an investigation was carried out into the role of mHeps and signalling activation. Data presented here suggested that the desulphated mHep6 and 7 may have a role promoting the canonical Wnt signalling pathway. Wnt signalling, specifically the canonical pathway, has been implicated in the activation of myelin genes and formation of compact myelin (Tawk et al. 2011). Using the commercially available ß-catenin inhibitor, the role of the canonical Wnt signalling pathway was assessed in its activation following treatment with the mHeps.

Here it was shown that following the co-treatment with mHep6 and 7 and the ß-catenin inhibitor, XAV, the promotion of myelination was abolished (Fig.4.11.H), suggesting that mHep6 and 7 are activating the canonical Wnt pathway.

It has previously been shown that the 2-*O*-sulphate in HS GAG chain is required for the activation of the canonical Wnt pathway (Cadwalader et al. 2012). Wnt signalling has long been implicated in OL myelination. ß-catenin has been shown to be present in the OLs and active in both a developmental and lesioned CNS (Fancy et al 2009). However, its involvement and dysregulation in demyelination and remyelination still remains unclear. A study identified Wnt/ß-catenin as an essential promotor of myelin-associated gene expression. This study also showed that blocking Wnt signalling reduces PLP (myelin) in OL but activating Wnt1 ligand increases the expression of myelin-associated genes through the promotion of ß-catenin binding to T-cell factor/lymphoid-enhancer factor transcription factor (Tawk et al 2011). Another study demonstrated that a continuous activation of Wnt signalling in OPCs displays a hypomyelination phenotype in ß-catenin dominant-active transgenic mice (Fancy et al 2009). This observation could potentially explain the data gathered in our study specifically relating to the treatment strategy employed; a single treatment followed by recovery. This suggests that ß-catenin could be initially upregulated by mHep7 then in the subsequent days the same pathway in no longer being activated, therefore, 'resetting' the pathway transiently leading to a beneficial effect.

OPC differentiation to OLs and a change in the microenvironment, such as through injury, involves intermediate cellular phenotypes or a 'spectrum of cells' which will have different receptors and ligand profiles which control the differentiation process. This suggests that signal manipulation by the mimetics can have the same biochemical effects on the ligand/receptor but the presentation or immobilisation of a signalling pathway depends upon the presence of the ligand/receptor on a cell.

FGF2 activation was investigated to demonstrate the function of the mimetics as a ligand 'sponge', specifically mHep6 which is 2-*O*-sulphated. However, due to the promiscuous nature of HS binding many other signalling pathways could also be influenced by the mimetics. One such signalling pathway which requires the loss of 6-*O*-sulphation of the cell surface HSPG for activation is Wnt signalling (Ai et al. 2003). This is due to 6-*O*-sulphate binding Wnt with high affinity and competing with the ligand for the Frizzled receptor. So through the introduction of mimetics lacking the 6-*O*-sulphate moiety, Wnt signalling could be initiated indirectly through none-active competition for the ligand (Dhoot et al. 2001). Thus, evidence was provided in this study that mHep6 does initiate Wnt signalling, leading to promotion in myelin following injury. This was

tested experimentally by, mHep6 and β-catenin inhibitor co-treatment, which demonstrated that the activation of the canonical Wnt pathway via the non-competitive binding of the ligand by mHep6 can be removed to 4.5% (Fig.4.11.H) through the inhibition of β-catenin. This was tested in the complex injury setting to demonstrate the mimetic effect in an injury environment and that Wnt signalling activation was taking place. This provides a more transferable demonstration of the mechanistic role of mHep6 in an injury setting which is difficult to recapitulate in a monoculture.

The culture used in this study identified mHep6 and 7 as a mediator of the Wnt/ ß-catenin signalling pathway. The specific cellular target for Wnt/ß-catenin in the SCI model remains unknown. Many studies have focused on OPCs/OLs, however there are multiple cell populations which could impose a Wnt signalling effect on the OPCs/OLs.

It has been shown that 2-*O* and 6-*O* sulphation positions are required for both the immobilisation and activation of FGF and Wnt signalling (4.3.8 and 4.11). Through the introduction of a mimetic which has 2-*O*-sulphation and 6-*O*-desulphation, it was demonstrated that both the inhibition and activation of FGF and Wnt signalling respectively is possible (Fig.4.9 and Fig.4.11). Previous studies have conferred with some of the observations made here specifically the biochemical interactions of mHep6 (Higginson et al. 2012). However, what was shown in this study is that N-sulphation (mHep7) can also initiate Wnt signalling, however, very little known about the role of *N*-sulphation and Wnt signalling activation. N-sulphation has been shown to be crucial in PDGF-B activation (Abramsson et al. 2007) and interestingly PDGF-B has been implicated in reductions in secondary damages after SCI.

What these experiments demonstrate is that the different mimetics have a diverse set of signalling modulation abilities. I have only scratched the surface of the exact mechanism of action. However, evidence has been provided implicating two signalling pathway interactions, the immobilisation of FGF signalling leading to the inhibition of OPC proliferation and subsequent OL differentiation and promotion in myelination and the activation of Wnt signalling and myelination. Continued study is required to provide a more detailed signalling profile picture of SCI and their manipulation by the mimetics. However, it can be clearly seen that there is great promise for heparin mimetics as a treatment strategy for SCI.

4.4.3 mHeps' effects on neurite outgrowth

This study recorded an increase in neurite outgrowth across the lesion following a single treatment of mHep5, 6, 7 and 8, at a concentration of 1 ng/ml 1 day post injury (Fig.4.3.G).

These mHeps could be directly affecting neurite outgrowth, rescuing the disrupted interaction of a the GAG chains of the resident HSPG or through artificially mimicking their interaction with the growing neurite (Lander et al. 1982). Or indirectly by altering surrounding cellular behaviour which then creates a permissive environment for outgrowth.

The introduction of single desulphated mHeps, mHep6, 7 and fully desulphated mHep8, resulted in the promotion neurite outgrowth across a lesion. Similar data has been generated by Karumbaiah and colleagues targeting CSPGs sulphation levels. In this study, siRNA knockdown of the astrocytic sulfotransferase enzyme (sulphates C4 and C6) led to the promotion of neurite outgrowth (Karumbaiah et al. 2011). This provides further evidence that the sulphation levels of heparin or resident GAGs, specifically a more desulphated environment, is permissive to neurite outgrowth.

It has been suggested in this study that the specific sulphation position on the disaccharide unit could be crucial. The specific sulphation pattern could dictate which signalling pathway is initiated. Data generated here has shown that 2-*O*-sulphation and *N*-sulphation occurring in isolation support neurite outgrowth. Other studies have observed similar results, mutants having defects is the Hst-2 gene which encodes the enzymatic activity of the 2-*O*-sulphation of the glucosamine on the HS display axonal patterning defects (Kinnunen et al. 2004). Suggesting that 2-*O*-sulphate is involved with neurite outgrowth and pathfinding. However, mHep8 which lacks any sulphated moiety in the three modification positions yet also promotes neurite outgrowth. This suggests that the overall level of sulphation may be in part the reason for the outgrowth observed.

Desulphated heparin mimetics have been shown in this study to promote neurite outgrowth (4.3). Once again the different sulphation patterns of the mHeps could be crucial in identifying their specific mode of function. For example, mHep6 mimics the sulphation pattern of syndecan, an HSPG, in that they both have 2-*O*-sulfation of the iduronic acid residue. Interestingly, syndecan has been implicated in what has been termed ligand 'shuttling' which presents ligands to the neuron and triggers outgrowth. Additionally, syndecan has been shown to be able to bind and present Wnt ligands to

neurons (Beller and Snow 2014) (Tkachenko et al. 2005). Therefore, treatment with mHep6 could be providing the neurite with growth factors which then initiates outgrowth.

An additional mimetic was shown to have neurite outgrowth benefit; one which did not have positive myelination properties – mHep5. However, criteria was set which states that only a mimetic which displays both promotion of myelination and neurite outgrowth will be subject to further study. For this reason mHep5 was not carried forward for more detailed study. However, mHep5 data has demonstrated that each of the three modification sites individually has neurite outgrowth activating potential. However, 6-*O*-sulphate position on the glucosamine along with 2-*O*-sulphate on the iduronic acid and *N*-sulphation on the glucosamine can initiate neurite outgrowth but when each of these sulphate positions are simultaneously sulphated there is no promotion of neurite outgrowth as seen with mHep1. This suggests that to increase potency of the effect, combinations of all sulphated sites is not the answer. This is valuable information for future mimetic designs and sulphated modification combinations. However, it is not known if dual sulphation for example 2-*O*-sulphation and *N*-sulphation, lacking 6-*O*-sulphation could increase neurite outgrowth, we do not know but is a logic next step in the pursuit of neurite outgrowth potency.

4.4.3.1 Desulphated mHeps promote neurite outgrowth partially through the activation of the Wnt pathway

The canonical Wnt pathway has been well documented. It acts via the presentation of ligands in a gradient manner, suggesting a strong link between neurite outgrowth and axonal pathfinding (Salinas 2012).

Data from this study suggests that ß-catenin may play a role in neurite outgrowth and possibly a partial target for mHep7 following treatment. In co-treatment of mHep7 with ß-catenin inhibitor, we saw a partial removal of the mHep7 effect on neurite outgrowth; less than that of mHep7 alone but still a statistically significant promotion of neurite outgrowth compared to untreated controls. These data suggest that mHep7 is in part acting via the activation of the Wnt pathway and that neurite outgrowth activation requires multiple signalling pathways, specifically ones provided by mHep7 and *N*-sulphation interactions.

The role of ß-catenin in neurite outgrowth remains unclear (Endo and Rubin 2007; Zou 2004). Several studies provide conflicting observations but this could be related to the use of non-neuronal cells in their studies. Whether our treatment is ‘resetting’ the Wnt

signalling or stabilising β-catenin, we are unsure. However, evidence has been provided previously implicating Wnt in myelination so it is follows that the mimetic is interacting with the canonical Wnt pathway but in neurite outgrowth process.

My data suggests promiscuity in the heparin mimetic interactions in the culture with an interaction of the mimetics with the Wnt signalling pathway. The mimetic neurite outgrowth mechanistic story still remains elusive. A potential (partial) mechanism has been shown for mHep7 via the Wnt pathway. However, the inability to study the neurons-neurites in monoculture or in a structured organised fashion makes uncovering the exact mechanism very difficult. There are many cofounding factors in the complex culture with many cell types potentially involved in the outgrowth process. So it cannot be shown here if the mimetics are directly or indirectly acting on neurite. This problem is what generated the development of a novel model in which to study neurites isolated from their cell bodies.

4.4.4 mHeps' effects on astrocytes

Treatment with desulphated heparin mimetics showed multiple beneficial outcomes following treatment by promoting myelination, neurite density, neurite outgrowth and decreasing lesion size. This suggests either multiple cellular targets or the targeting of a cell which interacts with several different cellular processes. Astrocytes have been shown to mediate between many cellular populations and cellular interactions.

The glial scar is a major feature of SCI pathology; astrocytosis occurs following injury which is characterised by an alteration in astrocyte phenotype to a more reactive state (Faulkner et al. 2004). This shift in phenotype has been linked with contributing to pathology creating an environment non-permissive to axonal regeneration and remyelination. GFAP and Nestin are upregulated in astrocytes following trauma and are well established markers of astrocytosis. Following SCI there is a focal increase in nestin, by astrocytes which, however, has been suggested to be potentially neuroprotective.

The mimetics used in this study were previously used as a tool to assess the role of differentially sulphated heparan sulphates on cell-cell interactions, specifically OECs and SCs with astrocytes in a confrontational assay (Higginson et al. 2012). This study was the premise behind their use in this SCI model. The major finding from the Higginson study was that desulphated heparins do not induce a (negative) boundary between the cell populations and suggesting a role for sulfatases in the formation of the boundary.

What this study and the SCI model have in common is the astrocyte. Astrocytes have been implicated in a plethora of pathologies including SCI and the glial scar, which is a characteristic of this SCI model. The observations in this study, specifically neurite outgrowth, lesion size and myelination, have strong links with and are potentially mediated by the astrocyte. This led to our prediction that the heparin mimetics, specifically the desulphated versions, have beneficial effects on astrocytes which results in the beneficial effects on the cells which are mediated by the astrocyte, such as the OPC/OL and the neurites.

However, we did not see any beneficial effect on two common reactive astrocytic markers; nestin and GFAP. These two markers have been shown in numerous studies to be increased following damage to the astrocyte and suggestive of a negative phenotype. GFAP was not affected at all and nestin was actually increased following treatment with the desulphated mimetics. Interestingly, a study has shown that an increase in GFAP in astrocytes can promote myelination through the increased expression of CNTF (Nash et al. 2011a).

Astrocytes have been implicated with an increased expression of HSPG following injury to the cord (Properzi et al. 2008). They showed a strong upregulation in Glypican-1 (a HSPG) and an increase of the detrimental highly sulphated GAGs that are 2-*O*-sulphated on the astrocyte surface. A similar increase seen of 2-*O*-sulphation on OPC HSPG suggested that treatment with the 2-*O*-sulphate mimetic mHep6 could indirectly compete for the FGF ligand and nullify the signalling initiation and negative response to injury. However, this competitive blocking of ligand binding does not alter the reactive astrocyte phenotype as there is no change in the levels of common reactive marker protein levels following treatment.

Due to the beneficial effects observed with the desulphated mimetics and the diverse effects (both promotion in myelination and neurite outgrowth) it was hypothesised that these compounds may be mediating a change in the reactive astrocyte. However, there was no change in levels of GFAP and nestin levels actually increased following treatment with mHep6 and 7.

This could be potentially related to the low number of astrocytes migrating into the lesion site, with decreased density of seeding and migratory cells *in vitro* being shown to upregulate Nestin. Also Nestin has been shown to be activated by certain growth factors, such as NGF, FGF and CNTF. All of these growth factors are in part mediated by HSPG by acting as co-factors for signalling activation. This suggests that the treatment

with mHeps could be mediating the activation of nestin expression through the presentation of these growth factors to the astrocytes.

The Nestin positive cells have also been linked with reverting to a more immature/progenitor-like state (Lin et al. 1995). Another study linked low sulphated HSPGs and restriction of embryonic stem cell neural differentiation suggesting a crucial ratio of HSPGs and FGF4 ligand is required to be present for stem cells to undergo differentiation and even enabling the cells to survive (Forsberg et al. 2012). This study suggests that low sulphated heparin could maintain a more immature phenotype or developmental state. If desulphated mimetics establish an environment similar to early developmental stages around the injury site, this could be why there is repair and regeneration after trauma in this injury model. Evidence has arisen which suggests that successful regeneration after SCI needs to be accompanied by a developmental state which can aid in neural pathfinding and circuit-refining mechanisms (Harel and Strittmatter 2006). However, astrocytes are not the only cells within this mixed population of glia and neurons in the CNS which express nestin. Radial glia cells also express Nestin and have been highlighted as a potential cell of interest in CNS repair, being linked with creating a more favourable developmental-like environment. Incidentally, mature astrocytes can de-differentiate to a radial glia phenotype, providing a scaffold for neurons to extend processes (Leavitt et al. 1999). This cellular shift could be responsible for the effects observed following treatment with desulphated mimetic. Radial glia have not been explored in this study, however, with this new evidence that nestin levels are increased following mHep treatment, these cells require further investigation.

4.4.5 Treatment strategy

The treatment strategy used (single treatment then recovery) could also be affecting the outcomes we recorded. Previous treatment strategies using this model as published in Boomkamp 2012 and 2014, employ a continuous presence of the compound with administration occurring from DIV25 every other day until DIV31. However, this method was detrimental to the cultures during the preliminary stages of the study. This lead to both a reduction in the concentration of the compound but also to the number of times the compound was administrated following injury, and this method of treatment was then subsequently applied to the beneficial desulphated mimetics.

The treatment method used here could be a crucial factor in the promotion of myelination. The desulphated heparin mimetic effect on OPC/OL could be a balancing act between proliferation and differentiation. Rosenberg and Chan use the phrase

'Timing is everything' and following injury to the culture the single treatment as opposed to repeated treatments could be a factor in the promotion of myelination. Potentially, a sustained treatment could have yielded a different result. As alluded to earlier, persistent activation of a signalling factor could actually hinder the repair process. A study highlighted that overexpression of β-catenin can be detrimental to microtubule/actin organization (Ligon et al. 2001), therefore indicating that persistent activation of the signalling pathway targeted by the mHeps could potentially be detrimental to the both myelination and neurite outgrowth.

4.5 Conclusion

Selective desulphation of heparin has shown potential as a treatment for SCI using this *in vitro* SCI myelinating culture. The results gathered in this study demonstrate a role for sulphation in injury, in the form of exogenous desulphated mHeps inducing beneficial effects in the form of promotion of myelination and neurite outgrowth.

There is a possibility that the different biochemical structures of each heparin mimetic could be mediating different or multiple signalling ligands and receptors. Therefore, each mimetic could have different mechanisms of action, which could initiate different, potentially beneficial, recovery mechanisms following injury.

The mimetics could be potentially acting as a sponge and clearing the availability of a detrimental ligand removing the hyperactivity of the negative signalling pathway, or enabling the activation of a beneficial pathway. It seems that both may be the case. The promiscuity of the mimetics may be the combinational treatment approach that SCI needs but in the form of a single orchestrator molecule.

There are other factors which have not been addressed in this study relating to other structural features of the heparin molecule, such as the size of the carbohydrate. The size of the polysaccharide could alter the effect observed either negatively or potentially beneficially adding to the benefits and repair strength of the molecule.

Chapter 5

Development of a novel microfluidic device to study CNS injury and regeneration

5 Result: Development of a novel Microfluidic device to study SCI and regeneration

It is now apparent that conventional *in vitro* models are inadequate for the study of the CNS specifically, the highly specialised neuronal cells. Neuronal cells are specialised cells which extend processes over substantial distances and encounter many differing microenvironments. Conventional *in vitro* models do not provide control of the neuronal microenvironments and also they are inadequate in the study of the individual sections of the neuron such as the axon, dendrite or soma. Therefore, it is difficult to study molecular and cellular changes that occur during different states such as, during development or following injury. For this reason compartmentalisation devices have been developed which allow for controlled isolation of the different parts of the neuron. The first devised technique for neuronal cell compartmentalisation was the Campenot chamber, which allowed for the study of axons independently from their cell body (Campenot 1977). Campenot chambers were primarily used for the study of peripheral nerve injury and regeneration processes (MacInnis and Campenot 2002).

The next stage in CNS study has led to micro-scaled compartmentalisation devices and methodologies. The subject of micro scaled technologies was introduced previously (section 1.6.3.2). Lab-on-chip technology has been applied to cell biology and has created a powerful arsenal of tools for the study of neuronal-glial interactions and the targeted study of axons. Microfluidic technology is at the forefront of the *in vitro* revolution and has pushed boundaries, not only in cell biology, but, in fields such as protein crystallography, drug discovery and microbiology (Maeki et al. 2016) (Chi et al. 2016) (Probst et al. 2013) (Saleh-Lakha and Trevors 2010).

The microfluidic platform provides a means of not only compartmentalisation but also control of the fluidic microenvironment. This is due to the physical phenomena that intercedes at sub-millimetre dimensions within the devices. Microfluidic devices (MFD) take advantage of the change in forces that dominate within the devices. These include, creation of laminar flow, fluidic resistance and surface tension (Beebe et al. 2002). Conventional *in vitro* models are dominated by turbulent flow, whereas, microfluidic devices are dominated by laminar flow. These two fluid regimes differ in that laminar is controlled directional particle fluid flow and turbulent is chaotic/ unpredictable (Beebe et al. 2002). The fluid dynamics of a system is defined by Reynolds number (Re). This number is calculated using the fluid density, velocity of the fluid, viscosity and hydraulic diameter (of the microchannels). Any device using microchannels almost always involves laminar flow (White.F. 1991). Therefore, a Re <

2300 indicates laminar flow whereas, >2300 indicates signs of turbulent flow. The creation of laminar flow can lead to the creation and manipulation of particle diffusion within the device (Dertinger et al. 2001). Thus, creating an *in vitro* model (as it more accurately represents the fluid dynamics *in vivo)*, which allows the movement of extracellular fluid carrying secreted molecules, which can create diffusion gradients within in a microenvironment.

Microfluid devices are economically viable as the 'master mould' from which a particular microfluidic device can be cast, can be repeatedly used. The device is casted in Polydimethylsiloxane (PDMS) which is a relatively cheap elastomer (Peterson et al. 2005). The concepts of microenvironment manipulation and regulation of diffusion gradients make microfluidics a promising prospect for the study of SCI and neuroscience in general.

Neuroscience, like other areas of biological sciences, can exploit the benefits of microfluidics. This experimental tool allows for a multifaceted approach to the study neuroscience. For example, the study of genetically manipulated cells and their responses to various potential therapeutic treatments can be investigated using a microfluidic platform. This enables individual neurons and their axonal/dendritic processes to be studied in isolation allowing genetic diseases such as Parkinson's disease and Alzheimer's disease and their responses to be mapped in greater detail than compared to standard *in vitro* cultures (Song et al. 2014) (Seidi et al. 2011).

Electrophysiology can be performed within the device using patch clamping so the electrical functionality of individual neurons can be assessed. In addition, the study of localised physiology of isolated cellular projections such as axons can allow for comparison between the axonal and somal proteome and gene expression patterns (Taylor and Jeon 2010). Even the investigation of neurological behaviour is possible,a device has been created which again exploits the microfluidic technology but this time focusing on the multicellular organism *C.Elegans* (Chronis 2010). Here, the device was used to study locomotion and olfactory sensing in a precisely controlled manner by controlling the diffusion gradient. This enabled visualisation of whole organism neural activity, which is not possible using a standard non-compartmental and fluidically control *in vitro* system. The examples discussed have utilised the many benefits of microfluidics, but for the purpose of my study the salient quality of the microfluidic technology is the compartmentalisation of neuronal and glial cells and the introduction of targeted injury in a closed system. This enables the investigation of neurite outgrowth and myelination in a primary spinal cord cell culture in a manner not possible with our previous model or any published model.

The standard myelinating culture and the SCI model have a number of limitations when it comes to the study of axonal outgrowth and understanding the mechanisms of repair. The neuronal organisation in the myelinating culture is not representative of the *in vivo* physiology, specifically the neurons are not aligned, which results in neurites and neuronal cell bodies being proximal to each other. In the case of injury this creates an injury environment which is not seen *in vivo*, and potentially generating inaccurate responses in repair and regeneration processes. Furthermore, due to the lack of defined neuronal orientation, injury induction can be inconsistent between cultures making the targeted study of axons and other neurites very difficult. Finally, there is no compartmentalisation and isolation of cellular populations so focused treatment is not possible. Addressing all of these factors is crucial to gaining a better understanding of CNS repair and regeneration.

5.1 Aims

To overcome the limitations of the standard myelinating culture, the aims were

- Use commercially available culture isolation devices to compartmentalise the CNS populations of cells of the myelinating culture.

- Develop a novel microfluidic device for the study of axonal injury and repair.

5.2 Result: Using Ibidi® culture inserts to compartmentalise CNS cells for injury and regeneration

Our primary investigation into the compartmentalisation of neuronal cell bodies from their projections involved the use of commercially available culture inserts, Ibidi® Culture Inserts. These inserts are composed of two chambers aligned side by side, into which cells or molecules can be placed, after which the insert can be removed to allow the interactions of the components of the both chambers to be analysed (Fig.5.1.Ai). These products have been used previously for studying cell migration, wound healing and cell invasion (Chang et al. 2015) (Tolg et al. 2014) (Shih et al. 2012) (Higginson et al. 2012).

We aimed to use the Ibidi® insert, to compartmentalise neuronal cell bodies from the neurite projections. Figure 5.1 visually demonstrates the conceptual parameters of the

insert design of the method we employed, including the specific seeding arrangement and orientation.

5.2.1 Establishment of the seeding protocol for Ibidi® culture inserts as a means of isolating different cellular populations

A single Ibidi ® culture insert was placed on top of a standard 13 mm PLL-coated coverslip and adhesion occurred with light pressure applied to the insert. These were then inserted into a 24 well culture plate. The chambers of the insert will be referred to as insert chamber 1 and 2 with left chamber being 1 and right chamber being 2 (See Fig.5.1. ii-iii).

The astrocyte seeding protocol was performed as described previously in (Higginson et al. 2012) with some minor modifications. Neurospheres were first differentiated into astrocytes, then trypsinised and counted, using a cell density of 2-3 x 10^4 cells in 70 µl in chambers 1+2 (Fig.5.1. iv). Astrocyte confluencey was achieved in each chamber prior to the seeding of spinal cord cells.

Dissociated rat mixed spinal cord cells were generated as previously described (section 2.3) with slight modifications. Insert chambers 1 and 2 were emptied of all media prior to the addition of the spinal cord cell mix. Spinal cord cells were seeded 15 x 10^4 cells in 70 µl PM/DM+ (neuronal cell media) to chamber 1 and 70 µl PM/DM+ only in chamber 2 (Fig.5.1.v). The spinal cord mix was left to adhere for 2 hours before the culture insert was removed, with each chamber being emptied prior to insert removal to prevent unadhered cells from washing over to the neighbouring chamber. The entire well containing the culture was flooded with 500 µl of PM/DM+ and maintained according to the previously described myelinating culture method (section 2.8).

Following the removal of the insert, we hypothesised that the neurites should extend across the insert interface to the neural-free chamber, creating an area for targeted neurite injury investigation (Fig.5.1.vi-vii).

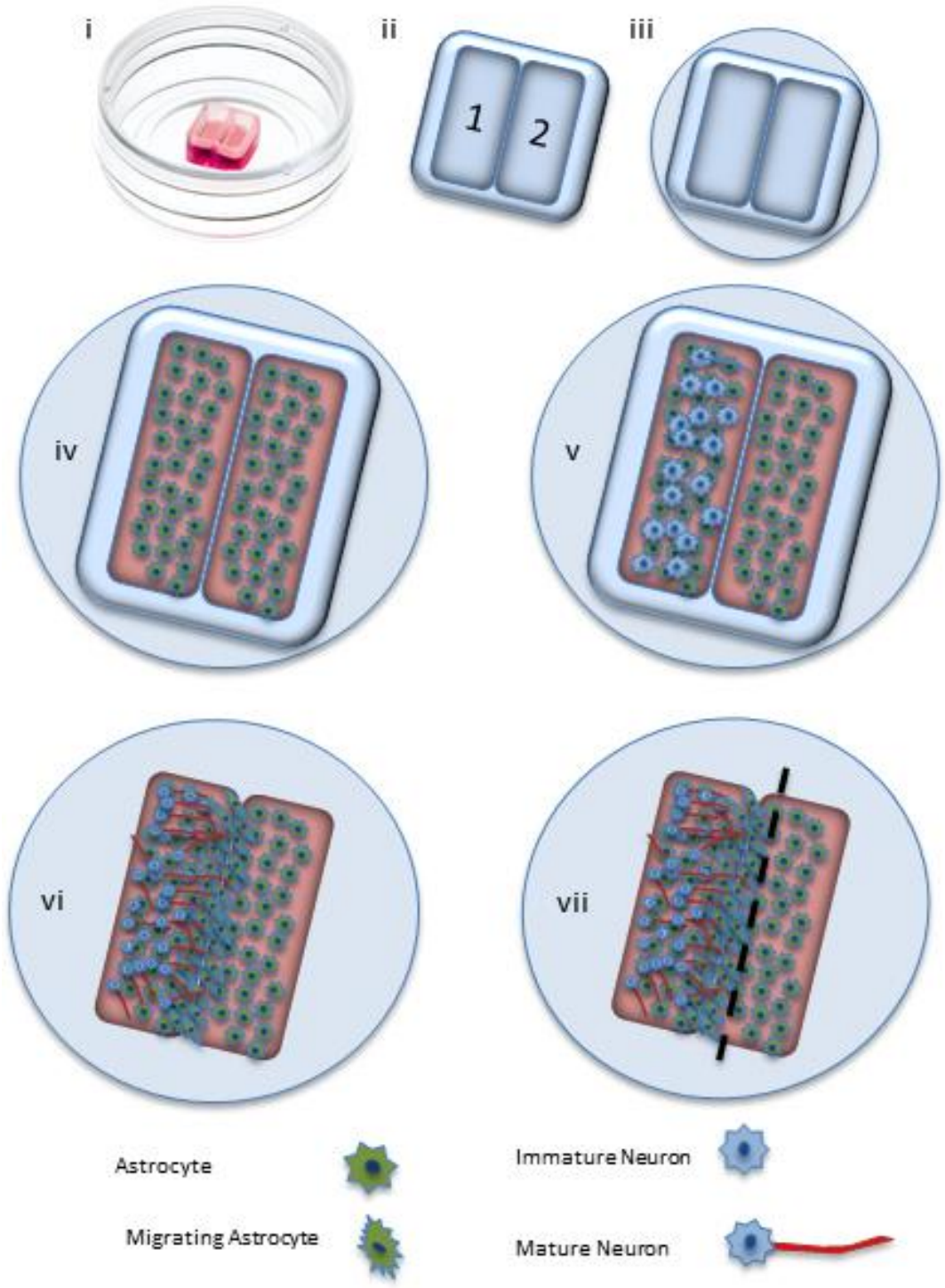

Figure 5.1 Myelinating culture compartmentalisation using Ibidi ® culture inserts.

The Ibidi ® insert was placed on a standard glass cover slip (ii and iii) Astrocytes were seeded in chambers 1 and 2 and allowed to become confluent taking ~4 days (iv), then disasociated spinal cord cells were seeded into chamber 1 only (v). Neurite extended from the seeding chamber out over the astrocyte space (vi) and injury induction applied to neurite which extend over to chamber 2-the astrocyte only side (vii).

5.2.2 Astrocytes in both chambers migrate into the cell free space created by the insert joining both populations

To assess the astrocyte response when placed in the culture inserts, astrocytes were cultured in the absence of the spinal cord cells.

Following astrocyte seeding, the cells became confluent at 3-5 DIV, then the insert was removed (Fig.5.2.Ai). Astrocyte migration into the cell free space created insert can be seen 2 days following the removal of the insert (Fig.5.2.A). Both astrocyte populations show cellular elongation and migration into the cell free space; whether that is the space between the chambers or the space surrounding the entire insert. The astrocytes migrated into the cell free space created by the insert at day 3 post insert removal.

The original cell free space can be located as the cellular morphology of the astrocyte in this space is more process bearing and elongated compared to the flat, 'cobble stone' morphology of the astrocytes in the seeding chamber (Fig.5.2.B). However, these cells are successful in forming a confluent monolayer between the two chambers, which is necessary for neurons to project neurites in culture.

These data support the use of these inserts, as the cells appear viable and can migrate into the cell free space and create a confluent monolayer connecting the two chambers. The cultures were fixed and stained using the same protocol described previously (section 2.10).

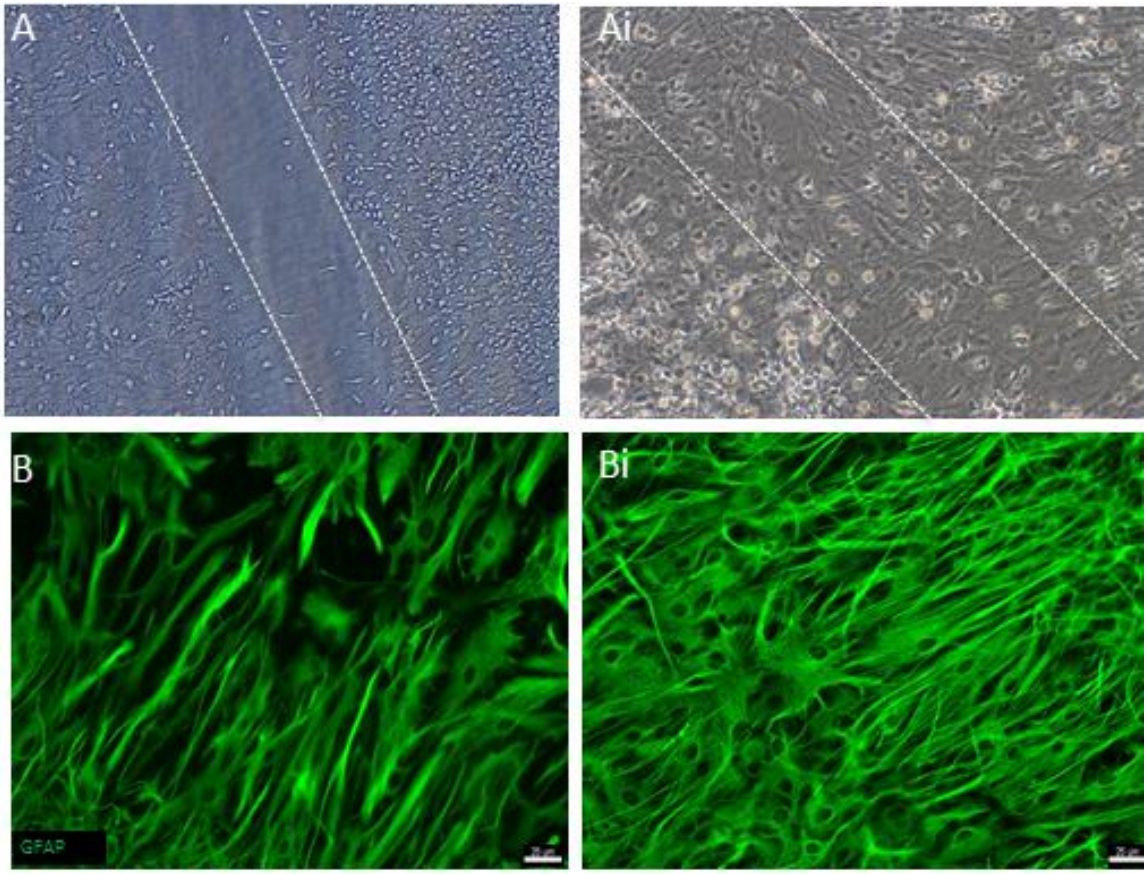

Figure 5.2 Astrocyte response to insert seeding and removal.

(A) Phase contrast images of the cell free space (depicted by dashed lines) taken at days 1-4 following insert removal. (B) Astrocytes stained with GFAP (green) following insert removal. Scale bar-25 µm.

5.2.3 Spinal cord cells have no defined directionality and neurite extension is too low to allow targeted injury of neurites

Following the investigation of astrocyte response to the culture insert system, we next assessed the properties of the dissociated rat spinal cord cells when added to chamber 1 of the inserts.

Following the formation of the astrocyte monolayers generated in chambers 1 and 2, spinal cord cell mix was added to chamber 1. These cultures were fixed and stained for β-tubulin to identify neurons and neurites, to map the progress of the neuronal processes.

The neuronal migratory response to the removal of the insert appears to be tied in with the astrocyte response. The neuronal cells moving into the cell free space with the astrocytes likened to 'riding a wave' (Fig.3-3.B). Neurites follow no apparent direction with neurite projecting in any given direction. β-tubulin staining was present in the neuronal free area after removal of insert (A), so prior to insert removal the wells are emptied and washed with fresh media to remove any unadhered cells.

Additionally, the identification of the neuronal cell body-free area, the area which is to be subjected to the injury was difficult to find, by eye, making accurate injury site induction difficult.

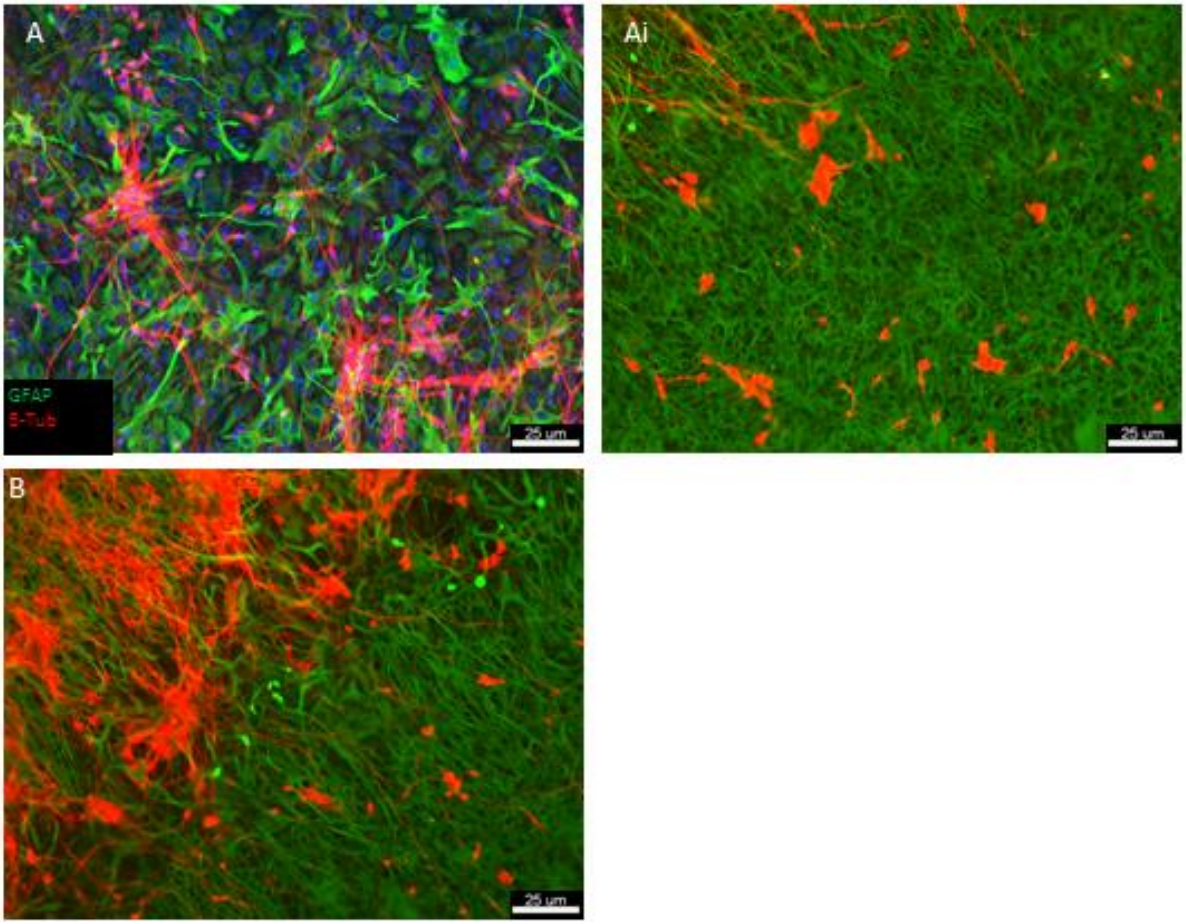

Figure 5.3 Seeding of spinal cord cells into the culture insert.

Spinal cord cells were seeded on top the astrocyte (green) monolayer in chamber 1. (A) β-tubulin (red) neurite staining in chamber 1 and (Ai) wash over of neurites in chamber 2. (B) Demonstrates the neurite 'wave' migration into the cell free space. Scale bar-25 µm.

5.2.4 Single Ibidi ® culture insert - Conclusion

The aim of this section was to compartmentalise the neuronal cell bodies from the neurite processes, using a commercially available culture insert. The insert allowed for the successful seeding of both astrocytes and spinal cord cells into the chambers. Astrocytes successfully migrated into the cell free space created by the removal of the insert. However, the extension of the neurites from the spinal cord cell mix seeded in chamber 1 into the adjacent compartment was unsuccessful.

The astrocytes were able to adhere and migrate into the cell free space created by the insert, forming a monolayer of cells. This was crucial as primary immature rat neurons and neurites require both physical and trophic support from a confluent monolayer of astrocytes to develop. Therefore, if a cell free space was maintained between the two chambers, the neurites would not be able to extend across into the soma-free space.

The original purpose of this design was to isolate the neuronal cell bodies from the processes so that injury could be targeted to the neurites alone, a more accurate representation of the *in vivo* injury state. Isolation of the cell bodies was partially achieved; they were seen to reside in the primary chamber site in which they were first seeded, however, there was no consistent neurite orientation towards the cell body free space which was required for targeted injury induction. The random orientation may be related to the lack of guidance cue gradients of certain neurotrophic factors (Kennedy et al. 2006) (Guan and Rao 2003), which would provide a neurite orientation to a defined location. Potentially, the neurotrophic factors are lost in the surrounding media, a product of turbulent flow, making neurite orientation seemingly random, but in fact just a product of the lack of definitive diffusion gradients.

Optimisation for this design would involve overcoming the lack of aligned neurite extension. This could be done by increasing the number of spinal cord cells seeded, to increase the number of neurites we see in the soma-free space. However, this idea is potentially detrimental, with increased cell number and density, so does the chance of the culture being lost from sloughing off the coverslip.

Furthermore, surface topographical cues could be used to promote alignment of the neurites. This idea was investigated by using aligned fibrillary collagen matrix to align white matter neurons using Ibidi® inserts (Lanfer et al. 2010). This approach however, may not be appropriate in this culture system as the astrocyte monolayer may mask the alignment potential of the collagen. However, astrocytic alignment has been shown to

increase neuronal growth and alignment in culture (East et al. 2010). This suggests that astrocyte alignment could increase the number of neurites seen in the soma-free space.

Another way to promote neurite extension would be to modify the insert design. The addition of a second culture insert directly adjacent to the first would allow for an additional spinal cord cell seeding chamber. Therefore, this could increase the number of neurites in the soma-free chamber. This new design may also help promote an increase in neurites due to the guidance cues secreted from the adjacent neuronal populations. In addition, this design would allow for easier identification of the soma-free area for precise injury induction.

To gain a deeper insight into the axonal response to injury there is need for the development of a model which allows for neurite compartmentalisation. However, as it is this culture design does not enable the investigation of neurites separate from their soma.

5.3 Result: Development of a dual insert compartmentalised co-culture model of CNS injury and regeneration

The single culture insert design investigated in the previous results section was limited in its capacity to provide adequate neurite numbers for injury analysis. This could be due to the number of initial spinal cord cells seeded or due to lack of neurite guidance. Furthermore, the identification of the potential injury area was difficult.

The subsequent compartmentalisation design accommodated two culture inserts. Figure 5.4 visually demonstrates the method employed, including the specific seeding arrangement of astrocytes and spinal cord cells and orientation of the inserts. Larger coverslips were required to accommodate the two inserts which were placed in 6 -well culture plates. This method created a second, much larger cell free space between the two individual inserts when the inserts were removed. This design also helped to identify the area which is subjected to injury, this is because a clear central cell area will be easily identifiable by eye. In this following section, the seeding wells are denoted as chambers when the insert is still in place and are denoted as cell areas once the insert is removed.

It was hypothesised that this set up would overcome the problems with neurite outgrowth the problem accompanying the single insert design. The aim of this was to

develop further the compartmentalisation design to increase the neurite number for injury induction.

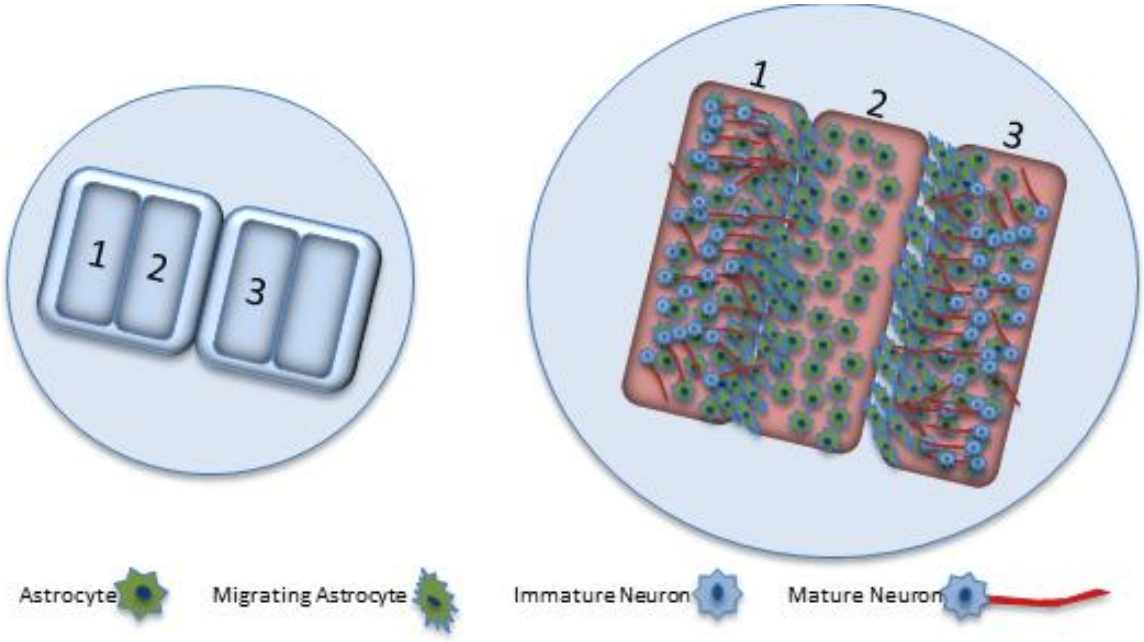

Figure 5.4 Dual insert compartmentalisation method

Two Ibidi® culture inserts were placed next to each other on a 30 mm coverslip. Astrocytes were seeded into all chambers. A cell free space was formed between chamber 1 and 2 but also between inserts so between chamber 2 and 3. Spinal cord cells were seeded into chamber 1 and 3.

5.3.1 Astrocytes seeded in chambers 2 and 3 do not migrate and fully close the cell free space created following insert-insert removal

To assess the astrocyte response in this new dual insert method, observations were made on astrocyte culture in the absence of spinal cord cells.

The seeding protocol was similar to that described above, with the addition of seeding astrocytes into chamber 3. The final cell seeding volume was 70 μl per insert at a cell density of 2-3 x 10^4 cells. Both culture inserts were removed from the coverslip after 3-5 DIV, creating two cell free spaces with the cell free space between the two inserts being larger than the cell free space between the two chambers of an individual insert.

The cell free space created by the insert-insert arrangement ranged from 1000 μm at the edges to 950 μm at the centre. The astrocytes failed to migrate fully into this cell free space resulting in a cell free space devoid of astrocytes (Fig.5.6.B-Bi). Astrocytes originating from chambers 2 and 3 both extended processes and displayed an elongated morphology in the cell free space but failed to form a confluent monolayer following 9 DIV. The cell free space created by the insert alone between chambers 1 and 2 was fully populated by cells as observed in (Fig.5.6.A). However, the closure time of this space was increased from 2-3 DIV to 4-6 DIV. The cultures were fixed and stained for astrocytes for GFAP to map the progress of the cells. As neurites require a confluent monolayer to support their extension, this design is not suitable for investigating neurite-specific injury.

5.3.2 Additional spinal cord cell seeding does not increase the observed number of neurites in the central area

Spinal cord cells were added to chamber 1 and chamber 3 following confluence of the astrocyte monolayer, at a concentration of 1.5 x 10^5 per 70 μl. The cells were allowed to adhere for 2 hours before each well was emptied of all media and washed with fresh media. Each insert was removed, followed by flooding of the cells with 1 ml of PM/DM+ media. The cultures were fixed and stained using the same protocol described above; neurons and neurites stained with B-tub and SMI31 depending on the maturity of the culture to map the progress of the neuronal processes, nuclei with DAPI.

Following the seeding protocol for spinal cord cells, few neurites projected from area 1 into the central area, which was observably no more than with the single insert design (Fig.5.A1). Due to the lack of cellular closure of the insert to insert cell free space, the

neurites from area 3 did not populate the central area and increase the observable neurite number. Furthermore, the astrocyte migration seemed to be additionally hindered in the presence of the spinal cord cells. Neurite trajectory was similar to that seen in the single insert experiment with no defined orientation (Fig.5.Bi)

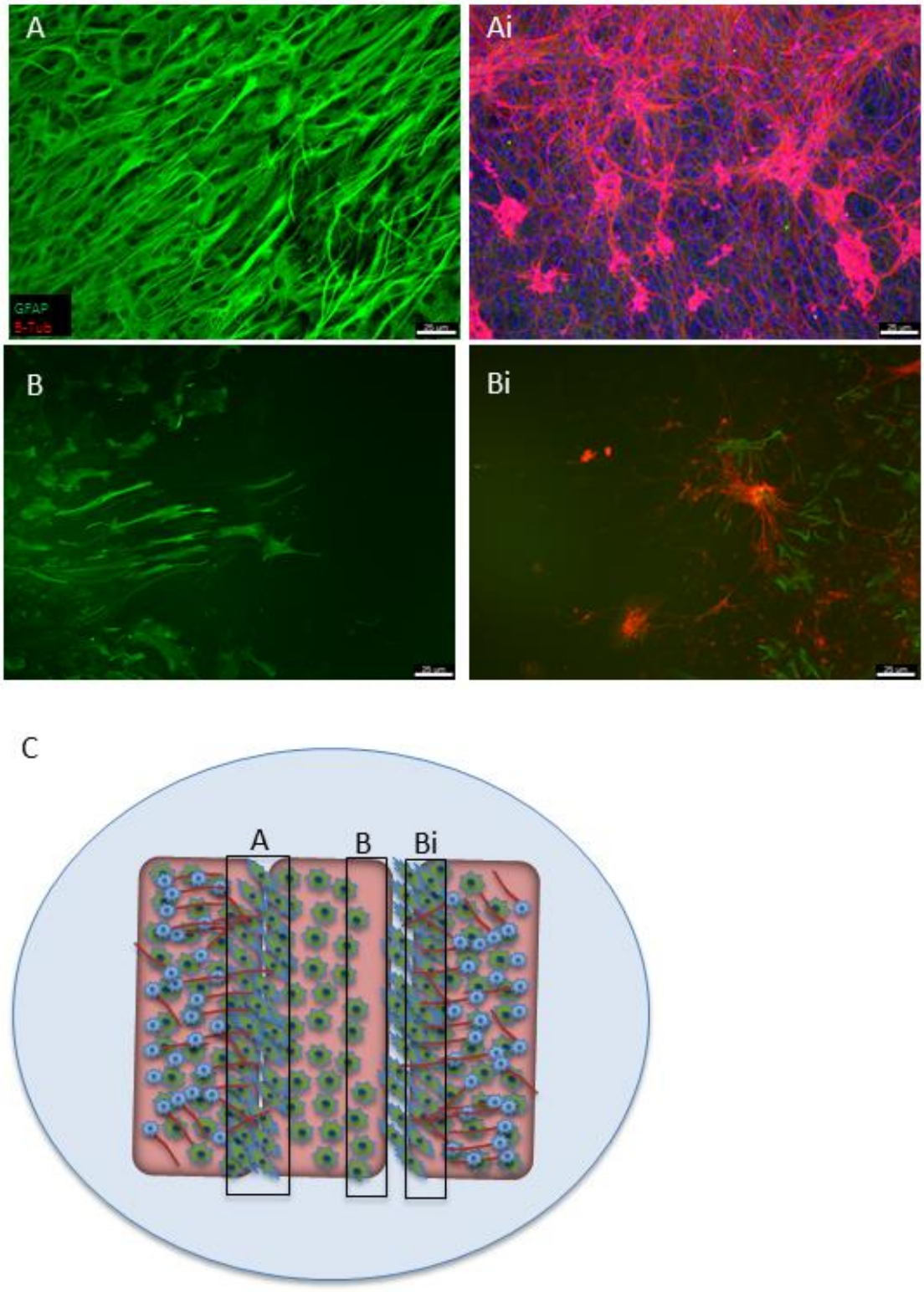

Figure 5.5 Astrocytes do not migrate and close the area between the two inserts leading to no improved neurite number in the central area.

Astrocytes were seeded into all chambers. Following 4 DIV spinal cord cells were seeded into chamber 1 and 3. (A) Astrocytes (GFAP, green) migrating and closing the cell free space created within the insert. (Ai) neurites seen extending from area 1 into soma-free space. (B) Astrocytes (GFAP, green) can be seen migrating into the space created between the two inserts, failing to form confluency. (Bii) neurites (β-tubulin, red) can be seen migrating as far as the leading astrocyte but no farther. (C) Is a schematic of the positions of the fluorescent images (A-Bi). Scale bar 25-µm.

5.3.3 Dual culture insert as a means of increasing targeted injury

Even though initial observations indicated that there were few neurites extending into the central area, neurites projected sporadically from area 1 into the central area are were then subjected to injury. The central area was more easily identified in the dual insert system than in the single insert system, which was why this was used for injury experimentation.

Following astrocyte and spinal cord cell seeding into the appropriate chambers, the central area was easily identified by eye. The cultures were matured for 14 days, then subjected to injury, using a single flat edge blade. However, due to the lack of neurites in the central area, the injury was induced at a site closer to area 1 and 2 rather than in the centre of area 2. Injury was induced directly proximal to area 1 which would allow for the greatest likelihood of neurite injury. The injury cultures were then visualised to determine the injury response, they were fixed and stained, for neurites using SMI31, nuclei with DAPI and myelin with PLP.

The central area was easily identified and injury was induced. The astrocyte response to injury was similar as seen previously within this thesis and published observations (Boomkamp et al. 2012), with an initial cell free space being invaded by astrocytes which have a reactive morphology (Fig.5.6.B). The limited number of neurites which had migrated into this area were severed and no neurites were observed entering the lesion site (Fig.5.6.B).

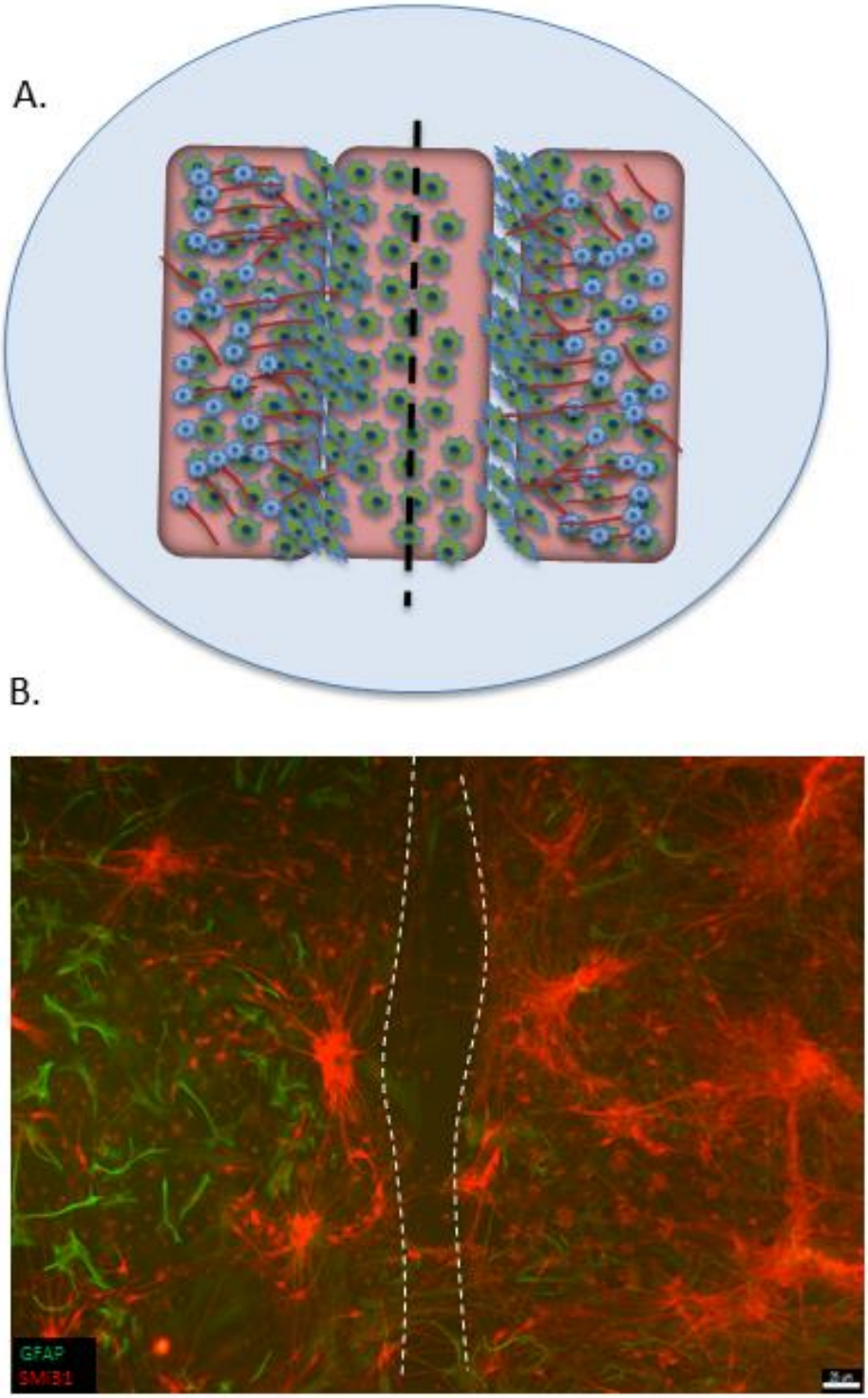

Figure 5.6 Dual insert lesion

Injury was performed by targeting the site between area 1 and 2 to increase chance of neurite injury. (A) Shows injury induction schematic. (B) Shows the lesion attempt, white dashed lines highlights lesion site, neurites (red) and astrocyte (green) and the few neurites growing out into the lesion site. Scale bar 25-µm.

5.3.4 Conclusion

The development of a dual insert design failed to meet the desired criteria set out at the start of this section, namely the separation of neurte projections from the soma. The design only overcome the pitfalls created with the single insert method, which was the lack of identification of the central area. Many of the limitations of the single insert method apply to the dual insert method as discussed in section 5.2.4. The first problem arose with the inability of the astrocytes to migrate and close the insert to insert cell free space. The lack of astrocytic migration, subsequently led to a lack of neurite presence in the central area, therefore failing to increase the number of neurites in the injury site.

There was no observable indirect promotion of neurites in the central area due to the addition of another neuronal population and a potential increase in guidance cues by the opposing neuronal populations. This failure could be again due to the lack of controlled diffusion of guidance cues in the culture dish as discussed previously with the single insert design. Any neuronal guidance factors released by the cells in the culture, such as those in the Netrin family (Kennedy et al. 1994) and slit proteins (Bashaw and Goodman 1999), diffuse uniformly through the entire culture due to turbulent flow, leading to a lack of defined growth and guidance of the neurites. Additionally, the lack of neurite extension could be related to the inability of any cell, including astrocytes, in a 2D environment to adequately form the ECM where the guidance cues would otherwise direct the growing neurites. It has been known for many years that the 2D *in vitro* models have limitations in the study CNS ECM-related function (Cullen et al. 2011) (Fawcett et al. 1989). However, decellularisation techniques could be employed to quantify ligands or guidance cues which are bound in the ECM of these cultures (Gao et al. 2013). This would test whether the 2D ECM of these cultures is capable of interacting and mediating neurite guidance in this system and would provide evidence whether the lack of guidance is not solely related to lack of fluidic diffusion gradients, but a lack of ECM to 'house' and sequester the guidance factors.

This dual insert design did allow for focused injury induction. The symmetry created by the two inserts allowed for easy identification of the central chamber, which was not possible with the single insert design. Injury to this area showed similar visual similarities to the previous cutting technique used in the myelinating cultures (Fig.5.6.B). Furthermore, neurites were severed and the underlying astrocyte monolayer was damaged, with the astrocytes responding as previously described (Boomkamp et al. 2014; Boomkamp et al. 2012) and observed elsewhere (Etienne-Manneville and Hall 2001).

Due to the lack of astrocyte closure at the insert-insert space there was no neurite extension across the cell free space to the central area. This process of astrocytic guidance has been observed elsewhere; *in vitro* models have demonstrated the need for astrocytes to support overlying neurons (Sorensen et al. 2008a) (Recknor et al. 2004), also during development neurons rely on astrocytic tracts to guide the neurons to their desired locations where they can mature and function (Lois et al. 1996). For this reason the lesion was created at a site closer to chamber 1 and 2, rather than at a more central position, so the neurites which extended into the central space were injured.

Logical progression from this design would be a new insert culture device which has a triple chamber design with a uniform space between chambers 1-2 and 2-3, to overcome the lack astrocyte migration seen in our dual insert design.

5.4 Novel Microfluidic device to study SCI and Regeneration

The culture insert techniques provided valuable preliminary results, specifically the requirement of multiple neuronal populations converging on a central area; which would allow for direct analysis of the effects of injury and treatment on neurites in the absence of any neuronal cell bodies. Also, the two designs highlighted the need for manipulation of the cellular microenvironment, through controlled diffusion gradient across the entire culture, if we aim to create a more accurate representation of the *in vivo* environment (Whitesides 2006). However, the culture insert designs hit major obstacles, specifically; the lack of design freedom to add or rearrange the chamber positions, the difficulty in neurite separation from cell body, inadequate neurite number and finally the inability to manipulate the microenvironment.

With these new criteria plus the formation of a new collaboration with Dr. M. Zagnoni at the University of Strathclyde, it was possible to develop a novel microfluidic device to study spinal cord injury which should meet all the criteria highlighted from the previous experiments.

A novel microfluidic platform to study axonal biology

Microfluidic technology has been shown to be a powerful *in vitro* tool, due to its ability to precisely control, monitor and manipulate cellular microenvironments. This is achieved by controlling volume differences between to culture chambers connected by microchannels. Microfluidics technology has been used in the study of localised physiology of isolated cellular projections such as axons (Taylor and Jeon 2011). These

microchannels are hijacked by growing neurite which enter and extend down the microchannel exiting in the adjacent chamber, where soma cannot. Therefore, allowing compartmentalisation of the neuronal cell body from the neurite (Gross et al. 2007; Taylor et al. 2005). Here we are adopting this technology and applying it to the study of axons.

Microfluidic technology has been accepted with open arms in the study of axonal biology. Device design freedom allows for complex biological interactions to be studied in greater detail than ever before. There is a lot of design freedom with a wide range of designs possible using the fabrication technique known as soft lithography (Whitesides et al. 2001). Soft lithography refers to the creation of a master mould which has the device design including seeding chambers and microchannels, which then can be stamped onto a material to create the device. Devices are fabricated from polydimethylsiloxane (PDMS), a plastic polymer which has useful characteristics such as elasticity, durability, biocompatibility and optical transparency (McDonald et al. 2000). PDMS-based microfluidic devices have several useful characteristics such as elasticity, durability, biocompatibility, optical transparency, gas permeability, no toxicity, and low electrical conductivity (McDonald et al. 2000). This system uses computer-aided design software for designing the compartment/chambers and microchannels, that are etched etched on to a photoresist material so that an inverse master mould is formed. PDMS is then cast on the mould creating a device which has the desired compartmentalised chambers and microchannels.

Axonal guidance cues have been studied in detail and many factors have been described in both repulsion and attraction (Dickson and Senti 2002). Microfluidic devices have been designed to study these factors in greater detail, (Joanne Wang et al. 2008) using a novel microfluidic device showing that the ECM bound molecule, laminin, plays an intricate role in the response of the axonal growth cone to brain-derived neurotrophic factor (BDNF). This observation was not possible using standard *in vitro* methods. These designs have capitalised on the physical microchannel guidance and axonal targeting towards a desired repulsion or attraction factor.

Microfluidic technology has also been used in the study of microglia-axonal interactions, specifically the response of microglia to health and injured/degenerating axons (Hosmane et al. 2010). A novel spherical multi-chambered device was created, which observed the migration of microglia along the axon with higher numbers being found around the injured axon (Hosmane et al. 2010). This study allowed the tracking of glial cells with individual and bundles of axons providing a far more detailed study of the interaction occurring along the axons. Microfluidic technology can allow for comparison

between the axonal and somal proteome and gene expression patterns (Taylor and Jeon 2011) and also the targeted injury of axons through compression and stretching techniques (Hosmane et al. 2011) (Yap et al. 2014).

For the purposes of this study, the most important quality of the microfluidic technology is the compartmentalisation of neuronal and glial cells which allows for the introduction of targeted injury in a closed system. This quality enabled the investigation of axonal outgrowth and myelination in primary spinal cord cell culture in a controlled manner not possible with our previous model or any published model. This technology has become available to this lab through collaborations with Michelle Zagnoni and Trevor Bushell at the University of Strathclyde, who provided help in designing the novel SCI-microfluidic device (SCI-MFD).

Controlling the media volumes in the seeding chamber and the central chamber can allow for the manipulation of diffusion gradients within the device by a process known as hydrostatic pressure-caused laminar flow. This property allows for isolated treatment of each of the chambers so that treatment in chamber 1 will not cross into the adjacent chambers. This allows for the study of targeted treatment of different neuronal populations and different sections of individual neurons, such as treating the injured axons and studying the knock on effects on the cell bodies, or vis-versa. This will allow for a more *in vivo*-like treatment strategy as treatment of the injury site through injection may not directly affect the neuronal cell bodies associated with injury site.

5.4.1 Microfluidic devices to study axonal injury

In collaboration with the University of Strathclyde we designed the first SCI-MFD. Fig.5.8.A shows the novel MFD; the SCI-MFD has a detailed micro-pattern which comprises the 2x inlet and outlet ports, 2x seeding chambers and 2 sets of microchannels 500 µm in length that converge onto a single central seeding chamber. The device is symmetrical down the central vertical axis, which enabled manipulation of diffusion gradients. Two variations on the device design were tested, differing only in width of the microchannel; 40 µm and 20 µm (Fig.5.7.B). Following device fabrication and assembly (see Materials and Methods 2.5) each compartment was PLL coated (4 µg/ml) for 1 hour. The cell seeding method is detailed in section 2.5; astrocytes were differentiated from neurospheres in a T75 flask for 4 days in 10% FBS and these astrocytes were seeded into chambers 1, 2 and 3 at a density of 5×10^4 in 5 µl for 15 mins then a further 115 µl added to each chamber. Neurospheres which were not differentiated were also seeded into the chamber to investigate if they could

differentiate into astrocytes and form a confluent monolayer. Disassociated spinal cord cells was then introduced into chamber 1 and 3 at a density of 3.5×10^5. The MFD was visualised live using phase contrast microscopy. The devices were fixed and stained using the protocol described in section 2.9. The cultures were stained for appropriate neuronal markers, ß-tubulin and SMI31 depending on the maturity of the culture, astrocytes were stained using marker-GFAP, myelin was stained using marker PLP and nuclei were stained using DAPI and Axio Fluorescent microscopy.

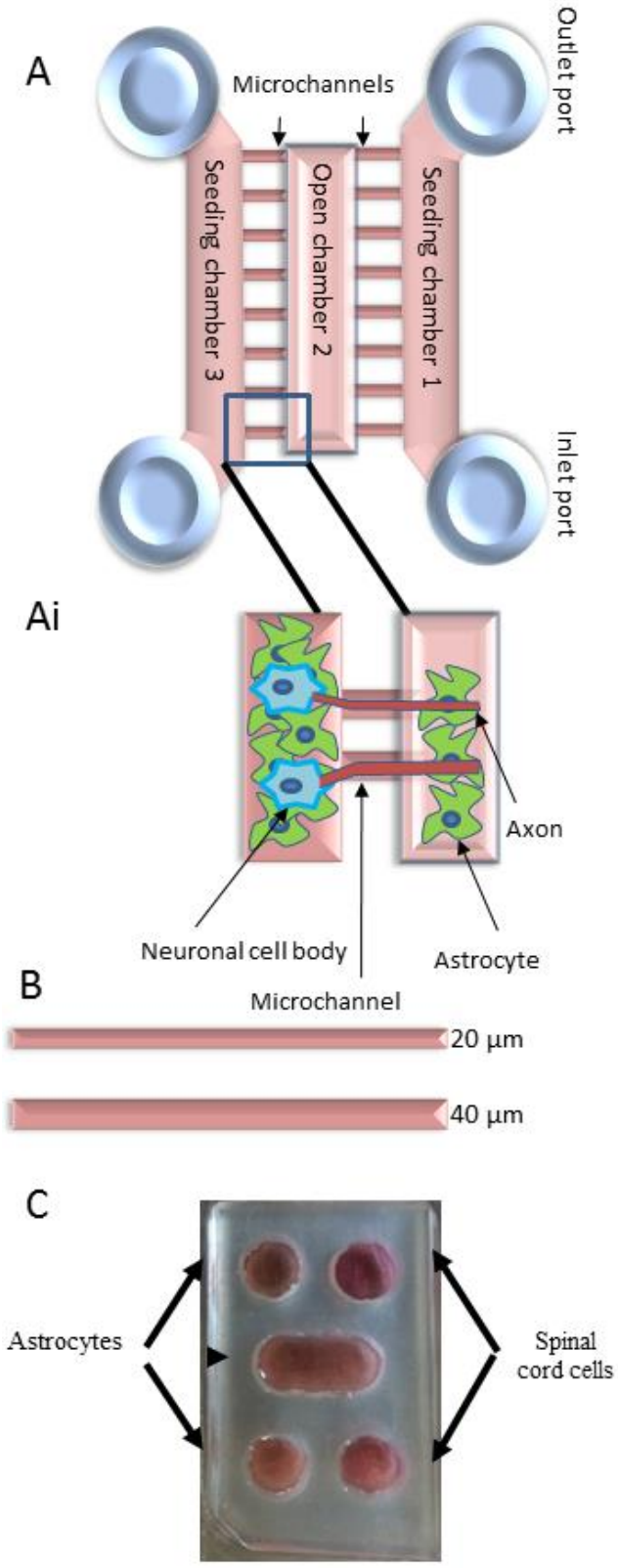

Figure 5.7 Spinal cord injury microfluidic device (SCI-MFD)

The SCI-MFD (A) which comprises of the 2x inlet and outlet ports, 2x seeding chambers and 2 sets of microchannels that converge onto a single central seeding chamber. The device is completely symmetrical down the central vertical axis. The schematic can be seen in (A) and an enlarged section depicting the seeding protocol for neurons and astrocytes and the axonal migration down the microchannel (Ai). (B) shows the widths of the microchannels 20 µm and 40 µm. (C) photograph of the device.

5.4.2 Astrocyte monolayer confluency was only observed in SCI-MFD with differentiated astrocytes

Astrocyte confluency was achieved after 3 DIV (Fig.5.8.B and D) in the microfluidic device by seeding differentiated astrocytes at a density of 3.5 x 10^5 per 5 µl volume into the inlet port of chamber 1 and 3 and directly into chamber 2. Following 15 minutes 145 µl of 10% FBS was added to each seeding chamber creating a final volume of 150 µl. Seeding with neurospheres did not allow for the formation of an astrocyte monolayer in chamber 1 and 3 (Fig.5.8.E), the closed seeding chambers.

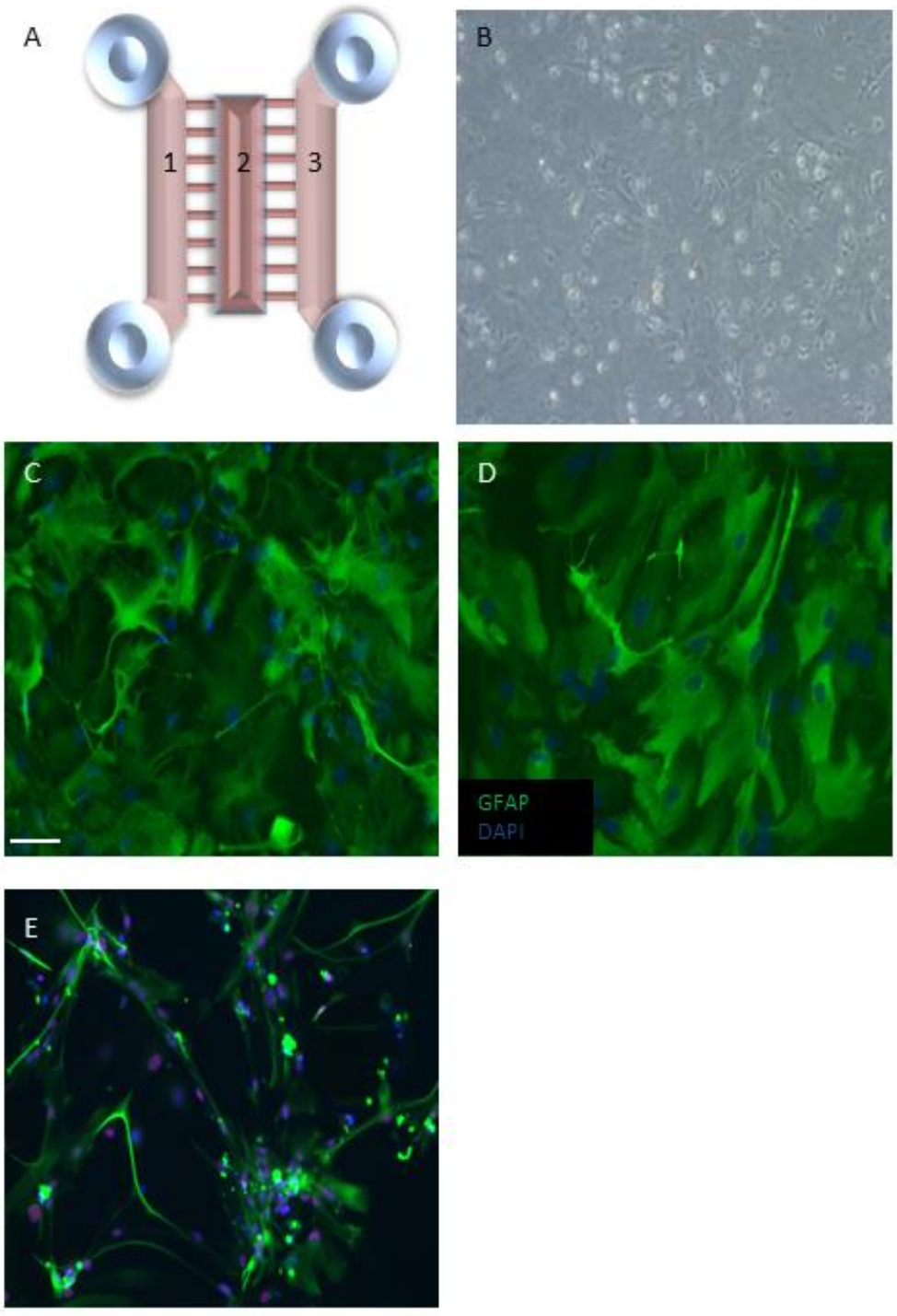

Figure 5.8 Astrocyte seeding in the MFD

Astrocytes were firstly differentiated from neurospheres in a T75 flask and seeded in the device at 3.5*105 at 5 µl volume. (A) number the chambers which are seeded with astrocytes/ (B) a representative phase images of the seeding chambers, (C-D) immmuocytochemisty images stained for GFAP (Green) and DAPI (Blue) for Chamber 1 and 2. (E) Neurosphere seeding into chamber 2. All immunostainings images were taken 3DIV, Scale bar-25µm.

5.4.3 Cellular invasion down the microchannel

From phase microscopy cellular components were seen down the microchannels which appear more in the injury device with 40 μm-wide microchannels not the 20 μm-wide channels (Fig.5.9. A+B).

To investigate the cellular invasion of the microchannels, immunohistochemistry was used to identify possible cells migrating down the microchannels. Initially, nuclei staining alone with DAPI showed massive infiltration of nuclei down the entire microchannel (see Fig.5.9.C). Upon further investigation the device design with 40 μm-wide channels had vastly more nuclei infiltration than the 20 μm-wide device (see Fig 9 A [40 μm] and C [20 μm]). Manipulation of the hydrostatic pressure across the microchannels resulted in a drastic decrease in the number of nuclei seen in the microchannels of both channel widths (Fig.5.9.F). Manipulation of hydrostatic pressure was achieved by maintaining identical volumes of media 50 μl in both central chamber and the adjacent chamber at the moment of seeding, (section 5.5.2). The 20 μm-wide device was taken forward for further experimentation.

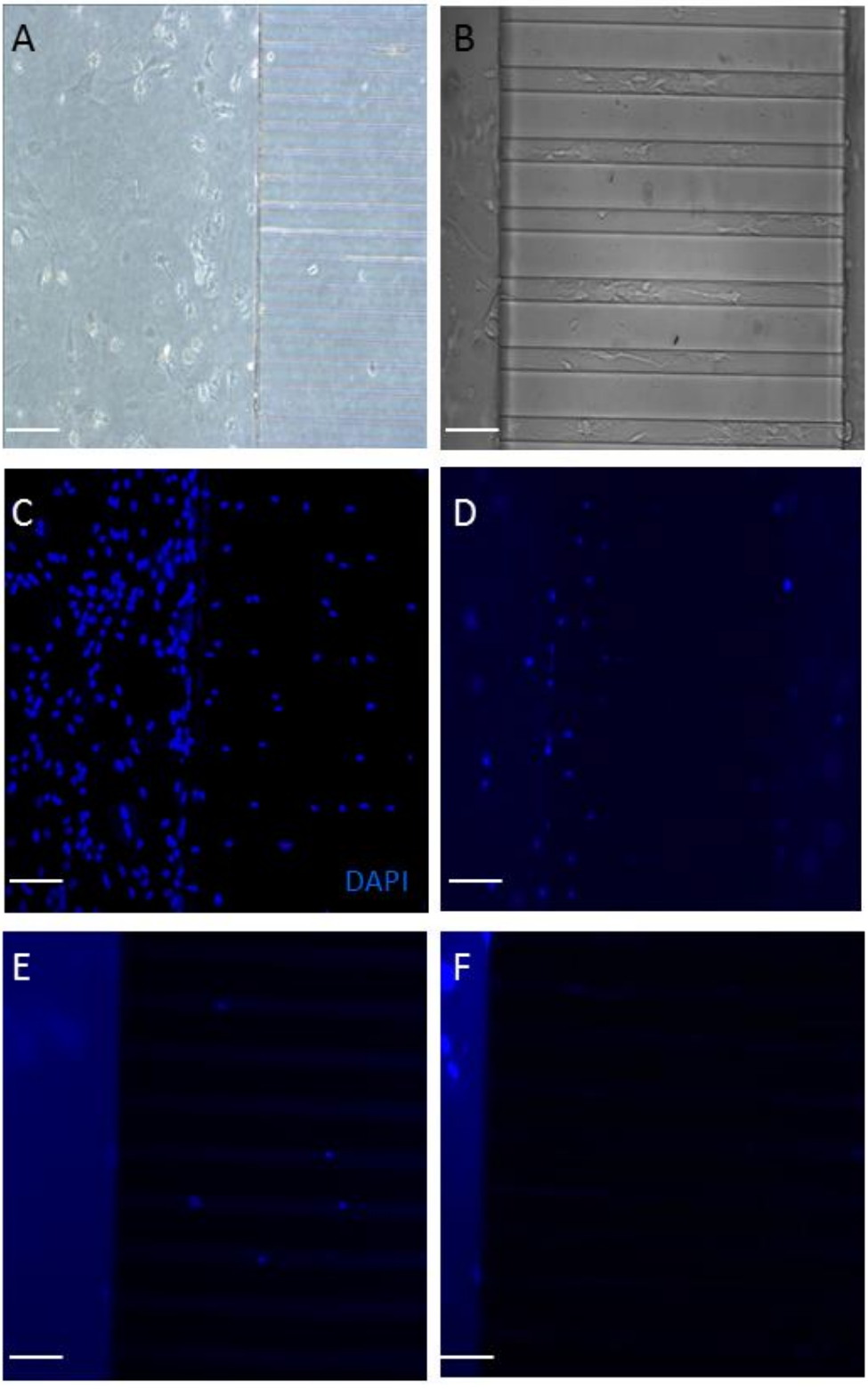

Figure 5.9 Nuclei seen in microchannels in the 20 µm and 40 µm wide microchannel devices

A and B show phase images of the channels with cellular intrusion .DAPI (blue) positive nuclei can be seen in the microchannel in both 20 µm 40 µm wide channels. 40 µm (C) have vastly more and down the entire channel length as compared to 20 µm (D). It is not known which cells types they are and if the nuclei presence is due to cellular migration or hydrostatic force acting upon the cells. Controlling volumes in the adjacent seeding chamber can remove nuclei present in the channel 20 µm (F) and 40 µm (E). Scale bar-25 µm.

5.4.4 Neuronal and astrocyte processes extend down the microchannels.

As the initial data showed that we could generate a confluent monolayer of astrocytes in each chamber, this gave us impetus to try the full, complex myelinating culture. Dissociated rat mixed spinal cord cells were generated as previously described from E15.5 Sprague Dawley rat embryos (Section 2.3). The seeding protocol was followed as previously described with slight modifications to the final seeding volume and cell density, so that 5 μl of 5 x 10^4 spinal cord mix cells was added to chamber 1 and chamber 2.

For optimal cell loading, all chambers were emptied of media prior to the addition of spinal cord cells. The spinal cord cell mix was added to chambers 1 and 3, and then the media DM+/10% FBS to chamber 2. Cells were observed by phase microscopy to determine if more or less media was needed to be added to the central chamber to adjust the hydrostatic pressure and manipulate the final position of the cells near the microchannels. The spinal cord mix was left to adhere for 2 hours then flooded with 145 μl of appropriate media to create a final volume of 150 μl in each chamber.

Following fixation, neurites were immunolabelled with β-tub and SMI31 depending on the maturity of the culture to map the progress of the neuronal processes in the chamber and microchannels. GFAP and DAPI were used to identify the astrocyte positions throughout the device.

Fig.5.10.A-B shows astrocyte processes entering the microchannels and extending up to 100 μm after 3 DIV. In these experiments it appears that the astrocyte nuclei do not follow the processes, with no GFAP+ nuclei present in the microchannel at the distances the processes were observed.

In addition to astrocyte processes, neurites (Fig.5.10.C-F) can be seen extending down the microchannels after 6 DIV and even exiting the channel into the open access chamber following a further 4 days in culture (see Fig.5.10.F).

This data suggests that the device is capable of fulfilling the criteria of neuronal cell compartmentalisation with neuronal cell bodies remaining in the seeding chamber and neurites entering and exiting into the central chamber. Astrocyte process can be seen in the channels but do not appear to hinder the neurite entry.

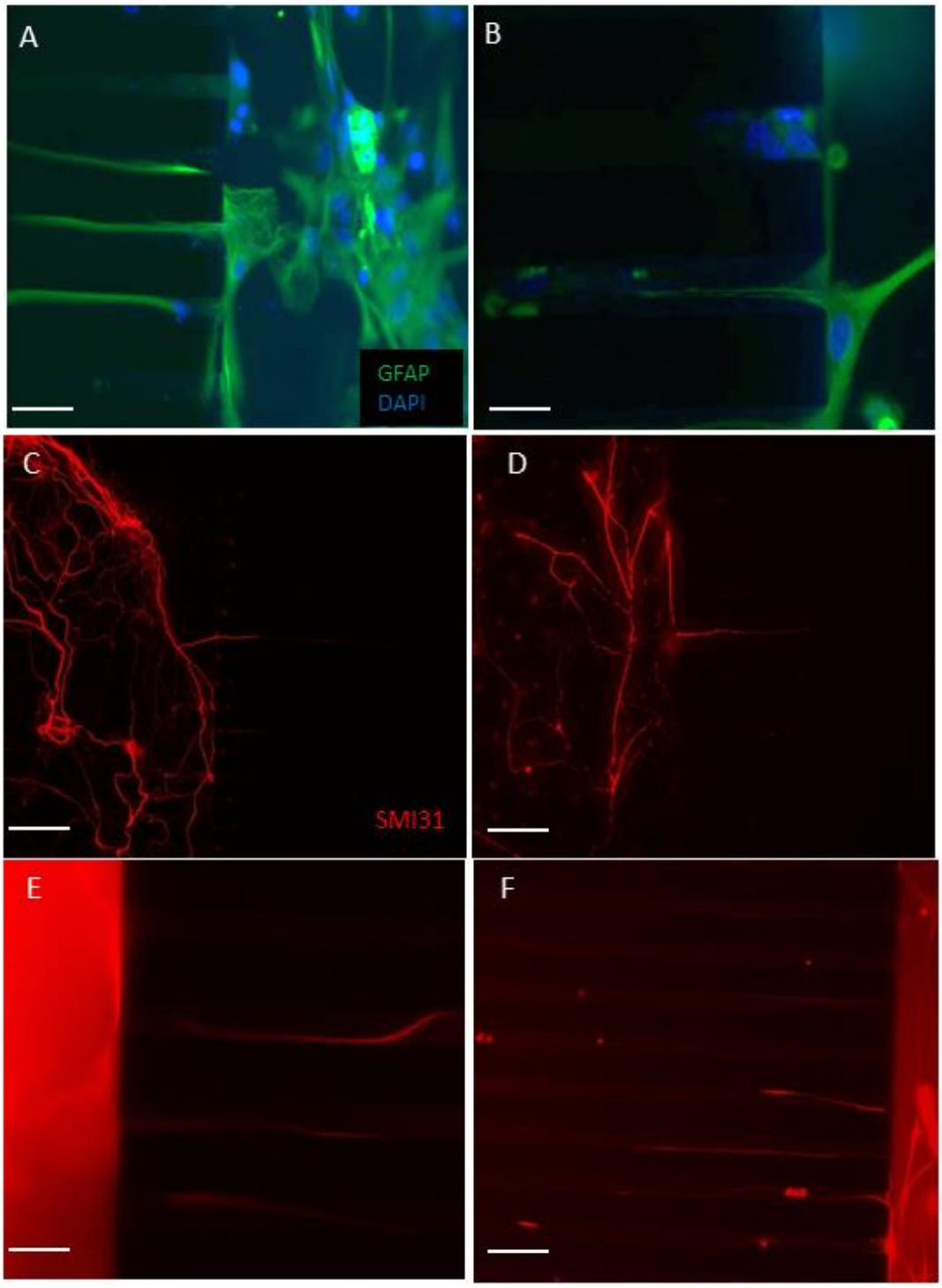

Figure 5.10 Neurite and Astrocyte processes can be seen to migrate into and along the microchannels.

Astrocytes (GFAP, green) were seeded into the device and following monolayer formation processes can be seen extending into the microchannels (A and B). Spinal cord cells were seeded and after 6 DIV neurites (β-Tubulin) can be seen in the microchannels (C-F). Scale bar; 15 µm (A-B and E-F) and 25 µm (C-D).

5.4.5 Antibody diffusion controlled by volumetric differences between chambers

Manipulation of diffusion gradients can occur between two chambers which are connected by microchannels. The diffusion site can be seen in Fig.5.11.B-D. This allows for fluidic isolation of a particular treatment, or in this case a fluorescent antibody. Differentiated astrocytes were seeded in chambers 1 and 3 as previously described (Section 5.5.2). GFAP staining was used in each chamber but three different secondary antibodies were applied to each chamber. The device was fixed and immunolabelled as described in Material and Methods: 2.7. Chamber 1 contained anti-rabbit Alexa Fluor® 488, chamber 2 containing anti-rabbit Alexa Fluor® 555 and chamber 3 anti-rabbit Alexa Fluor® 350, all targeting Anti-GFAP. Diffusion gradients can be seen between the chambers, with certain individual cells being co-stained with two different secondary antibodies without overlap (Fig.5.11.B-D). This dual staining is caused by the controlled diffusion gradient between the two chambers, making it so that the media solutions in each chamber do not mix. This creates a site where the two media solutions meet but do not overlap.

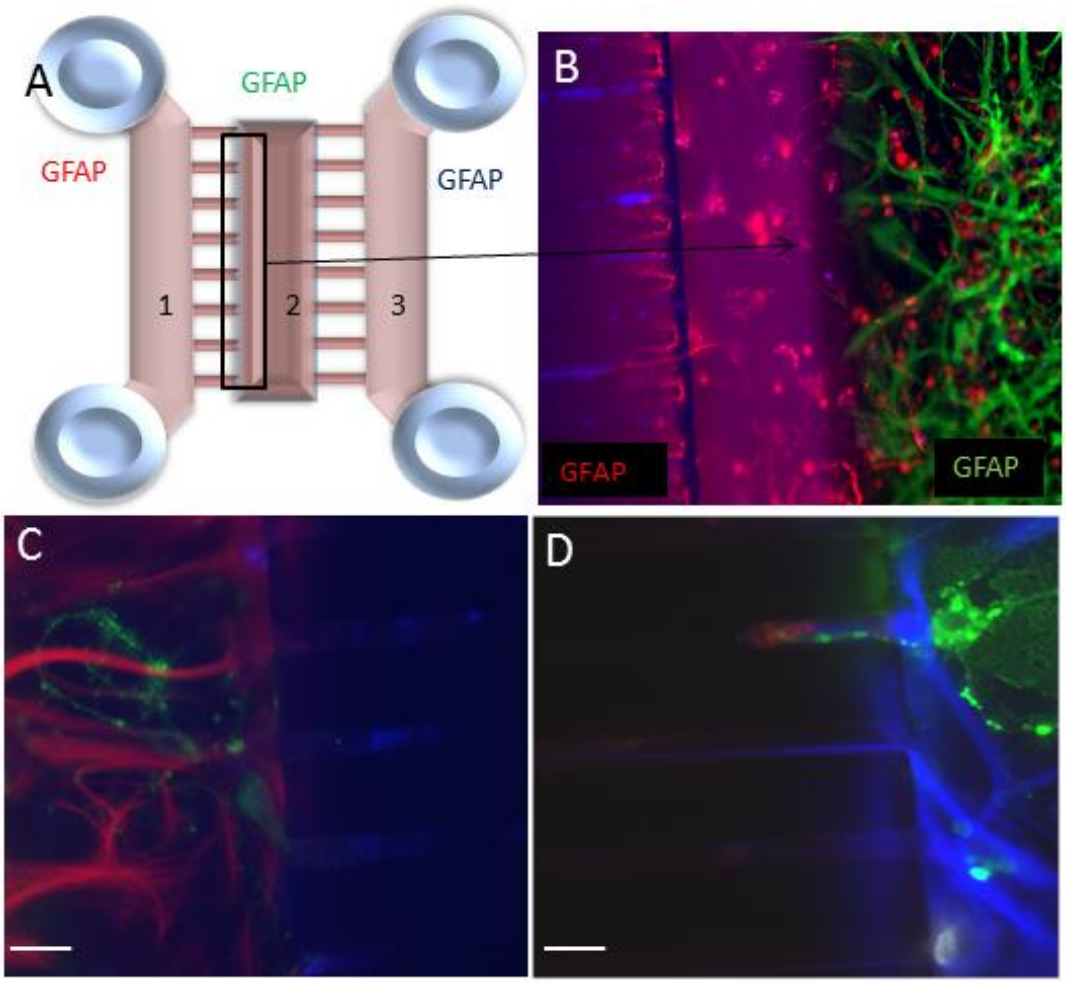

Figure 5.11 Antibody diffusion control within the SCI-MFD

Astrocytes were seeded into the device and allowed to become confluent. The diffusion gradient created by media volume differences in chamber 1 and 2 can be seen A-B. Each chamber was stained for GFAP, chamber 1 GFAP-red (C), chamber 2 GFAP-green (B) and chamber 3 GFAP-blue (D). Scale bar-15 µm.

5.4.6 Injury Induction to the open access chamber resulted in no spontaneous axonal outgrowth.

The device was seeded with astrocytes and spinal cord cells as previously described and cultured for 16 days to allow axonal migration down the microchannels. Injury to the open access chamber was performed using a P200 pipette tip, as the flat edge blade used in previous experimentation was too large. The culture was fixed and stained for axons (SMI31) and nuclei (DAPI) to identify the lesion site. The injury created a cell free space, which was subsequently closed by migrating astrocytes (Fig.5.12.B) and no spontaneous axonal outgrowth was observed, with no SMI31 positive processes in the lesion site (Fig.5.12.C).

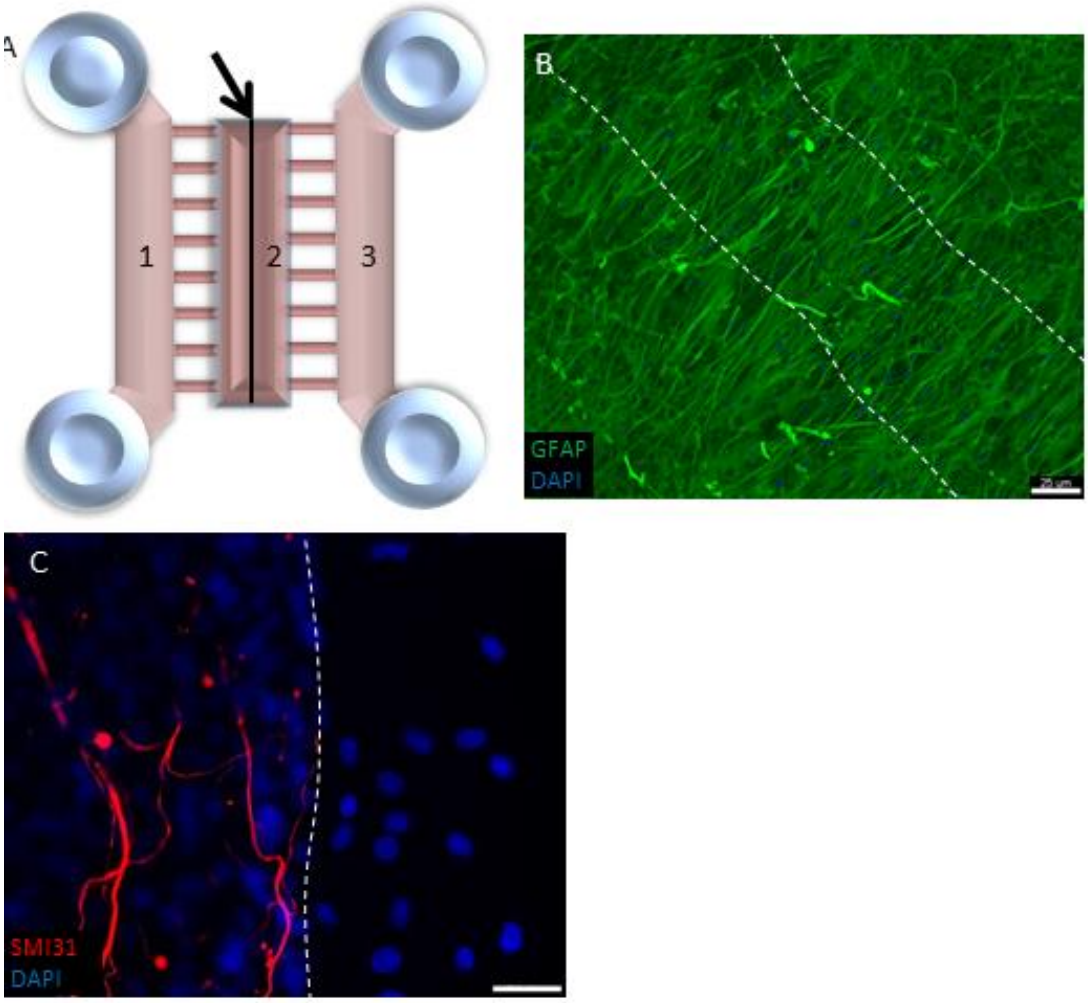

Figure 5.12 Injury to open access chamber, shows no spontaneous axonal outgrowth

Astrocyte confluency was achieved in all chamber then spinal cord cells were seeded into chamber 1 and 3. The cultures were matured for 16 days then subjected to injury, the injury position is marked with a line on the schematic (A). The cultures were fixed and stained 5 days later, (B) for astrocytes (GFAP-green) which migrate and close the lesion and for axons (SMI31-red) no axons can be seen in the lesion site. White dashed line marks injury site (B-C). Scale bar 25 µm (B) and 15 µm (C).

5.4.7 Discussion

This microfluidic culture device provides a novel method to align, isolate, lesion and analyse primary CNS axons and their glial interactions (Kim et al. 2009) (Park et al. 2009b). The technique is reproducible due to the use of soft lithography and computer aided design machine to create the master mould of the device, leading to consistent device reproducibility (Wittig et al. 2005). This design of a SCI-MFD has to meet the desired criteria of neuronal compartmentalization, accessibility for injury induction and diffusionally controllable compartments.

This novel SCI-MFD utilises the microchannels which generate the fluidic dynamics and diffusion gradients, but also allows for the compartmentalisation of the soma from the axons. This occurs as the axons can enter the microchannels but the neuronal cell bodies cannot.

There are several prominent findings within this study:

1. Axonal growth down the microchannels

It appears the primary aim of this study to compartmentalise the soma from neurites was achieved. This was accomplished by the minimal diameter of the microchannels inhibiting the neuronal cell body from moving into the open access chamber, whilst being big enough to allow for neurite projection down the microchannels. Neurites/axons can and been seen to enter, travel down and exit the microchannels.

However, optimisation is required to promote the number of axons entering the central chamber. This could be achieved by the addition of neurotrophic factors into the central chamber to attract axons, in a similar way to that which was discussed previously (section 5.3.2). A study has shown that neurites can respond and alter their growth pattern through the interaction with ECM molecules and guidance cues in a MFD (Joanne Wang et al. 2008). However, the use of neurotrophic factors may alter the response of the cells within the chamber as neurotrophic factors have also been shown to promote and affect the response of cells (Jordan-Sciutto et al. 2001). Therefore, the addition of neurotrophic factors could alter the culture conditions and in turn the response of the cells to injury, potentially confounding the results, making the use of chemical guidance cues a poor option for promoting axons in the central chamber. Additionally, more neurites/axons could be persuaded to enter the microchannels through manipulating the hydrostatic pressure so that the neurites are physically pulled into and down the microchannel.

Work by Gu and colleagues utilised the hydrostatic pressure aspect of the device, using the physical flow of the media on axonal mechano-sensing (Gu et al. 2014). Their novel device, using microsyringe pumps, showed an effective approach in directing axonal growth, in the absence of any biochemical guidance cues. This approach was novel in that the actual hydrostatic pressure and physical flow was shown to be a factor in the axonal guidance.

The device design ensured that only axons not dendrites entered the central chamber. This was achieved by controlling the length of microchannels between the seeding chamber and the central chamber, a channel length of 500 µm was used to ensure there was no dendritic contamination of the central chamber. However, other studies have concluded that 200 µm was sufficient to isolate dendrites (Park et al. 2009b). Modifying our device to reduce the size may be an interesting option as this could potentially increase the number of axons in the central chamber.

2. OPC/OL microchannel migration?

An unexpected finding was nuclei in the microchannels seen in the astrocyte monolayer culture. Data has yet to be collected to ascertain which cell types they are and which chamber they came from by immunostaining. There are many potential theories to explain why these cells are in the channels but two will be discussed as these can be approached experimentally in future studies:

1) Cellular migration down the channels.

2) Hydrostatic pressure caused the cells to be forced down the channel.

Both potential theories could be investigated through a single strategy. Controlling the hydrostatic pressure would lead to 1) the removal of any migratory signals which will cause the cells to enter and migrate down the channel and 2) volumetrically identical chambers prior to seeding so that no hydrostatic pressure is physically forcing the cells down the microchannels.

However, if the cells are in fact OPCs then their presence down the microchannel could open up potential axonal myelination studies including the investigation of injury and repair in mature myelinated axons. Myelination has been studied previously with a microfluidic platform using a co-culture of OLs and axons (Park et al. 2009a). However, the SCI-MFD offers the chance to study myelination following mechanical induced injury, whereas the microfluidic platform in the previous study did not.

3. Fluidic isolation

Microfluidic technology offers the ability to control diffusion gradient across a cell culture environment. Previous studies have demonstrated diffusion control, through the use of analytical methods and visual colourmetic methods to demonstrate fluid isolation (Robertson et al. 2014) (Park et al. 2009b). However, the demonstration of the diffusion gradients within the SCI-MFD was performed though preferential co-staining of individual cells in the chamber at the site of the diffusion gradient (see section 5.5.5). Here, two different secondary antibodies targeting the same primary antibody (GFAP) were able to stain the same cell without overlapping. This highlighted the potential scope of this device in terms of diffusion isolation and treatment options for different cell populations, specifically injured axons. This ability to control and manipulate diffusion gradients can avoid problems arising in standard *in vitro* model studies such as off-target effects of treatment due to the turbulent flow, which could confound observations and results. The co-staining result better represents the diffusion manipulation capacity of a device than previously demonstrated colorimetric methods because we showed that large macromolecules such proteins (IgG antibodies) can be precisely manipulated. Therefore, this demonstrates that treatments with macromolecules, such as antibodies, which is a popular treatment strategy in SCI, specifically, anti-NOGO (Freund et al. 2007) and anti-LINGO (Mi et al. 2005) can be precisely controlled within this device.

4. Axonal injury

The novel design feature of this MFD was the open access chamber which allowed for targeted injury of axons. This compartment housed a confluent monolayer of astrocytes and axons, which entered from the adjacent chambers. The preliminary results for injury using this device suggested that there was no spontaneous axonal regeneration following injury, which is a similar axonal response *in vivo* (Yiu and He 2006). Furthermore, this experiment lays the foundation for the study of treatments, such as desulphated mHeps, for the regeneration of injured axons in the absence of soma. Alternatively, treatments can be applied to the somal compartment only and the effects on the injured axons in the central compartment studied, providing the optimal target for a particular treatment.

- Limitation

A potential limitation in this study is the time frame for device fabrication and preparation. The device preparation is very time consuming with on average 20 devices

being made each day (based on a single photoresist mould) versus being able to PLL coat hundreds of coverslip per day as in the standard myelinating culture. It may be an unfair comparison as the SCI myelinating culture is a basic *in vitro* system with no complex use of technology which a limitation of the system. However, what I propose is using both techniques employing the SCI myelinating culture as a screen before then taking the findings to the MFD for more advanced detailed study of the axonal injury/repair process.

- Further Investigation

Further investigation is required to characterise the injury response of axons by looking at key injury markers to determine what factors are involved at the immediate injury site, when only axons and astrocytes are present. This could be achieved using the parameter employed by (Boomkamp et al. 2012), specifically, but not limited to, the astrocytic upregulation of GFAP and CSPG. More detailed investigations will be carried out looking at the differences in axonal-related injury and regeneration markers such as GAP-43 (Bomze et al. 2001), a known regenerative marker, between the axons and the isolated cell body.

Optimisation is needed to increase the number of axons crossing the channel to increase our experimental material (axons) in the open access chamber. This could be achieved by manipulating the hydrostatic pressure by altering the volumes of media between the compartments to provide physical guidance cues to the neurites.

Finally, to validate this SCI-MFD in context of SCI treatment, we could employ previously published compounds of repair, which have shown promise in neurite outgrowth such as Chondroitinase ABC and Rho pathway targeted treatments (Bradbury et al. 2002) (Dergham et al. 2002). Obtaining similar data to that published in these studies would endorse our SCI-MFD model as being a suitable platform to study SCI as it is reflective of the *in vivo* environment.

5.5 Conclusion

The aim of this chapter was to develop a compartmentalisation device to study neurite outgrowth and repair. The first step to address this aim was the use of the commercially available Ibidi® culture inserts. These culture inserts highlighted the need for a multiple chamber device, with more neuronal populations converging on a single open access chamber from distances no more than 800 µm. The insert experiments were only brief investigations into the cellular growth and migration within the inserts. Each

experiment was a stepping stone which led to the next design, each addressing a limitation of the last. Throughout this study it became apparent that for compartmentalisation to be achieved there was a requirement to provide artificial guidance to the neurites and control of the fluid microenvironment around the cells in culture. Both of these criteria could be met through the use of microfluidic technology.

The Ibidi® culture insert was a valuable starting point, and these experiments provided the preliminary data which led to the development of the final MFD designs. This device enabled compartmentalisation of the axons from the soma in a neuronal-glia co-culture through providing artificial guidance to the neurites, provided by the microchannels and through the control of the fluid microenvironment. Together, these culminated in being able to injure axons independently from the soma. Although no spontaneous axonal regeneration was observed, this model could provide the means to investigate the effects of treatments on axons specifically by adding these treatments to the central compartment.

This novel SCI-MFD presented here describes an innovative approach to the study of axonal injury and regeneration. This device offers the chance to overcome several major limitations in the study of axonal biology such as the study of axonal response to injury and treatment in a complex multi-cultured system.

Chapter 6

Discussion

6 Discussion

The overall aims of this PhD were to identify novel compounds to support repair and regeneration after SCI using a medium throughput screen and to develop a compartmentalised culture model of SCI to study targeted axonal injury.

There are two principle findings of this thesis: 1) the identification of a subset of novel compounds, desulphated heparin mimetics, for SCI repair and their proposed mechanism of action and, 2) the development of a novel microfluidic culture platform to study axonal injury.

6.1 Use of SCI model as a medium throughput screen

Using the injured myelinating culture, and monocultures I was able to suggest a new therapeutic family of compounds for SCI relating to neurite outgrowth and myelination, namely heparin mimetics. It is well known that a successful intervention for SCI would be a combinatorial therapeutic approach including targeting the aberrant immune response, promotion and reconnection of damaged axons, manipulation of intracellular signalling and implementation of artificial scaffolds (Thuret et al. 2006). What has been suggested in this study is that a compound which in itself has multiple repair properties (promotion of myelination and neurite outgrowth) could remove the need for several different or multiple combinations of treatments for SCI. However, this can only be substantiated through the use of *in vivo* model of SCI, models such as the contusion impactors and clip compression (Alluin et al. 2011) (Krishna et al. 2013). Using these injury models and looking at parameters such as axonal outgrowth and myelination in and around the site of injury would determine if multiple therapeutic benefits are seen *in vivo* after treatment with mHeps.

High throughput screening of potential drug targets has now adopted microfluidic technology. The MF platform has the properties of low cost, able to handle nanolitre-volumes, low sample requirements and ability to accommodate cell culture (Yin and Marshall 2012). Taking the MF technology and its proven use in high throughput screening, potential therapeutic compounds can be assessed for SCI repair and regenerative properties. Chung and colleagues created a MFD which enables assessment of thousands of single cells and their response to kinetic and chemical stimuli (Chung et al. 2011). Such techniques could be adopted and the response of glial cells to potential therapeutic compounds such as mHeps could be assessed, and compound targets identified using single cell screens could be further investigated in the complex SCI-MFD

and SCI model. Utilising many methodologies could potentially lead to a 'production line' of models to identify potential therapeutic targets.

The heparin mimetic panel was a set of specific modifications of the commercially available Heparin. Each compound was modified relating to the level or position of the sulphate group(s) on the heparin polysaccharide (Yates et al. 2004). In this study it was observed that the mimetics may be involved in the mediation of FGF and Wnt signalling pathways, that appear to be dysregulated or disrupted following injury. Data presented here corroborate the results of other studies using oligosaccharide heparin mimetics, looking to understand the dysregulation of HSPG production with FGF signalling in certain diseases such as cancer. In a study it was demonstrated that GAG mimetics can interact with FGF-2 and mediate signalling through FGFR4 (Saxena et al. 2010). Similarly, a study using mHeps as a tool to understand astrocytes and transplantation candidates concluded that the mimetics mediate FGF signalling (Higginson et al. 2012). The Saxena and Higginson studies used the mimetics as a tool for understanding the dysregulation of the FGF pathway, however, the work also showed the potential benefits of a heparin mimetic as a FGF2 signalling agonist as a treatment.

In this thesis I show evidence that the sulphation state of the heparin mimetic is crucial in the promotion of both neurite outgrowth and of myelination following injury. Using the SCI model, desulphated mHep6, 7 and 8 had a positive effect on neurite density, myelination and neurite outgrowth (Fig.4.2-4.3), whereas, highly sulphated mHeps had adverse effects including the reduction in myelination and no increase in neurite outgrowth and exasperated the injury response (Fig.4.4). To identify the signalling mechanisms involved following treatment with mHeps, commercially available, signalling pathway inhibitors were used to selectively inhibit Wnt and FGF signalling (results:4.3.8 and 4.3.10-11). Evidence was provided that suggests canonical Wnt and FGF2 signalling pathways could be involved and targets for the heparin mimetics (Fig.4.9, 4.11-4.12). Similar observations were recorded in (Higginson et al. 2012), which also demonstrated FGF being mediated by heparin mimetics. However, the cell type(s) and the exact signalling target(s) of the effective mHeps still remain unclear. To identify cell populations that could be responsible for the response of the mixed complex culture, monocultures of OPC/OLs were used to investigate the cells responsible for myelin formation in isolation. This enabled the identification of mHep manipulation of OPC proliferation and OL sheath size (Fig.4.3.5 and 4.3.7). However, a monoculture of primary rat spinal neuronal cells was not possible using the standard methods available in our lab. Therefore, targeted neurite outgrowth study required the development of a new culture technique.

This study did provide an unexpected result in that there was no effect of the mono and desulphated mHeps 6, 7 and 8, on the reactive phenotype of the astrocyte specifically GFAP (Fig.4.5.D). Following treatment with the monosulphated mimetics there was no decrease in GFAP and Nestin, two common reactivity markers (4.3.4). This was unexpected as astrocyte reactivity is central in SCI and is targeted for reduction by regenerative therapies (Schwab and Bartholdi 1996) (Dergham et al. 2002) (Bradbury et al. 2002). However, this thesis has implicated Nestin as a potential marker for a repair phenotype as its upregulation occurred in conjunction with promotion in myelination and neurite outgrowth (Fig.4.5.E and discussed in 4.4.4).

6.2 Selective desulphated mHeps as a treatment for SCI

Heparin mimetics are potentially a valuable treatment for SCI. The modification of commercially available Heparin to create different isoforms which have different levels and positions of sulphate moieties is a novel approach for SCI treatment (Higginson et al. 2012). The molecular size of the mHeps is roughly around 10,000 kDa which translates to 20-24 disaccharides in length. The composition of the mHep polysaccharide consists of a repeating chain of iduronic acid and glucosamine which have sulphate moieties at either C2, C6 or N positions (Patey et al. 2006; Yates et al. 2004). This thesis highlighted two specific sulphate positions which were shown to have greatest therapeutic effect in this SCI model, 2-*O*-sulphated (mHep6) and *N*-sulphated (mHep7). Application of mHep6 and mHep7 demonstrated both promotion of neurite outgrowth and myelination following a single treatment of our SCI model at a concentration of 1 ng/ml (Fig.4.1-2).

Heparin is routinely used during SCI treatment, LMWH is an administered within 72 hours following SCI to help minimise vascular complications such as DVT (Christie et al. 2011). Following the identification of mHeps with therapeutic properties these mHeps could be administered alongside the LMWH and the other acute treatment options. Moreover, the mHeps have been shown to have no anti-thrombotic properties so their presence will not cause any complications for surgical procedures allowing their administration to continue if required.

An important set of results which could have far reaching implications for the routine treatment of SCI are the effect of mHep1 (Heparin) following injury to the neural cell co-culture. Discussed previously, LMWH is used as prophylaxis and treatment of DVT within 72 hours following SCI (Kulkarni et al. 1992) (Christie et al. 2011). Within this 72 hour time period the BBB is still disrupted (Hay et al. 2015) (Whetstone et al. 2003), therefore, molecules which may not be able to breach an intact BBB will have access to

the spinal cord. However, this study has implicated mHep1 as detrimental for CNS repair and regeneration. mHep1 was observed to significantly exacerbate the lesion size (Fig.4.4), increase GFAP a marker for reactive astrocytosis (Fig.4.5), decrease myelination and OL number adjacent to the lesion (Fig.4.2), decrease OL cell size (Fig.4.10), and finally decrease myelination in a healthy culture (Fig.4.10). However, these multiple negative effects were observed using the commercial Heparin but not with the clinically used LMWH, the difference being LMWH is a fraction of heparin with a mean molecular weight below 10 kDa (Nurmohamed et al. 1992). LMWH is a potent modified version of Heparin itself. As LMWH is in clinical use and different from mHep1 it would be interesting to investigate LMWH on the SCI model and assay its effects on myelination, neurite outgrowth, astrocytosis and OPC/OL proliferation/differentiation. This would clarify if heparin (LMWH) administration during SCI treatment could have, similar to mHep1 negative effects on regeneration and repair.

An obstacle with any potential treatment is that it has to breach the BBB. Even though the permeability of the BBB is disrupted following SCI which does allow drugs to reach their target (Popovich et al. 1996), over time the BBB reforms and will, therefore, reduce the effectiveness of long term treatment of the damaged cord of drugs that are not inherently BBB permeable (Koziara et al. 2006) (Tamai and Tsuji 1996). The mHeps have been shown to be able to pass the BBB, with other heparin derived mimetics (ultra-low molecular weight heparin fragment C3) also been shown to do the same and elicit their effects on CNS targets (Ma et al. 2002). MA and colleagues used C3, a mixture of heparin oligosaccharides which can penetrate the BBB which was demonstrated using radiolabelled C3 and detected in the CSF following intravenous injection. Furthermore, demonstrating C3 can enter and exhort anti-protease properties and inhibitory effect on activated factor X, providing potential attenuation of Alzheimer symptoms (Ma et al. 2002) (Passeri and Cucinotta 1989) (Leveugle et al. 1998).

Of the other major naturally occurring GAGs, chondroitin sulphates have been highlighted as major components of the inhibitory environment of the glial scar (Rolls et al. 2008). However, as this thesis has highlighted that varying the degree of sulphation at the injury site could present a new therapeutic avenue in SCI, could targeting not only HS but CS also enhance the repair and regeneration of the spinal cord? CS have been shown to both attract and repel neuronal processes (Brittis et al. 1992; Dou and Levine 1995; Nadanaka et al. 1998), suggesting they could be harnessed to induce axonal outgrowth.

Work by Tully and colleagues synthesised and assessed the effects of varying sulphation of CS on neuronal growth. They found that sulphated tetrasaccharide and not the

desulphated saccharides promoted outgrowth (Tully et al. 2004). These observations are the opposite of the sulphation requirements of the mHeps promotion of outgrowth. Such studies suggest that CS should not only be seen as a factor which needs to be removed or overcome, but a target with beneficial repair and regenerative properties. Furthermore, opening up our research, using the SCI model to assess effects of other GAGs present at the site of injury and the creation/ modification of these GAGs could generate new therapeutic compounds for the treatment for SCI.

Having heparin-derived mimetics in the clinic, which have been shown to transverse an intact BBB and have therapeutic properties (Passeri and Cucinotta 1989) (Cornelli 1996), adds to the mHeps as a more desirable treatment option in other neurological disease such as SCI. Moreover, not only as a treatment option in the acute phase, but also potentially as a long term therapy.

6.3 Off-target effects of mHeps

An advantage of the mHeps as a treatment option in the context of SCI has been the multiple beneficial effects observed: promotion of myelination and neurite outgrowth. The data shows that the heparin mimetics are in part mediating their effects on these processes through the Wnt and FGF signalling pathways (Fig.4.9, 11-12). Furthermore, the heparin mimetics have multiple cellular targets with the culture system. This suggests that the heparin mimetics probably have other cellular and signalling targets which are as of yet undiscovered. However, the *in vitro* SCI model used in this study does not encapsulate fully the *in vivo* environment: for instance there is no peripheral immune component. Previous studies have shown that HS mimetics can modulate chemokine activity, thus, altering the inflammatory cascade (Sheng et al. 2013) (Casu et al. 2010). Therefore, the multiple effects being observed in the *in vitro* model used could be amplified in an *in vivo* setting. It was observed that, mHep 7 in a healthy culture resulted in loss of myelination. This is an important consideration for the use of mHep7 in an *in vivo* model of SCI which could interact with both injured and uninjured regions of the CNS (Stieger and Gao 2015). The differential effect of mHep 7 between the states of pathology/steady state suggests the heparin mimetics can have different effects in a given microenvironment where different cells are more active (Douglas et al. 2009).

The control of off-target effects is a common focus following compound screens. The identification of such targets has been aided through the use of gene microarrays to identify changes in gene expression patterns following exposure to compounds

(MacDonald et al. 2006). These gene expression fingerprints may be cell specific but could point towards specific cellular mechanisms and cellular populations which could be vulnerable to a drug's mechanisms. Using the *in vitro* models in combination with another methodology, such as microarray analysis would enable greater confidence in targets identified. In addition to a gene centered study, a high-content cellular analysis of changes in protein-protein interactions using protein-fragment complementary assay (PFCA) strategies could strengthen the pursuit of potential off-targeted candidates (MacDonald et al. 2006). The PFCA analysis allows for a high throughput study of the structure-function relationship of a given drug with protein targets (MacDonald et al. 2006). This technique could be used to understand the specific binding targets of the mHeps to relay this data back to any potential cellular 'hot-spots' where the mHeps may have off-target effects. The use of both experimental approaches, microarray and PCA analysis, could elucidate undetermined targets of the heparin mimetics.

Ma and colleagues tracked the accumulation of the heparin-derived mimetic following intravenous injection. Their study concluded that the high accumulation was the brain, with the kidney having the second highest mimetic levels (Ma et al. 2002). This suggests that the mHeps could have other target sites around the body.

Off-target effects have been seen with other treatments for SCI. The first proven pharmacological treatment for SCI was high dose steroid methyl-prednisolone (MPSS). A cohort of clinical studies showed reduced disability when MPSS was given in the early hours following injury (Bracken et al. 1990). This drug, like the mHeps, has multiple effects, such as reduction in swelling and inflammation (Bracken et al. 1997). However, MPSS is a controversial treatment choice as complications and off-target effects such as gastric bleeding and wound infections have been reported (Hurlbert 2000).

The identification of off-target effects and the underlying mechanisms can be valuable. Understanding these would allow for further modifications to be made to the mimetics so as to remove the unwanted off-target interactions (MacDonald et al. 2006), therefore, increasing the therapeutic potential of heparin mimetics in SCI repair.

6.4 Microfluidics

The MFD technology used here could be an extremely useful tool for the study of axonal biology (Siddique and Thakor 2014; Taylor et al. 2005). The design of this device creates a better representation of some of the structural aspects of the spinal cord compared to the myelinating co-culture (Sorensen et al. 2008a) (Boomkamp et al. 2012). Specifically,

the compartmentalisation of the neuronal cell bodies from the neuronal processes and the organisation of isolated populations of neurons (Fig.5.8) are more reflective of certain aspects of the *in vivo* environment compared to the random seeding and undetermined neurite outgrowth of the SCI model. Additionally, the MFD allows for the targeted injury and study of axonal outgrowth verses neurite outgrowth, due to the size of the microchannels (500 µm) which only allows axons (not dendrites) to enter the central chamber (Fig.5.7). This allows for the investigation of compound effect on axonal outgrowth which is a key regenerative target following injury.

The SCI-MFD used in this thesis is the next generation SCI-MFD. It is built on the work specifically by Taylor and colleagues, who devised a novel MFD to isolate and lesion axons (Taylor et al. 2005). However, their simple device does not allow for immediate access to the axons. The SCI-MFD used in this thesis has an open access central chamber (Fig.5.7) which allows for direct and controlled injury and treatment of the axons insolation (Fig.5.12).

The MFD developed in this study can be used to investigate SCI in more depth. The device's cell seeding protocol can be adapted to accommodate many cellular populations aiming to help understand the injury process and repair mechanisms (Fig.5.7.A). For example, this specific device can be used to help understand the role of immune cells in SCI with the possibility of seeding immune cells into any of the chambers. Such an investigation could enable the characterisation of certain chemotactic factors released at the injury site by recording the migration to the injury site (Li et al. 2012b) (Cho et al. 2013). This could potentially aid the identification of a therapeutic intervention pertaining to immune cell migration, with subsequent investigation into the effects of the mimetics on this process (Sheng et al. 2013). Also, the device can be used to study the BBB as this structure plays a pivotal role in drug delivery success (Bicker et al. 2014) (Prabhakarpandian et al. 2013). The device could be used to investigate the mimetics' effects on the penetration and the cellular populations of the BBB (Gumbleton and Audus 2001). For example, the device could be seeded with the endothelial cells which are a component of the BBB, lining the microchannels and the mimetics could be introduced into the adjacent chambers and effects recorded.

A characterisation requirement for the MFD, which will strengthen the validity of the regenerative potential of compounds tested, would be to characterise the exact neuronal age within the device. This can be done by first identifying the time point in which no further neuronal cell division takes place, by staining the culture for NeuN (soma marker) and a proliferation stain (BrdU) or loss of PC3 gene expression of

(Iacopetti et al. 1994). This will allow for the exact neural age to be calculated, and the inclusion of neuronal age as a factor in the regenerative process and response to certain compounds such as mHeps.

The use of microfluidic platform in life science studies has drastically increased in the recent years with vast numbers of publications and patents relating to the use of this technology (Mark et al. 2010). The MF platform used in the lab for understanding basic biological processes and use in targeted study of axonal injury appears to be of great benefit (Siddique and Thakor 2014) (Taylor et al. 2005). MFD could be one of many technologies used in the early stages of compound development used to help guide towards drug mechanism and further the understanding of a complex biological process. Evidence provided herein supports a role for microfluidic technology allowing for the investigation of targeted axonal injury and treatment.

6.5 The experimental design

To critically analyse any study there are two focuses 1) the data retrieved and how this related to literature and future experimentation and 2) returning to assess the actual experimental design and the methodologies used. In this section I will focus on (2) and attempt to discuss the methodology used and how it can be improved.

A potential caveat of this study was the emphasis on a single culture method with no deviation from the cellular source material. The compounds have not been validated in other model organisms, therefore, there is a lack of interspecies toxicity/effectiveness correlation. This could hinder the progression of the mimetics to clinical level (Astashkina et al. 2012).

This culture system uses embryonic tissue as source material, so the responses to treatment and injury could potentially not representation of the effects in a mature system. The embryonic or immature cell will respond differently to extracellular stimuli compared to mature/terminally differentiated cells counter parts. However, the main reason why embryonic tissues are used is due to the comparative ease of culturing when compared to primary differentiated cells. Embryonic cells have a higher growth capacity and adapt more easily to deviations in external factors such as culture flasks and coverslips (Sato and Yasumura 1966). Additionally, the current scientific community's drive for reduction, replacement and refinement (3R's principle) of animal use in scientific experimentation places emphasis on sustainable or embryonic samples. Embryonic samples can be amplified readily in culture, thus, maximising sample outputs

from small tissue sources. This reduction in the beginnings of a pursuit for a compound will limit the number of *in vivo* models required at later stages for compound development.

For these reasons I advocate the use of embryonic CNS tissue but strongly suggest future work to accompany this culture with: both complex cultures varying in their source material (ones more translatable to human; i.e. human cell lines) and *in vivo* model systems (only following an exhaustive *in vitro* approach) but also simple and even biochemical assays which can both validate and strengthen our findings with our current *in vitro* models.

6.6 Future work

Previously in the discussion I have alluded to work which could strengthen the data which has already been generated, such as experimentation including the use other source material such as human cell lines for toxicology studies, and alternative models such as mouse transgenic strains. These will provide further validation of the compounds and the microfluid device used in this thesis.

The data and evidence generated in this study also hold promise in other neurological diseases; ones concerned with signalling dysregulation and alterations in the sulphation state at the area of trauma. This study has focused on the CNS but these compounds could have benefit in the peripheral nervous system (PNS). Current attempts at identifying a role for mimetics in PNS injury and remyelination are underway in our lab; a recent study highlighted heparin as a promotor in Schwann cell myelination. This begs the question which sulphate position and signalling pathway is responsible and these questions can be pursued using the mHep library.

There are a multitude of demyelinating diseases which may benefit from the desulphated mimetics' effects (modulation of disrupted signalling) on OPC proliferation and OL differentiation (Levine et al. 2001) (Rodgers et al. 2013). Multiple sclerosis (MS) is a chronic demyelinating disease which can be studied experimentally using a modified version of the myelinating culture model used in this study (Lindner et al. 2015). This offers a readily available tool to investigate the role of the mHeps in demyelinating conditions and a potential role for mHeps in the treatment of MS.

If we switch the focus slightly looking to our treatment with the heparin mimetics as a substitute for loss of function or presence of resident HSPG, we could approach

disorders which have shown reductions in the levels of HSPG. Autism is one such disease which could potentially benefit from our heparin mimetic compounds, especially as there are strong rodent models which have alterations in *N*-sulphated heparan sulphate (Meyza et al. 2012). Therefore, potentially demonstrating a multi-disease benefit of the mHeps and increasing the pharma/economical prospect of the mHeps.

Mentioned previously in the discussion, more experimentation is required to fully understand the signalling pathways such as Wnt and FGF involved in (this culture's) development to maturity and following injury. Given more time, focus would be applied to this characterisation as it will not only add to the strength of the culture system but most importantly, help to understand in greater detail any other potential compound's mechanism of function pertaining to these pathways.

The next logical avenue of research is to take the mHeps to the SCI-MFD. It was hypothesised that the mHeps could act similarly to their HSPG relatives and in part perform co-factor functions creating morphogenic gradients for signalling activation or competitively binding ligands leading to deactivation (Fuerer et al. 2010) (Yan and Lin 2009). However, the SCI model used in the mHep investigation is limited in the study of targeted treatment and diffusion (morphogenic) gradients. Thus, investigating whether the presence of diffusion gradients will impact the effects of the mHeps is not possible in the SCI model system. Furthermore, the SCI-MFD is capable of creating and manipulating diffusion gradients (Fig.5.11). Therefore, using the SCI-MFD in which a lesion is induced followed by treatment with mHep6 and mHep7, would allow data to be gathered on how the mHeps act in the presence of diffusion gradients. This would provide data on mHeps in a more *in vivo* like environment.

6.7 Overall Conclusion

SCI is a devastating condition with limited effective therapies available. The consensus is that a combinational approach is needed to overcome the complex pathology of SCI. Though research presented in this thesis suggests promise, there is need for clarity into the exact mechanisms of function for the mHeps and the impact these compounds have on targeted axonal injury. In this study I have identified a novel therapeutic compound and focused on understanding the specific biochemical component responsible for the therapeutic benefit. Moreover, I have also isolated a cellular target in which the compounds are acting and even dissected individual differences between related desulphated mimetics effects on these cells. I have provided evidence suggesting that targeting the OPC proliferation status and forcing OL differentiation can increase

myelination adjacent to the lesion site. Additionally, neurite outgrowth was promoted but using the established SCI injury model was not sufficient to delve deeper into the exact mechanism of effect. For this reason a novel microfluidic model was developed, with the aim for creating a more *in vivo*-like environment in which to study axonal outgrowth. This new model would also prove invaluable in the study of the mimetic compounds. We hypothesised that the mimetics would act similarly to their HSPG relatives which mediate cell signalling through ligand/morphogenic gradients but the established SCI model does not encompass the fluid dynamics of the *in vivo* microenvironment rendering these gradients potentially non-existent. However, the microfluid device can create and even allow manipulation of such gradients, resulting in a model that not only allows for targeted axonal study but also an environment in which the mimetics will exhort their greatest impact as signalling pathway manipulators. To end, this study has provided a foundation for two novel avenues of future study 1) heparin mimetics as a treatment for SCI and 2) a compartmentalised open access injury microfluidic device for vastly more detailed study of SCI. It is my hope that these two advancements may provide future improvement of treatment options for this devastating condition.

7 References

2002. Pharmacological therapy after acute cervical spinal cord injury. Neurosurgery 50:S63-72.

Abbott NJ, Ronnback L, Hansson E. 2006. Astrocyte-endothelial interactions at the blood-brain barrier. Nat Rev Neurosci 7:41-53.

Abe N, Cavalli V. 2008. Nerve injury signaling. Current Opinion in Neurobiology 18:276-283.

Abramsson A, Kurup S, Busse M, Yamada S, Lindblom P, Schallmeiner E, Stenzel D, Sauvaget D, Ledin J, Ringvall M and others. 2007. Defective N-sulfation of heparan sulfate proteoglycans limits PDGF-BB binding and pericyte recruitment in vascular development. Genes Dev 21:316-31.

Achyuta AK, Conway AJ, Crouse RB, Bannister EC, Lee RN, Katnik CP, Behensky AA, Cuevas J, Sundaram SS. 2013. A modular approach to create a neurovascular unit-on-a-chip. Lab Chip 13:542-53.

Adeeb N, Mortazavi MM. 2014. The role of FGF2 in spinal cord trauma and regeneration research. Brain Behav 4:105-7.

Ai X, Do AT, Lozynska O, Kusche-Gullberg M, Lindahl U, Emerson CP, Jr. 2003. QSulf1 remodels the 6-O sulfation states of cell surface heparan sulfate proteoglycans to promote Wnt signaling. J Cell Biol 162:341-51.

Ajioka I, Ichinose S, Nakajima K, Mizusawa H. 2011. Basement membrane-like matrix sponge for the three-dimensional proliferation culture of differentiated retinal horizontal interneurons. Biomaterials 32:5765-72.

Alberts B, Johnson A, Lewis J. 2002. Molecular Biology of the Cell. 4th edition. New York: Garland Science.

Allen A. 1911. Surgery of experimental lesion of spinal cord equivalent to crush injury of fracture dislocation of spinal column: A preliminary report. Journal of the American Medical Association LVII:878-880.

Allen DD, Caviedes R, Cardenas AM, Shimahara T, Segura-Aguilar J, Caviedes PA. 2005. Cell lines as in vitro models for drug screening and toxicity studies. Drug Dev Ind Pharm 31:757-68.

Alluin O, Karimi-Abdolrezaee S, Delivet-Mongrain H, Leblond H, Fehlings MG, Rossignol S. 2011. Kinematic study of locomotor recovery after spinal cord clip compression injury in rats. J Neurotrauma 28:1963-81.

Andersson H, van den Berg A. 2003. Microfluidic devices for cellomics: a review. Sensors and Actuators B: Chemical 92:315-325.

Araque A, Parpura V, Sanzgiri RP, Haydon PG. 1999. Tripartite synapses: glia, the unacknowledged partner. Trends Neurosci 22:208-15.

Ashton RS, Conway A, Pangarkar C, Bergen J, Lim KI, Shah P, Bissell M, Schaffer DV. 2012. Astrocytes regulate adult hippocampal neurogenesis through ephrin-B signaling. Nat Neurosci 15:1399-406.

Ashwell KWS. 2009. Chapter 2 - Development of the Spinal Cord. In: Kayalioglu CWP, editor. The Spinal Cord. San Diego: Academic Press. p 8-16.

Astashkina A, Mann B, Grainger DW. 2012. A critical evaluation of in vitro cell culture models for high-throughput drug screening and toxicity. Pharmacol Ther 134:82-106.

Bansal R, Kumar M, Murray K, Morrison RS, Pfeiffer SE. 1996. Regulation of FGF receptors in the oligodendrocyte lineage. Mol Cell Neurosci 7:263-75.

Barnett SC, Hutchins AM, Noble M. 1993. Purification of olfactory nerve ensheathing cells from the olfactory bulb. Dev Biol 155:337-50.

Barnett SC, Riddell JS. 2004. Olfactory ensheathing cells (OECs) and the treatment of CNS injury: advantages and possible caveats. Journal of Anatomy 204:57-67.

Barrowcliffe TW. 2012. History of heparin. Handb Exp Pharmacol:3-22.

Bartholdi D, Schwab ME. 1997. Expression of pro-inflammatory cytokine and chemokine mRNA upon experimental spinal cord injury in mouse: an in situ hybridization study. Eur J Neurosci 9:1422-38.

Bashaw GJ, Goodman CS. 1999. Chimeric Axon Guidance Receptors: The Cytoplasmic Domains of Slit and Netrin Receptors Specify Attraction versus Repulsion. Cell 97:917-926.

Basu A, Krady JK, O'Malley M, Styren SD, DeKosky ST, Levison SW. 2002. The type 1 interleukin-1 receptor is essential for the efficient activation of microglia and the induction of multiple proinflammatory mediators in response to brain injury. J Neurosci 22:6071-82.

Beattie MS, Bresnahan JC, Komon J, Tovar CA, Van Meter M, Anderson DK, Faden AI, Hsu CY, Noble LJ, Salzman S and others. 1997. Endogenous repair after spinal cord contusion injuries in the rat. Exp Neurol 148:453-63.

Beck KD, Nguyen HX, Galvan MD, Salazar DL, Woodruff TM, Anderson AJ. 2010. Quantitative analysis of cellular inflammation after traumatic spinal cord injury: evidence for a multiphasic inflammatory response in the acute to chronic environment. Brain 133:433-47.

Becker-Catania SG, Nelson JK, Olivares S, Chen SJ, DeVries GH. 2011. Oligodendrocyte progenitor cells proliferate and survive in an immature state following treatment with an axolemma-enriched fraction. ASN Neuro 3:e00053.

Beebe DJ, Mensing GA, Walker GM. 2002. Physics and applications of microfluidics in biology. Annu Rev Biomed Eng 4:261-86.

Beller JA, Snow DM. 2014. Proteoglycans: road signs for neurite outgrowth. Neural Regen Res 9:343-55.

Belmiro CL, Castelo-Branco MT, Melim LM, Schanaider A, Elia C, Madi K, Pavao MS, de Souza HS. 2009. Unfractionated heparin and new heparin analogues from ascidians (chordate-tunicate) ameliorate colitis in rats. J Biol Chem 284:11267-78.

Berlly M, Shem K. 2007. Respiratory Management During the First Five Days After Spinal Cord Injury. The Journal of Spinal Cord Medicine 30:309-318.

Bernfield M, Gotte M, Park PW, Reizes O, Fitzgerald ML, Lincecum J, Zako M. 1999. Functions of cell surface heparan sulfate proteoglycans. Annu Rev Biochem 68:729-77.

Bhatia SN, Ingber DE. 2014. Microfluidic organs-on-chips. Nat Biotech 32:760-772.

Bhatt JM, Gordon PH. 2007. Current clinical trials in amyotrophic lateral sclerosis. Expert Opin Investig Drugs 16:1197-207.

Bicker J, Alves G, Fortuna A, Falcão A. 2014. Blood–brain barrier models and their relevance for a successful development of CNS drug delivery systems: A review. European Journal of Pharmaceutics and Biopharmaceutics 87:409-432.

Bishop JR, Schuksz M, Esko JD. 2007. Heparan sulphate proteoglycans fine-tune mammalian physiology. Nature 446:1030-7.

Blakemore WF. 1977. Remyelination of CNS axons by Schwann cells transplanted from the sciatic nerve. Nature 266:68-9.

Bomze HM, Bulsara KR, Iskandar BJ, Caroni P, Skene JH. 2001. Spinal axon regeneration evoked by replacing two growth cone proteins in adult neurons. Nat Neurosci 4:38-43.

Bond LM, McKerracher L. 2014. Cervical spinal cord injury: tailoring clinical trial endpoints to reflect meaningful functional improvements. Neural Regeneration Research 9:1493-1497.

Boomkamp SD, McGrath MA, Houslay MD, Barnett SC. 2014. Epac and the high affinity rolipram binding conformer of PDE4 modulate neurite outgrowth and myelination using an in vitro spinal cord injury model. Br J Pharmacol 171:2385-98.

Boomkamp SD, Riehle MO, Wood J, Olson MF, Barnett SC. 2012. The development of a rat in vitro model of spinal cord injury demonstrating the additive effects of Rho and ROCK inhibitors on neurite outgrowth and myelination. Glia 60:441-56.

Booth R, Kim H. 2012. Characterization of a microfluidic in vitro model of the blood-brain barrier (muBBB). Lab Chip 12:1784-92.

Bowers SL, Banerjee I, Baudino TA. 2010. The extracellular matrix: at the center of it all. J Mol Cell Cardiol 48:474-82.

Bracken MB, Shepard MJ, Collins WF, Holford TR, Young W, Baskin DS, Eisenberg HM, Flamm E, Leo-Summers L, Maroon J and others. 1990. A randomized, controlled trial of methylprednisolone or naloxone in the treatment of acute spinal-cord injury. Results of the Second National Acute Spinal Cord Injury Study. N Engl J Med 322:1405-11.

Bracken MB, Shepard MJ, Holford TR, Leo-Summers L, Aldrich EF, Fazl M, Fehlings M, Herr DL, Hitchon PW, Marshall LF and others. 1997. Administration of methylprednisolone for 24 or 48 hours or tirilazad mesylate for 48 hours in the treatment of acute spinal cord injury. Results of the Third National Acute Spinal Cord Injury Randomized Controlled Trial. National Acute Spinal Cord Injury Study. Jama 277:1597-604.

Bradbury EJ, Moon LDF, Popat RJ, King VR, Bennett GS, Patel PN, Fawcett JW, McMahon SB. 2002. Chondroitinase ABC promotes functional recovery after spinal cord injury. Nature 416:636-640.

Brambilla R, Bracchi-Ricard V, Hu W-H, Frydel B, Bramwell A, Karmally S, Green EJ, Bethea JR. 2005. Inhibition of astroglial nuclear factor κB reduces inflammation and improves functional recovery after spinal cord injury. The Journal of Experimental Medicine 202:145-156.

Briona LK, Poulain FE, Mosimann C, Dorsky RI. 2015. Wnt/ss-catenin signaling is required for radial glial neurogenesis following spinal cord injury. Dev Biol 403:15-21.

Brittis PA, Canning DR, Silver J. 1992. Chondroitin sulfate as a regulator of neuronal patterning in the retina. Science 255:733-6.

Bush TG, Puvanachandra N, Horner CH, Polito A, Ostenfeld T, Svendsen CN, Mucke L, Johnson MH, Sofroniew MV. 1999. Leukocyte infiltration, neuronal degeneration, and neurite outgrowth after ablation of scar-forming, reactive astrocytes in adult transgenic mice. Neuron 23:297-308.

Bushong EA, Martone ME, Jones YZ, Ellisman MH. 2002. Protoplasmic astrocytes in CA1 stratum radiatum occupy separate anatomical domains. J Neurosci 22:183-92.

Buss A, Pech K, Kakulas BA, Martin D, Schoenen J, Noth J, Brook GA. 2009. NG2 and phosphacan are present in the astroglial scar after human traumatic spinal cord injury. BMC Neurol 9:32.

Cadwalader EL, Condic ML, Yost HJ. 2012. 2-O-sulfotransferase regulates Wnt signaling, cell adhesion and cell cycle during zebrafish epiboly. Development 139:1296-305.

Caja Ry. 1928. Degeneration and Regeneration of the Nervous System.

Campenot RB. 1977. Local control of neurite development by nerve growth factor. Proc Natl Acad Sci U S A 74:4516-9.

Canoll PD, Musacchio JM, Hardy R, Reynolds R, Marchionni MA, Salzer JL. 1996. GGF/neuregulin is a neuronal signal that promotes the proliferation and survival and inhibits the differentiation of oligodendrocyte progenitors. Neuron 17:229-43.

Capila I, Linhardt RJ. 2002. Heparin-protein interactions. Angew Chem Int Ed Engl 41:391-412.

Carlson SL, Parrish ME, Springer JE, Doty K, Dossett L. 1998. Acute inflammatory response in spinal cord following impact injury. Exp Neurol 151:77-88.

Castillo GM, Cummings JA, Yang W, Judge ME, Sheardown MJ, Rimvall K, Hansen JB, Snow AD. 1998. Sulfate content and specific glycosaminoglycan backbone of perlecan are critical for perlecan's enhancement of islet amyloid polypeptide (amylin) fibril formation. Diabetes 47:612-20.

Casu B, Guerrini M, Torri G. 2004. Structural and conformational aspects of the anticoagulant and anti-thrombotic activity of heparin and dermatan sulfate. Curr Pharm Des 10:939-49.

Casu B, Naggi A, Torri G. 2010. Heparin-derived heparan sulfate mimics to modulate heparan sulfate-protein interaction in inflammation and cancer. Matrix Biol 29:442-52.

Cepko CL, Austin CP, Yang X, Alexiades M, Ezzeddine D. 1996. Cell fate determination in the vertebrate retina. Proc Natl Acad Sci U S A 93:589-95.

Chan CC, Khodarahmi K, Liu J, Sutherland D, Oschipok LW, Steeves JD, Tetzlaff W. 2005. Dose-dependent beneficial and detrimental effects of ROCK inhibitor Y27632 on axonal sprouting and functional recovery after rat spinal cord injury. Exp Neurol 196:352-64.
Chang YH, Chiu YJ, Cheng HC, Liu FJ, Lai WW, Chang HJ, Liao PC. 2015. Down-regulation of TIMP-1 inhibits cell migration, invasion, and metastatic colonization in lung adenocarcinoma. Tumour Biol 36:3957-67.
Chapman E, Best MD, Hanson SR, Wong C-H. 2004. Sulfotransferases: Structure, Mechanism, Biological Activity, Inhibition, and Synthetic Utility. Angewandte Chemie International Edition 43:3526-3548.
Chari DM, Zhao C, Kotter MR, Blakemore WF, Franklin RJ. 2006. Corticosteroids delay remyelination of experimental demyelination in the rodent central nervous system. J Neurosci Res 83:594-605.
Chen G, Hu YR, Wan H, Xia L, Li JH, Yang F, Qu X, Wang SG, Wang ZC. 2010. Functional recovery following traumatic spinal cord injury mediated by a unique polymer scaffold seeded with neural stem cells and Schwann cells. Chin Med J (Engl) 123:2424-31.
Chen J, Leong SY, Schachner M. 2005. Differential expression of cell fate determinants in neurons and glial cells of adult mouse spinal cord after compression injury. Eur J Neurosci 22:1895-906.
Chen ZJ, Ughrin Y, Levine JM. 2002. Inhibition of axon growth by oligodendrocyte precursor cells. Mol Cell Neurosci 20:125-39.
Chi CW, Ahmed AR, Dereli-Korkut Z, Wang S. 2016. Microfluidic cell chips for high-throughput drug screening. Bioanalysis 8:921-37.
Cho H, Hashimoto T, Wong E, Hori Y, Wood LB, Zhao L, Haigis KM, Hyman BT, Irimia D. 2013. Microfluidic chemotaxis platform for differentiating the roles of soluble and bound amyloid-beta on microglial accumulation. Sci Rep 3:1823.
Chong SY, Rosenberg SS, Fancy SP, Zhao C, Shen YA, Hahn AT, McGee AW, Xu X, Zheng B, Zhang LI and others. 2012. Neurite outgrowth inhibitor Nogo-A establishes spatial segregation and extent of oligodendrocyte myelination. Proc Natl Acad Sci U S A 109:1299-304.
Christie S, Thibault-Halman G, Casha S. 2011. Acute Pharmacological DVT Prophylaxis after Spinal Cord Injury. Journal of Neurotrauma 28:1509-1514.
Chronis N. 2010. Worm chips: microtools for C. elegans biology. Lab Chip 10:432-7.
Chung K, Rivet CA, Kemp ML, Lu H. 2011. Imaging single-cell signaling dynamics with a deterministic high-density single-cell trap array. Anal Chem 83:7044-52.
Cole GJ, Loewy A, Glaser L. 1986. Neuronal cell-cell adhesion depends on interactions of N-CAM with heparin-like molecules. Nature 320:445-7.
Coleman ML, Sahai EA, Yeo M, Bosch M, Dewar A, Olson MF. 2001. Membrane blebbing during apoptosis results from caspase-mediated activation of ROCK I. Nat Cell Biol 3:339-345.
Collins MN, Birkinshaw C. 2013. Hyaluronic acid based scaffolds for tissue engineering--a review. Carbohydr Polym 92:1262-79.
Coombe DR, Kett WC. 2005. Heparan sulfate-protein interactions: therapeutic potential through structure-function insights. Cell Mol Life Sci 62:410-24.
Coombe DR, Kett WC. 2012. Heparin mimetics. Handb Exp Pharmacol:361-83.
Cornelli U. 1996. Non-Anticoagulant Actions of Glycosaminoglycans (GAGs). In: Harenberg J, Casu B, editors. Nonanticoagulant Actions of Glycosaminoglycans. Boston, MA: Springer US. p 249-279.
Court FA, Hendriks WT, MacGillavry HD, Alvarez J, van Minnen J. 2008. Schwann cell to axon transfer of ribosomes: toward a novel understanding of the role of glia in the nervous system. J Neurosci 28:11024-9.
Crang AJ, Blakemore WF. 1991. Remyelination of demyelinated rat axons by transplanted mouse oligodendrocytes. Glia 4:305-13.
Crossman AR, Neary D. 2010. Neuroanatomy: An Illustrated Colour Text. In: 4th, editor. Neuroanatomy: An Illustrated Colour Text
Churchill Livingstone Elsevier. p 67-87.

Cui H, Freeman C, Jacobson GA, Small DH. 2013. Proteoglycans in the central nervous system: role in development, neural repair, and Alzheimer's disease. IUBMB Life 65:108-20.
Cullen DK, Wolf JA, Vernekar VN, Vukasinovic J, LaPlaca MC. 2011. Neural tissue engineering and biohybridized microsystems for neurobiological investigation in vitro (Part 1). Crit Rev Biomed Eng 39:201-40.
Cuzzocrea S, Genovese T, Mazzon E, Crisafulli C, Di Paola R, Muia C, Collin M, Esposito E, Bramanti P, Thiemermann C. 2006. Glycogen synthase kinase-3 beta inhibition reduces secondary damage in experimental spinal cord trauma. J Pharmacol Exp Ther 318:79-89.
Dalton PD, Flynn L, Shoichet MS. 2002. Manufacture of poly(2-hydroxyethyl methacrylate-co-methyl methacrylate) hydrogel tubes for use as nerve guidance channels. Biomaterials 23:3843-51.
Damus PS, Hicks M, Rosenberg RD. 1973. Anticoagulant action of heparin. Nature 246:355-7.
Dawson MR, Levine JM, Reynolds R. 2000. NG2-expressing cells in the central nervous system: are they oligodendroglial progenitors? J Neurosci Res 61:471-9.
Dergham P, Ellezam B, Essagian C, Avedissian H, Lubell WD, McKerracher L. 2002. Rho signaling pathway targeted to promote spinal cord repair. J Neurosci 22:6570-7.
Dertinger SKW, Chiu DT, Jeon NL, Whitesides GM. 2001. Generation of Gradients Having Complex Shapes Using Microfluidic Networks. Analytical Chemistry 73:1240-1246.
Dhoot GK, Gustafsson MK, Ai X, Sun W, Standiford DM, Emerson CP. 2001. Regulation of Wnt Signaling and Embryo Patterning by an Extracellular Sulfatase. Science 293:1663-1666.
Dibaj P, Nadrigny F, Steffens H, Scheller A, Hirrlinger J, Schomburg ED, Neusch C, Kirchhoff F. 2010. NO mediates microglial response to acute spinal cord injury under ATP control in vivo. Glia 58:1133-44.
Dickson BJ, Senti KA. 2002. Axon guidance: growth cones make an unexpected turn. Curr Biol 12:R218-20.
Donnelly DJ, Popovich PG. 2008. Inflammation and its role in neuroprotection, axonal regeneration and functional recovery after spinal cord injury. Experimental Neurology 209:378-388.
Dou CL, Levine JM. 1995. Differential effects of glycosaminoglycans on neurite growth on laminin and L1 substrates. J Neurosci 15:8053-66.
Douglas MR, Morrison KC, Jacques SJ, Leadbeater WE, Gonzalez AM, Berry M, Logan A, Ahmed Z. 2009. Off-target effects of epidermal growth factor receptor antagonists mediate retinal ganglion cell disinhibited axon growth. Brain 132:3102-21.
Drake R, Vogl AW, Mitchell AWM. 2015. Gray's Anatomy, for Students
The Anatomical Basis of Clinical Practice. Grays Anatomy: Elsevier.
Dudas B, Semeniken K. 2012. Glycosaminoglycans and Neuroprotection. In: Lever R, Mulloy B, Page PC, editors. Heparin - A Century of Progress. Berlin, Heidelberg: Springer Berlin Heidelberg. p 325-343.
Dumont RJ, Verma S, Okonkwo DO, Hurlbert RJ, Boulos PT, Ellegala DB, Dumont AS. 2001. Acute spinal cord injury, part II: contemporary pharmacotherapy. Clin Neuropharmacol 24:265-79.
East E, de Oliveira DB, Golding JP, Phillips JB. 2010. Alignment of astrocytes increases neuronal growth in three-dimensional collagen gels and is maintained following plastic compression to form a spinal cord repair conduit. Tissue Eng Part A 16:3173-84.
Ekwall B. 1980. Screening of toxic compounds in tissue culture. Toxicology 17:127-42.
Elkabes S, DiCicco-Bloom EM, Black IB. 1996. Brain microglia/macrophages express neurotrophins that selectively regulate microglial proliferation and function. J Neurosci 16:2508-21.
Endo Y, Rubin JS. 2007. Wnt signaling and neurite outgrowth: insights and questions. Cancer Sci 98:1311-7.

Escobar Galvis ML, Jia J, Zhang X, Jastrebova N, Spillmann D, Gottfridsson E, van Kuppevelt TH, Zcharia E, Vlodavsky I, Lindahl U and others. 2007. Transgenic or tumor-induced expression of heparanase upregulates sulfation of heparan sulfate. Nat Chem Biol 3:773-8.

Etienne-Manneville S, Hall A. 2001. Integrin-mediated activation of Cdc42 controls cell polarity in migrating astrocytes through PKCzeta. Cell 106:489-98.

Eyre JA. 2003. Development and plasticity of the corticospinal system in man. Neural Plast 10:93-106.

Fairless R, Barnett SC. 2005. Olfactory ensheathing cells: their role in central nervous system repair. Int J Biochem Cell Biol 37:693-9.

Fancy SP, Baranzini SE, Zhao C, Yuk DI, Irvine KA, Kaing S, Sanai N, Franklin RJ, Rowitch DH. 2009. Dysregulation of the Wnt pathway inhibits timely myelination and remyelination in the mammalian CNS. Genes Dev 23:1571-85.

Fancy SP, Zhao C, Franklin RJ. 2004. Increased expression of Nkx2.2 and Olig2 identifies reactive oligodendrocyte progenitor cells responding to demyelination in the adult CNS. Mol Cell Neurosci 27:247-54.

Farbman AI. 1990. Olfactory neurogenesis: genetic or environmental controls? Trends Neurosci 13:362-5.

Faulkner JR, Herrmann JE, Woo MJ, Tansey KE, Doan NB, Sofroniew MV. 2004. Reactive astrocytes protect tissue and preserve function after spinal cord injury. J Neurosci 24:2143-55.

Fawcett JW. 2006. Overcoming inhibition in the damaged spinal cord. J Neurotrauma 23:371-83.

Fawcett JW, Asher RA. 1999. The glial scar and central nervous system repair. Brain Res Bull 49:377-91.

Fawcett JW, Housden E, Smith-Thomas L, Meyer RL. 1989. The growth of axons in three-dimensional astrocyte cultures. Dev Biol 135:449-58.

Fehlings MG. 2001. Summary statement: the use of methylprednisolone in acute spinal cord injury. Spine (Phila Pa 1976) 26:S55.

Fehlings MG, Hawryluk GW. 2010. Scarring after spinal cord injury. J Neurosurg Spine 13:165-7; discussion 167-8.

Feldblum S, Arnaud S, Simon M, Rabin O, D'Arbigny P. 2000. Efficacy of a new neuroprotective agent, gacyclidine, in a model of rat spinal cord injury. J Neurotrauma 17:1079-93.

Feng G, Mellor RH, Bernstein M, Keller-Peck C, Nguyen QT, Wallace M, Nerbonne JM, Lichtman JW, Sanes JR. 2000. Imaging neuronal subsets in transgenic mice expressing multiple spectral variants of GFP. Neuron 28:41-51.

Ferreira Chacon JM, Mello de Andrea ML, Blanes L, Ferreira LM. 2010. Effects of topical application of 10,000 IU heparin on patients with perineal dermatitis and second-degree burns treated in a public pediatric hospital. J Tissue Viability 19:150-8.

Festoff BW, Ameenuddin S, Arnold PM, Wong A, Santacruz KS, Citron BA. 2006. Minocycline neuroprotects, reduces microgliosis, and inhibits caspase protease expression early after spinal cord injury. J Neurochem 97:1314-26.

Filbin MT. 2003. Myelin-associated inhibitors of axonal regeneration in the adult mammalian CNS. Nat Rev Neurosci 4:703-713.

Fitch MT, Doller C, Combs CK, Landreth GE, Silver J. 1999. Cellular and molecular mechanisms of glial scarring and progressive cavitation: in vivo and in vitro analysis of inflammation-induced secondary injury after CNS trauma. J Neurosci 19:8182-98.

Fitch MT, Silver J. 1997. Activated macrophages and the blood-brain barrier: inflammation after CNS injury leads to increases in putative inhibitory molecules. Exp Neurol 148:587-603.

Fitch MT, Silver J. 2008. CNS Injury, Glial Scars, and Inflammation: Inhibitory extracellular matrices and regeneration failure. Experimental neurology 209:294-301.

Ford-Perriss M, Turner K, Guimond S, Apedaile A, Haubeck HD, Turnbull J, Murphy M. 2003. Localisation of specific heparan sulfate proteoglycans during the proliferative phase of brain development. Dev Dyn 227:170-84.
Forsberg M, Holmborn K, Kundu S, Dagalv A, Kjellen L, Forsberg-Nilsson K. 2012. Undersulfation of heparan sulfate restricts differentiation potential of mouse embryonic stem cells. J Biol Chem 287:10853-62.
Fournier AE, GrandPre T, Strittmatter SM. 2001. Identification of a receptor mediating Nogo-66 inhibition of axonal regeneration. Nature 409:341-6.
Fournier AE, Takizawa BT, Strittmatter SM. 2003. Rho kinase inhibition enhances axonal regeneration in the injured CNS. J Neurosci 23:1416-23.
Franklin RJ, Bayley SA, Blakemore WF. 1996. Transplanted CG4 cells (an oligodendrocyte progenitor cell line) survive, migrate, and contribute to repair of areas of demyelination in X-irradiated and damaged spinal cord but not in normal spinal cord. Exp Neurol 137:263-76.
Franssen EH, de Bree FM, Verhaagen J. 2007. Olfactory ensheathing glia: their contribution to primary olfactory nervous system regeneration and their regenerative potential following transplantation into the injured spinal cord. Brain Res Rev 56:236-58.
Freeman C, Liu L, Banwell MG, Brown KJ, Bezos A, Ferro V, Parish CR. 2005. Use of sulfated linked cyclitols as heparan sulfate mimetics to probe the heparin/heparan sulfate binding specificity of proteins. J Biol Chem 280:8842-9.
Freier T, Montenegro R, Shan Koh H, Shoichet MS. 2005. Chitin-based tubes for tissue engineering in the nervous system. Biomaterials 26:4624-32.
Freund P, Wannier T, Schmidlin E, Bloch J, Mir A, Schwab ME, Rouiller EM. 2007. Anti-Nogo-A antibody treatment enhances sprouting of corticospinal axons rostral to a unilateral cervical spinal cord lesion in adult macaque monkey. J Comp Neurol 502:644-59.
Friese RS, Rehring TF, Wollmering M, Moore EE, Ketch LL, Banerjee A, Harken AH. 1994. Trauma primes cells. Shock 1:388-94.
Fuerer C, Habib SJ, Nusse R. 2010. A study on the interactions between Heparan Sulfate Proteoglycans and Wnt proteins. Developmental dynamics : an official publication of the American Association of Anatomists 239:184-190.
Fujita Y, Yamashita T. 2014. Axon growth inhibition by RhoA/ROCK in the central nervous system. Front Neurosci 8:338.
Gao X, Wang Y, Chen J, Peng J. 2013. The role of peripheral nerve ECM components in the tissue engineering nerve construction. Rev Neurosci 24:443-53.
Garg HG, Mrabat H, Yu L, Freeman C, Li B, Zhang F, Linhardt RJ, Hales CA. 2008. Significance of the 2-O-sulfo group of L-iduronic acid residues in heparin on the growth inhibition of bovine pulmonary artery smooth muscle cells. Carbohydr Res 343:2406-10.
Geoffroy CG, Zheng B. 2014. Myelin-associated inhibitors in axonal growth after CNS injury. Curr Opin Neurobiol 27:31-8.
Ghodbane M, Stucky EC, Maguire TJ, Schloss RS, Shreiber DI, Zahn JD, Yarmush ML. 2015. Development and validation of a microfluidic immunoassay capable of multiplexing parallel samples in microliter volumes. Lab on a Chip 15:3211-3221.
Goldberg LC, Barkoff JR. 1960. Treatment of dermatoses with intravenously given methylprednisolone sodium succinate. J Am Med Assoc 172:1514-7.
Goldshmit Y, Frisca F, Pinto AR, Pebay A, Tang JK, Siegel AL, Kaslin J, Currie PD. 2014. Fgf2 improves functional recovery-decreasing gliosis and increasing radial glia and neural progenitor cells after spinal cord injury. Brain Behav 4:187-200.
Gonzalez-Fernandez C, Fernandez-Martos CM, Shields SD, Arenas E, Javier Rodriguez F. 2014. Wnts are expressed in the spinal cord of adult mice and are differentially induced after injury. J Neurotrauma 31:565-81.
Gonzalez P, Fernandez-Martos CM, Gonzalez-Fernandez C, Arenas E, Rodriguez FJ. 2012. Spatio-temporal expression pattern of frizzled receptors after contusive spinal cord injury in adult rats. PLoS One 7:e50793.
Graziadei PP. 1973. Cell dynamics in the olfactory mucosa. Tissue Cell 5:113-31.

Graziadei PP, Graziadei GA. 1979. Neurogenesis and neuron regeneration in the olfactory system of mammals. I. Morphological aspects of differentiation and structural organization of the olfactory sensory neurons. J Neurocytol 8:1-18.
Greek R, Menache A. 2013. Systematic reviews of animal models: methodology versus epistemology. Int J Med Sci 10:206-21.
Greene LA, Tischler AS. 1976. Establishment of a noradrenergic clonal line of rat adrenal pheochromocytoma cells which respond to nerve growth factor. Proceedings of the National Academy of Sciences 73:2424-2428.
Grosberg A, Alford PW, McCain ML, Parker KK. 2011. Ensembles of engineered cardiac tissues for physiological and pharmacological study: heart on a chip. Lab Chip 11:4165-73.
Gross PG, Kartalov EP, Scherer A, Weiner LP. 2007. Applications of microfluidics for neuronal studies. J Neurol Sci 252:135-43.
Gu L, Black B, Ordonez S, Mondal A, Jain A, Mohanty S. 2014. Microfluidic control of axonal guidance. Sci Rep 4:6457.
Guan KL, Rao Y. 2003. Signalling mechanisms mediating neuronal responses to guidance cues. Nat Rev Neurosci 4:941-56.
Gumbleton M, Audus KL. 2001. Progress and limitations in the use of in vitro cell cultures to serve as a permeability screen for the blood-brain barrier. J Pharm Sci 90:1681-98.
Gumy LF, Tan CL, Fawcett JW. 2010. The role of local protein synthesis and degradation in axon regeneration. Experimental Neurology 223:28-37.
Hall ED. 1992. The neuroprotective pharmacology of methylprednisolone. J Neurosurg 76:13-22.
Hamilton NB, Attwell D. 2010. Do astrocytes really exocytose neurotransmitters? Nat Rev Neurosci 11:227-38.
Hantaz-Ambroise D, Vigny M, Koenig J. 1987. Heparan sulfate proteoglycan and laminin mediate two different types of neurite outgrowth. J Neurosci 7:2293-304.
Harel NY, Strittmatter SM. 2006. Can regenerating axons recapitulate developmental guidance during recovery from spinal cord injury? Nat Rev Neurosci 7:603-616.
Hausmann ON. 2003. Post-traumatic inflammation following spinal cord injury. Spinal Cord 41:369-78.
Hay JR, Johnson VE, Young AM, Smith DH, Stewart W. 2015. Blood-Brain Barrier Disruption Is an Early Event That May Persist for Many Years After Traumatic Brain Injury in Humans. J Neuropathol Exp Neurol 74:1147-57.
Hayball PJ, Cosh DG, Ahern MJ, Schultz DW, Roberts-Thomson PJ. 1992. High dose oral methylprednisolone in patients with rheumatoid arthritis: pharmacokinetics and clinical response. Eur J Clin Pharmacol 42:85-8.
Haydon PG, Carmignoto G. 2006. Astrocyte control of synaptic transmission and neurovascular coupling. Physiol Rev 86:1009-31.
He MM, Smith AS, Oslob JD, Flanagan WM, Braisted AC, Whitty A, Cancilla MT, Wang J, Lugovskoy AA, Yoburn JC and others. 2005. Small-molecule inhibition of TNF-alpha. Science 310:1022-5.
Hering TM, Beller JA, Calulot CM, Centers A, Snow DM. 2015. Proteoglycans of reactive rat cortical astrocyte cultures: abundance of N-unsubstituted glucosamine-enriched heparan sulfate. Matrix Biol 41:8-18.
Hermann GE, Rogers RC, Bresnahan JC, Beattie MS. 2001. Tumor necrosis factor-alpha induces cFOS and strongly potentiates glutamate-mediated cell death in the rat spinal cord. Neurobiol Dis 8:590-9.
Higashida T, Kreipke CW, Rafols JA, Peng C, Schafer S, Schafer P, Ding JY, Dornbos D, 3rd, Li X, Guthikonda M and others. 2011. The role of hypoxia-inducible factor-1alpha, aquaporin-4, and matrix metalloproteinase-9 in blood-brain barrier disruption and brain edema after traumatic brain injury. J Neurosurg 114:92-101.
Higginson JR, Thompson SM, Santos-Silva A, Guimond SE, Turnbull JE, Barnett SC. 2012. Differential sulfation remodelling of heparan sulfate by extracellular 6-O-sulfatases regulates fibroblast growth factor-induced boundary formation by glial cells: implications for glial cell transplantation. J Neurosci 32:15902-12.

Hirata K, Kawabuchi M. 2002. Myelin phagocytosis by macrophages and nonmacrophages during Wallerian degeneration. Microsc Res Tech 57:541-7.
Hirsh J. 2001. New anticoagulants. Am Heart J 142:S3-8.
Hosmane S, Fournier A, Wright R, Rajbhandari L, Siddique R, Yang IH, Ramesh KT, Venkatesan A, Thakor N. 2011. Valve-based microfluidic compression platform: single axon injury and regrowth. Lab Chip 11:3888-95.
Hosmane S, Yang IH, Ruffin A, Thakor N, Venkatesan A. 2010. Circular compartmentalized microfluidic platform: Study of axon-glia interactions. Lab Chip 10:741-7.
Huebner EA, Strittmatter SM. 2009. Axon Regeneration in the Peripheral and Central Nervous Systems. Results and problems in cell differentiation 48:339-351.
Hurlbert RJ. 2000. Methylprednisolone for acute spinal cord injury: an inappropriate standard of care. J Neurosurg 93:1-7.
Iacopetti P, Barsacchi G, Tirone F, Maffei L, Cremisi F. 1994. Developmental expression of PC3 gene is correlated with neuronal cell birthday. Mech Dev 47:127-37.
Inman D, Guth L, Steward O. 2002. Genetic influences on secondary degeneration and wound healing following spinal cord injury in various strains of mice. J Comp Neurol 451:225-35.
Jessen KR. 2004. Glial cells. The International Journal of Biochemistry & Cell Biology 36:1861-1867.
Joanne Wang C, Li X, Lin B, Shim S, Ming GL, Levchenko A. 2008. A microfluidics-based turning assay reveals complex growth cone responses to integrated gradients of substrate-bound ECM molecules and diffusible guidance cues. Lab Chip 8:227-37.
Johns P. 2014. Clinical Neuroscience: An illustrated text. Elsevier Health Sciences. p 13.
Johnson KG, Ghose A, Epstein E, Lincecum J, O'Connor MB, Van Vactor D. 2004. Axonal heparan sulfate proteoglycans regulate the distribution and efficiency of the repellent slit during midline axon guidance. Curr Biol 14:499-504.
Jones LL, Margolis RU, Tuszynski MH. 2003. The chondroitin sulfate proteoglycans neurocan, brevican, phosphacan, and versican are differentially regulated following spinal cord injury. Exp Neurol 182:399-411.
Jordan-Sciutto KL, Murray Fenner BA, Wiley CA, Achim CL. 2001. Response of cell cycle proteins to neurotrophic factor and chemokine stimulation in human neuroglia. Exp Neurol 167:205-14.
Jullien J, Gurdon J. 2005. Morphogen gradient interpretation by a regulated trafficking step during ligand–receptor transduction. Genes & Development 19:2682-2694.
Jung H, Yoon BC, Holt CE. 2012. Axonal mRNA localization and local protein synthesis in nervous system assembly, maintenance and repair. Nat Rev Neurosci 13:308-324.
Kabu S, Gao Y, Kwon BK, Labhasetwar V. 2015. Drug delivery, cell-based therapies, and tissue engineering approaches for spinal cord injury. Journal of Controlled Release 219:141-154.
Kacem K, Lacombe P, Seylaz J, Bonvento G. 1998. Structural organization of the perivascular astrocyte endfeet and their relationship with the endothelial glucose transporter: a confocal microscopy study. Glia 23:1-10.
Kalinski AL, Sachdeva R, Gomes C, Lee SJ, Shah Z, Houle JD, Twiss JL. 2015. mRNAs and Protein Synthetic Machinery Localize into Regenerating Spinal Cord Axons When They Are Provided a Substrate That Supports Growth. J Neurosci 35:10357-70.
Karumbaiah L, Anand S, Thazhath R, Zhong Y, McKeon RJ, Bellamkonda RV. 2011. Targeted downregulation of N-acetylgalactosamine 4-sulfate 6-O-sulfotransferase significantly mitigates chondroitin sulfate proteoglycan-mediated inhibition. Glia 59:981-96.
Karus M, Samtleben S, Busse C, Tsai T, Dietzel ID, Faissner A, Wiese S. 2012. Normal sulfation levels regulate spinal cord neural precursor cell proliferation and differentiation. Neural Dev 7:20.
Kayalioglu G. 2009. Chapter 3 - The Vertebral Column and Spinal Meninges. In: Kayalioglu CWP, editor. The Spinal Cord. San Diego: Academic Press. p 17-36.

Kennedy TE, Serafini T, de la Torre JR, Tessier-Lavigne M. 1994. Netrins are diffusible chemotropic factors for commissural axons in the embryonic spinal cord. Cell 78:425-35.
Kennedy TE, Wang H, Marshall W, Tessier-Lavigne M. 2006. Axon guidance by diffusible chemoattractants: a gradient of netrin protein in the developing spinal cord. J Neurosci 26:8866-74.
Kettenmann H, Verkhratsky A. 2008. Neuroglia: the 150 years after. Trends Neurosci 31:653-9.
Khakh BS, Sofroniew MV. 2015. Diversity of astrocyte functions and phenotypes in neural circuits. Nat Neurosci 18:942-52.
Kim YT, Karthikeyan K, Chirvi S, Dave DP. 2009. Neuro-optical microfluidic platform to study injury and regeneration of single axons. Lab Chip 9:2576-81.
Kinnunen T, Townsend J, Turnbull J. 2004. Heparan sulfate is essential for neuron migration and axon outgrowth in Caenorhabditis elegans. International Journal of Experimental Pathology 85:A69-A70.
Kippert A, Trajkovic K, Rajendran L, Ries J, Simons M. 2007. Rho regulates membrane transport in the endocytic pathway to control plasma membrane specialization in oligodendroglial cells. J Neurosci 27:3560-70.
Kirshblum SC, Burns SP, Biering-Sorensen F, Donovan W, Graves DE, Jha A, Johansen M, Jones L, Krassioukov A, Mulcahey MJ and others. 2011. International standards for neurological classification of spinal cord injury (Revised 2011). The Journal of Spinal Cord Medicine 34:535-546.
Klapka N, Hermanns S, Straten G, Masanneck C, Duis S, Hamers FP, Muller D, Zuschratter W, Muller HW. 2005. Suppression of fibrous scarring in spinal cord injury of rat promotes long-distance regeneration of corticospinal tract axons, rescue of primary motoneurons in somatosensory cortex and significant functional recovery. Eur J Neurosci 22:3047-58.
Knoller N, Auerbach G, Fulga V, Zelig G, Attias J, Bakimer R, Marder JB, Yoles E, Belkin M, Schwartz M and others. 2005. Clinical experience using incubated autologous macrophages as a treatment for complete spinal cord injury: phase I study results. J Neurosurg Spine 3:173-81.
Kocsis JD, Lankford KL, Sasaki M, Radtke C. 2009. Unique in vivo properties of olfactory ensheathing cells that may contribute to neural repair and protection following spinal cord injury. Neuroscience Letters 456:137-142.
Komoly S, Hudson LD, Webster HD, Bondy CA. 1992. Insulin-like growth factor I gene expression is induced in astrocytes during experimental demyelination. Proc Natl Acad Sci U S A 89:1894-8.
Koshinaga M, Sanon HR, Whittemore SR. 1993. Altered acidic and basic fibroblast growth factor expression following spinal cord injury. Exp Neurol 120:32-48.
Kotter MR, Li WW, Zhao C, Franklin RJ. 2006. Myelin impairs CNS remyelination by inhibiting oligodendrocyte precursor cell differentiation. J Neurosci 26:328-32.
Koziara JM, Lockman PR, Allen DD, Mumper RJ. 2006. The blood-brain barrier and brain drug delivery. J Nanosci Nanotechnol 6:2712-35.
Krishna G, Goel S, Krishna KA. 2014. Chapter 7 - Alternative animal toxicity testing and biomarkers A2 - Gupta, Ramesh C. Biomarkers in Toxicology. Boston: Academic Press. p 129-147.
Krishna V, Andrews H, Jin X, Yu J, Varma A, Wen X, Kindy M. 2013. A contusion model of severe spinal cord injury in rats. J Vis Exp.
Kubota Y, Morita T, Kusakabe M, Sakakura T, Ito K. 1999. Spatial and temporal changes in chondroitin sulfate distribution in the sclerotome play an essential role in the formation of migration patterns of mouse neural crest cells. Dev Dyn 214:55-65.
Kuhlengel KR. 1988. Effect of implants prepared from tissue culture of dorsal root ganglion neurons and Schwann cells on growth of corticospinal fibers after spinal cord injury in neonatal rats. Prog Brain Res 78:199-204.
Kuhlengel KR, Bunge MB, Bunge RP. 1990. Implantation of cultured sensory neurons and Schwann cells into lesioned neonatal rat spinal cord. I. Methods for preparing implants from dissociated cells. J Comp Neurol 293:63-73.

Kulkarni JR, Burt AA, Tromans AT, Constable PDL. 1992. Prophylactic low dose heparin anticoagulant therapy in patients with spinal cord injuries: a retrospective study. Paraplegia 30:169-172.
Kumar S, Chakraborty S, Barbosa C, Brustovetsky T, Brustovetsky N, Obukhov AG. 2012. Mechanisms controlling neurite outgrowth in a pheochromocytoma cell line: The role of TRPC channels. Journal of cellular physiology 227:1408-1419.
Kundi S, Bicknell R, Ahmed Z. 2013. SPINAL CORD INJURY: CURRENT MAMMALIAN MODELS. American Journal of Neuroscience 4:1-12.
Laabs T, Carulli D, Geller HM, Fawcett JW. 2005. Chondroitin sulfate proteoglycans in neural development and regeneration. Current Opinion in Neurobiology 15:116-120.
Lakatos A, Barnett SC, Franklin RJ. 2003. Olfactory ensheathing cells induce less host astrocyte response and chondroitin sulphate proteoglycan expression than Schwann cells following transplantation into adult CNS white matter. Exp Neurol 184:237-46.
Lakatos A, Franklin RJM, Barnett SC. 2000. Olfactory ensheathing cells and Schwann cells differ in their in vitro interactions with astrocytes. Glia 32:214-225.
Lamond R, Barnett SC. 2013. Schwann cells but not olfactory ensheathing cells inhibit CNS myelination via the secretion of connective tissue growth factor. J Neurosci 33:18686-97.
Lander AD, Fujii DK, Gospodarowicz D, Reichardt LF. 1982. Characterization of a factor that promotes neurite outgrowth: evidence linking activity to a heparan sulfate proteoglycan. J Cell Biol 94:574-85.
Lanfer B, Hermann A, Kirsch M, Freudenberg U, Reuner U, Werner C, Storch A. 2010. Directed growth of adult human white matter stem cell-derived neurons on aligned fibrillar collagen. Tissue Eng Part A 16:1103-13.
Lapierre F, Holme K, Lam L, Tressler RJ, Storm N, Wee J, Stack RJ, Castellot J, Tyrrell DJ. 1996. Chemical modifications of heparin that diminish its anticoagulant but preserve its heparanase-inhibitory, angiostatic, anti-tumor and anti-metastatic properties. Glycobiology 6:355-66.
Larner AJ, Johnson AR, Keynes RJ. 1995. Regeneration in the vertebrate central nervous system: phylogeny, ontogeny, and mechanisms. Biol Rev Camb Philos Soc 70:597-619.
Leal-Filho MB. 2011. Spinal cord injury: From inflammation to glial scar. Surg Neurol Int 2:112.
Leavitt BR, Hernit-Grant CS, Macklis JD. 1999. Mature astrocytes transform into transitional radial glia within adult mouse neocortex that supports directed migration of transplanted immature neurons. Exp Neurol 157:43-57.
Lee DH, Lee JK. 2013. Animal models of axon regeneration after spinal cord injury. Neurosci Bull 29:436-44.
Lee JM, Yan P, Xiao Q, Chen S, Lee KY, Hsu CY, Xu J. 2008. Methylprednisolone protects oligodendrocytes but not neurons after spinal cord injury. J Neurosci 28:3141-9.
Lee PJ, Hung PJ, Lee LP. 2007. An artificial liver sinusoid with a microfluidic endothelial-like barrier for primary hepatocyte culture. Biotechnol Bioeng 97:1340-6.
Lee SI, Jeong SR, Kang YM, Han DH, Jin BK, Namgung U, Kim BG. 2010. Endogenous expression of interleukin-4 regulates macrophage activation and confines cavity formation after traumatic spinal cord injury. J Neurosci Res 88:2409-19.
Leveugle B, Ding W, Laurence F, Dehouck MP, Scanameo A, Cecchelli R, Fillit H. 1998. Heparin oligosaccharides that pass the blood-brain barrier inhibit beta-amyloid precursor protein secretion and heparin binding to beta-amyloid peptide. J Neurochem 70:736-44.
Levine JM, Reynolds R, Fawcett JW. 2001. The oligodendrocyte precursor cell in health and disease. Trends in Neurosciences 24:39-47.
Li GL, Farooque M, Holtz A, Olsson Y. 1999. Apoptosis of oligodendrocytes occurs for long distances away from the primary injury after compression trauma to rat spinal cord. Acta Neuropathol 98:473-80.

Li J, Li JP, Zhang X, Lu Z, Yu SP, Wei L. 2012a. Expression of heparanase in vascular cells and astrocytes of the mouse brain after focal cerebral ischemia. Brain Res 1433:137-44.
Li J, Zhu L, Zhang M, Lin F. 2012b. Microfluidic device for studying cell migration in single or co-existing chemical gradients and electric fields. Biomicrofluidics 6:24121-2412113.
Liebner S, Corada M, Bangsow T, Babbage J, Taddei A, Czupalla CJ, Reis M, Felici A, Wolburg H, Fruttiger M and others. 2008. Wnt/beta-catenin signaling controls development of the blood-brain barrier. J Cell Biol 183:409-17.
Ligon LA, Karki S, Tokito M, Holzbaur EL. 2001. Dynein binds to beta-catenin and may tether microtubules at adherens junctions. Nat Cell Biol 3:913-7.
Lin RC, Matesic DF, Marvin M, McKay RD, Brustle O. 1995. Re-expression of the intermediate filament nestin in reactive astrocytes. Neurobiol Dis 2:79-85.
Lindahl U. 2007. Heparan sulfate-protein interactions--a concept for drug design? Thromb Haemost 98:109-15.
Lindahl U, Kusche-Gullberg M, Kjellen L. 1998. Regulated diversity of heparan sulfate. J Biol Chem 273:24979-82.
Lindner M, Thummler K, Arthur A, Brunner S, Elliott C, McElroy D, Mohan H, Williams A, Edgar JM, Schuh C and others. 2015. Fibroblast growth factor signalling in multiple sclerosis: inhibition of myelination and induction of pro-inflammatory environment by FGF9. Brain 138:1875-93.
Lingor P, Teusch N, Schwarz K, Mueller R, Mack H, Bahr M, Mueller BK. 2007. Inhibition of Rho kinase (ROCK) increases neurite outgrowth on chondroitin sulphate proteoglycan in vitro and axonal regeneration in the adult optic nerve in vivo. J Neurochem 103:181-9.
Lipson AC, Widenfalk J, Lindqvist E, Ebendal T, Olson L. 2003. Neurotrophic properties of olfactory ensheathing glia. Exp Neurol 180:167-71.
Logan A, Green J, Hunter A, Jackson R, Berry M. 1999. Inhibition of glial scarring in the injured rat brain by a recombinant human monoclonal antibody to transforming growth factor-beta2. Eur J Neurosci 11:2367-74.
Lois C, Garcia-Verdugo JM, Alvarez-Buylla A. 1996. Chain migration of neuronal precursors. Science 271:978-81.
Lord MS, Whitelock JM. 2014. Bioengineered heparin: is there a future for this form of the successful therapeutic? Bioengineered 5:222-6.
Luo J, Shi R. 2004. Diffusive oxidative stress following acute spinal cord injury in guinea pigs and its inhibition by polyethylene glycol. Neurosci Lett 359:167-70.
Lytle JM, Chittajallu R, Wrathall JR, Gallo V. 2009. NG2 cell response in the CNP-EGFP mouse after contusive spinal cord injury. Glia 57:270-85.
Lyuksyutova AI, Lu CC, Milanesio N, King LA, Guo N, Wang Y, Nathans J, Tessier-Lavigne M, Zou Y. 2003. Anterior-posterior guidance of commissural axons by Wnt-frizzled signaling. Science 302:1984-8.
Ma Q, Cornelli U, Hanin I, Jeske WP, Linhardt RJ, Walenga JM, Fareed J, Lee JM. 2007. Heparin oligosaccharides as potential therapeutic agents in senile dementia. Curr Pharm Des 13:1607-16.
Ma Q, Dudas B, Hejna M, Cornelli U, Lee JM, Lorens S, Mervis R, Hanin I, Fareed J. 2002. The blood-brain barrier accessibility of a heparin-derived oligosaccharides C3. Thromb Res 105:447-53.
MacDonald ML, Lamerdin J, Owens S, Keon BH, Bilter GK, Shang Z, Huang Z, Yu H, Dias J, Minami T and others. 2006. Identifying off-target effects and hidden phenotypes of drugs in human cells. Nat Chem Biol 2:329-337.
MacInnis BL, Campenot RB. 2002. Retrograde support of neuronal survival without retrograde transport of nerve growth factor. Science 295:1536-9.
Maeki M, Yamaguchi H, Tokeshi M, Miyazaki M. 2016. Microfluidic Approaches for Protein Crystal Structure Analysis. Anal Sci 32:3-9.
Marchand R, Woerly S, Bertrand L, Valdes N. 1993. Evaluation of two cross-linked collagen gels implanted in the transected spinal cord. Brain Res Bull 30:415-22.

Mark D, Haeberle S, Roth G, von Stetten F, Zengerle R. 2010. Microfluidic lab-on-a-chip platforms: requirements, characteristics and applications. Chemical Society Reviews 39:1153-1182.
Masuda T, Fukamauchi F, Takeda Y, Fujisawa H, Watanabe K, Okado N, Shiga T. 2004. Developmental regulation of notochord-derived repulsion for dorsal root ganglion axons. Mol Cell Neurosci 25:217-27.
Matsumoto T, Tamaki T, Kawakami M, Yoshida M, Ando M, Yamada H. 2001. Early complications of high-dose methylprednisolone sodium succinate treatment in the follow-up of acute cervical spinal cord injury. Spine (Phila Pa 1976) 26:426-30.
Mautes AE, Weinzierl MR, Donovan F, Noble LJ. 2000. Vascular events after spinal cord injury: contribution to secondary pathogenesis. Phys Ther 80:673-87.
McAdoo DJ, Hughes MG, Nie L, Shah B, Clifton C, Fullwood S, Hulsebosch CE. 2005. The effect of glutamate receptor blockers on glutamate release following spinal cord injury. Lack of evidence for an ongoing feedback cascade of damage --> glutamate release --> damage --> glutamate release --> etc. Brain Res 1038:92-9.
McCarthy ST, Turner JJ, Robertson D, Hawkey CJ, Macey DJ. 1977. Low-dose heparin as a prophylaxis against deep-vein thrombosis after acute stroke. Lancet 2:800-1.
McConnell SK. 1992. The control of neuronal identity in the developing cerebral cortex. Curr Opin Neurobiol 2:23-7.
McDonald JC, Duffy DC, Anderson JR, Chiu DT, Wu H, Schueller OJ, Whitesides GM. 2000. Fabrication of microfluidic systems in poly(dimethylsiloxane). Electrophoresis 21:27-40.
McKeon RJ, Höke A, Silver J. 1995. Injury-Induced Proteoglycans Inhibit the Potential for Laminin-Mediated Axon Growth on Astrocytic Scars. Experimental Neurology 136:32-43.
McKinnon RD, Matsui T, Dubois-Dalcq M, Aaronson SA. 1990. FGF modulates the PDGF-driven pathway of oligodendrocyte development. Neuron 5:603-14.
McTigue DM, Popovich PG, Morgan TE, Stokes BT. 2000. Localization of transforming growth factor-beta1 and receptor mRNA after experimental spinal cord injury. Exp Neurol 163:220-30.
McTigue DM, Wei P, Stokes BT. 2001. Proliferation of NG2-positive cells and altered oligodendrocyte numbers in the contused rat spinal cord. J Neurosci 21:3392-400.
Mei F, Fancy SP, Shen YA, Niu J, Zhao C, Presley B, Miao E, Lee S, Mayoral SR, Redmond SA and others. 2014. Micropillar arrays as a high-throughput screening platform for therapeutics in multiple sclerosis. Nat Med 20:954-60.
Meyza KZ, Blanchard DC, Pearson BL, Pobbe RL, Blanchard RJ. 2012. Fractone-associated N-sulfated heparan sulfate shows reduced quantity in BTBR T+tf/J mice: a strong model of autism. Behav Brain Res 228:247-53.
Mi S, Miller RH, Lee X, Scott ML, Shulag-Morskaya S, Shao Z, Chang J, Thill G, Levesque M, Zhang M and others. 2005. LINGO-1 negatively regulates myelination by oligodendrocytes. Nat Neurosci 8:745-51.
Miao QL, Ye Q, Zhang XH. 2014. Perineuronal net, CSPG receptor and their regulation of neural plasticity. Sheng Li Xue Bao 66:387-97.
Miller AC, Rivero A, Ziad S, Smith DJ, Elamin EM. 2009. Influence of nebulized unfractionated heparin and N-acetylcysteine in acute lung injury after smoke inhalation injury. J Burn Care Res 30:249-56.
Mimura F, Yamagishi S, Arimura N, Fujitani M, Kubo T, Kaibuchi K, Yamashita T. 2006. Myelin-associated glycoprotein inhibits microtubule assembly by a Rho-kinase-dependent mechanism. J Biol Chem 281:15970-9.
Miron VE, Kuhlmann T, Antel JP. 2011. Cells of the oligodendroglial lineage, myelination, and remyelination. Biochim Biophys Acta 1812:184-93.
Mocchetti I, Rabin SJ, Colangelo AM, Whittemore SR, Wrathall JR. 1996. Increased basic fibroblast growth factor expression following contusive spinal cord injury. Exp Neurol 141:154-64.

Mothe AJ, Tator CH. 2012. Advances in stem cell therapy for spinal cord injury. The Journal of Clinical Investigation 122:3824-3834.
Nadanaka S, Clement A, Masayama K, Faissner A, Sugahara K. 1998. Characteristic hexasaccharide sequences in octasaccharides derived from shark cartilage chondroitin sulfate D with a neurite outgrowth promoting activity. J Biol Chem 273:3296-307.
Nadir Y, Brenner B. 2014. Heparanase multiple effects in cancer. Thromb Res 133 Suppl 2:S90-4.
Naggi A, Casu B, Perez M, Torri G, Cassinelli G, Penco S, Pisano C, Giannini G, Ishai-Michaeli R, Vlodavsky I. 2005. Modulation of the heparanase-inhibiting activity of heparin through selective desulfation, graded N-acetylation, and glycol splitting. J Biol Chem 280:12103-13.
Nagoshi N, Kaneko S, Fujiyoshi K, Takemitsu M, Yagi M, Iizuka S, Miyake A, Hasegawa A. 2015. Characteristics of neuropathic pain and its relationship with quality of life in 72 patients with spinal cord injury.
Nakajima K, Honda S, Tohyama Y, Imai Y, Kohsaka S, Kurihara T. 2001. Neurotrophin secretion from cultured microglia. J Neurosci Res 65:322-31.
Nash B, Ioannidou K, Barnett SC. 2011a. Astrocyte phenotypes and their relationship to myelination. J Anat 219:44-52.
Nash B, Thomson CE, Linington C, Arthur AT, McClure JD, McBride MW, Barnett SC. 2011b. Functional duality of astrocytes in myelination. J Neurosci 31:13028-38.
Nisbet DR, Crompton KE, Horne MK, Finkelstein DI, Forsythe JS. 2008. Neural tissue engineering of the CNS using hydrogels. Journal of Biomedical Materials Research Part B: Applied Biomaterials 87B:251-263.
Nobes CD, Hall A. 1999. Rho GTPases control polarity, protrusion and adhesion during cell movement. J Cell Biol 144:1235-1244.
Noble M. 2000. Precursor Cell Transitions in Oligodendrocyte Development. The Journal of Cell Biology 148:839-842.
Noble M, Murray K, Stroobant P, Waterfield MD, Riddle P. 1988. Platelet-derived growth factor promotes division and motility and inhibits premature differentiation of the oligodendrocyte/type-2 astrocyte progenitor cell. Nature 333:560-2.
Nomura H, Tator CH, Shoichet MS. 2006. Bioengineered strategies for spinal cord repair. J Neurotrauma 23:496-507.
Norenberg MD, Smith J, Marcillo A. 2004. The pathology of human spinal cord injury: defining the problems. J Neurotrauma 21:429-40.
NSCISC. 2013. Spinal cord injury facts and figures at a glance. J Spinal Cord Med 36:170-1.
Nurmohamed MT, Rosendaal FR, Buller HR, Dekker E, Hommes DW, Vandenbroucke JP, Briet E. 1992. Low-molecular-weight heparin versus standard heparin in general and orthopaedic surgery: a meta-analysis. Lancet 340:152-6.
Obermair FJ, Schroter A, Thallmair M. 2008. Endogenous neural progenitor cells as therapeutic target after spinal cord injury. Physiology (Bethesda) 23:296-304.
Ogata K, Kosaka T. 2002. Structural and quantitative analysis of astrocytes in the mouse hippocampus. Neuroscience 113:221-33.
Orange JS, May MJ. 2008. Cell penetrating peptide inhibitors of nuclear factor-kappa B. Cell Mol Life Sci 65:3564-91.
Oudega M, Vargas CG, Weber AB, Kleitman N, Bunge MB. 1999. Long-term effects of methylprednisolone following transection of adult rat spinal cord. European Journal of Neuroscience 11:2453-2464.
Pannek J. 2011. Treatment of urinary tract infection in persons with spinal cord injury: guidelines, evidence, and clinical practice: A questionnaire-based survey and review of the literature. The Journal of Spinal Cord Medicine 34:11-15.
Park E, Velumian AA, Fehlings MG. 2004. The role of excitotoxicity in secondary mechanisms of spinal cord injury: a review with an emphasis on the implications for white matter degeneration. J Neurotrauma 21:754-74.
Park J, Koito H, Li J, Han A. 2009a. Microfluidic compartmentalized co-culture platform for CNS axon myelination research. Biomed Microdevices 11:1145-53.

Park J, Koito H, Li J, Han A. 2009b. A multi-compartment CNS neuron-glia Co-culture microfluidic platform. J Vis Exp.
Park KK, Liu K, Hu Y, Smith PD, Wang C, Cai B, Xu B, Connolly L, Kramvis I, Sahin M and others. 2008. Promoting axon regeneration in the adult CNS by modulation of the PTEN/mTOR pathway. Science 322:963-6.
Passeri M, Cucinotta D. 1989. Ateroid in the clinical treatment of multi-infarct dementia. Mod Probl Pharmacopsychiatry 23:85-94.
Patey SJ, Edwards EA, Yates EA, Turnbull JE. 2006. Heparin Derivatives as Inhibitors of BACE-1, the Alzheimer's β-Secretase, with Reduced Activity against Factor Xa and Other Proteases. Journal of Medicinal Chemistry 49:6129-6132.
Pedraza CE, Taylor C, Pereira A, Seng M, Tham CS, Izrael M, Webb M. 2014. Induction of oligodendrocyte differentiation and in vitro myelination by inhibition of rho-associated kinase. ASN Neuro 6.
Perry VH, Brown MC, Gordon S. 1987. The macrophage response to central and peripheral nerve injury. A possible role for macrophages in regeneration. J Exp Med 165:1218-23.
Persidsky Y, Ghorpade A, Rasmussen J, Limoges J, Liu XJ, Stins M, Fiala M, Way D, Kim KS, Witte MH and others. 1999. Microglial and astrocyte chemokines regulate monocyte migration through the blood-brain barrier in human immunodeficiency virus-1 encephalitis. Am J Pathol 155:1599-611.
Peterson SL, McDonald A, Gourley PL, Sasaki DY. 2005. Poly(dimethylsiloxane) thin films as biocompatible coatings for microfluidic devices: cell culture and flow studies with glial cells. J Biomed Mater Res A 72:10-8.
Pfrieger FW, Barres BA. 1997. Synaptic Efficacy Enhanced by Glial Cells in Vitro. Science 277:1684-1687.
Pike DB, Cai S, Pomraning KR, Firpo MA, Fisher RJ, Shu XZ, Prestwich GD, Peattie RA. 2006. Heparin-regulated release of growth factors in vitro and angiogenic response in vivo to implanted hyaluronan hydrogels containing VEGF and bFGF. Biomaterials 27:5242-51.
Pineau I, Lacroix S. 2007. Proinflammatory cytokine synthesis in the injured mouse spinal cord: multiphasic expression pattern and identification of the cell types involved. J Comp Neurol 500:267-85.
Pitts LH, Ross A, Chase GA, Faden AI. 1995. Treatment with thyrotropin-releasing hormone (TRH) in patients with traumatic spinal cord injuries. J Neurotrauma 12:235-43.
Popovich PG, Horner PJ, Mullin BB, Stokes BT. 1996. A quantitative spatial analysis of the blood-spinal cord barrier. I. Permeability changes after experimental spinal contusion injury. Exp Neurol 142:258-75.
Powell AK, Yates EA, Fernig DG, Turnbull JE. 2004. Interactions of heparin/heparan sulfate with proteins: appraisal of structural factors and experimental approaches. Glycobiology 14:17r-30r.
Prabhakarpandian B, Shen MC, Nichols JB, Mills IR, Sidoryk-Wegrzynowicz M, Aschner M, Pant K. 2013. SyM-BBB: a microfluidic Blood Brain Barrier model. Lab Chip 13:1093-101.
Probert L, Eugster HP, Akassoglou K, Bauer J, Frei K, Lassmann H, Fontana A. 2000. TNFR1 signalling is critical for the development of demyelination and the limitation of T-cell responses during immune-mediated CNS disease. Brain 123 (Pt 10):2005-19.
Probst C, Grunberger A, Wiechert W, Kohlheyer D. 2013. Microfluidic growth chambers with optical tweezers for full spatial single-cell control and analysis of evolving microbes. J Microbiol Methods 95:470-6.
Properzi F, Lin R, Kwok J, Naidu M, van Kuppevelt TH, Ten Dam GB, Camargo LM, Raha-Chowdhury R, Furukawa Y, Mikami T and others. 2008. Heparan sulphate proteoglycans in glia and in the normal and injured CNS: expression of sulphotransferases and changes in sulphation. Eur J Neurosci 27:593-604.
Purves D, Augustine GJ, D F. 2001. Neuroscience 2nd.

Raisman G. 2001. Olfactory ensheathing cells - another miracle cure for spinal cord injury? Nat Rev Neurosci 2:369-75.
Ramon-Cueto A. 2000. Olfactory ensheathing glia transplantation into the injured spinal cord. Prog Brain Res 128:265-72.
Rapalino O, Lazarov-Spiegler O, Agranov E, Velan GJ, Yoles E, Fraidakis M, Soloman A, Gepstein R, Katz A, Belkin M and others. 1998a. Implantation of stimulated homologous macrophages results in partial recovery of paraplegic rats. Nat Med 4:814-821.
Rapalino O, Lazarov-Spiegler O, Agranov E, Velan GJ, Yoles E, Fraidakis M, Solomon A, Gepstein R, Katz A, Belkin M and others. 1998b. Implantation of stimulated homologous macrophages results in partial recovery of paraplegic rats. Nat Med 4:814-21.
Rauvala H, Peng HB. 1997. HB-GAM (heparin-binding growth-associated molecule) and heparin-type glycans in the development and plasticity of neuron-target contacts. Prog Neurobiol 52:127-44.
Recknor JB, Recknor JC, Sakaguchi DS, Mallapragada SK. 2004. Oriented astroglial cell growth on micropatterned polystyrene substrates. Biomaterials 25:2753-67.
Reichert F, Saada A, Rotshenker S. 1994. Peripheral nerve injury induces Schwann cells to express two macrophage phenotypes: phagocytosis and the galactose-specific lectin MAC-2. J Neurosci 14:3231-45.
Reynolds BA, Weiss S. 1996. Clonal and population analyses demonstrate that an EGF-responsive mammalian embryonic CNS precursor is a stem cell. Dev Biol 175:1-13.
Richardson PM, McGuinness UM, Aguayo AJ. 1980. Axons from CNS neurons regenerate into PNS grafts. Nature 284:264-5.
Riento K, Ridley AJ. 2003. ROCKs: multifunctional kinases in cell behaviour. Nat Rev Mol Cell Biol 4:446-456.
Robertson G, Bushell TJ, Zagnoni M. 2014. Chemically induced synaptic activity between mixed primary hippocampal co-cultures in a microfluidic system. Integr Biol (Camb) 6:636-44.
Rochkind S, Shahar A, Amon M, Nevo Z. 2002. Transplantation of embryonal spinal cord nerve cells cultured on biodegradable microcarriers followed by low power laser irradiation for the treatment of traumatic paraplegia in rats. Neurol Res 24:355-60.
Rodgers JM, Robinson AP, Miller SD. 2013. Strategies for Protecting Oligodendrocytes and Enhancing Remyelination in Multiple Sclerosis. Discovery medicine 16:53-63.
Rodriguez JP, Coulter M, Miotke J, Meyer RL, Takemaru K. 2014. Abrogation of beta-catenin signaling in oligodendrocyte precursor cells reduces glial scarring and promotes axon regeneration after CNS injury. 34:10285-97.
Rolls A, Shechter R, London A, Segev Y, Jacob-Hirsch J, Amariglio N, Rechavi G, Schwartz M. 2008. Two faces of chondroitin sulfate proteoglycan in spinal cord repair: a role in microglia/macrophage activation. PLoS Med 5:e171.
Rosen SD, Lemjabbar-Alaoui H. 2010. Sulf-2: an extracellular modulator of cell signaling and a cancer target candidate. Expert Opin Ther Targets 14:935-49.
Rossi F, Perale G, Papa S, Forloni G, Veglianese P. 2013. Current options for drug delivery to the spinal cord. Expert Opin Drug Deliv 10:385-96.
Rothman SM, Olney JW. 1986. Glutamate and the pathophysiology of hypoxic--ischemic brain damage. Ann Neurol 19:105-11.
Saleh-Lakha S, Trevors JT. 2010. Perspective: microfluidic applications in microbiology. J Microbiol Methods 82:108-11.
Salinas PC. 2012. Wnt signaling in the vertebrate central nervous system: from axon guidance to synaptic function. Cold Spring Harb Perspect Biol 4.
Sarrazin S, Lamanna WC, Esko JD. 2011. Heparan sulfate proteoglycans. Cold Spring Harb Perspect Biol 3.
Sato GH, Yasumura Y. 1966. Retention of differentiated function in dispersed cell culture. Trans N Y Acad Sci 28:1063-79.

Saxena K, Schieborr U, Anderka O, Duchardt-Ferner E, Elshorst B, Gande SL, Janzon J, Kudlinzki D, Sreeramulu S, Dreyer MK and others. 2010. Influence of heparin mimetics on assembly of the FGF.FGFR4 signaling complex. J Biol Chem 285:26628-40.

Schmitt AB, Breuer S, Liman J, Buss A, Schlangen C, Pech K, Hol EM, Brook GA, Noth J, Schwaiger FW. 2003. Identification of regeneration-associated genes after central and peripheral nerve injury in the adult rat. BMC Neurosci 4:8.

Schwab ME, Bartholdi D. 1996. Degeneration and regeneration of axons in the lesioned spinal cord. Physiol Rev 76:319-70.

Schwartz G, Fehlings MG. 2001. Evaluation of the neuroprotective effects of sodium channel blockers after spinal cord injury: improved behavioral and neuroanatomical recovery with riluzole. J Neurosurg 94:245-56.

Scremin OU. 2009. Chapter 5 - The Spinal Cord Blood Vessels. In: Kayalioglu CWP, editor. The Spinal Cord. San Diego: Academic Press. p 57-63.

Seidi A, Kaji H, Annabi N, Ostrovidov S, Ramalingam M, Khademhosseini A. 2011. A microfluidic-based neurotoxin concentration gradient for the generation of an in vitro model of Parkinson's disease. Biomicrofluidics 5:22214.

Sheng GJ, Oh YI, Chang SK, Hsieh-Wilson LC. 2013. Tunable heparan sulfate mimetics for modulating chemokine activity. J Am Chem Soc 135:10898-901.

Shih YT, Wang MC, Peng HH, Chen TF, Chen L, Chang JY, Chiu JJ. 2012. Modulation of chemotactic and pro-inflammatory activities of endothelial progenitor cells by hepatocellular carcinoma. Cell Signal 24:779-93.

Shoichet MS, Tate CC, Baumann MD, Reichert WM. 2008. Strategies for Regeneration and Repair in the Injured Central Nervous System. Indwelling Neural Implants: Strategies for Contending with the In Vivo Environment: Boca Raton (FL): CRC Press/Taylor & Francis.

Siddique R, Thakor N. 2014. Investigation of nerve injury through microfluidic devices. Journal of the Royal Society Interface 11:20130676.

Silbert JE, Sugumaran G. 2002. Biosynthesis of chondroitin/dermatan sulfate. IUBMB Life 54:177-86.

Simard JM, Schreibman D, Aldrich EF, Stallmeyer B, Le B, James RF, Beaty N. 2010. Unfractionated heparin: multitargeted therapy for delayed neurological deficits induced by subarachnoid hemorrhage. Neurocrit Care 13:439-49.

Simons M, Lyons DA. 2013. Axonal selection and myelin sheath generation in the central nervous system. Curr Opin Cell Biol 25:512-9.

Simons M, Nave KA. 2015. Oligodendrocytes: Myelination and Axonal Support. Cold Spring Harb Perspect Biol.

Small DH, Mok SS, Williamson TG, Nurcombe V. 1996. Role of Proteoglycans in Neural Development, Regeneration, and the Aging Brain. Journal of Neurochemistry 67:889-899.

Smith PD, Coulson-Thomas VJ, Foscarin S, Kwok JC, Fawcett JW. 2015. "GAG-ing with the neuron": The role of glycosaminoglycan patterning in the central nervous system. Exp Neurol.

Snaidero N, Simons M. 2014. Myelination at a glance. Journal of Cell Science 127:2999-3004.

Snow AD, Kisilevsky R, Willmer J, Prusiner SB, DeArmond SJ. 1989. Sulfated glycosaminoglycans in amyloid plaques of prion diseases. Acta Neuropathol 77:337-42.

Snow AD, Willmer JP, Kisilevsky R. 1987. Sulfated glycosaminoglycans in Alzheimer's disease. Hum Pathol 18:506-10.

Snyder EY, Teng YD. 2012. Stem cells and spinal cord repair. N Engl J Med 366:1940-2.

Sofroniew MV. 2015. Astrocyte barriers to neurotoxic inflammation. Nat Rev Neurosci 16:249-63.

Sofroniew MV, Vinters HV. 2010. Astrocytes: biology and pathology. Acta Neuropathol 119:7-35.

Song HL, Shim S, Kim DH, Won SH, Joo S, Kim S, Jeon NL, Yoon SY. 2014. beta-Amyloid is transmitted via neuronal connections along axonal membranes. Ann Neurol 75:88-97.
Sorensen A, Moffat K, Thomson C, Barnett SC. 2008a. Astrocytes, but not olfactory ensheathing cells or Schwann cells, promote myelination of CNS axons in vitro. Glia 56:750-63.
Sorensen A, Moffat K, Thomson C, Barnett SC. 2008b. Astrocytes, but not olfactory ensheathing cells or Schwann cells, promote myelination of CNS axons in vitro. Glia 56:750-763.
Sotelo-Silveira JR, Calliari A, Kun A, Koenig E, Sotelo JR. 2006. RNA trafficking in axons. Traffic 7:508-15.
Steeves JD, Lammertse D, Curt A, Fawcett JW, Tuszynski MH, Ditunno JF, Ellaway PH, Fehlings MG, Guest JD, Kleitman N and others. 2007. Guidelines for the conduct of clinical trials for spinal cord injury (SCI) as developed by the ICCP panel: clinical trial outcome measures. Spinal Cord 45:206-21.
Stenman JM, Rajagopal J, Carroll TJ, Ishibashi M, McMahon J, McMahon AP. 2008. Canonical Wnt signaling regulates organ-specific assembly and differentiation of CNS vasculature. Science 322:1247-50.
Sterne GD, Brown RA, Green CJ, Terenghi G. 1997. Neurotrophin-3 delivered locally via fibronectin mats enhances peripheral nerve regeneration. Eur J Neurosci 9:1388-96.
Stevens B, Porta S, Haak LL, Gallo V, Fields RD. 2002. Adenosine: a neuron-glial transmitter promoting myelination in the CNS in response to action potentials. Neuron 36:855-68.
Stieger B, Gao B. 2015. Drug transporters in the central nervous system. Clin Pharmacokinet 54:225-42.
Straley K, Heilshorn SC. 2009. Designer protein-based scaffolds for neural tissue engineering. Conf Proc IEEE Eng Med Biol Soc 2009:2101-2.
Straley KS, Foo CW, Heilshorn SC. 2010. Biomaterial design strategies for the treatment of spinal cord injuries. J Neurotrauma 27:1-19.
Su Z, Yuan Y, Chen J, Cao L, Zhu Y, Gao L, Qiu Y, He C. 2009. Reactive Astrocytes in Glial Scar Attract Olfactory Ensheathing Cells Migration by Secreted TNF-α in Spinal Cord Lesion of Rat. PLoS ONE 4:e8141.
Swarup VP, Mencio CP, Hlady V, Kuberan B. 2013. Sugar glues for broken neurons. Biomol Concepts 4:233-57.
Tabakow P, Jarmundowicz W, Czapiga B, Fortuna W, Miedzybrodzki R, Czyz M, Huber J, Szarek D, Okurowski S, Szewczyk P and others. 2013. Transplantation of autologous olfactory ensheathing cells in complete human spinal cord injury. Cell Transplant 22:1591-612.
Tamai I, Tsuji A. 1996. Drug delivery through the blood-brain barrier. Advanced Drug Delivery Reviews 19:401-424.
Taoka Y, Okajima K. 2000. Role of leukocytes in spinal cord injury in rats. J Neurotrauma 17:219-29.
Tator CH, Koyanagi I. 1997. Vascular mechanisms in the pathophysiology of human spinal cord injury. J Neurosurg 86:483-92.
Tawk M, Makoukji J, Belle M, Fonte C, Trousson A, Hawkins T, Li H, Ghandour S, Schumacher M, Massaad C. 2011. Wnt/beta-catenin signaling is an essential and direct driver of myelin gene expression and myelinogenesis. J Neurosci 31:3729-42.
Taylor AM, Blurton-Jones M, Rhee SW, Cribbs DH, Cotman CW, Jeon NL. 2005. A microfluidic culture platform for CNS axonal injury, regeneration and transport. Nature methods 2:599-605.
Taylor AM, Jeon NL. 2010. Micro-scale and microfluidic devices for neurobiology. Curr Opin Neurobiol 20:640-7.
Taylor AM, Jeon NL. 2011. Microfluidic and compartmentalized platforms for neurobiological research. Crit Rev Biomed Eng 39:185-200.

Tewarie RSN, Hurtado A, Bartels RH, Grotenhuis A, Oudega M. 2009. Stem Cell–Based Therapies for Spinal Cord Injury. The Journal of Spinal Cord Medicine 32:105-114.
Tharin S, Kothapalli CR, Ozdinler PH, Pasquina L, Chung S, Varner J, DeValence S, Kamm R, Macklis JD. 2012. A microfluidic device to investigate axon targeting by limited numbers of purified cortical projection neuron subtypes. Integr Biol (Camb) 4:1398-405.
Thietje R, Pouw MH, Schulz AP, Kienast B, Hirschfeld S. 2011. Mortality in patients with traumatic spinal cord injury: descriptive analysis of 62 deceased subjects. J Spinal Cord Med 34:482-7.
Thomson CE, McCulloch M, Sorenson A, Barnett SC, Seed BV, Griffiths IR, McLaughlin M. 2008. Myelinated, synapsing cultures of murine spinal cord – validation as an in vitro model of the central nervous system. European Journal of Neuroscience 28:1518-1535.
Thuret S, Moon LDF, Gage FH. 2006. Therapeutic interventions after spinal cord injury. Nat Rev Neurosci 7:628-643.
Tian B, Liu J, Dvir T, Jin L, Tsui JH, Qing Q, Suo Z, Langer R, Kohane DS, Lieber CM. 2012. Macroporous nanowire nanoelectronic scaffolds for synthetic tissues. Nat Mater 11:986-94.
Tkachenko E, Rhodes JM, Simons M. 2005. Syndecans: new kids on the signaling block. Circ Res 96:488-500.
Toft A, Tome M, Lindsay SL, Barnett SC, Riddell JS. 2012. Transplant-mediated repair properties of rat olfactory mucosal OM-I and OM-II sphere-forming cells. J Neurosci Res 90:619-31.
Tolg C, Telmer P, Turley E. 2014. Specific sizes of hyaluronan oligosaccharides stimulate fibroblast migration and excisional wound repair. PLoS One 9:e88479.
Tripathi R, McTigue DM. 2007. Prominent oligodendrocyte genesis along the border of spinal contusion lesions. Glia 55:698-711.
Tully SE, Mabon R, Gama CI, Tsai SM, Liu X, Hsieh-Wilson LC. 2004. A Chondroitin Sulfate Small Molecule that Stimulates Neuronal Growth. Journal of the American Chemical Society 126:7736-7737.
Tumova S, Woods A, Couchman JR. 2000. Heparan sulfate proteoglycans on the cell surface: versatile coordinators of cellular functions. The International Journal of Biochemistry & Cell Biology 32:269-288.
Turnbull J, Powell A, Guimond S. 2001. Heparan sulfate: decoding a dynamic multifunctional cell regulator. Trends in Cell Biology 11:75-82.
Turner N, Grose R. 2010. Fibroblast growth factor signalling: from development to cancer. Nat Rev Cancer 10:116-129.
Ughrin YM, Chen ZJ, Levine JM. 2003. Multiple regions of the NG2 proteoglycan inhibit neurite growth and induce growth cone collapse. J Neurosci 23:175-86.
Vallstedt A, Klos JM, Ericson J. 2005. Multiple dorsoventral origins of oligodendrocyte generation in the spinal cord and hindbrain. Neuron 45:55-67.
van Kesteren RE, Mason MRJ, MacGillavry HD, Smit AB, Verhaagen J. 2011. A Gene Network Perspective on Axonal Regeneration. Frontiers in Molecular Neuroscience 4:46.
Verma P, Chierzi S, Codd AM, Campbell DS, Meyer RL, Holt CE, Fawcett JW. 2005. Axonal protein synthesis and degradation are necessary for efficient growth cone regeneration. J Neurosci 25:331-42.
Villegas J. 1972. Axon-Schwann cell interaction in the squid nerve fibre. J Physiol 225:275-96.
Vlodavsky I, Ilan N, Naggi A, Casu B. 2007. Heparanase: structure, biological functions, and inhibition by heparin-derived mimetics of heparan sulfate. Curr Pharm Des 13:2057-73.
Wade A, McKinney A, Phillips JJ. 2014. Matrix regulators in neural stem cell functions. Biochimica et Biophysica Acta (BBA) - General Subjects 1840:2520-2525.

Wall D, Douglas S, Ferro V, Cowden W, Parish C. 2001. Characterisation of the anticoagulant properties of a range of structurally diverse sulfated oligosaccharides. Thromb Res 103:325-35.
Wang H-Y, Lu C. 2008. Microfluidic electroporation for delivery of small molecules and genes into cells using a common DC power supply. Biotechnology and Bioengineering 100:579-586.
Wang KC, Koprivica V, Kim JA, Sivasankaran R, Guo Y, Neve RL, He Z. 2002. Oligodendrocyte-myelin glycoprotein is a Nogo receptor ligand that inhibits neurite outgrowth. Nature 417:941-4.
Wang L, Liang Z, Li G. 2011. Rab22 controls NGF signaling and neurite outgrowth in PC12 cells. Mol Biol Cell 22:3853-60.
Wang S, Sdrulla AD, diSibio G, Bush G, Nofziger D, Hicks C, Weinmaster G, Barres BA. 1998. Notch receptor activation inhibits oligodendrocyte differentiation. Neuron 21:63-75.
Watson C, Kayalioglu G. 2009. Chapter 1 - The Organization of the Spinal Cord. In: Kayalioglu CWP, editor. The Spinal Cord. San Diego: Academic Press. p 1-7.
Weitz JI. 1997. Low-molecular-weight heparins. N Engl J Med 337:688-98.
Wells MR, Kraus K, Batter DK, Blunt DG, Weremowitz J, Lynch SE, Antoniades HN, Hansson HA. 1997. Gel matrix vehicles for growth factor application in nerve gap injuries repaired with tubes: a comparison of biomatrix, collagen, and methylcellulose. Exp Neurol 146:395-402.
Wen Y, Yu S, Wu Y, Ju R, Wang H, Liu Y, Wang Y, Xu Q. 2015. Spinal cord injury repair by implantation of structured hyaluronic acid scaffold with PLGA microspheres in the rat. Cell Tissue Res.
Wessel HP, Chucholowski A, Fingerle J, Iberg N, Märki HP, Müller R, Pech M, Pfister-Downar M, Rouge M, Schmid G and others. 2005. From Glycosaminoglycans to Heparinoid Mimetics with Antiproliferative Activity. Carbohydrate Mimics: Wiley-VCH Verlag GmbH & Co. KGaA. p 417-431.
Whetstone WD, Hsu J-YC, Eisenberg M, Werb Z, Noble-Haeusslein LJ. 2003. Blood-Spinal Cord Barrier After Spinal Cord Injury: Relation to Revascularization and Wound Healing. Journal of neuroscience research 74:227-239.
Whitesides GM. 2006. The origins and the future of microfluidics. Nature 442:368-73.
Whitesides GM, Ostuni E, Takayama S, Jiang X, Ingber DE. 2001. Soft lithography in biology and biochemistry. Annu Rev Biomed Eng 3:335-73.
Wilhelmsson U, Faiz M, de Pablo Y, Sjoqvist M, Andersson D, Widestrand A, Potokar M, Stenovec M, Smith PL, Shinjyo N and others. 2012. Astrocytes negatively regulate neurogenesis through the Jagged1-mediated Notch pathway. Stem Cells 30:2320-9.
Willis D, Li KW, Zheng JQ, Chang JH, Smit AB, Kelly T, Merianda TT, Sylvester J, van Minnen J, Twiss JL. 2005. Differential transport and local translation of cytoskeletal, injury-response, and neurodegeneration protein mRNAs in axons. J Neurosci 25:778-91.
Wittig JH, Jr., Ryan AF, Asbeck PM. 2005. A reusable microfluidic plate with alternate-choice architecture for assessing growth preference in tissue culture. J Neurosci Methods 144:79-89.
Wolman L. 1965. The disturbance of circulation in traumatic paraplegia in acute and late stages: A pathological study. Paraplegia 2:213-26.
Xu X, Dai Y. 2010. Heparin: an intervenor in cell communication. Journal of Cellular and Molecular Medicine 14:175-180.
Yan D, Lin X. 2009. Shaping Morphogen Gradients by Proteoglycans. Cold Spring Harbor Perspectives in Biology 1:a002493.
Yap YC, Dickson TC, King AE, Breadmore MC, Guijt RM. 2014. Microfluidic culture platform for studying neuronal response to mild to very mild axonal stretch injury. Biomicrofluidics 8:044110.
Yates EA, Guimond SE, Turnbull JE. 2004. Highly diverse heparan sulfate analogue libraries: providing access to expanded areas of sequence space for bioactivity screening. J Med Chem 47:277-80.

Yin H, Marshall D. 2012. Microfluidics for single cell analysis. Curr Opin Biotechnol 23:110-9.
Yiu G, He Z. 2006. Glial inhibition of CNS axon regeneration. Nat Rev Neurosci 7:617-27.
Zhang LX, Yin YM, Zhang ZQ, Deng LX. 2015. Grafted bone marrow stromal cells: a contributor to glial repair after spinal cord injury. Neuroscientist 21:277-89.
Zhang SC, Lundberg C, Lipsitz D, O'Connor LT, Duncan ID. 1998. Generation of oligodendroglial progenitors from neural stem cells. J Neurocytol 27:475-89.
Zhang Y, Gazit Z, Pelled G, Gazit D, Vunjak-Novakovic G. 2011. Patterning osteogenesis by inducible gene expression in microfluidic culture systems. Integr Biol (Camb) 3:39-47.
Zhang Y, Yeung MN, Liu J, Chau CH, Chan YS, Shum DK. 2006. Mapping heparanase expression in the spinal cord of adult rats. J Comp Neurol 494:345-57.
Zhong Y, Bellamkonda RV. 2008. Biomaterials for the central nervous system. J R Soc Interface 5:957-75.
Zhou X, He X, Ren Y. 2014. Function of microglia and macrophages in secondary damage after spinal cord injury. Neural Regeneration Research 9:1787-1795.
Zivraj KH, Tung YC, Piper M, Gumy L, Fawcett JW, Yeo GS, Holt CE. 2010. Subcellular profiling reveals distinct and developmentally regulated repertoire of growth cone mRNAs. J Neurosci 30:15464-78.
Zorner B, Schwab ME. 2010. Anti-Nogo on the go: from animal models to a clinical trial. Ann N Y Acad Sci 1198 Suppl 1:E22-34.
Zou Y. 2004. Wnt signaling in axon guidance. Trends Neurosci 27:528-32.